Devensian Ice-Sheet history of the western North Sea

GRIMOLDI, ELENA

DEVENSIAN ICE-SHEET HISTORY OF THE WESTERN NORTH SEA

ELENA GRIMOLDI

A thesis submitted for the degree of Doctor of Philosophy

SEPTEMBER 2017

Supervisors: Dave Roberts, David Evans, Heather Stewart, Hans Petter Sejrup, Berit Hjelstuen & Haflidi Haflidason

Department of Geography
UNIVERSITY OF DURHAM

Durham University

DEVENSIAN ICE-SHEET HISTORY OF THE WESTERN NORTH SEA

ELENA GRIMOLDI

A thesis submitted for the degree of Doctor of Philosophy

SEPTEMBER 2017

Supervisors: Dave Roberts, David Evans, Heather Stewart, Hans Petter Sejrup, Berit Hjelstuen & Haflidi Haflidason

Department of Geography
UNIVERSITY OF DURHAM

Abstract

The ice masses of present-day Greenland and Antarctica are characterised by marine-terminating ice streams and outlet glaciers, which deliver the majority of ice to the surrounding ocean and have a large impact on the ice sheet stability and sea-level. Understanding the break-up of palaeo-ice sheets and ice streams is thus considered crucial for understanding contemporary ice sheet behaviour and ice sheet response to global climate change.

The history of the former eastern margin of the last British and Irish Ice Sheet (BIIS) is still poorly understood, particularly in the western North Sea. The BIIS is known to have overrun the eastern coasts of England and Scotland at different times during the Pleistocene and to have extended offshore. It was drained by numerous ice streams, which experienced different phases of activity during the Last Glacial Maximum (LGM). However, despite recent improvements in the understanding of the onshore glacial history of the region, still little is known about the offshore sector. In particular, significant gaps remain in the knowledge of the deglacial history of the BIIS from the western North Sea, and of the dynamic behaviour of the North Sea Lobe (NSL) ice stream as it retreated from the offshore region.

This research incorporates different bathymetric, seismic and sedimentological datasets collected in the western North Sea, to investigate the geomorphological and sedimentary imprint left on the seafloor by the passage of the BIIS and by the NSL during the last glacial phase. The findings provide new insights on the seafloor geomorphology and on the stratigraphic architecture of the Quaternary sediments of the area, and better reconstruct the advance and retreat behaviour of the NSL in the region. The results demonstrate that the geomorphological imprint found on the seafloor of the western North Sea can be ascribable to the action of the NSL, which was flowing from NW to SE. The presence of Grounding Zone Wedges and of glaciomarine sediments characterised by cold temperature foraminifera species, known to be indicators of extreme glacial marine environments, indicates that the NSL was a marine-terminating ice lobe in the investigated area during retreat and that its decay was episodic, punctuated by phases of temporary stability. Bedrock strata, which is present at or very close to the seabed, is thought to have provided pinning points that facilitated periods of ice stillstand. In addition, new radiocarbon ages constrain ice retreat towards southern Scotland between $\sim$19 - 16 ka BP, and suggest that deglaciation of this sector of the North Sea started earlier than previously thought.

Contents

List of Figures

List of Tables

Acknowledgements

First and foremost, my sincerest gratitude goes to my supervisor Dave Roberts, who has supported me throughout my three years at Durham and was always available to discuss my thesis and my data. I have really appreciated your encouragement, ideas, and also your efforts in helping me set up new collaborations that would benefit my PhD. I am equally grateful to my second Durham supervisor, Dave Evans, who always provided great insights and suggestions throughout the project.

A special thank you also goes to my external supervisors. Hans Petter Sejrup and Berit Hjelstuen, thank you for being of great support during my visit at Bergen University and every time we met at the GLANAM meetings or conferences. You always listened to my progress with interest and provided valuable insights. Heather Stewart, thank you for giving me the chance to peek through the BGS archives and for providing me with great datasets that really helped to shape and develop this project.

My colleagues and friends, Katharina Streuff and Kasper Weilbach, it was great to share an office (and at one point even a house) with you both. I felt part of a team, and you were always available to help and provide advice and suggestions. I really enjoyed our office discussions on software, data, possible interpretations, and our many, many shared coffees. Katharina, thanks for your endless patience in listening to me talking during the many ups and especially downs. It was great to share a house with you and I really appreciate your friendship.

I am so very grateful for the fantastic GLANAM team, who I don't think could have been any better. Despite being in different countries, we always managed to keep in touch and help each other with our respective projects, and also have a great time at every single project meeting. Such a great group of people, from my fellow PhD students, to the many GLANAM collaborators. Thank you for making this project possible, and giving me the opportunity to be part of it.

I would like to express my gratitude to the People Programme (Marie Curie Actions) of the European Union's Seventh Framework Programme (FP7/2007-2013/ under REA grant agreement no°317217), that provided the funding for developing the GLANAM project and, as part of it, this research. A special thanks also goes to Durham University and the many members of staff who provided the facilities, software, and the necessary resources for this project, together with assistance whenever needed.

I would also like to thank the Britice-Chrono project (and team), for bringing me aboard the *James Cook* for the JC123 oceanographic survey and for providing great new datasets for

this project and the necessary funds for the radiocarbon dating.

To my parents, a big thank you for your endless support, throughout my University years but also each and every day. I am really grateful for everything you do and have done for me, and for your patience and guidance. You always supported every single opportunity I wanted to take, even and especially when that involved me moving abroad and travelling around all the time. Not only you manage to keep up and be present, even from far away, but I love how you enjoyed every experience I made, almost as much as me.

My partner Niko, what can I say if not thank you, for being right by my side, even when we were apart, and for being part of this crazy experience with me. Your patience and support throughout this project were vital and much appreciated. You had to listen to me rant about work, but were always reminding me what's important. I am so grateful for that Geology class in 2004.

Last but not least, my brother Daniele and my fantastic friends who, despite being far away most of the time, are always present. Giulia, Laura, Monica, Karen, your support is endless and I am really grateful you are in my life!

Declaration:

This thesis incorporates the results of original research carried out by myself. Some of the data presented in this work were obtained from the Marine Data Exchange portal of The Crown Estate, from the United Kingdom Hydrographic Office, and from the British Geological Survey. In addition, some of the data were collected in collaboration with the Britice-Chrono project. However, the majority of the work as presented here and the final interpretations of the data were carried out by myself at Durham University as part of my PhD.

Copyright permission was obtained where necessary and references to existing work were made as appropriate. Any errors or omissions are the responsibility of the author.

Elena Grimoldi
September, 2017

Chapter 1

Introduction

1.1 Project outline

This project is part of an Initial Training Network (ITN) called GLANAM (Glaciated North Atlantic Margins; www.glanam.org), funded under the EU Marie Curie Programme. The GLANAM project is a multi-partner project which comprises both academics and industrial partners, from Norway, the UK and Denmark, together with 11 Early Stage Researchers and 4 Experienced Researchers (15 "Fellows"). The main scientific goal of the GLANAM project is to determine the controls and developments in time and space of glaciated continental margins, with specific reference to the North Atlantic. The work of the 15 fellows focusses on different research areas of the North Atlantic (Fig. 1.1), with the aim of investigating and better understanding former glacial environments.

Despite the large research effort from both European industry and academia to understand the modes and evolution of ice sheet-influenced continental margins, significant gaps remain in the understanding of the evolution of the North Atlantic continental margins and especially of the role and influence of past ice sheets growth and decay. Within the GLANAM network, this work focusses on the western North Sea (Fellow 7, Fig. 1.1) and on its Pleistocene and particularly Devensian (Weichselian) glacial history.

1.2 Rationale

The investigation of past ice sheets is critical for understanding contemporary ice sheet behaviour and ice sheet response to global climate change (Stokes & Clark, 2001; Golledge & Stoker, 2006; Stokes *et al.*, 2015; Livingstone *et al.*, 2015). Recent observations of both the Antarctic and Greenland Ice Sheets have recognized an increase in the their overall retreat and mass loss in recent years, in response to climatic warming (Alley *et al.*, 2005; Dowdeswell, 2006; Alley *et al.*, 2010; Shepherd *et al.*, 2012; Stokes *et al.*, 2015). It is thus crucial to understand the mechanisms responsible for ice sheet growth and decay, in order to better understand current ice sheets evolution, the ice sheet - ocean - climate interactions over time, and their future role with respect to sea-level rise (Stokes & Clark, 2001; Alley *et al.*, 2005; Stokes *et al.*, 2015; Hughes *et al.*, 2014).

Ice sheets are regarded as dynamic and complex systems, and their evolution in time

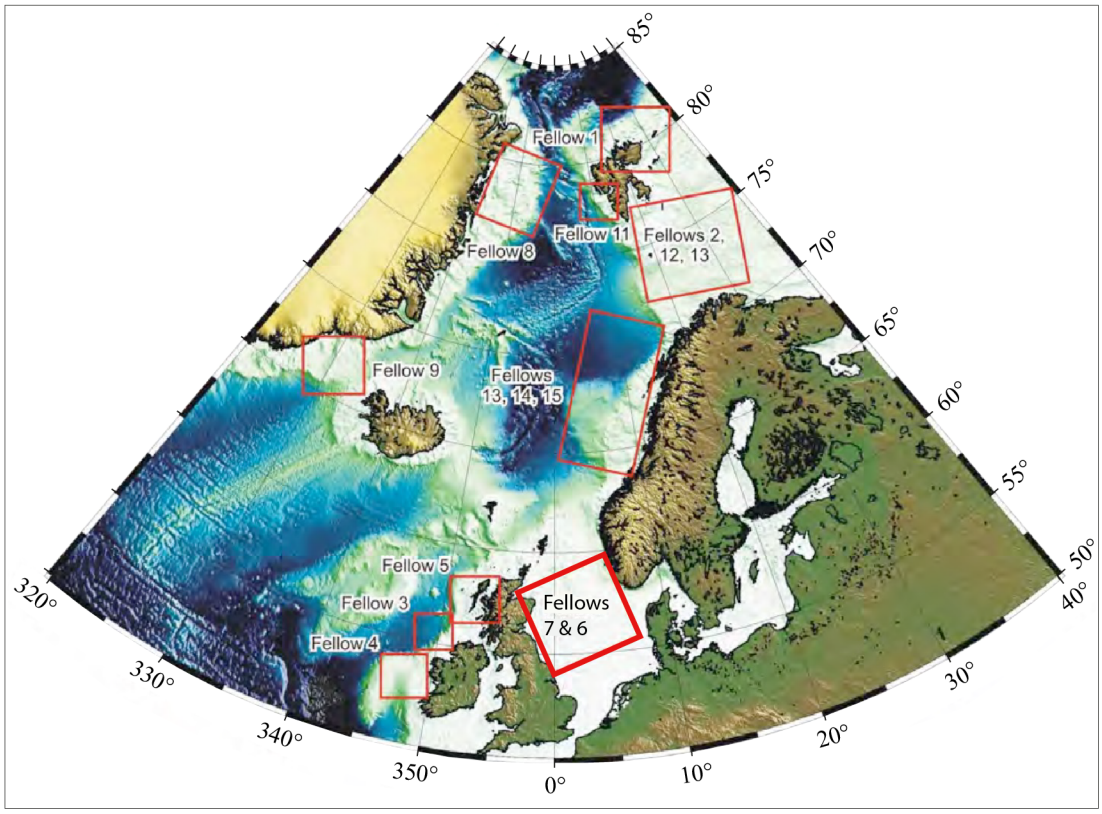

Figure 1.1: The GLANAM project main research areas (red squares). The red square labelled "Fellows 7 & 6" shows both western and eastern North Sea areas of interest.

has the potential to leave an imprint in the geologic record, which comprises distinctive geomorphic and sedimentary zones of erosion and deposition (Boulton, 1996a,b; Benn & Evans, 2010). Boulton (1996b) proposed a schematic reconstruction of the erosional and depositional imprints generated during complex patterns of ice fluctuations (Fig. 1.2), suggesting that the type of evidence observed on the bed of present-day and palaeo-ice sheets can give important information on their development, flow patterns and extent over time. The study of contemporary ice sheets is often difficult and restricted, given that their beds are, for the most part, still covered and inaccessible. Also, the observational window of present-day ice sheets is relatively short and often limited to a few decades (Stokes & Clark, 2001; Stokes *et al.*, 2015). This is why the research of palaeo-ice sheets has been increasingly important, as they are considered analogues of contemporary ice sheets, and can provide a long-term perspective on their dynamic evolution. This information is necessary to better predict and model how present-day ice masses might change and behave in the future (Stokes *et al.*, 2015; Hughes *et al.*, 2016).

Contemporary ice sheets are often characterised by marine-terminating ice streams and outlet glaciers, which are responsible for the majority of the ice drainage and delivery to the surrounding oceans (Boulton, 1990; Stokes & Clark, 2001; Dowdeswell *et al.*, 2004; Dowdeswell, 2006; Ó Cofaigh *et al.*, 2013). Ice streams are fast-flowing ice arteries that move at a faster rate in respect to the surrounding slow-moving ice, and, when marine-terminating, they are sensitive to sea-level changes and changes in ocean temperature; they can rapidly

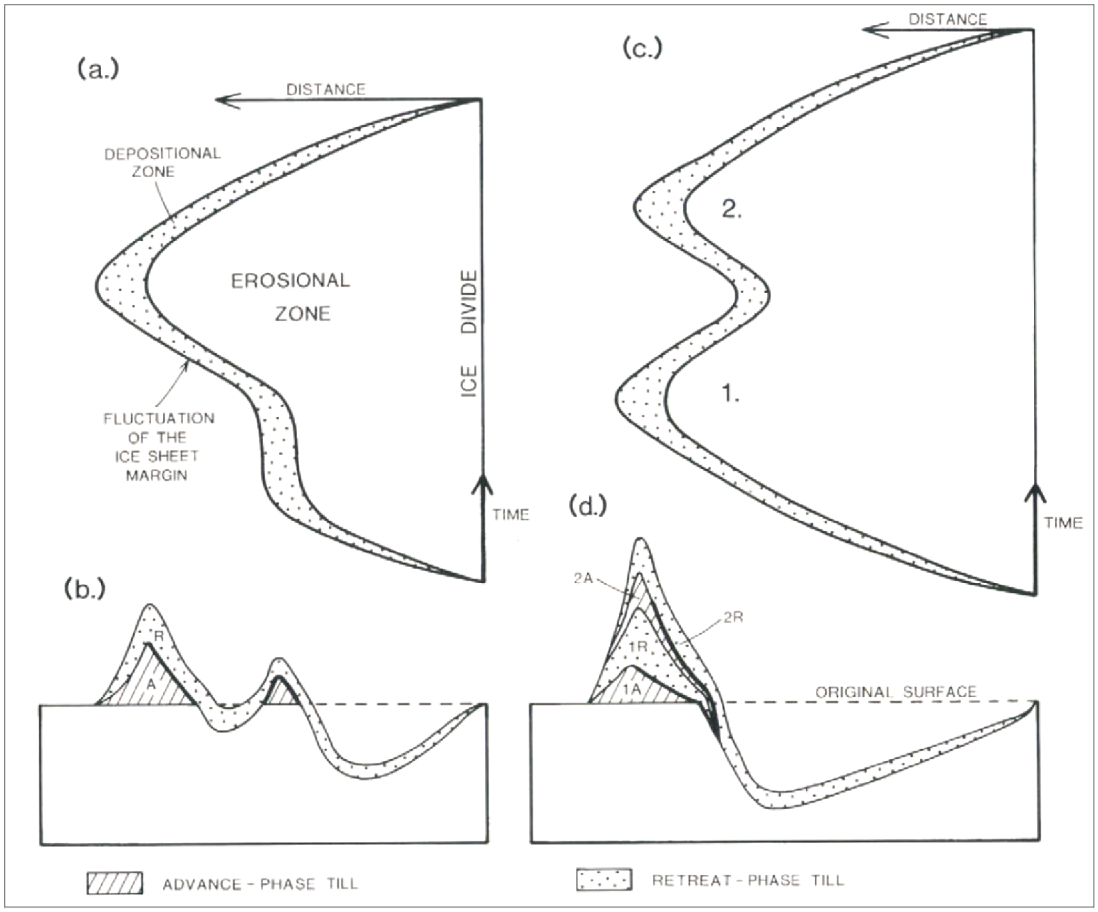

Figure 1.2: A schematic diagram showing till sequences generated by more complex patterns of ice sheet fluctuation, from Boulton (1996b). a-b: an ice sheet with prolonged period of standstill during advance. A substantial thickness of till is deposited in the terminal zone during the standstill, which is not entirely removed by erosion during the ice sheet's subsequent advance to its maximum. c-d: stacked till units with intervening erosion surfaces (potentially marked by boulder pavements) produced by re-advance (2) after initial retreat of its maximum (1).

contribute to ice sheet instability and mass loss (Alley *et al.*, 2005; Stokes *et al.*, 2015; Stroeven *et al.*, 2016; Peters *et al.*, 2016). Their large flux and activity thus have a great effect on the dynamic behaviour of ice sheets (Stokes & Clark, 2001; Clark *et al.*, 2012; Livingstone *et al.*, 2012a; Stokes *et al.*, 2015). Ice streams are known to leave behind a series of diagnostic geomorphic signature at their beds. The recognition of these geomorphological imprints has not only permitted the identification of palaeo-ice stream locations, but also allowed for the reconstruction of palaeo-ice streams flow patterns and extent, and for the collection of important information on the processes that occurred at the ice-bed interface and on their evolution throughout their glacial history (Stokes & Clark, 2001; Livingstone *et al.*, 2012a; Stokes *et al.*, 2015).

The North Atlantic was characterised by the presence of numerous ice sheets in the past. The Eurasian ice sheet complex (EISC) was the third largest ice mass after the North American and Antarctic ice sheets during the Last Glacial Maximum (LGM), and was formed by the coalescence of the British and Irish Ice Sheet, the Scandinavian Ice Sheet and the Barents Sea

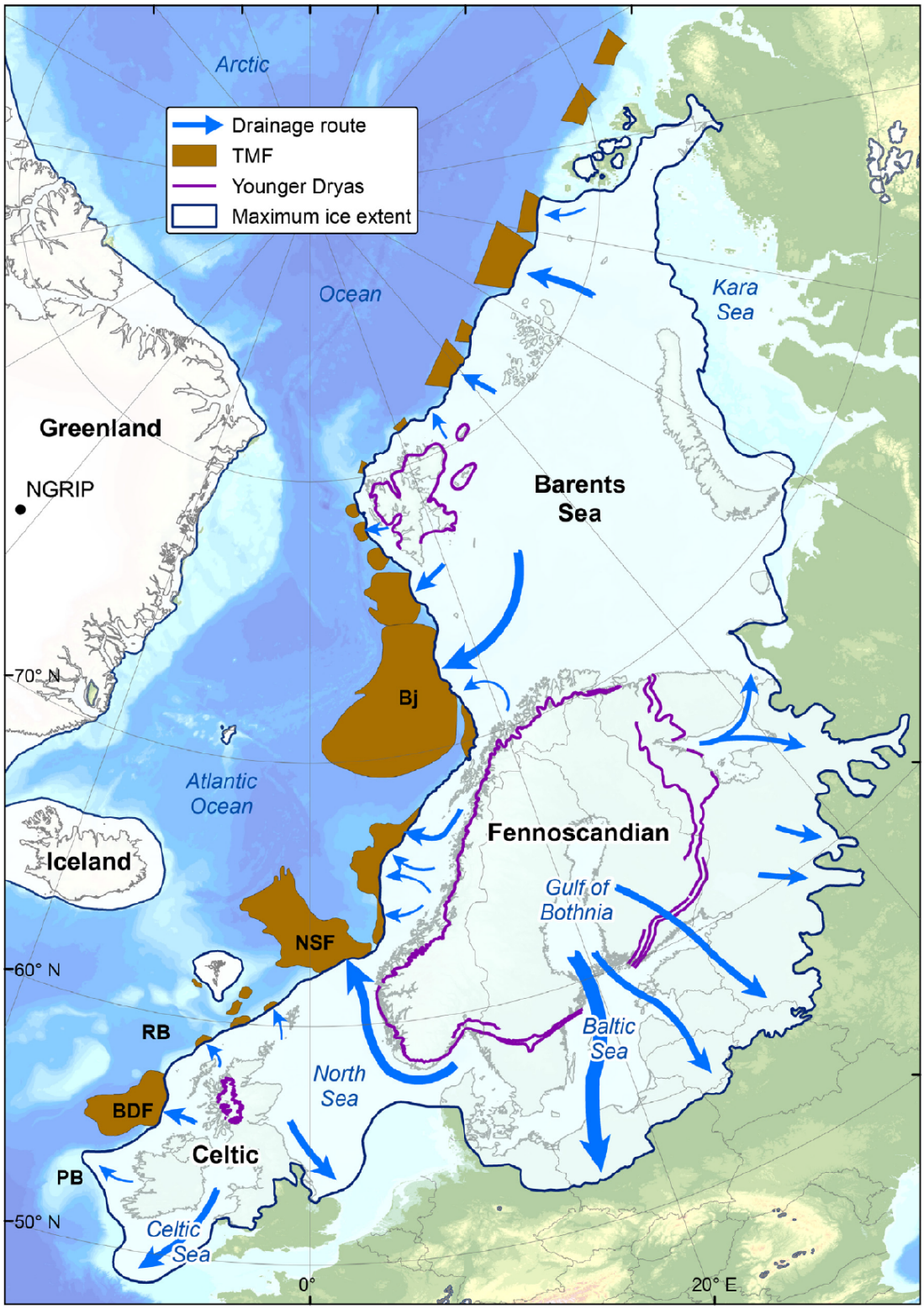

Figure 1.3: Major drainage routes of the Eurasian ice sheet complex during the Last Glacial Maximum, from Patton *et al.* (2017). Locations of major trough mouth fans (brown). PB: Porcupine Bank; BDF: Barra and Donegal Fans; RB: Rosemary Bank; NSF: North Sea Fan; Bj: Bjørnøyrenna Fan.

and Svalbard Ice Sheets (Fig. 1.3; Clark *et al.*, 2012; Hughes *et al.*, 2016; Patton *et al.*, 2016, 2017). This complex was characterised by marine-terminating, marine-based and terrestrial-

based ice sheets and was drained by numerous fast-slowing ice streams, which deposited large volumes of sediments at the continental shelf (Hughes *et al.*, 2016; Patton *et al.*, 2016, 2017). The study of the different independent ice sheets that formed the EISC has received increasing attention, considering their geological record holds important information on their evolution and final demise (Hubbard *et al.*, 2009; Clark *et al.*, 2012; Hughes *et al.*, 2016; Patton *et al.*, 2016, 2017). In particular, numerous studies have focussed on the reconstruction of the British and Irish Ice Sheet (BIIS), which was characterised by marine and terrestrial margins and was also drained by numerous ice streams which extended in the offshore regions and which influenced its dynamic behaviour during both advance and retreat phases (Evans *et al.*, 2005; Boulton & Hagdorn, 2006; Catt, 2007; Hubbard *et al.*, 2009; Davies *et al.*, 2011, 2012b; Clark *et al.*, 2012; Livingstone *et al.*, 2012b, 2015). A well constrained empirical reconstruction of its growth, and timing and rate of deglaciation is critical for the current modelling efforts to help better predict the controls on present-day ice sheets retreat in Greenland and Antarctica (Clark *et al.*, 2012).

1.3 The GLANAM project - western North Sea: research aims and objectives

It is known that ice sheets have advanced into the North Sea at various times during the Pleistocene, contributing to its spatially variable patterns of erosion and infilling (Gatliff *et al.*, 1994; Sejrup *et al.*, 2000; Lonergan *et al.*, 2006; Graham *et al.*, 2011; Stewart & Lonergan, 2011). The British and Irish Ice Sheet (BIIS) and the Scandinavian Ice Sheet (SIS) were at some point confluent during the Pleistocene, covering the central part of the North Sea before retreating towards the British and Scandinavian mainlands, respectively, during deglaciation (Sejrup *et al.*, 1994, 2009; Graham *et al.*, 2011; Davies *et al.*, 2012b; Stewart *et al.*, 2013), and up to $\sim$800 m of Quaternary sequences were accumulated in the deepest part of the basin (Gatliff *et al.*, 1994; Sejrup *et al.*, 2000; Lonergan *et al.*, 2006; Graham *et al.*, 2011; Stewart & Lonergan, 2011). Numerous studies have tried to reconstruct the BIIS/SIS extent and interaction during the Pleistocene, their extensional limits offshore and the mechanisms and timings of their retreat, but significant gaps still remain in our knowledge of the North Sea Pleistocene stratigraphic architecture. Furthermore, during the Late Devensian, the central sector of the BIIS was characterized by multi-sourced and competing ice dispersal centres in the Southern Uplands, Pennines, Lake District and Cheviots and was drained by fast-flowing ice streams in the Celtic and Irish Sea, in the north-western and north-eastern margins of Scotland and onshore and offshore the eastern coast of the UK (Boulton & Hagdorn, 2006; Roberts *et al.*, 2007; Bradwell *et al.*, 2008b; Hubbard *et al.*, 2009; Davies *et al.*, 2009a, 2012a; Livingstone *et al.*, 2010, 2012b, 2015; Yorke *et al.*, 2012; Bateman *et al.*, 2015). The North Sea is thus considered as a key location for the study of Pleistocene glacial/interglacial conditions and holds evidence of both complex changes in ice sheet dynamics as well as changing pattern of glacigenic sediment transport (Graham *et al.*, 2011).

Different studies, focussed on onshore eastern England, have provided information on

the BIIS evolution and particularly on the dynamic behaviour of the BIIS ice streams as they moved into the North Sea during the Last Glacial Maximum (LGM; Eyles *et al.*, 1994; Catt, 2007; Evans & Thomson, 2010; Boston *et al.*, 2010; Roberts *et al.*, 2013; Livingstone *et al.*, 2015; Bateman *et al.*, 2015), but the linkage between onshore glacial sediments and offshore facies is still poorly understood.

This research aims to reconstruct the glacial evolution of the western North Sea. Specifically, it will focus on the following objectives:

1. To provide an assessment of the near-shore and offshore shallow seismic facies off the coasts of eastern England using new 2D seismic datasets, together with additional seismic datasets from the British Geological Survey (BGS) archives
2. To establish the Devensian glacial geomorphology of the western North Sea using new bathymetry datasets
3. To reconstruct the deglacial history of the North Sea Lobe off Durham and Northumberland coasts using new sediment cores
4. To link these findings to the wider Pleistocene glacial history of the western North Sea

The project focusses on new bathymetry, 2D seismic profiles and sediment cores acquired from offshore eastern England and southern Scotland during several oceanographic surveys and combines this information with previous onshore and offshore literature. In particular, we concentrate on the Blyth survey and the Britice-Chrono survey (research areas 1 and 2, Fig. 1.4), and analyse the new datasets together with pre-existing data collected in the region in order to fully characterise the geomorphological and sedimentary imprint left on the seafloor by the passage of the last BIIS.

1.3.1 Thesis structure

In addition to this first introductory chapter, this thesis is divided into 4 chapters (chapters 2 - 5). Chapter 2 provides information on the geological background of the study area, while the results of this work are presented in chapters 3 - 4 and discussed in chapter 5.

Chapter 2: Geological background
Chapter 2 provides a review of the geological setting that characterises the North Sea. It presents key information on the formation of the basin and on the pre-Quaternary and Quaternary glacial history of the area and sets the scene for the following chapters. This chapter also summarises the current knowledge of the evolution of the former eastern margin of the last BIIS, of its growth and decay, and focusses particularly on the sedimentary imprint left by this ice sheet onshore and offshore, and on the chronology of its retreat.

Chapter 3: Seismic stratigraphy of the Blyth survey area

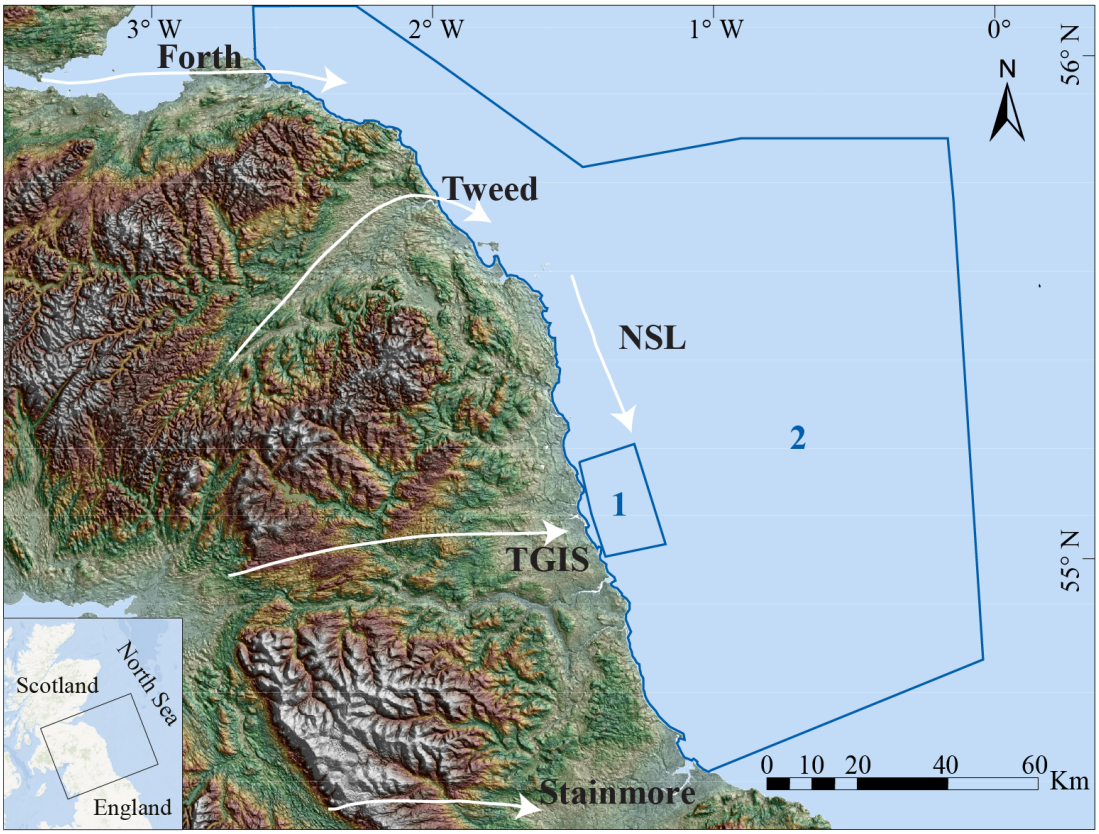

Figure 1.4: NEXTMap image of northern England and Southern Scotland (location shown in the insert map). The extension of research areas 1 (Blyth survey) and 2 (Britice-Chrono survey) in the western North Sea are shown with blue polygons. The locations and flow directions of the Forth, Tweed, Tyne Gap Ice Stream (TGIS), Stainmore and North Sea Lobe (NSL) palaeo-ice streams are shown with white arrows.

Chapter 3 is focussed on the geophysical datasets collected in the Blyth survey area (Fig. 1.4). The Blyth survey is located in an area that was covered by the BIIS and particularly by the passage of the Tyne Gap Ice Stream (TGIS) and North Sea Lobe (NSL) ice stream. It has thus the potential to provide important information on both the geomorphological and sedimentary imprint of the last BIIS and of older Pleistocene glaciations that affected the area. In this chapter the analyses of both multibeam bathymetry and 2D seismic data provide an assessment of the pre-Quaternary and Quaternary seismic architecture of this sector of the western North Sea. The results are also analysed in close correlation to the glacial stratigraphy immediately onshore. The information presented in this chapter complements and develops the existing knowledge of the Quaternary glacial stratigraphy of the area.

Chapter 4: The geomorphological imprint and sedimentary signature of the North Sea Lobe, and chronology of the last BIIS retreat in the western North Sea

Chapter 4 combines new geophysical and sedimentological datasets collected in the Britice-Chrono survey area (Fig. 1.4) with the available bathymetry provided by the United Kingdom Hydrographic Office and with seismic datasets collected in the past by the BGS. It provides the first real assessment of the geomorphological and sedimentary imprint left on the seafloor by the last BIIS, and particularly by the NSL during both advance and retreat. Bathymetry and

seismic datasets are analysed in this chapter to provide an assessment of the different landforms observed and to produce a new geomorphological map of the seafloor. In addition, the seismic architecture of the region is reconstructed and the pattern of ice advance and retreat offshore established. The sediment cores are analysed from a lithological and micropalaeontological point of view and are correlated to the seismic stratigraphy and geomorphology. The findings are reviewed together with the existing knowledge of the glacial history of this area and are discussed in a wider contextual framework. This chapter presents new information on the nature of the Quaternary glacial sediments that characterise the area and on the glacial environments associated with the NSL, and proposes a new theory for the evolution of the NSL and for the style of its final retreat. In addition, two new radiocarbon ages are presented from this sector of the western North Sea, and a preliminary chronology for the retreat of the NSL offshore is proposed.

Chapter 5: Discussion

Chapter 5 reviews and discusses the new information presented in the previous chapters and proposes a reconstruction of the last phases of the NSL. In particular, this chapter combines the evidence for the advance and retreat phases of the NSL identified in the western North Sea and considers them within the wider reconstructions of the collapse of the BIIS and SIS ice sheets. The new chronology proposed in Chapter 4 is added to the previously published chronology of ice retreat from the North Sea basin and from onshore eastern England and south-eastern Scotland. Finally, the drivers for deglaciation of this sector of the western North Sea are discussed and a new model which reconstructs the final phases of activity of the NSL is proposed. The new datasets proposed in this thesis provide new insights on the last phases of the NSL offshore and help to better understand its final demise.

Chapter 2

Geological background

The North Sea is a shallow epicontinental sea located between the east coasts of England and Scotland to the west, and Norway and Denmark to the east. It is bordered by the Shetland Islands in the north and by Germany, The Netherlands, Belgium and France in the south, and it is connected to the Norwegian Sea and Baltic Sea and, via the English Channel, to the Atlantic Ocean. Its present-day structural configuration is the result of a very long and complex geological history which resulted in the formation of the N - S trending Central Graben, initiated during mid-Jurassic rifting (Stewart *et al.*, 2013). Research into the stratigraphy of Upper Paleozoic, Mesozoic and Cenozoic formations found on eastern England and Scotland has provided a basis for the study of offshore deposits. Interests in hydrocarbon exploration, windfarm developments and the acquisition and investigation, by the British Geological Survey (BGS), of seismic profiles, shallow boreholes and sediment cores collected in the North Sea, has resulted in the compilation of pre-Quaternary and Quaternary geological maps for the entire basin (Cameron *et al.*, 1992; Glennie, 1998; Graham *et al.*, 2011; Stoker *et al.*, 2011; Cotterill *et al.*, 2017).

In this chapter, the pre-Quaternary and Quaternary sediments are described according to the BGS Offshore Regional Reports and their location is assigned to different sectors of the North Sea, according to the subdivision utilised by the BGS. Figure 2.1 shows the location and extension of the southern, central and northern North Sea, and of the Moray Firth sectors (Cameron *et al.*, 1992; Gatliff *et al.*, 1994). For simplicity, the Moray Firth and northern North Sea sectors are here considered together and generally referred to as the northern North Sea. The extension of the western North Sea as per the study area of this thesis is shown in red and extends from the coast to the red dashed line (Fig. 2.1).

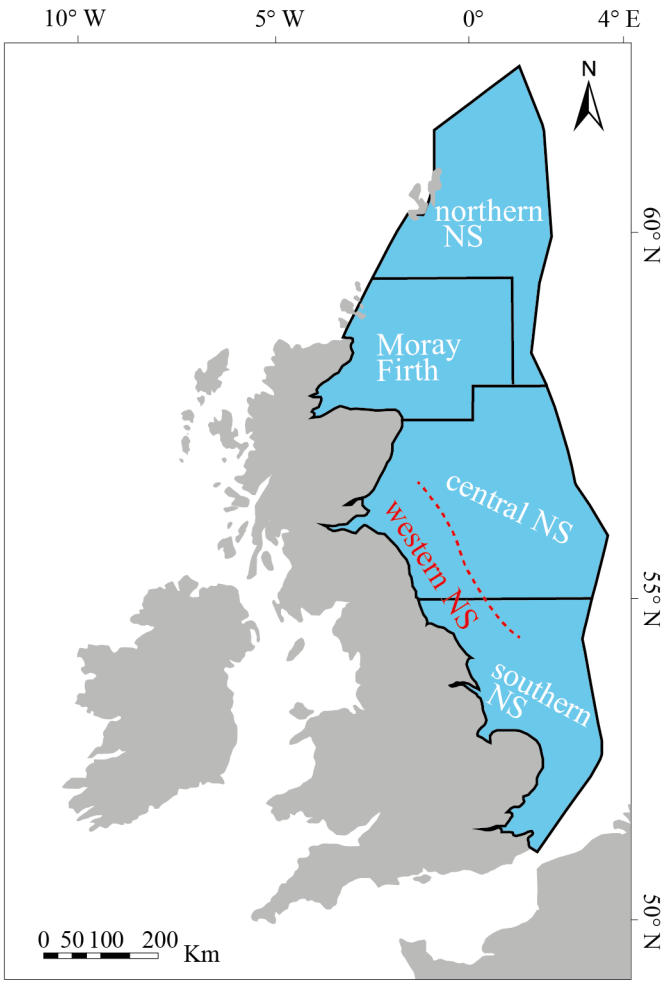

Figure 2.1: Extension of the southern, central, and northern North Sea and of the Moray Firth sectors, as outlined in the BGS Offshore Regional Reports (Cameron *et al.*, 1992; Gatliff *et al.*, 1994). NS: North Sea. The extension of the western North Sea which refers to the study area of this thesis is shown in red and extends from the coast to the dashed line. Modified from Cameron *et al.* (1992) and Gatliff *et al.* (1994).

2.1 Pre-Quaternary

2.1.1 Pre-Carboniferous

One of the major events that influenced the structure and geology of the North Sea basin is the Caledonian orogeny, which marked the collision between the Baltica, Laurentia and Avalonia plates, and the closure of the Iapetus Ocean during early Ordovician to mid-Devonian times (Gatliff *et al.*, 1994; Mona Lisa Working Group, 1997; Artemieva & Thybo, 2013). Lower Paleozoic sediments constitute the basement rocks of the central and southern North Sea and were extensively deformed during the Caledonian collision (Cameron *et al.*, 1992; Gatliff *et al.*, 1994; Glennie, 1998).

Following the Caledonian orogeny, most of the southern North Sea remained an upland area. The Devonian period was predominantly a time of continental, terrestrial and lacustrine

sedimentation which concentrated in numerous widespread depocentres, and was also characterised by the deposition of the Old Red Sandstone (Cameron *et al.*, 1992; Gatliff *et al.*, 1994; Glennie, 1998).

2.1.2 Carboniferous to Neogene

Post-Caledonian rifting and regional thermal subsidence allowed for the sea to transgress from the south to the north, and for a major change in facies sedimentation, from the predominant Old Red Sandstone to the establishment of fluvio-deltaic and shallow-marine environments (Cameron *et al.*, 1992; Gatliff *et al.*, 1994). During the Late Carboniferous, the sedimentation in the North Sea was increasingly affected by the Variscan orogeny, which led to a change of the tectonics in the basin, from crustal extension and subsidence to regional compression and strike-slip. Uplift in the southern North Sea region led to the erosion of up to 1500 m of Upper Carboniferous sediments (Cameron *et al.*, 1992; Gatliff *et al.*, 1994; Mona Lisa Working Group, 1997; Glennie, 1998; Artemieva & Thybo, 2013).

Following the Variscan orogeny, intraplate extension led to the formation of numerous Permo-Triassic basins and the southern North Sea began to subside, allowing the accumulation of thick Permian and Triassic sequences (Cameron *et al.*, 1992; Glennie, 1998). In the southern and central North Sea, fluvial and aeolian sediments were deposited during the Early Permian in an arid or semi-arid tropical desert environment, while during the Late Permian, various transgressions into the basin resulted in the deposition of shales, carbonates and evaporites into the Zechstein Sea. Post-Permian halokinesis led to the deformation of the Zechstein evaporites, and resulted in the formation of salt diapirs and zones of salt withdrawal. This led to a variation in the overall thickness of the Upper Permian sequence, which varies from 50 m up to 2500 m throughout the basin (Cameron *et al.*, 1992; Gatliff *et al.*, 1994; Glennie, 1998).

The beginning of the Triassic period was initially characterised by the deposition of sandstones and mudstones, while fully marine conditions were established in the southern North Sea during the Late Triassic (Cameron *et al.*, 1992; Gatliff *et al.*, 1994). The Middle Jurassic was characterised by a phase of domal uplift and erosion and subsequently, during the Upper Jurassic, the onset of a major phase of extensional activity, rifting and subsidence contributed to the present architectural configuration of the North Sea (Cameron *et al.*, 1992; Gatliff *et al.*, 1994; Glennie, 1998; Graham *et al.*, 2011). After the Late Jurassic - Early Cretaceous extensional phase, regional thermal cooling and subsidence allowed for the accumulation of thick Cretaceous chalk beds and of up to 3000 m of Cenozoic sequences in the North Sea (Gatliff *et al.*, 1994; Stewart *et al.*, 2012). Paleogene and Neogene sequences were mainly accumulated in the central part of the basin and are not found up until $\sim$100 km off the coasts of the UK (Fig. 2.2; Cameron *et al.*, 1992; Gatliff *et al.*, 1994). They were deposited in deltaic, shallow marine and deep marine environments (Cameron *et al.*, 1992; Gatliff *et al.*, 1994; Glennie, 1998). Subsidence and marine conditions continued at the beginning of the Pleistocene until changes in the cyclicity of orbital forcing, which led to insolation minima, caused different ice sheet transgressions in the North Sea, with glacial and glaciomarine sediments being deposited across the basin.

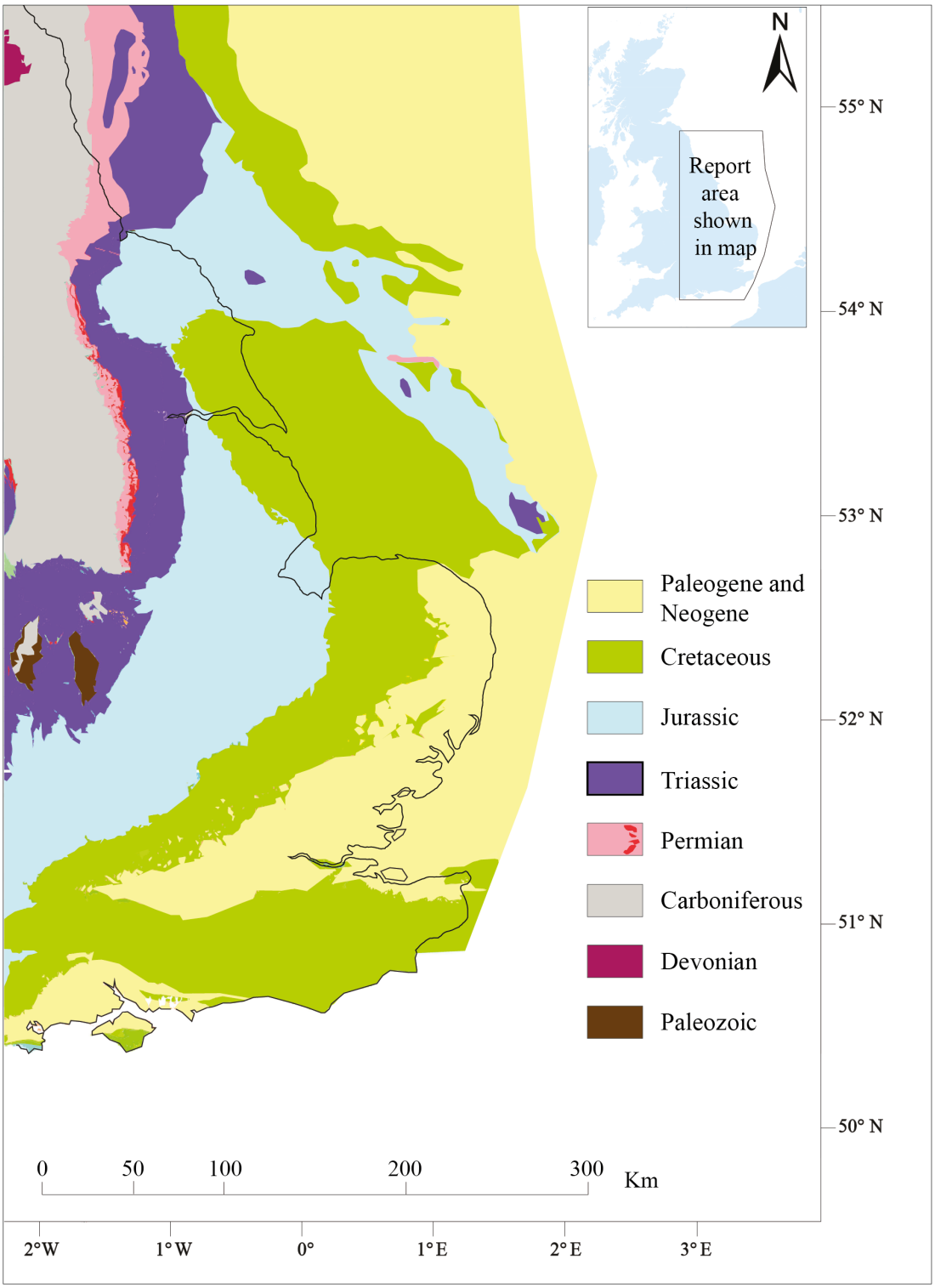

Figure 2.2: Pre-Quaternary bedrock outcrops in eastern England and western North Sea. Based on Cameron *et al.* (1992) and Gatliff *et al.* (1994) and on the British Geological Survey geological map of Britain. With permission of the British Geological Survey.

2.2 Quaternary glaciations in the North Sea

2.2.1 Early - Mid Quaternary

Early Pleistocene sedimentation was characterised by a deltaic sequence deposited in a prodelta/shallow marine setting extending from continental Europe. This sequence has been recognized and subdivided into several different formations in the southern North Sea, and progrades towards the central North Sea, where it passes into the Aberdeen Ground Formation (Fig. 2.3; Graham *et al.*, 2011). The Aberdeen Ground Formation is mainly composed of marine clays and fine sands and records the presence, towards its base, of the Bruhnes-Matuyama boundary (dated at 780 ka BP, Fig. 2.3; Stoker *et al.*, 1983; Graham *et al.*, 2011). The sequence is also incised by an extensive network of tunnel valleys that can be constrained as being younger than Early Pleistocene in age (Stoker & Bent, 1985; Cameron *et al.*, 1992; Gatliff *et al.*, 1994; Lonergan *et al.*, 2006; Graham *et al.*, 2011; Stewart *et al.*, 2013). Although the Early Pleistocene is generally thought to be an ice-free period, evidence for the earliest known glaciation of the North Sea basin comes from the Norwegian Channel, where the oldest identified and dated glacial deposit, the Fedje Till, is found (Fig. 2.3). It was assigned an age close to 1.1 Ma (Marine Isotope Stages [MIS] 34–36) based on micropalaeontology, Sr-isotopes, palaeomagnetism and amino acid geochronology (Sejrup *et al.*, 2000; Ehlers & Gibbard, 2008; Graham *et al.*, 2011). Iceberg scoured surfaces have also been observed within the Aberdeen Ground Formation at different levels, implying the occurrence of glacial conditions earlier than the Mid-Pleistocene (Stoker *et al.*, 2011).

Three major glaciations have been recognized from the Mid Pleistocene (0.5 Ma) onwards in the North Sea: the Anglian (Elsterian, MIS 12), Wolstonian (Saalian, MIS 10 – 6) and Devensian (Weichselian, MIS 5d – 2; Lonergan *et al.*, 2006; Ehlers & Gibbard, 2007, 2008; Gibbard & Cohen, 2008; Toucanne *et al.*, 2009; Stewart & Lonergan, 2011; Graham *et al.*, 2011; Stoker *et al.*, 2011; Cotterill *et al.*, 2017). These glaciations have been inferred as the major glacial events that characterised the Quaternary in the North Sea, although different studies have shown that additional glacial episodes probably occurred in the region and are preserved in the sedimentary sequence (Gatliff *et al.*, 1994; Graham *et al.*, 2011; Stewart & Lonergan, 2011).

The Anglian (MIS 12)

The Anglian glaciation was probably the most extensive Pleistocene glaciation in the North Sea. Full glacial conditions led to the erosion of a major system of NNW - SSE orientated tunnel valleys in the central and southern part of the basin (Davies *et al.*, 2011; Graham *et al.*, 2011; Stewart *et al.*, 2013), which were then infilled with the Swarte Bank Formation (Fig. 2.4). The Swarte Bank facies is a subglacial till, the first and only offshore trace of ice advance in the North Sea during this time (Cameron *et al.*, 1992; Gatliff *et al.*, 1994; Davies *et al.*, 2011, 2012a). In the onshore record, the Swarte Bank Formation is correlated with the Anglian Till in East Anglia, based on their similar lithological properties (Davies *et al.*, 2011). Ice is thought to have overridden the contemporary valley of the River Thames, advanced into its

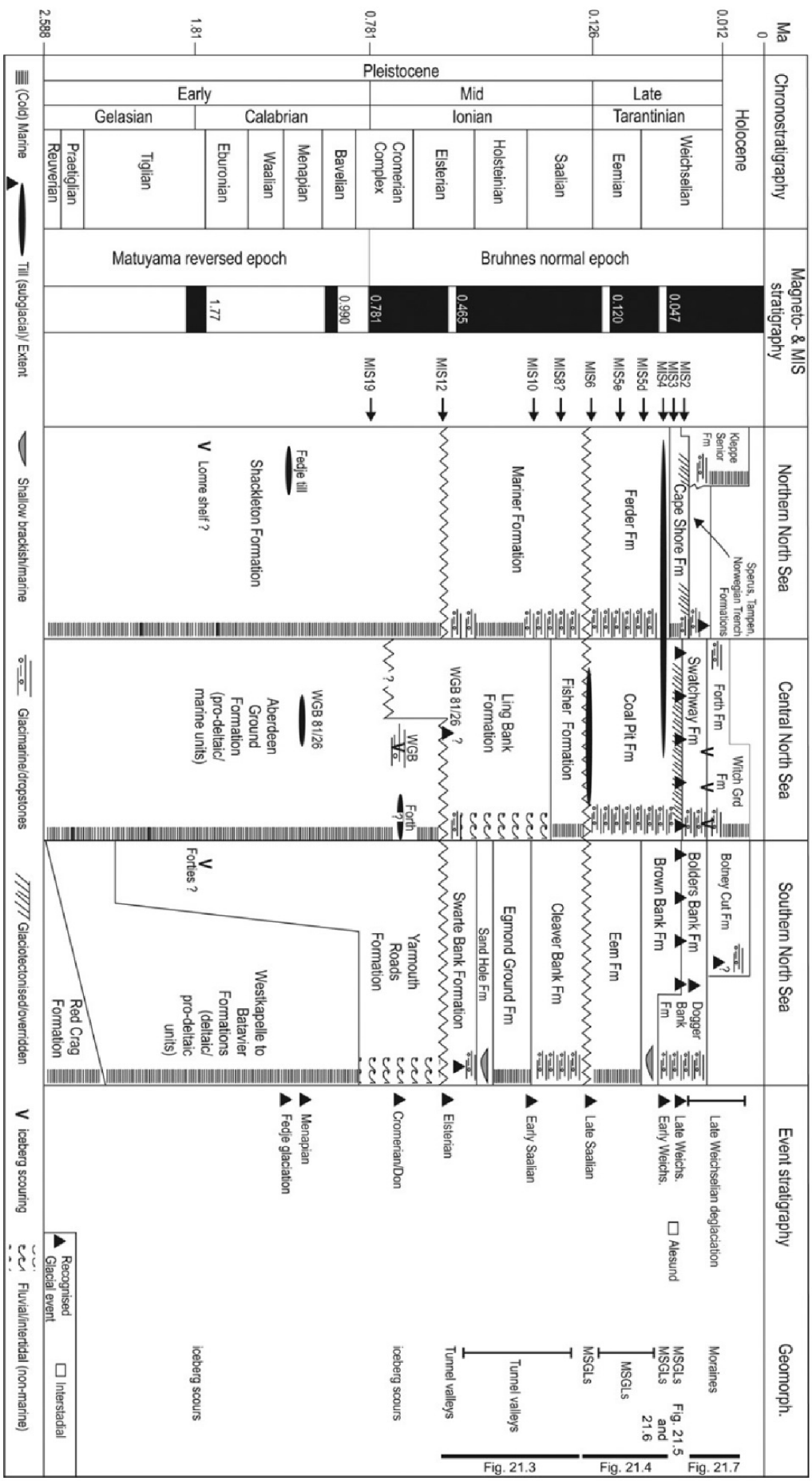

Figure 2.3: Quaternary framework of the North Sea basin. From Graham *et al.* (2011).

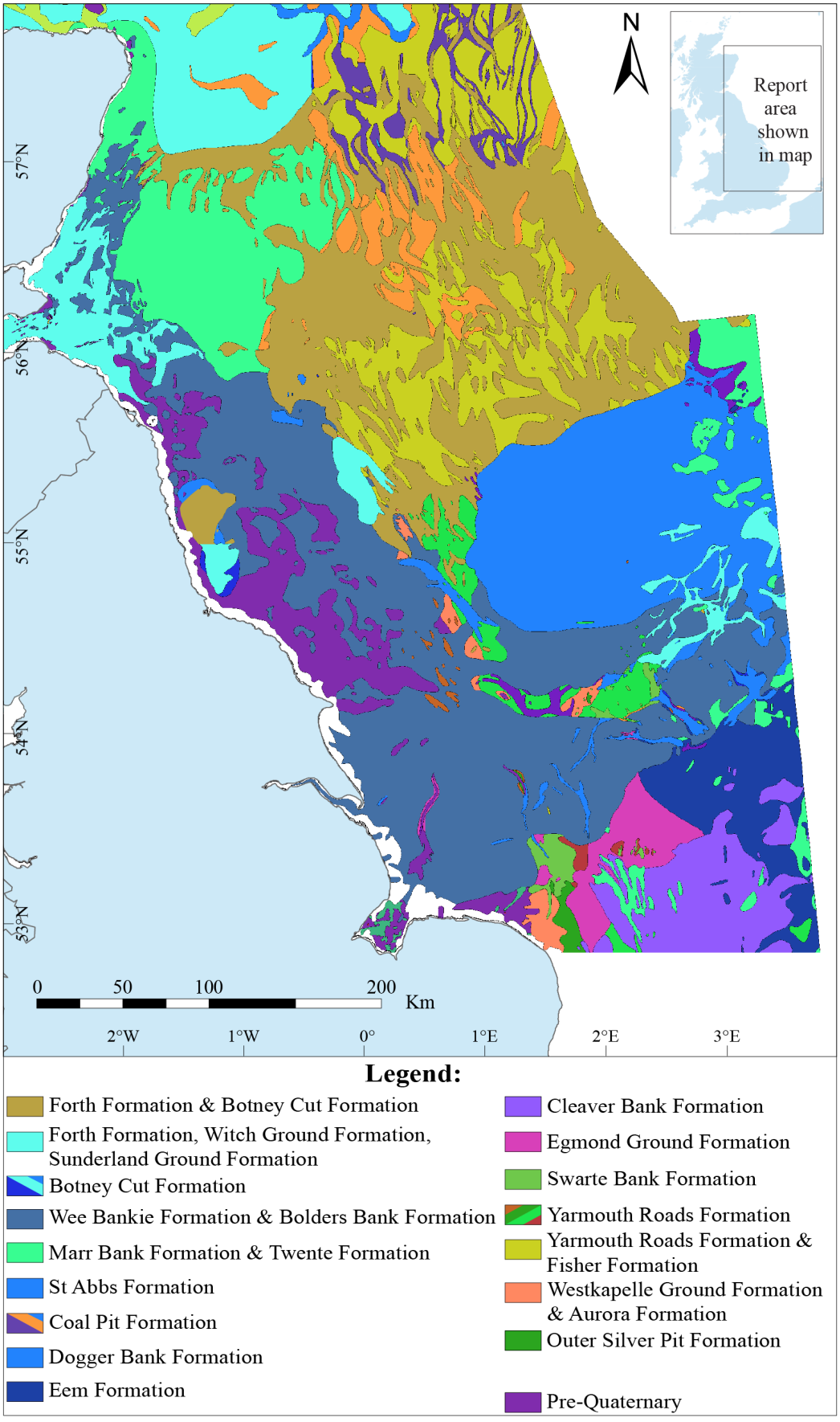

Figure 2.4: Quaternary sediments of the western North Sea compiled from the British Geological Survey Quaternary sheets and based on Gatliff *et al.* (1994) and Cameron *et al.* (1992). With the permission of the British Geological Survey.

southern tributary valleys and terminated in a large ice-dammed lake in the southern North Sea basin (Ehlers & Gibbard, 2008). The onshore evidence and the overall distribution of tunnel valleys suggest that the ice sheet covered the North Sea basin at its maximum extent during the Anglian (Lonergan *et al.*, 2006; Graham *et al.*, 2011; Stewart *et al.*, 2013).

After the decay of the Anglian ice sheet, the Sand Hole Formation and the Egmond Ground Formation (MIS 11; Cameron *et al.*, 1992; Stoker *et al.*, 2011), were deposited during the Hoxnian (Holsteinian) in a marine environment (Fig. 2.4). The latter is found on top of the Swarte Bank Formation (Fig. 2.3 and 2.4) and truncates its upper reflector on seismic profiles (Cameron *et al.*, 1992; Gatliff *et al.*, 1994).

The Wolstonian (MIS 10 – 6)

The Wolstonian cold stage has been correlated to MIS 10 – 6 (Gibbard & Cohen, 2008; Toucanne *et al.*, 2009; Graham *et al.*, 2011; Stoker *et al.*, 2011). Ehlers (1990) has suggested two possible different phases of Wolstonian glaciation in the North Sea. Evidence for the earliest of these phases (MIS 8; Graham *et al.*, 2011) demonstrates that major parts of the present North Sea basin must have been covered with ice at the time in order to explain an ice advance from NNW into The Netherlands and north-west Germany. Beets *et al.* (2005) also described the presence of till of MIS 8 age in the southern North Sea (Dutch Survey borehole 89/2) which was subsequently overlain by shallow marine sands of MIS 7 age (Graham *et al.*, 2011). This MIS 8 widespread glacial phase is also supported by new evidence from onshore south-eastern England (White *et al.*, 2010; Bridgland *et al.*, 2015).

Evidence for a later Wolstonian glacial event (MIS 6; Graham *et al.*, 2011) comes from a single glacial erosion surface that can be traced through large parts of the North Sea. This feature is overlain by glacigenic sediments, including till and glaciomarine deposits within the Fisher and the Coal Pit formations in the central North Sea and the Ferder Formation in the northern region of the basin (Fig. 2.3 and 2.4; Cameron *et al.*, 1992; Gatliff *et al.*, 1994; Davies *et al.*, 2011; Graham *et al.*, 2011). Furthermore, in addition to the Anglian tunnel valleys observed in the central North Sea, tunnel valleys of supposed Wolstonian age are also relatively common across the basin (Huuse & Lykke-Anderson, 2000; Graham *et al.*, 2011). Stewart & Lonergan (2011) recognized 7 generations of tunnel valleys in the central North Sea that span from MIS 12 to MIS 2 in age, and correlated some of them to MIS 10, 8 and 6. Several cold phases have probably contributed to their formation and it is believed that the complex cross-cutting tunnel valleys document a complicated pattern of reoccupation and overprinting during extensive Mid to Late Pleistocene glaciations (Graham *et al.*, 2011; Stewart *et al.*, 2012, 2013).

2.2.2 Early Devensian and the Last Glacial Maximum (MIS 4 – 2)

After the re-establishment of marine conditions during the Ipswichian (Eemian) Stage, reversion to glacial conditions and a sea-level fall characterised the Devensian Stage (Cameron *et al.*, 1992; Gatliff *et al.*, 1994). There appears to be good evidence for at least two different phases of ice-sheet growth in the North Sea during the Devensian Cold Stage (MIS 5d – 2): the Early Devensian (MIS 4) and the Late Devensian (Last Glacial Maximum, MIS 3/2; Graham

et al., 2011). Evidence for glaciation during the Early Devensian comes from the upper part of the Ferder Formation in the northern North Sea, which overlies Ipswichian deposits and consists of fine-grained matrix-supported diamictons. It extends from the Norwegian Channel to the continental shelf west of the Shetland Isles and is thought to be evidence for extensive glaciation across the northern North Sea with confluence of British and Scandinavian ice sheets (Fig. 2.4; Carr *et al.*, 2006; Graham *et al.*, 2011).

During the Late Devensian, the Bolders Bank and Dogger Bank formations were deposited in the southern North Sea (Fig. 2.4; Cameron *et al.*, 1992; Carr *et al.*, 2006; Graham *et al.*, 2011). These two facies were described as composed of a reddish-brown stiff diamicton and of a clay-rich diamicton respectively, and they were reported by Cameron *et al.* (1992) to be laterally equivalent. Both formations are believed to have deposited by the action of the North Sea Lobe (NSL; Cameron *et al.*, 1992; Carr *et al.*, 2006; Davies *et al.*, 2009a, 2011, 2012a; Livingstone *et al.*, 2012b). The southern limit of the NSL extension (and thus of the BIIS) in the North Sea is still largely debated, although it is often correlated to the southern limit of the Bolders Bank Formation (Dove *et al.*, 2017; Roberts *et al.*, In prep.). In the central North Sea, additional Late Devensian formations, such as the Wee Bankie, Marr Bank and Swatchaway formations, have been recognized and mapped (Fig. 2.3 and 2.4; Gatliff *et al.*, 1994; Carr *et al.*, 2006). The Marr Bank Formation has been mapped extensively offshore eastern Scotland and consists of glacigenic sediments (Gatliff *et al.*, 1994). The formation becomes acoustically indistinguishable from the upper part of the Coal Pit sequence to the east and seems to continue into the Wee Bankie Formation to the west and south (Fig. 2.4; Cameron *et al.*, 1992; Gatliff *et al.*, 1994). The Wee Bankie Formation has been mapped offshore Scotland and England and it is mainly composed of a stiff diamicton. Its south-eastwards extension is represented by the Bolders Bank Formation and the facies has also been related to the action of the NSL (Fig. 2.4; Cameron *et al.*, 1992; Gatliff *et al.*, 1994; Evans *et al.*, 2005).

Investigations of core samples from offshore areas and the continuous improvements in acoustic technology have led to a more precise reconstruction of the ice sheet limits in the North Sea basin during the Last Glacial Maximum (Carr *et al.*, 2006; Sejrup *et al.*, 2009, 2016). Radiocarbon data from the central part of the North Sea suggest that the area was ice free during the Sandnes/Ålesund Interstadial, between ~38 and 29 ka (Sejrup *et al.*, 1994, 2000). Evidence from marine sediments in the Fladen/Witch Ground Basin areas suggests that this period was followed by a major glaciation which took place between ~29 and 25 ka. Large shelf-edge end moraines and tunnel valleys indicate that the British and Irish Ice Sheet and the Scandinavian Ice Sheet were confluent in the North Sea basin (Carr *et al.*, 2006; Sejrup *et al.*, 2009; Davies *et al.*, 2011; Graham *et al.*, 2011; Livingstone *et al.*, 2012b). The maximum ice extent and the starting points for ice retreat vary across the North Sea basin. One of the most important sediment and ice discharge routes of the Scandinavian Ice Sheet (SIS) was represented by the Norwegian Channel Ice Stream (NCIS), which was located in the Norwegian Channel and flowed along the coast from southern Norway and Sweden, extending northwards to the continental shelf edge in the northern North Sea (Fig. 2.5, see also Fig. 1.3 in Chapt. 1; Sejrup *et al.*, 2003; Ottesen *et al.*, 2016). This ice stream is thought to have been active in this area of the North Sea various times throughout the Pleistocene, and is believed to have been a major

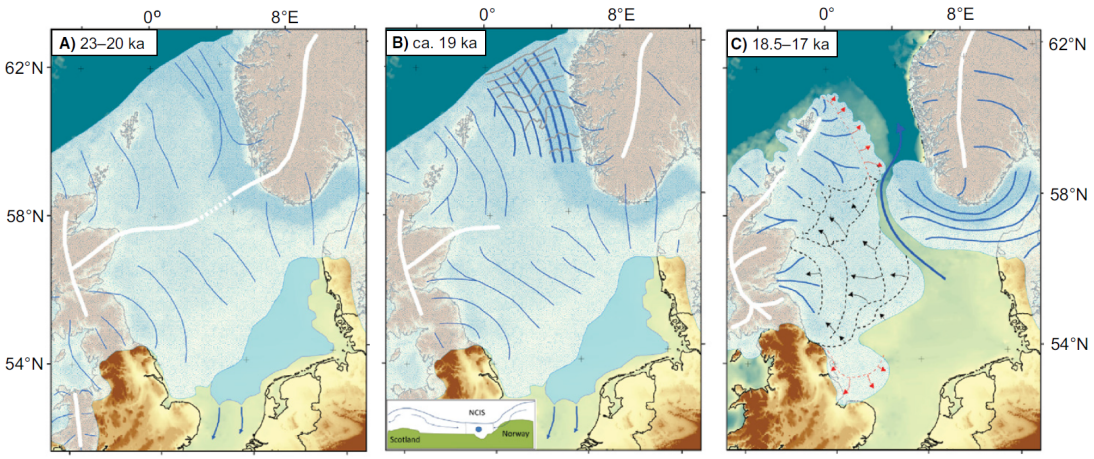

Figure 2.5: Reconstructions of maximum ice extent at different times, from Sejrup *et al.* (2016). A: maximum configuration with ice divides meeting in a saddle and an ice-dammed lake. B: Initiation of collapse. Norwegian Channel Ice Stream (NCIS) grew, increasing the drawdown of ice and destroying the ice divide. Grounding line retreat (gray) up the Norwegian Channel debuttressed ice on either side as it thinned and withdrew. C: Unzipping and collapse. NCIS narrows down and separates from British Ice and the ice-dammed lake discharges through the Link Bank drainage channel (blue arrow). Known re-advances are in red.

pathway for transportation of erosion products from southern Scandinavia to the Norwegian Sea during this time (Sejrup *et al.*, 2003). Evidence for its passage is well preserved below and at the seafloor of the Norwegian Channel, where different glacial landforms, which include Mega-Scale Glacial Lineations, Grounding-Zone Wedges and a series of terminal and lateral moraines have been observed (Sejrup *et al.*, 2003; Ottesen *et al.*, 2016; Morén *et al.*, 2017). The NCIS is thought to have played an important role in the final ice retreat and deglaciation phase of both the BIIS and SIS. The break-up of the last ice sheets is thought to have probably initiated in the northern North Sea around 25 ka (Sejrup *et al.*, 2009; Graham *et al.*, 2011; Clark *et al.*, 2012). Although, recent reconstructions from Sejrup *et al.* (2016) suggest that the NCIS increased its velocity between 20 and 19 ka, with flow acceleration and calving triggering rapid retreat and ice loss (Fig. 2.5; Bradwell *et al.*, 2008b; Sejrup *et al.*, 2016), and that by 18.5 - 17 ka the Scandinavian ice was constrained in the Norwegian Channel and was rapidly retreating towards land, leaving an ice-free corridor between the two ice sheets (Fig. 2.5; Sejrup *et al.*, 2016). The retreat of the NCIS towards southern Norway is thought to have been interrupted by stillstands off western Norway, as indicated by the presence of Grounding-Zone Wedges on the seafloor. (Morén *et al.*, 2017). This phase was followed by a more restricted glacial event in the western part of the North Sea, between ∼22 and 15 ka (the Dimlington Stadial), which was probably the correlative of the Tampen Formation advance that affected the eastern part of the basin (Sejrup *et al.*, 1994, 2009; Evans *et al.*, 2005, 2017; Davies *et al.*, 2011; Graham *et al.*, 2011; Clark *et al.*, 2012; Bateman *et al.*, 2015, 2017). In the southern and central North Sea, Dimlington ice limits are demarcated by the Bolders Bank and the Wee Bankie formations (Carr *et al.*, 2006; Davies *et al.*, 2011).

2.2.3 Evidence of Quaternary glaciations onshore eastern England

Eastern England is characterised by the outcrops of glacial and interglacial sediments that have been studied intensively in recent years (Eyles *et al.*, 1994; Clark *et al.*, 2004b; Pawley *et al.*, 2004, 2008; Catt, 2007; Preece *et al.*, 2009; Davies *et al.*, 2009a, 2012b; Boston *et al.*, 2010; Evans & Thomson, 2010; Roberts *et al.*, 2013; Bateman *et al.*, 2015, 2017; Evans *et al.*, 2017). The glacigenic sediments observed in County Durham, together with the sequences exposed in Yorkshire and Norfolk provide extensive evidence for Mid- to Late-Pleistocene glaciations, although the correlation of these sequences to the glacial formations observed in the North Sea basin remains a challenge.

Pre-Late Devensian

The Anglian tills are thought to be the first evidence of widespread glaciation in Britain (Ehlers & Gibbard, 2008). In Norfolk, the Lowestoft Formation and the Briton's Lane Formation are found. The Lowestoft Formation till is the most extensive glacial sequence in the UK and is defined as a clay rich diamicton comprising chalk and flint clasts (Clark *et al.*, 2004b; Ehlers & Gibbard, 2008). It extends throughout eastern England and its deposition has been correlated to MIS 12. This is based on dating of interglacial deposits overlying the till, correlated to MIS 11 (Fish & Whiteman, 2001; Clark *et al.*, 2004b; Pawley *et al.*, 2004, 2008; Davies *et al.*, 2012b). The ice sheet responsible for the deposition of the Lowestoft Formation is thought to be Scottish-sourced (Clark *et al.*, 2004b; Davies *et al.*, 2012b). The Briton's Lane Formation also occurs in Norfolk. It is composed of glacifluvial deposits characterised by a Scandinavian clast component and it overlies the Lowestoft Formation (Clark *et al.*, 2004b; Davies *et al.*, 2012b). The presence of Scandinavian ice has been suggested for its deposition, although reworking of older Scandinavian erratics is also considered as a possible scenario (Pawley *et al.*, 2004; Davies *et al.*, 2012b). The "new glacial stratigraphy" challenged the conventional stratigraphic framework proposed for north Norfolk, which argues against the presence of evidence for a pre-MIS 12 glaciation (Lee *et al.*, 2012), and suggested an alternative scenario, confirming a MIS 12 age for the Lowestoft Formation, but proposing the presence of sediments deposited by successive ice advances during MIS 16, 12, 10 and 6 on eastern England (Hamblin *et al.*, 2005; Preece *et al.*, 2009). In particular, this new stratigraphy suggested a MIS 6 age for the Briton's Lane Formation (Hamblin *et al.*, 2005; Preece *et al.*, 2009). Recent OSL and amino acid data collected from the Briton's Lane Formation and the sediments above it suggest that the formation is of MIS 12 age and are thus consistent with the traditional view of an Anglian glacial succession in Norfolk (Pawley *et al.*, 2008; Preece *et al.*, 2009; Lee *et al.*, 2012). In addition, recent studies have highlighted that the glacial-interglacial deposits found within the River Trent catchment are of MIS 8 and MIS 7 age, indicating they relate to a MIS 8 or older glaciation, and thus suggesting that the occurrence of an extensive MIS 6 glaciation south of the Humber area seems unlikely (Bridgland *et al.*, 2015; Westaway *et al.*, 2015).

The Bridlington Member (Basement Till) is the oldest known till in Holderness, east Yorkshire. It comprises erratics of north-eastern England, Scotland and Scandinavia provenance and is thought to represent evidence of a MIS 6 glaciation in the UK, implying

the presence of Scandinavian ice on England at that time (Clark *et al.*, 2004b; Catt, 2007; Boston *et al.*, 2010). There has been a long debate on the exact age of the Basement Till. Eyles *et al.* (1994) proposed that the till sequence found on the Yorkshire coast, which includes the Basement, Skipsea and Withernsea Tills, is of MIS 2 age and specifically that its deposition was a result of a surging glacier from the North Sea during the Last Glacial Maximum (LGM). Despite this, the Basement Till is overlain by the Sewerby Raised Beach, which has been dated to be of MIS 5e age, and is thus considered to be older, belonging to the MIS 6 glaciation or to an earlier cold stage (Eyles *et al.*, 1994; Bateman & Catt, 1996; Catt, 2007; Davies *et al.*, 2012b). The exact age of the sequence though is still uncertain (Catt, 2007; Davies *et al.*, 2012a; Roberts *et al.*, 2013).

Evidence for a pre-LGM glaciation is also found on County Durham. The Warren House Gill Formation crops out at Warren House Gill and is defined by Davies *et al.* (2012b) as composed of two members: the Ash Gill Member, a glaciomarine diamicton, and the Whitesides Member, characterised by pink estuarine silts. The Ash Gill Member is overlain by the Easington Raised Beach, which has been dated to be of MIS 7 age (Davies *et al.*, 2009b), thus implying that the Ash Gill Member belongs to MIS 8 or to an older glaciation (Davies *et al.*, 2009a, 2012b). The deposition of this diamicton is thought to be related to the advance of British ice, suggesting that Scandinavian ice did not reach as far as the eastern coasts of the UK at that time (Davies *et al.*, 2012b).

Late Devensian and ice stream flow

Evidence for Late Devensian glaciation is widespread in eastern England. On the Yorkshire coast, the Skipsea Till and the Withernsea Till are found. The Skipsea Till is the most extensive unit characterising the Holderness glacial sequence and is defined as a dark-greyish-brown, massive to laminated diamicton, rich in erratics from Scotland, Northumberland and the Cheviots (Evans & Thomson, 2010; Boston *et al.*, 2010). It is separated from the underlying Basement Till by the discontinuous Dimlington Silts unit, which is defined as a lacustrine deposit, radiocarbon dated to 18.5 cal. ka BP (Catt, 2007; Evans & Thomson, 2010; Boston *et al.*, 2010). The Withernsea Till is located stratigraphically above the Skipsea Till and occurs in a smaller and more confined area in Holderness. It is described as a matrix-supported diamicton with stratified intrabeds (Evans & Thomson, 2010; Boston *et al.*, 2010). The two units are thought to have been deposited during the Dimlington Stadial (Evans & Thomson, 2010; Bateman *et al.*, 2011, 2015, 2017; Roberts *et al.*, 2013). It is believed that the Skipsea Till represents an initial advance of the NSL into the Humber Gap region that reached its maximum extent at around 21.6 ka, while the Withernsea Till is thought to have been deposited during the most significant re-advance of the NSL during overall recession around $\sim$16.8 ka (Evans & Thomson, 2010; Bateman *et al.*, 2015, 2017). Above the Magnesian Limestone cliffs located on the eastern coasts of County Durham, the Blackhall Till and the Horden Till formations are found (Davies *et al.*, 2012a). The Blackhall Till is defined as a grey-brown diamicton containing Permian and Carboniferous erratics (Davies *et al.*, 2009b, 2011; Livingstone *et al.*, 2012b), while the Horden Till is a dark brown diamicton with Cheviot, Carboniferous and Permian erratics (Davies *et al.*, 2011; Livingstone *et al.*, 2012b). Both units are thought to

be of MIS 2 age (Livingstone *et al.*, 2012b; Davies *et al.*, 2009b, 2012a). Ice responsible for the Blackhall Till deposition is thought to have originated in north-western England, due to the local clasts observed in the formation (Davies *et al.*, 2009b). The Horden Till instead is thought to have been deposited by ice originated as far north as the Grampian Highlands, dominated by Cheviots and Northumbrian erratics (Davies *et al.*, 2009b).

As mentioned above, during the Late Devensian, the central sector of the BIIS was highly dynamic and underwent a complex sequence of flow events often linked to ice stream activity and shifting ice divides (Boulton & Hagdorn, 2006; Bradwell *et al.*, 2008b; Livingstone *et al.*, 2008, 2010, 2012b; Hubbard *et al.*, 2009; Davies *et al.*, 2009a, 2012a; Yorke *et al.*, 2012). This led to a complicated geomorphological ice flow signature (Livingstone *et al.*, 2012b). The Forth, Tweed, Tyne Gap Ice Stream (TGIS), Stainmore Gap Ice Stream and North Sea Lobe (NSL) ice streams affected north-east England and south-east Scotland during the last deglaciation (Everest *et al.*, 2005; Davies *et al.*, 2012a; Livingstone *et al.*, 2012b, 2015). Different studies have mapped numerous subglacial bedforms beneath the eastern margins of the last BIIS and identified ice flow lineations and cross-cutting relationships, which have led to the reconstruction of several chronologically distinct flow phases sourced from different dispersal centres (Evans *et al.*, 2005; Livingstone *et al.*, 2008, 2012b; Davies *et al.*, 2012a). Based on the geomorphological mapping of the central sector of the BIIS and on the onshore stratigraphy, Livingstone *et al.* (2012b, 2015) proposed a reconstruction of the last BIIS which included several flow phases. These are summarized by a six-stage model (Fig. 2.6; Davies *et al.*, 2012a; Livingstone *et al.*, 2012b, 2015). The model shows how ice was flowing from west to east through the Stainmore Gap Ice Stream and the TGIS, both active around $\sim$ 29 - 23 ka cal. BP and transferring ice to the eastern side of the country (Stage 1, Fig. 2.6). Successively, both ice streams weakened due to a gradual reduction of ice volume (Stage 2, Fig. 2.6), and the central sector of the last BIIS underwent widespread collapse between 18 and 16 ka BP (Stage 5, Fig. 2.6), while regions sourced from Scottish ice continued to stream southwards during this time. The NSL, flowing from north to south, was still active during later phases (Stage 5–6, Fig. 2.6; Livingstone *et al.*, 2012b, 2015; Bateman *et al.*, 2015) and moved onshore forming numerous proglacial lakes between the higher terrain of the east coast and its western margin (Stage 5 – 6, Fig. 2.6; Livingstone *et al.*, 2012b, 2015; Bateman *et al.*, 2017; Evans *et al.*, 2017). The TGIS was fed by ice originated from the Lake District and Southern Uplands regions and was a major tributary of the NSL (Livingstone *et al.*, 2012b, 2015). Livingstone *et al.* (2008, 2010, 2012b, 2015) identified three distinct flow sets in the central sector of the last BIIS, related to the activity of the TGIS and NSL ice streams (Fig. 2.7). Flow set (1) consists of W - E to SW - NE lineated terrain (demarcated by black dotted lines, in Fig. 2.7) in the Tyne Gap corridor. Flow set (2) is represented by numerous lineations stretching SE down the North Tyne Valley, and flow set (3) consists of a small set of N - S orientated lineations on the eastern coasts of England. The first flow set has been related to the action of the TGIS. The resulted W - E orientated streamlined features are inferred to become less dominant towards the east coast and appear overprinted by flow set (3). Flow set (2) has been correlated to the weakening of the TGIS which probably coincided with the southwards and onshore expansion of the NSL (flow set (3), Fig. 2.7; Davies *et al.*, 2012a; Livingstone

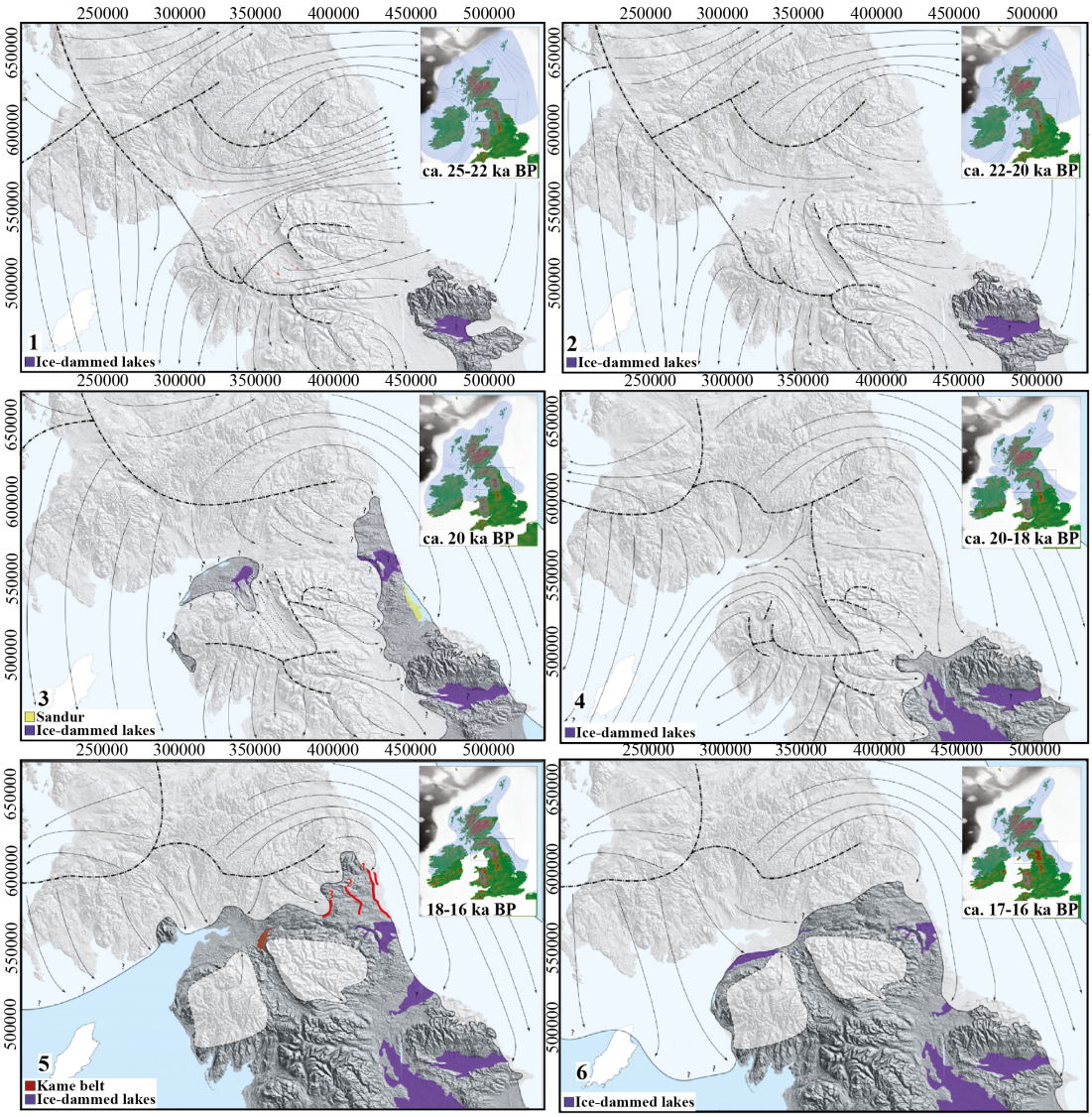

Figure 2.6: Six stage model for ice flow history and behaviour in the central sector of the last BIIS. The red lines numbered 1–3 in Stage 5 refer to three moraine systems identified in Livingstone *et al.* (2015). Compiled from Livingstone *et al.* (2012b, 2015).

et al., 2015). Furthermore, new evidence from three moraine assemblages mapped in the TGIS corridor reveals three significant ice-marginal positions in the area (Fig. 2.7; Livingstone *et al.*, 2015). The easternmost ice-margin position is represented by the "Crowden Hill Moraine" (moraine ridge 1 in Fig. 2.7), which has a NNW - SSE orientation and is thought to be related to the onshore movement of the NSL (Teasdale, 2013; Livingstone *et al.*, 2015). The other two moraine sets mapped inland of the Crowden Hill Moraine (moraine ridges 2 and 3 in Fig. 2.7) document uncoupling of the TGIS from the NSL and probably mark the continuous retreat of the TGIS into the North Tyne system (Livingstone *et al.*, 2015). The westward retreat of the TGIS is thought to have begun by 18.7 - 17.1 ka BP and to have reached the Solway Lowlands by 16.4 - 15.7 ka BP. Uncoupling of the TGIS from the NSL was necessary to dam Glacial Lake Wear, which was probably formed before 18.7 - 17.1 ka BP in the area deglaciated by the retreating TGIS (Livingstone *et al.*, 2015).

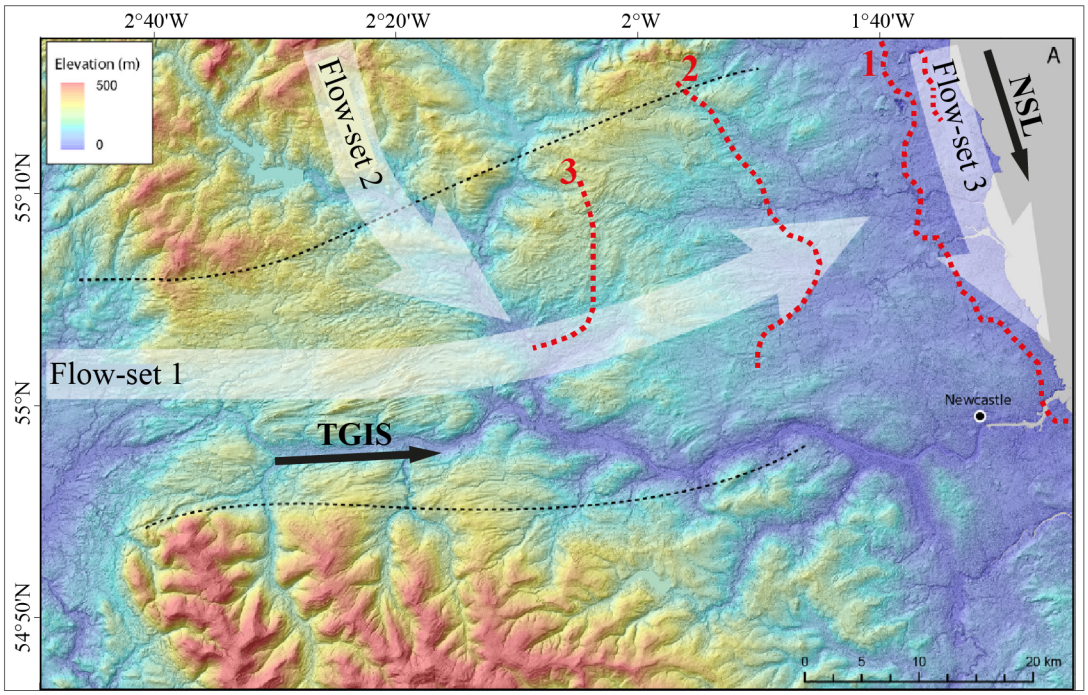

Figure 2.7: NEXTMap image showing the geomorphology of the Tyne Gap corridor (north-east England) and the landforms identified by Livingstone *et al.* (2015). The three main ice flow sets are indicated with white arrows. The three recognized moraines are shown with dashed red lines. The black dotted lines indicate the edge of the lineated terrain. The generalised flow direction of the TGIS and NSL is also shown with black arrows. Modified from Livingstone *et al.* (2015).

Evidence for the flow and signature of the TGIS and NSL ice streams is also recorded within the glacial sediments of eastern England. The Blackhall Till in county Durham is thought to have deposited during the LGM from ice originated in north-western England. Its deposition is thought to be related to the westward flow of the TGIS at that time (Davies *et al.*, 2009b, 2012a; Livingstone *et al.*, 2012b). During the Dimlington Stadial, the initial advance of the NSL flowing southwards resulted in the deposition of the Horden Till in County Durham and of the Skipsea Till in Yorkshire, which are thought to be correlatives (Carr *et al.*, 2006; Davies *et al.*, 2009a, 2011, 2012a; Evans & Thomson, 2010; Bateman *et al.*, 2011; Livingstone *et al.*, 2012b, 2015). Both the Skipsea and Horden tills are correlated to the offshore Bolders Bank Formation, which is thought to represent the easternmost extension of the NSL (Carr *et al.*, 2006; Davies *et al.*, 2009a, 2011, 2012a; Livingstone *et al.*, 2012b). Despite the fact that the BBF was initially regarded as one single unit (Cameron *et al.*, 1992; Gatliff *et al.*, 1994), Dove *et al.* (2017) presented new bathymetric and seismic evidence from the marine sector offshore Holderness in the southern North Sea, and divided the BBF into at least five different seismostratigraphic units (SU; Fig. 2.8). These units, which display a wedge-like structure in profile and have been correlated to arcuate wedges/moraines observed on the seafloor (Fig. 2.8), are believed to relate to stillstand episodes of the NSL and to indicate an oscillating ice margin (Dove *et al.*, 2017). Furthermore, the nature of the Dogger Bank Formation (DBF) was also recently revised. Cotterill *et al.* (2017) provided a new reconstruction of the DBF, subdividing it into three different seismostratigraphic units (termed ”Basal”, ”Older” and

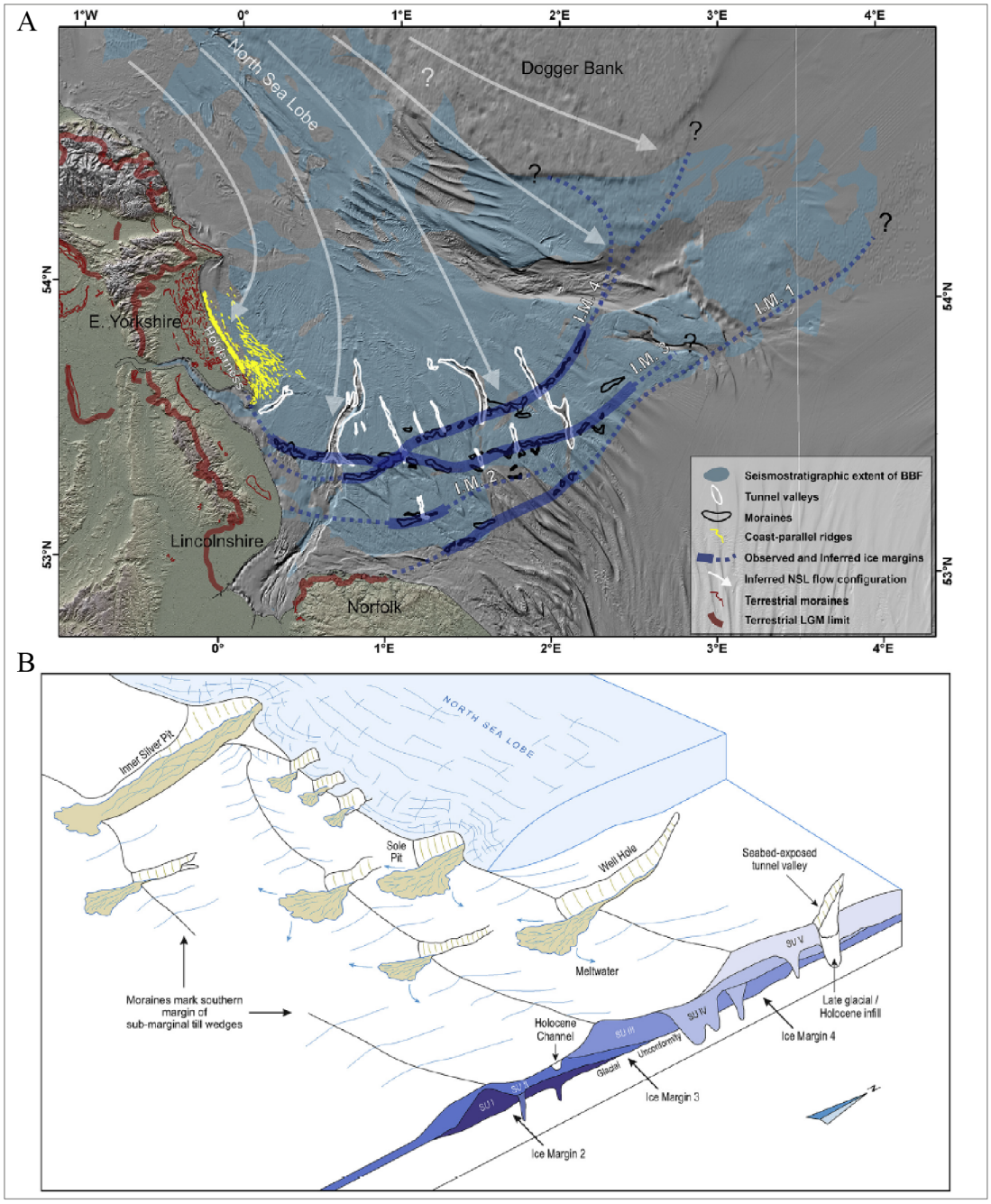

Figure 2.8: Recent reconstructions of the NSL occupation and retreat in the southern North Sea from Dove *et al.* (2017). A) Regional extent of the Bolders Bank Formation (BBF) and ice flow configuration (white arrows) of the NSL. B) Simplified conceptual diagram demonstrating the relationships between the glacial landforms present at seabed (broad wedges, moraines, tunnel valleys), and the revised stratigraphy of the BBF (shallow stacked wedges). This combined landform and sub-surface stratigraphic assemblage elucidates the phased stillstand occupation of the NSL at an oscillating southern margin prior to final retreat from the region.

"Younger" Dogger Bank) and highlighting how this facies has a much more complex internal structure than previously thought. New evidence suggests that the DBF is characterised by a thrust-moraine complex, which developed through glaciotectonic deformation at an oscillating ice margin during the last glacial phase (Cotterill *et al.*, 2017). A later re-advance of the NSL,

during overall retreat, is represented by the Withernsea Till in Holderness, deposited around ∼ 16.8 ka (Evans & Thomson, 2010; Bateman *et al.*, 2011, 2015, 2017).

Deglacial to Holocene sedimentary environments

The St Abbs, Forth, Witch Ground and Botney Cut formations (Fig. 2.4) have been mapped in the central and northern North Sea and assigned an age of Late Devensian - Early Holocene (Gatliff *et al.*, 1994; Stoker *et al.*, 2011). The St Abbs Formation is generally less than 20 m thick and has been mapped off the east coast of northern England and Scotland. It is composed of soft to stiff, weakly laminated and locally silty muds with sporadic pebbles and was deposited in glaciomarine conditions during MIS 2 (Gatliff *et al.*, 1994; Stoker *et al.*, 2011). It is found on top of either the Wee Bankie Formation or of pre-Quaternary sequences and its deposition was contemporaneous with the deposition of the lower parts of the Forth and Witch Ground formations (Gatliff *et al.*, 1994). The Forth Formation crops out extensively in the central North Sea (Fig. 2.4) and is typically less than 20 m thick but can occur as a channel fill and reach up to 150 m in thickness. It has been divided into four members due to the different nature of the sediments that constitute it: marine, glaciomarine, fluviomarine and estuarine sequences have all been observed in the formation, which is thought to be of MIS 2 - 1 age (Gatliff *et al.*, 1994; Stoker *et al.*, 2011; Graham *et al.*, 2011). The Witch Ground Formation occurs in the northern part of the central North Sea (Fig. 2.4) and is composed of soft to very soft clays and silts with some sandy beds, and is divided into three members which record deposition from glaciomarine to warmer and modern environments. It has also been assigned a MIS 2 - 1 age (Gatliff *et al.*, 1994; Stoker *et al.*, 2011). The Botney Cut Formation occurs extensively as valley/channel fill to the west and north of the Dogger Bank (Fig. 2.4; Cotterill *et al.*, 2017) and can be divided into two members, the lower of which is composed of stiff, reddish-brown diamicton with interbedded sand. The upper member instead comprises sandy and pebbly muds of partly glaciomarine origin, and is thought to be equivalent to the St Abbs Formation and to much of the Forth Formation to the north of 56° N and west of 0° (Gatliff *et al.*, 1994). The St Abbs, Forth and Witch Ground formations are part of the Reaper Glacigenic Group, while the Botney Cut Formation instead is part of the California Glacigenic Group (Stoker *et al.*, 2011).

Sea-level rise during the Holocene left a cover of superficial sediments at the seabed throughout the whole basin (Cameron *et al.*, 1992; Gatliff *et al.*, 1994; Sejrup *et al.*, 2000). At present, the North Sea is generally characterised by very shallow waters. The two study areas analysed in this work, the Blyth survey and the Britice-Chrono survey, located in the western North Sea, are characterised by water depths of ∼30 and ∼70 m on average, respectively, which reach a maximum of ∼110 m in the Britice-Chrono survey. In contrast, the North Sea basin is deeper in the Norwegian Channel (eastern North Sea), with waters reaching approximately 200 - 400 m depths, and at its northern margin, delimited by the continental shelf edge, where water depths increase rapidly from ∼200 m to more than 1500 m.

In summary, this chapter provides a review of the current knowledge of the complex geological history and stratigraphic architecture of the North Sea basin. Its present-day

structural configuration is the result of Jurassic - Early Cretaceous rifting followed by thermal cooling and subsidence, which allowed for the accumulation of up to 3000 m of Oligocene to Holocene sediments in the central part of the basin, including up to ∼800 m of Quaternary sediments. Both the BIIS and SIS ice sheets are known to have advanced into the North Sea numerous times during the Pleistocene and to have deposited thick glacigenic sequences offshore, which hold important information on the ice sheets dynamic and behaviour. The information provided in this review chapter constitutes the base for the research carried out in this work and presented in chapters 3 - 5, which builds on the current knowledge of the last BIIS and of its deglacial phase and suggests a new reconstruction for the evolution of the NSL in the western North Sea.

Chapter 3

Seismic stratigraphy of the Blyth survey area

3.1 Introduction

This work focusses on the analysis of a 2D geophysical investigation carried out east of Blyth (north-eastern UK, Fig. 3.1), which consists of both bathymetric and seismic data. The survey is of particular interest due to the fact that it is located on the former eastern margin of the BIIS, in an area hypothetically overrun by both the Tyne Gap Ice Stream (TGIS) and the North Sea Lobe (NSL; Fig. 3.1; Davies *et al.*, 2011; Livingstone *et al.*, 2012b, 2015). In

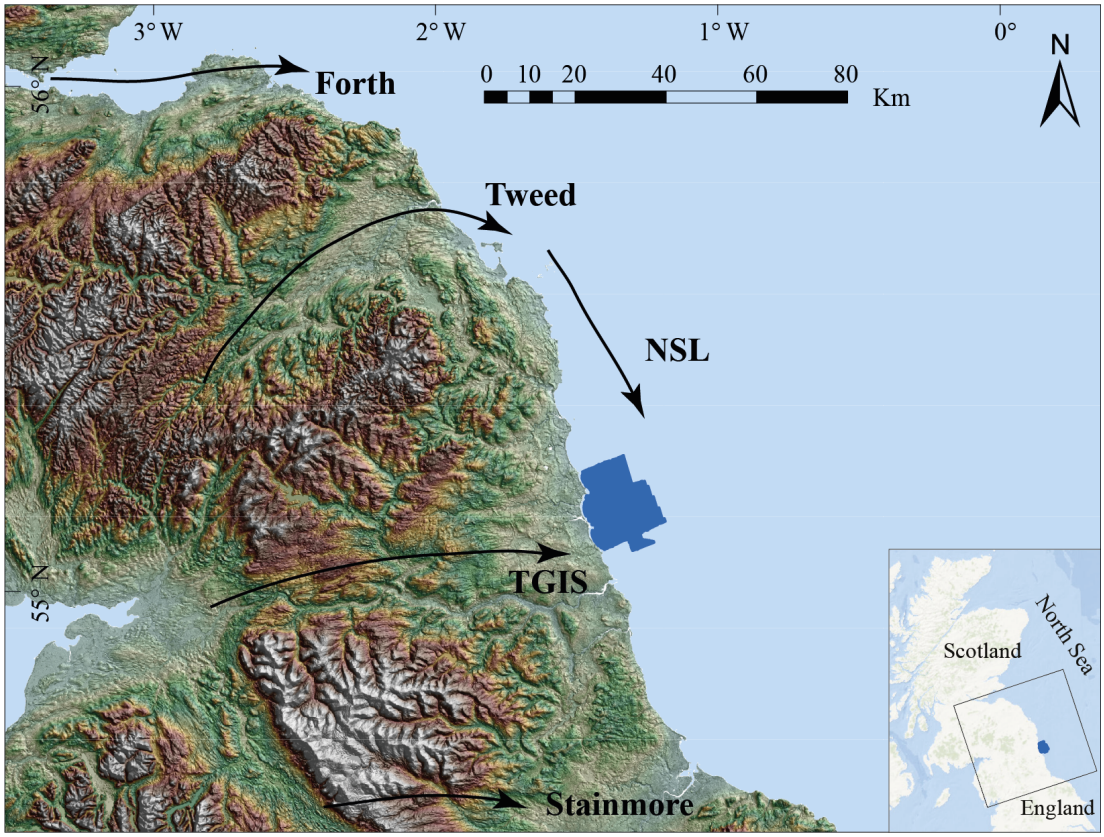

Figure 3.1: NEXTmap image of northern England and southern Scotland (location shown in the insert map) and location and generalised ice flow directions of the Forth, Tweed, Tyne Gap Ice Stream (TGIS), Stainmore and North Sea Lobe (NSL) ice streams. The location of the Blyth survey area is indicated with the blue polygon.

addition, the Blyth survey area is located just offshore of the Crowden Hill Moraine (Fig. 2.6, see also Chapt. 2) which is thought to represent the onshore movement of the NSL ice stream (Teasdale, 2013; Livingstone *et al.*, 2015), in a region of the western North Sea where Carboniferous, Permian and Triassic formations represent the pre-Quaternary geology which outcrops both offshore and onshore and which is overlain by Quaternary sequences (Cameron *et al.*, 1992; Gatliff *et al.*, 1994; Davies *et al.*, 2012a). Specifically, the Blyth survey is located where the Wee Bankie Formation, the Forth Formation and the St Abbs Formation were previously mapped by the British Geological Survey (BGS; Fig. 2.4). The survey could thus hold important information on the sedimentary and geomorphic signature of the last BIIS and of older Pleistocene glaciations that affected the area.

Here, the seismic sequence that characterises the Blyth survey area is analysed and interpreted to develop the existing Quaternary glacial stratigraphy of the western North Sea, and to investigate possible correlations of offshore and onshore stratigraphy. The research is focussed on the following aims:

1. To provide an assessment of the seismic stratigraphy of the Blyth survey area
2. To review the BGS data available for this area
3. To assess the Blyth seismic stratigraphy and the BGS data in the context of the wider onshore and offshore glacial history of the region

3.2 Materials and Methods

The geophysical survey (the Blyth survey) analysed in this chapter was downloaded from the Marine Data Exchange (MDE) portal of the Crown Estate (©Crown Copyright (2013)). It was originally acquired by EGS Ltd in 2011, who later shared it with the MDE. The MDE website is a system developed by the Crown Estate to store, manage and distribute offshore survey data, which is supplied by their offshore renewable and marine aggregates customers, and provides access to survey data and reports. These can be obtained from the MDE portal free of charge.

The Blyth survey area is located off Blyth harbour (Northumberland) in north-eastern England. It extends to a maximum of ∼15 km offshore from the coast to the east and around ∼20 km from Cresswell in the north and St. Mary's Island in the south (location indicated in the insert map in Fig. 3.2). The survey was carried out in 2011 by EGS Ltd for NAREC Ltd for the Narec Offshore Wind Farm Demonstration Site off the coast of Blyth, and it consists of both bathymetry and seismic datasets. Two vessels were employed simultaneously by EGS Ltd to survey the site both inshore and offshore (Fig. 3.2). A total area of approximately 221 km^2 was covered by Multibeam echosounder (MBES) using a Kongsberg EM3002D, a high resolution system working nominally at 300 kHz. Approximately 990 line km were surveyed to acquire 2D seismic profiles using a surface towed C-Products low-voltage Boomer and C-Products C-Phone hydrophone. Both the bathymetry and seismic data processing were undertaken by EGS Ltd. Caris HIPS/SIPS 7.1 software was utilised for MBES data processing and the data were gridded at 1 m cell size (1 m spatial resolution) and then exported in ASCII format as an .xyz file. The 2D seismic profiles were processed with C-View SDMP software.

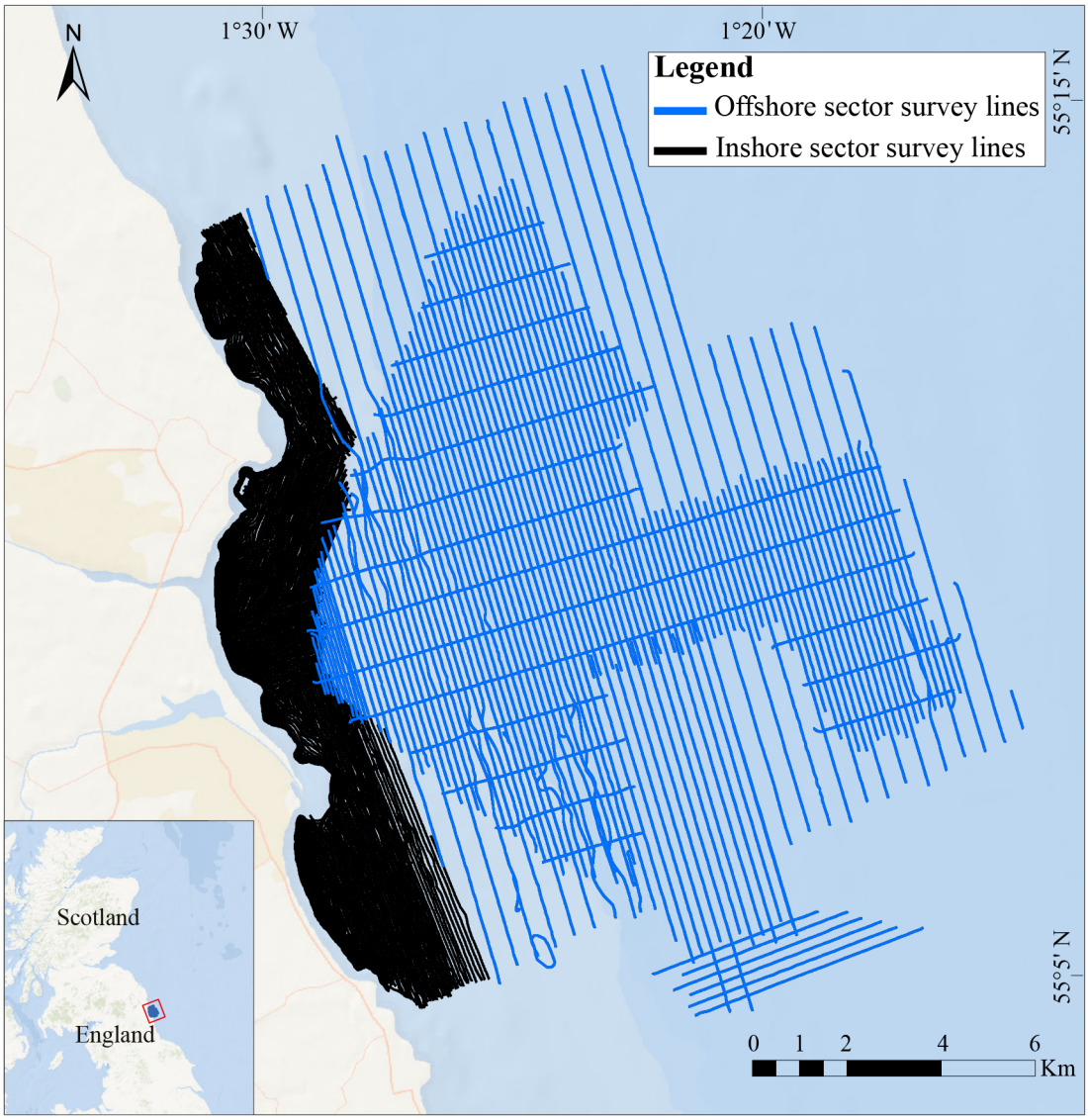

Figure 3.2: Blyth survey area: inshore (black) and offshore (blue) track lines. The location of the survey is indicated with the red rectangle in the insert map.

The datasets downloaded from the MDE website and analysed further in this study consist of the resulted MBES .xyz file and of the seismic profiles. No further re-processing was applied to the bathymetry data and the .xyz file was analysed and interpreted using QPS Fledermaus. This software was used to visualise the bathymetry in 3D and to better analyse and measure any relevant landforms observed on the seafloor. ArcGIS software was used to produce a Slope layer of the bathymetry which enhanced the bedrock structures and the presence of faults (Sect. 3.3.1) and also to create the bathymetric contours. The seismic profiles were analysed and interpreted with Seisee and IHS Kingdom. Different attempts were made to re-process the profiles with various software in order to reduce the noise and obtain a better quality image, but no substantial improvement was achieved. The analysis of the seismic data consisted in the recognition and mapping of the visible horizons, and in the identification of different seismic units, according to their seismic appearance and to the geometry of their internal reflectors. The seismic lines were also visualised in 3D using the VuPAK extension of the IHS Kingdom

software, in order to achieve a better understanding of the geometry and lateral extension of the encountered units. This 3D view also permitted the production of the fence diagrams shown in this chapter. Note that all the figures of the seismic profiles shown in this chapter have a depth scale shown in time (milliseconds (ms)), instead of meters. This was done in order to display the original acquired data. EGS Ltd employed two different values, of 1650 m/s and 1750 m/s to estimate the speed of sound in the sediments (EGS, 2012), so a mean value of 1700 m/s can be used to obtain an approximate depth conversion from time to meters. This means that, in this chapter, 10 ms correspond to $\sim$8.5 m.

Additional datasets were analysed in combination with the Blyth survey for comparison and to help with the interpretations. The BGS 1982-3 2D seismic survey and the BGS core logs, which were made available by the BGS for this study, provided useful information on the area analysed. The 1982-3 2D seismic survey was acquired by the BGS in the 1980's using various instruments (Cameron *et al.*, 1992; Gatliff *et al.*, 1994), and the profiles presented in this study were acquired with a Sparker. It is also to be noted that the 1982-3 survey consists of paper records, so it was not possible to import the seismic lines into IHS Kingdom, and the analysis and interpretations were made using CorelDRAW. The BGS geological maps available for the study area also provided valuable background information.

3.3 Results

3.3.1 Bathymetry data

The Multibeam echosounder swath data extend from the coast to ∼16 km offshore and cover an area of ∼10 - 19 km from north to south. Full multibeam coverage was achieved close to the coast and in the central part of the survey, while a partial coverage was achieved on its northern, eastern and southern sides (Fig. 3.3). The bathymetry data show how the seafloor in the survey area appears to be relatively flat. The seabed slopes gently from the shore towards the east, reaching a maximum depth of ∼61 m (south-eastern corner), and the bathymetric contours appear to be generally parallel to the coastline (Fig. 3.3a). Bedrock outcrops are visible in the north-western and south-western areas of the survey, predominantly from the shore up to the 20 m contour line, although smaller outcrops can also be found close to the 50 m contour line (Fig. 3.3a). According to the BGS Offshore Regional Reports, it is known that bedrock outcropping at this location close to the coast consists of Carboniferous coal-bearing sediments (from the BGS rocks nomenclature: Pennine Coal Measures Group, previously defined as Carboniferous Coal Measures), while Upper Permian (Zeichstein) shales, carbonates and evaporites are found further offshore (see also Chapt. 2; Taylor *et al.*, 1971; Cameron *et al.*, 1992; Gatliff *et al.*, 1994). The Carboniferous strata is generally characterised by sub-horizontal to inclined parallel bedding planes, which are often deformed and at times display faults. Close to the coast these beds appear to be dipping in a W - SW direction (detail in Fig. 3.3b, their appearance has here been enhanced using the Slope Geoprocessing Tool in ArcGIS), but their deformation is better observed on seismic profile. The rest of the dataset appears flat and is generally characterised by a gentle increase in depth moving from the shore towards the east. In addition to the bedrock outcrops, the only other notable landform observed in the area is represented by a series of regular, rectangular-shaped depressions, located at ∼45 m depth towards the central part of the survey (detail in Fig. 3.3c). These features are approximately 900 m long, 220 m wide on average and only 1 - 2 m deep. Because of their regular geometric shape and spacing, these depressions are thought to be anthropogenic and to be possibly related to the collapse of sub-seafloor mine shafts (EGS, 2012).

No geomorphological landforms and/or landforms of potentially glacial origin (i.e. lineations and moraines) were identified on the seafloor at this location. This is in contrast with the area immediately onshore the Blyth survey area, where numerous glacial landforms have been observed and mapped (Clark *et al.*, 2004a, 2018; Livingstone *et al.*, 2015). Figure 3.4 shows the location and extent of different moraines, subglacial lineations, streamlined bedrock and former glacial lake, which were downloaded from the BRITICE Glacial Map (a map and GIS database of glacial landforms and features related to the last British Ice Sheet; Clark *et al.*, 2004a, 2018). Despite the fact that these landforms, and particularly the subglacial lineations (Fig. 3.4, black polygons), appear to be widespread inland, only a few have been mapped closer to the eastern coast of England and immediately inland of the Blyth survey. Nevertheless, considering the glacial history of the site, which is thought to have been affected by the passage of both the TGIS and NSL ice streams, as previously discussed (see Sect. 3.1 and Chapt. 2; Davies *et al.*, 2011; Livingstone *et al.*, 2012b, 2015), it would be reasonable to

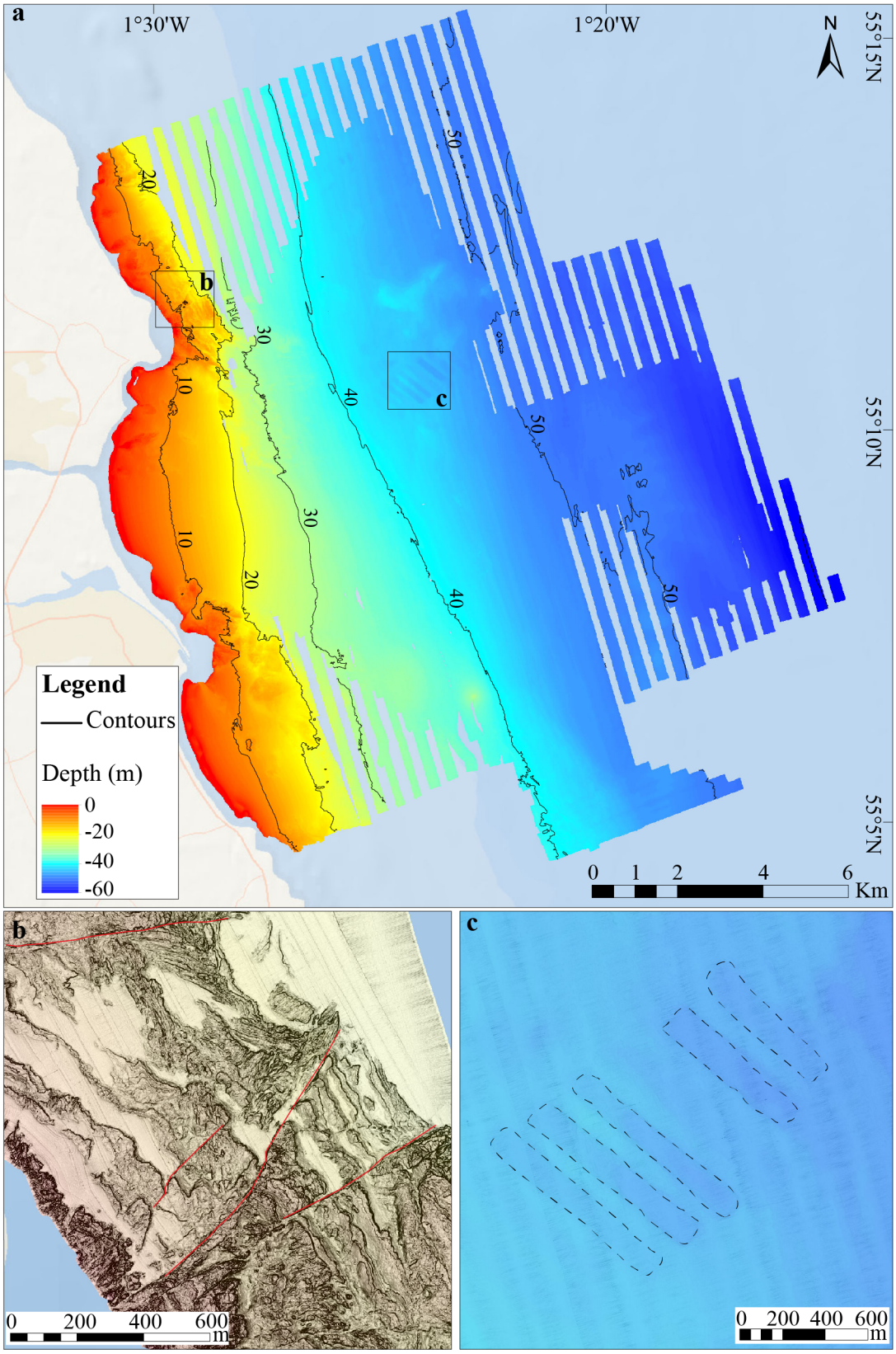

Figure 3.3: a: Blyth survey swath bathymetry and contour lines. Locations of b and c are shown with black squares. b: detail of the Pennine Coal Measures Group outcrops, showing bedrock bedding planes and faults (in red). c: detail of the regular, rectangular-shaped depressions (dashed lines).

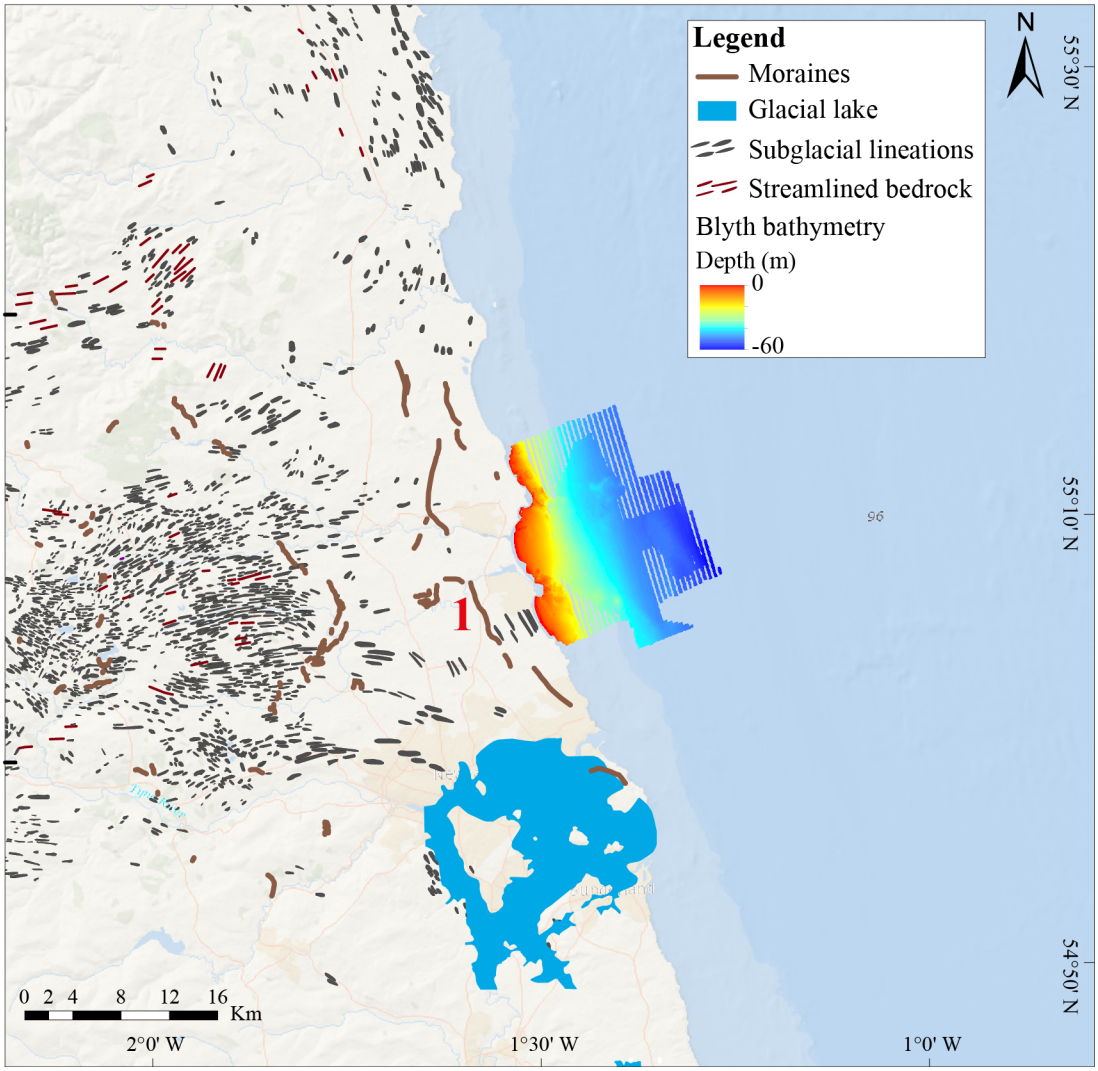

Figure 3.4: Location and extent of different glacial landforms inland of the Blyth survey. The red 1 indicates the Crowden Hill Moraine (Teasdale, 2013; Livingstone *et al.*, 2015). The onshore landforms were downloaded from the BRITICE Glacial Map (Clark *et al.*, 2004a, 2018).

assume the presence of these types of landforms also offshore. This is clearly not the case, as was observed on the bathymetry data of the Blyth survey, and the subject will be further discussed in Section 3.4.

3.3.2 Seismic profiles

2D seismic profiles were acquired at a very high resolution across the survey area and the Boomer system reached a maximum penetration of ~75 ms below the seabed. N - S orientated lines are located 150 m apart and provide a dense acquisition grid (Fig. 3.5). Both N - S and W - E orientated profiles were analysed. The latter, although less in number, provide more information on the shallow geology of the area which changes considerably within the survey. These changes are more apparent if observed along a W - E direction. Six different acoustic facies (AF) were recognized in the study area according to their acoustic signature and to the geometry of their internal reflectors.

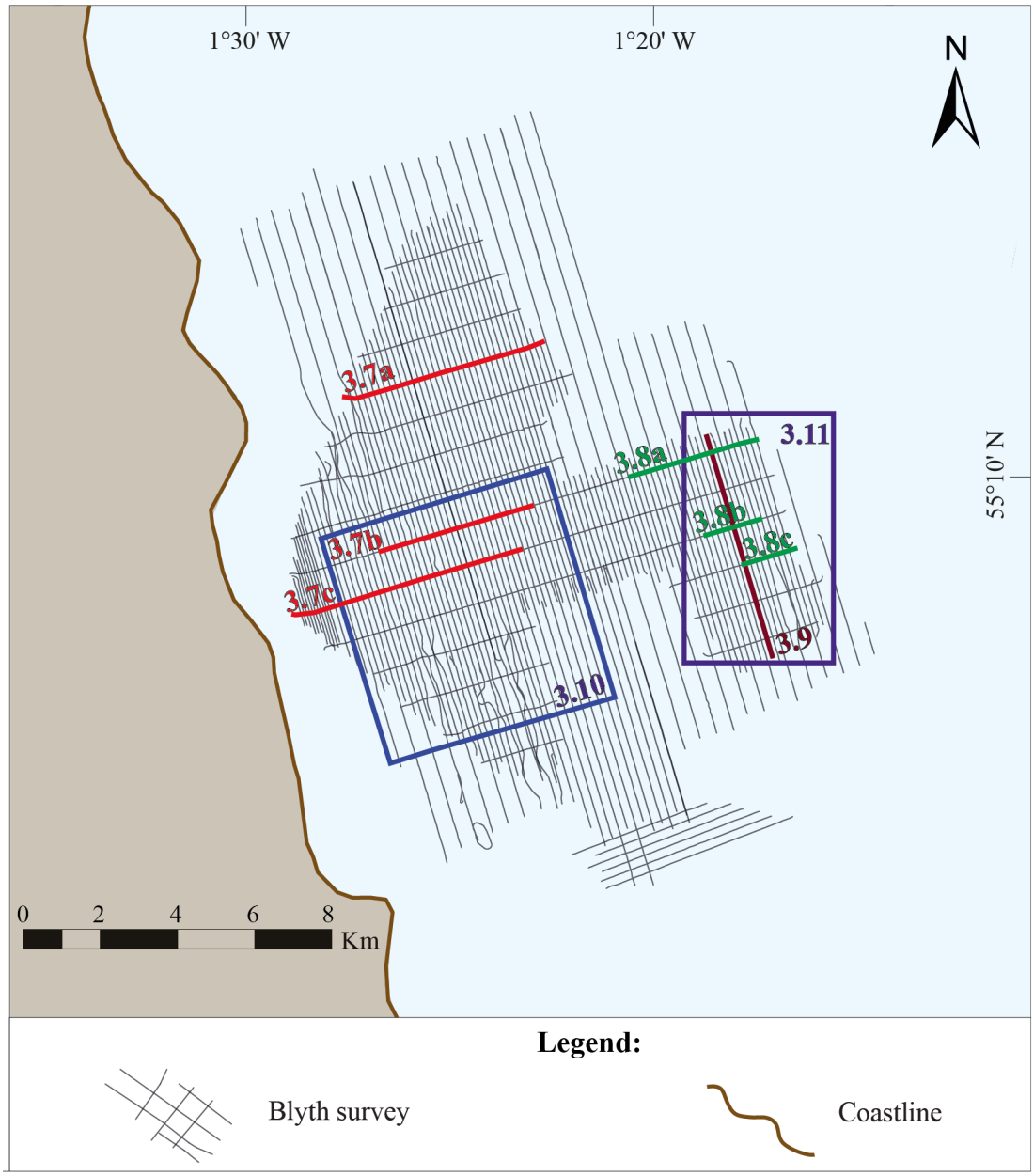

Figure 3.5: Overview of the Blyth offshore survey acquisition grid. The location of the profiles shown in Figure 3.7 (a, b, c), 3.8 (a, b, c) and 3.9, and of the fence diagrams shown in Figure 3.10 and 3.11 are indicated with different colours and the correspondent figure number.

The typical seismic appearances of these facies are shown in Figure 3.6 and described below.

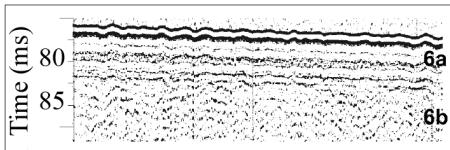	High amplitude seafloor reflector, overlying parallel reflectors (AF 6a), and sometimes chaotic reflectors (AF 6b)	AF 6
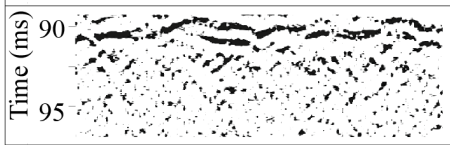	Flat, at times undulated upper boundary. Chaotic appearance of internal reflectors	AF 5
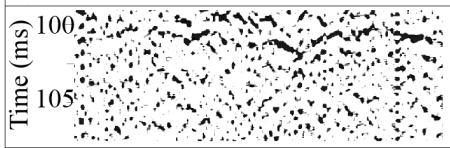	Low amplitude and undulated upper boundary. Chaotic appearance of internal reflectors	AF 4
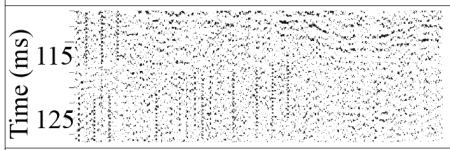	Weak wavy parallel reflectors	AF 3
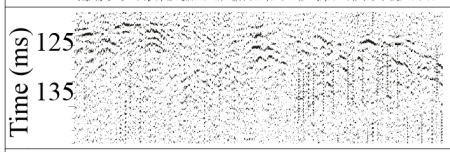	Low amplitude and undulated upper boundary. Chaotic appearance of internal reflectors	AF 2 (Permian)
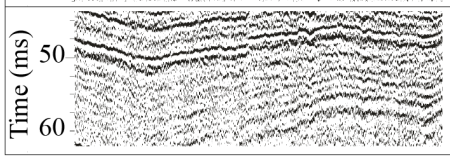	Folded high frequency parallel reflectors which at times appear faulted	AF 1 (Carboniferous)

Figure 3.6: Acoustic signatures of the six different seismic facies recognized and mapped along the profiles. Interpretation of pre-Quaternary strata based on the BGS literature (Cameron *et al.*, 1992; Gatliff *et al.*, 1994).

AF 1

AF 1 is the lowermost facies of the sequence. It has only been observed in the western part of the survey, from the start of the profiles close to the coast, where it often crops out at the seabed (as visible in Fig. 3.3b), to ∼6.5 km towards the east (Fig. 3.7, location of the profiles in Fig. 3.5). Internally, AF 1 is characterised by continuous, high frequency, wavy parallel reflectors, which appear folded and, at times, faulted (Fig. 3.6 and 3.7). This is also visible from the bathymetry data (Fig. 3.3b). The lower boundary of AF 1 is not visible from the seismic profiles due to the loss of penetration of the acoustic signal. At ∼6.5 km from the coastline, AF 1 deepens in the sequence and is overlain by AF 2 (Fig. 3.7). Based on the mapped geology of the area, AF 1 is interpreted as Carboniferous strata (Pennine Coal Measures Group; BGS Offshore Regional Report, Cameron *et al.*, 1992; Gatliff *et al.*, 1994).

AF 2

AF 2 is present at a relatively shallow depth below the seabed towards the west, but it deepens towards the east, and is overlain by AF 3 - 6. AF 2 is characterised by discontinuous and

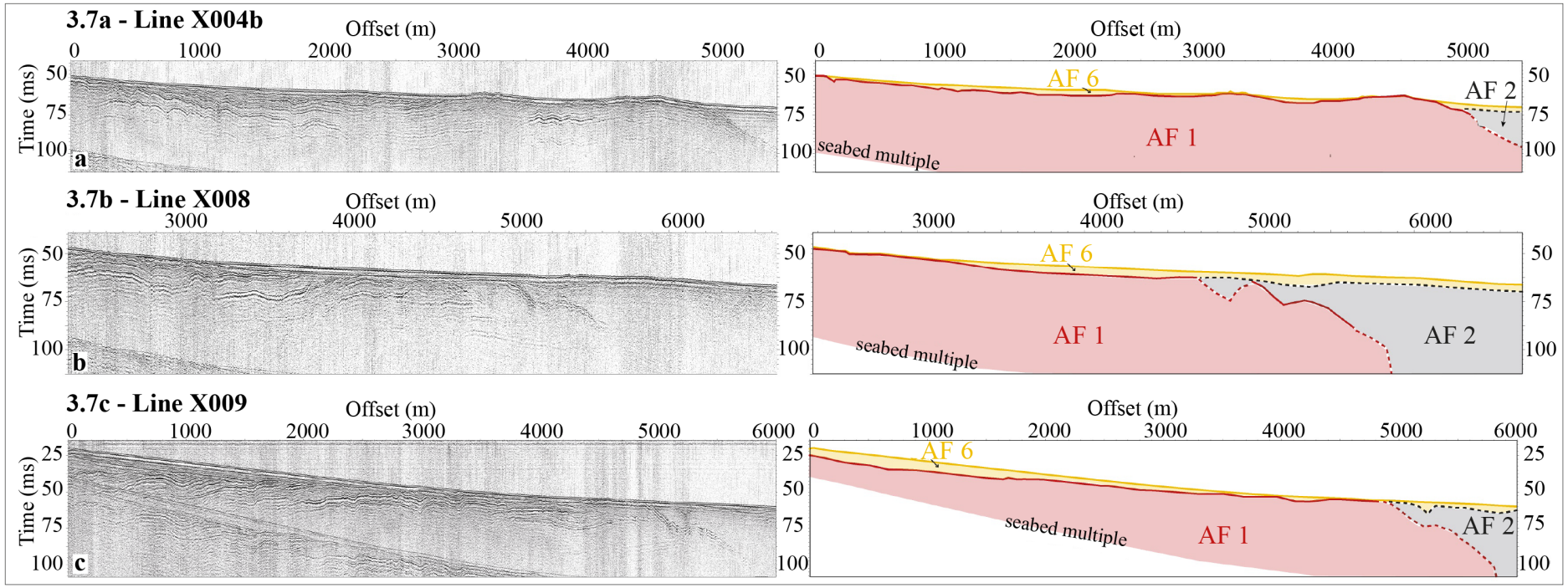

Figure 3.7: (left) W - E orientated profiles X004b (3.7a), X008 (3.7b) and X009 (3.7c) and their correspondent facies interpretation (right). The dashed lines represent inferred boundaries. The location of the profiles are indicated in red in Fig. 3.5 (3.7a, 3.7b, 3.7c).

chaotic reflectors (Fig. 3.6 and 3.7) which are generally difficult to observe along the profiles. Towards the easternmost part of the survey, the reflectors are mostly visible in the vicinity of the irregular and wavy upper boundary of the facies (Fig. 3.7 and 3.8). The limit between AF 1 and AF 2 is clear (Fig. 3.7), but the lower boundary of AF 2 is not visible from the profiles (Fig. 3.7 and 3.8). Only the upper boundary of the facies can be observed, particularly towards the east (Fig. 3.8). Based on the mapped geology of the area, AF 2 is interpreted as composed of Upper Permian sequences (BGS Offshore Regional Report; Cameron *et al.*, 1992; Gatliff *et al.*, 1994).

AF 3

In the easternmost part of the survey, at ∼12 km from the coast along the profiles, AF 2 deepens into the sequence and is overlain by AF 3, which extends to the east for ∼2.5 km from its first appearance until the end of the profiles (Fig. 3.8). When observing the sequence in a W - E direction, AF 3 generally appears at ∼100 ms depth as a thin layer, and then becomes thicker, reaching up to ∼40 ms thickness (∼34 m) and ∼140 ms depth in the most eastern part of the profiles (Fig. 3.8). The upper boundary of AF 3 appears to be flat (Fig. 3.8 and 3.9) and, while the internal structure of its reflectors is not always clear, at times the reflectors show a weak wavy parallel configuration (Fig. 3.6, 3.8 and 3.9). At the upper boundary of the facies, the reflectors of AF 3 appear truncated, thus showing evidence of erosion, while at the lower boundary of the facies, the reflectors appear conformable with the underlying AF 2 (Fig. 3.8). Laterally, AF 3 appears to onlap the unit below (Fig. 3.8a).

AF 4

AF 4 (in pink, Fig. 3.8 and 3.9) appears in the sequence at ∼12 km from the coast, where it is found at ∼96 ms depth. The facies overlies AF 3 and extends laterally for ∼2.5 km towards east until the end of the profiles. The upper boundary of AF 4 appears to be relatively flat, although wavy at times, and is often discontinuous, thus making it difficult to clearly follow the facies' geometry. AF 4 is relatively thin throughout the entire survey and reaches a maximum thickness of ∼10 - 12 ms (∼8.5 - 10.2 m, Fig. 3.8 and 3.9). The internal structure of its reflectors is very difficult to detect, although at times they appear to be discontinuous and chaotic (Fig. 3.6, 3.8 and 3.9). Towards the west, it is not clear if AF 4 onlaps the facies underneath (Fig. 3.8).

AF 5

AF 5 is found on top of AF 4 and is acoustically very similar to it (Fig. 3.6). The facies also appears from ∼12 km from the coast and extends laterally towards the east. It is relatively thin throughout the entire survey and reaches a maximum thickness of ∼10 ms (∼8.5 m, Fig. 3.8). The upper boundary of AF 5 appears relatively flat, although wavy at times, and the geometry of its internal reflectors is also not clearly defined, although, when visible, the reflectors appear chaotic (Fig. 3.6, 3.8 and 3.9). Towards the west, it is not clear if AF 5 onlaps the facies underneath.

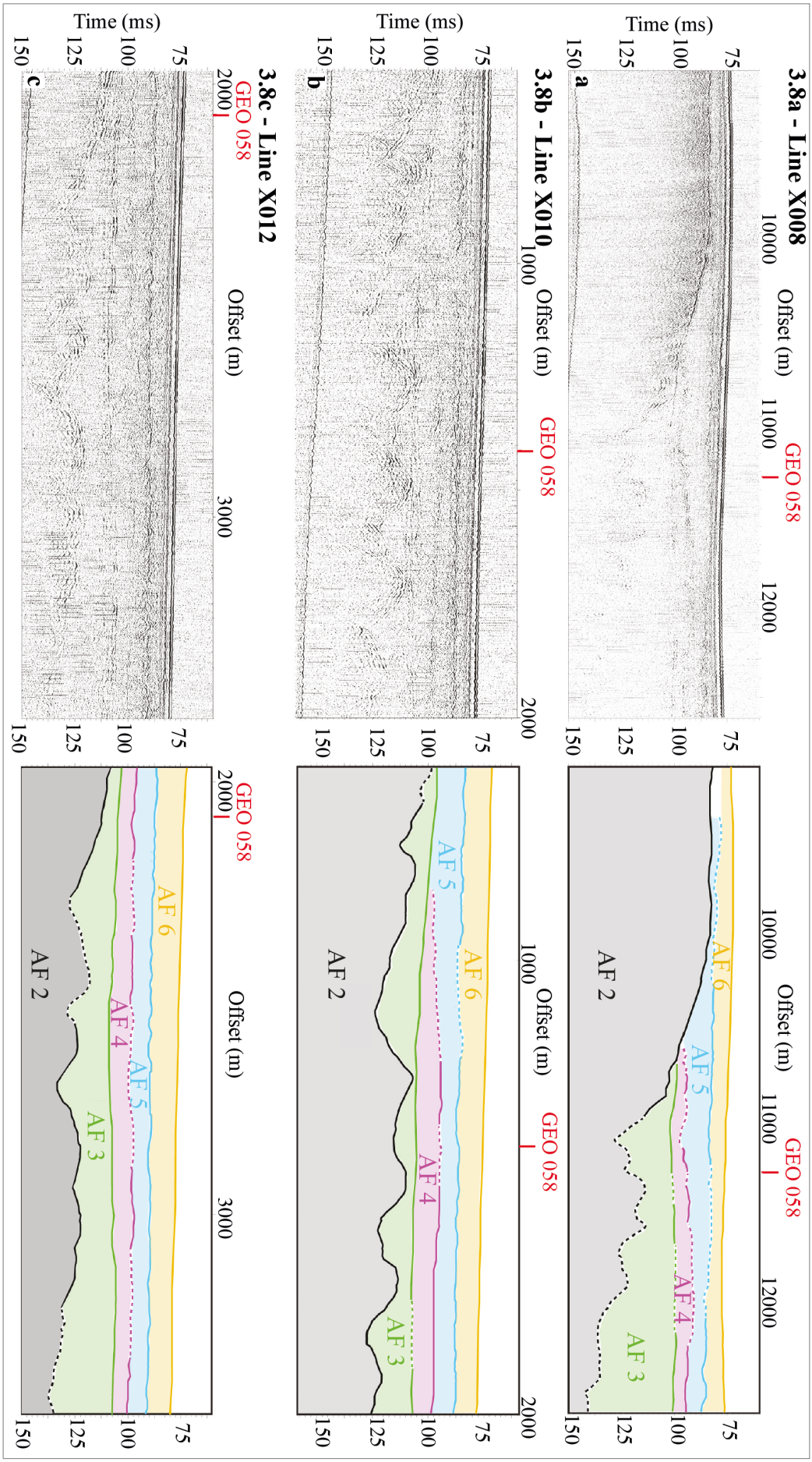

Figure 3.8: (left) W - E orientated profiles X008 (3.8a), X010 (3.8b) and X012 (3.8c) and their correspondent facies interpretation (right). The intersection with cross-profile GEO 058 (Fig. 3.9) is shown with red tick marks. The location of the profiles are indicated in green in Fig. 3.5 (3.8a, 3.8b, 3.8c).

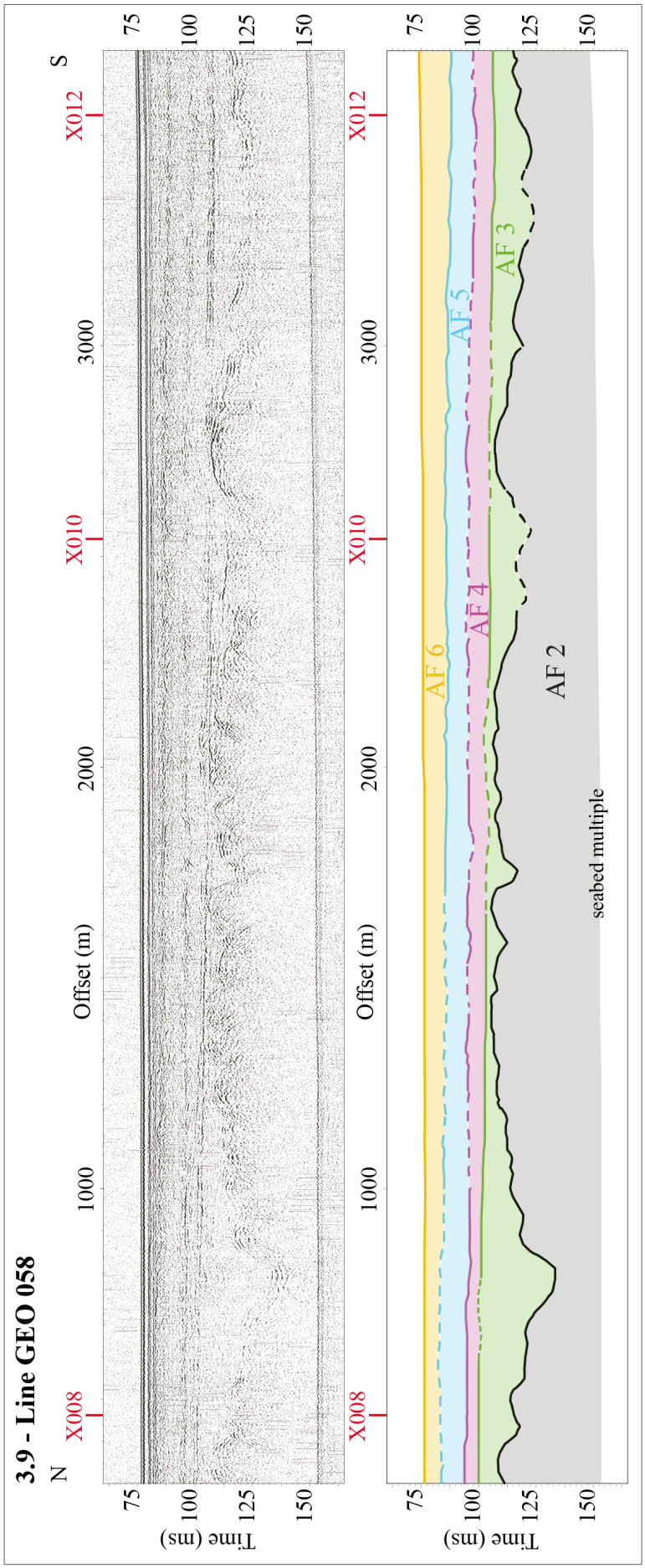

Figure 3.9: N - S orientated profile GEO 058 (top) and facies interpretation (bottom). The location of the profiles from Figure 3.8 that intersect this seismic line are shown with red tick marks. The dashed lines represent uncertain mapping of the horizons. The location of this profile is shown in brown in Figure 3.5 (3.9).

AF 6

The uppermost facies of the sequence, AF 6, has been mapped in the survey on top of AF 1 and AF 2 close to the coast, where it is discontinuous and interrupted by bedrock outcrops (Fig. 3.7), and on top of AF 5 towards the east (Fig. 3.8 and 3.9). The thickness of the facies varies throughout the survey, from an average of ∼4 ms (∼3.4 m) to a maximum of ∼10 - 15 ms (∼8.5 - 12.7 m) towards the easternmost part of the survey (Fig. 3.8 and 3.9), and the facies is delimited at the top by the seabed. The internal reflectors of AF 6 show two different geometries, a parallel one (AF 6a) which lies on top of a discontinuous and chaotic one (AF 6b; Fig. 3.6). It is at times difficult to identify a limit between the two, possibly also due to the vicinity of the facies to the seabed and to the presence of background noise in the profiles.

An example of the geometry of the entire seismic sequence, as observed both close to the coast and in the easternmost part of the survey, is shown in Figure 3.10 and 3.11 (location shown in Fig. 3.5 and in the insert maps). W - E orientated profiles X008 and X015 are shown together with the N - S orientated cross-profile ENV 010 in Figure 3.10. Here, it is possible to see the typical geometry of the bedrock strata close to the coast, which is characterised by the presence of Carboniferous bedrock (AF 1) that crops out at the seabed or is present at a very shallow depth below AF 6. It is also possible to see how the internal bedding planes of AF 1 are truncated at their upper boundary and dip at a relatively high angle towards the west close to the coast. Following the profiles towards the east, we can observe how the Carboniferous strata deepens in the sequence and the Permian bedrock appears on top of it (AF 2). The upper limit of this facies is very difficult to follow along the profiles and has been indicated with a black dashed line. AF 6 is present at the top of the sequence. N - S orientated profile GEO 061 is shown in Figure 3.11, together with the W - E orientated cross-profiles X008, X010 and X014. The figure shows a change in the geological sequence. While AF 2 deepens in the sequence, facies AF 3, AF 4, AF 5 and AF 6 appear on top of it, with the latter once again representing the uppermost facies of the sequence. It is possible to see how the upper boundary of AF 2 dips at a relatively high angle where AF 3 onlaps it. This latter facies extends until the end of the profiles and seems to infill the Permian bedrock (AF 2) underneath. At this scale, we can see how the upper boundary of AF 3 is relatively flat, which could indicate that it is erosional, although this will be further discussed in Section 3.4. AF 4 and AF 5 are present on top of AF 3 and they both display similar thickness and slightly irregular upper boundaries, both of which are often difficult to detect (dashed lines, Fig. 3.11).

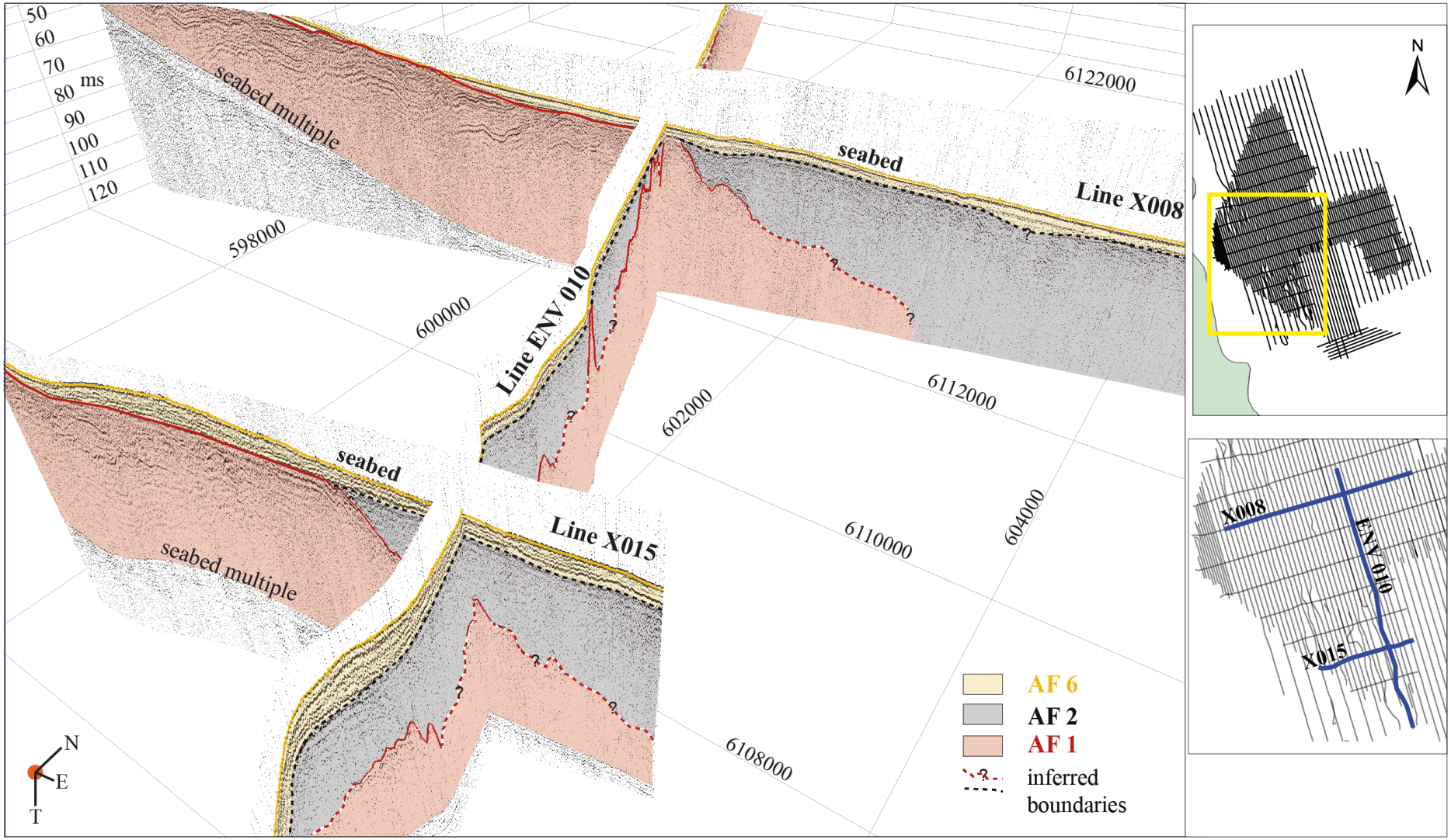

Figure 3.10: Fence diagram representative of the facies architecture observed in the western part of the Blyth survey.

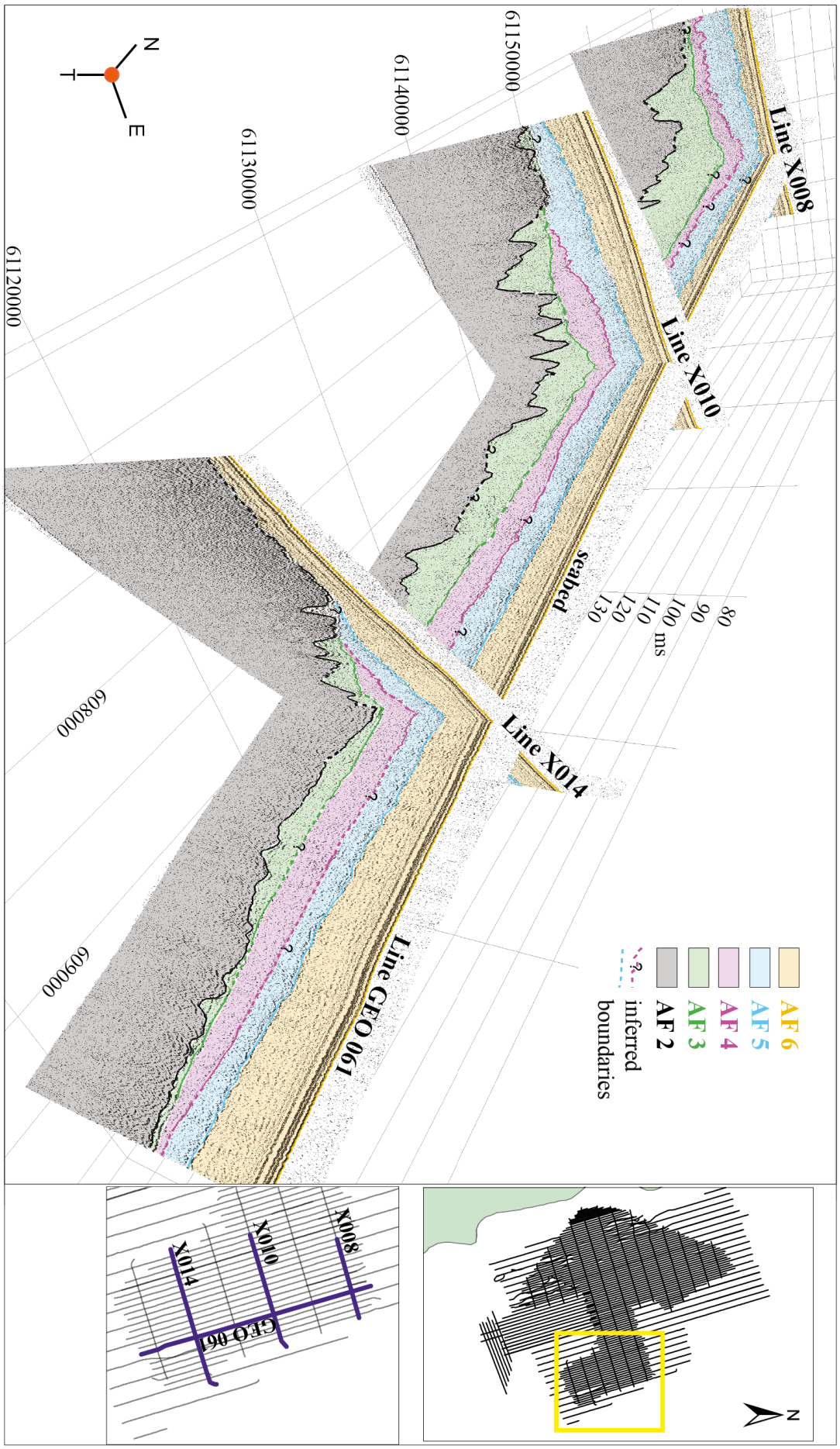

Figure 3.11: Fence diagram representative of the facies architecture observed in the eastern part of the Blyth survey.

3.4 Interpretations and Discussion

AF 1 and AF 2 have been previously interpreted as pre-Quaternary strata, specifically as composed of Carboniferous and Permian sediments (Cameron *et al.*, 1992; Gatliff *et al.*, 1994). AF 3 is more challenging to interpret but occurs directly on top of the Permian strata. It appears to infill the geology underneath (Fig. 3.11) and the reflectors at its lower boundary appear to be conformable with the underlying bedrock surface. Furthermore, the internal reflectors of AF 3 appear to have a weak, wavy parallel configuration (Fig. 3.6). Considering the acoustic signature of this facies and the information gathered from the BGS geological maps (Cameron *et al.*, 1992; Gatliff *et al.*, 1994), we interpret AF 3 to be composed of Triassic sediments.

AF 4 and AF 5 display similar acoustic signatures to one another. They are both characterised by discontinuous chaotic reflectors, are delimited at the top by an irregular upper boundary (Fig. 3.6 and 3.11), and have a relatively low thickness ($\sim$10 - 12 ms). Based on the BGS geology maps and information on the area (Cameron *et al.*, 1992; Gatliff *et al.*, 1994), and on the seismic character of the two facies, we interpret AF 4 and AF 5 as possibly composed of glacigenic diamicts.

Finally, AF 6 is found at the top of the seismic sequence in the study area. It has a varying thickness, being generally thinner close to the coast, where bedrock strata often outcrop, and thicker towards the easternmost part of the survey (Fig. 3.10 and 3.11). It is characterised by parallel to chaotic reflectors and is bounded at the top by the seafloor. Based on the BGS Offshore Regional Reports we interpret AF 6 as being composed of deglacial to Holocene sediments (Cameron *et al.*, 1992; Gatliff *et al.*, 1994).

3.4.1 Pre-Quaternary

The BGS has mapped the bedrock outcrops in the North Sea basin (as shown in Fig. 2.2, in Chapt. 2), and a close-up of the bedrock outcrops mapped in correspondence to the Blyth survey is shown in Figure 3.12. The Carboniferous and Permian strata (in grey and pink, respectively, in Fig. 3.12) are the principal bedrock formations that crop out within the Blyth survey area (Cameron *et al.*, 1992; Gatliff *et al.*, 1994). Figure 3.13 shows a comparison between two seismic profiles acquired from the BGS with a Sparker (Line 2 and 3 from the BGS survey 1982-3, Fig. 3.13a and b), and two Blyth profiles (X008 and X009, Fig. 3.13c and d), all orientated W - E and located across the mapped Carboniferous-Permian limit (the location of these profiles is marked in yellow in Fig. 3.12 with their correspondent figure number). The four profiles show a clear change in the acoustic response from west to east, in the lower part of the sequence, and the two different facies identified were correlated to the Carboniferous and Upper Permian formations. Along the BGS profiles, the geometry of the internal reflectors in the Carboniferous formation is clearly visible and was highlighted with solid red lines (Fig. 3.13a and b). The reflectors display a parallel configuration, and appear folded and at times faulted. The Permian unit displays mainly chaotic reflectors. The Blyth profiles correlate well with those of the BGS and they show similar characteristics. The parallel reflectors of the Carboniferous sediments are evident, while the Permian reflectors are

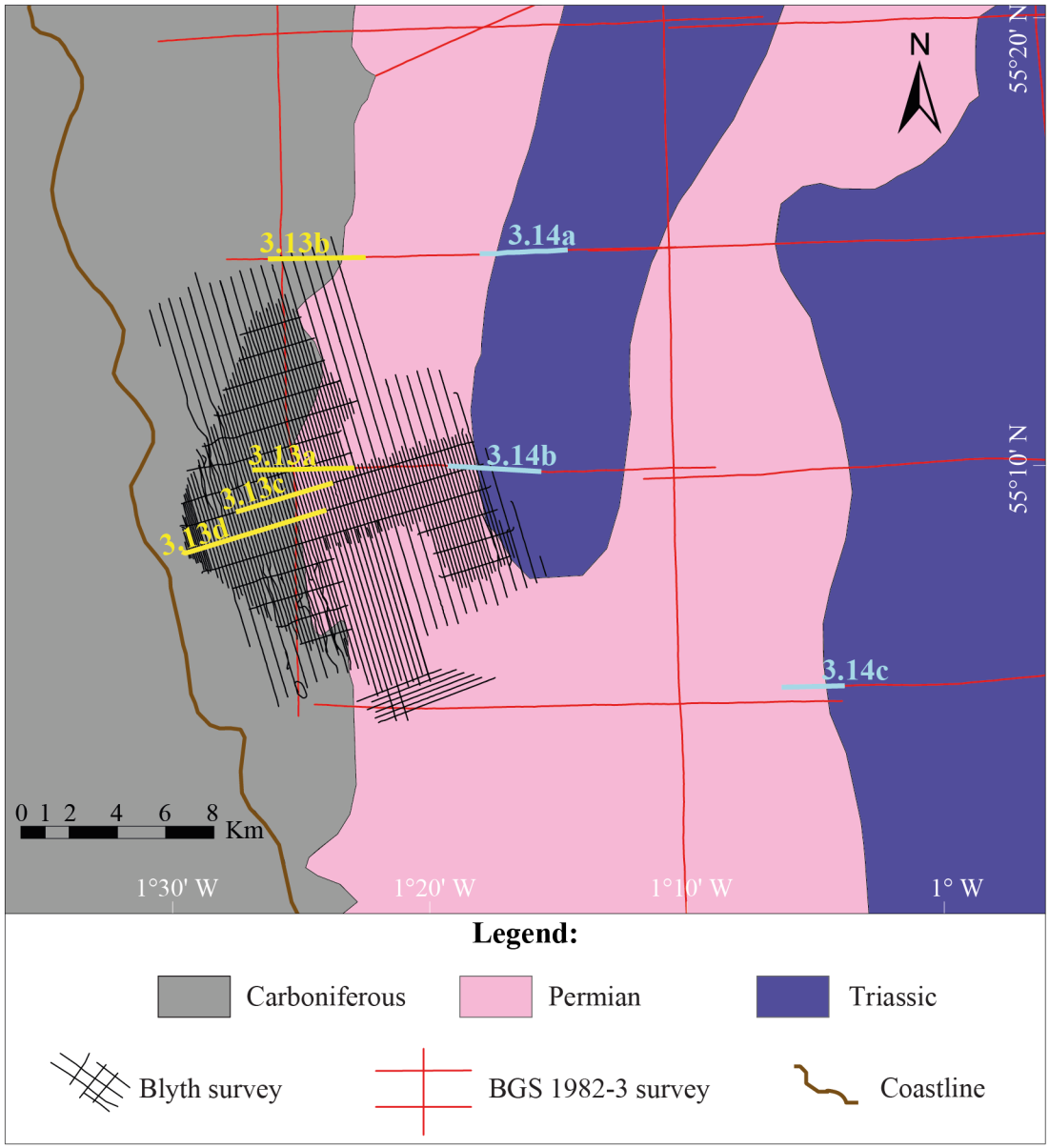

Figure 3.12: Pre-Quaternary units outcropping in the Blyth survey area, modified from the BGS Offshore Regional Reports and the BGS DigRock250k map. The location of the profiles shown in Figure 3.13 and 3.14 are indicated with different colours and the correspondent figure number.

less visible, and appear to be better detected in the Sparker profiles. The limit between the two facies is also clear from the acoustic profiles (dashed red line, Fig. 3.13). It is inclined and dips towards the south-east. The Carboniferous sediments in the North Sea basin are known to be displaced by numerous faults, which developed in response to the Variscan orogeny (see Chapt. 2; Cameron *et al.*, 1992; Glennie, 1998). These faults often propagate upwards into the overlying strata, and cause further deformation. The presence of faults in the Carboniferous strata has also been observed on the bathymetry data and along the seismic profiles of the Blyth survey (Fig. 3.3 and 3.7). The faults are believed to cause displacement and folding, resulting in the deformation of the Upper Permian strata above.

The Upper Permian (Zechstein) sediments are known to be composed of shale, carbonates

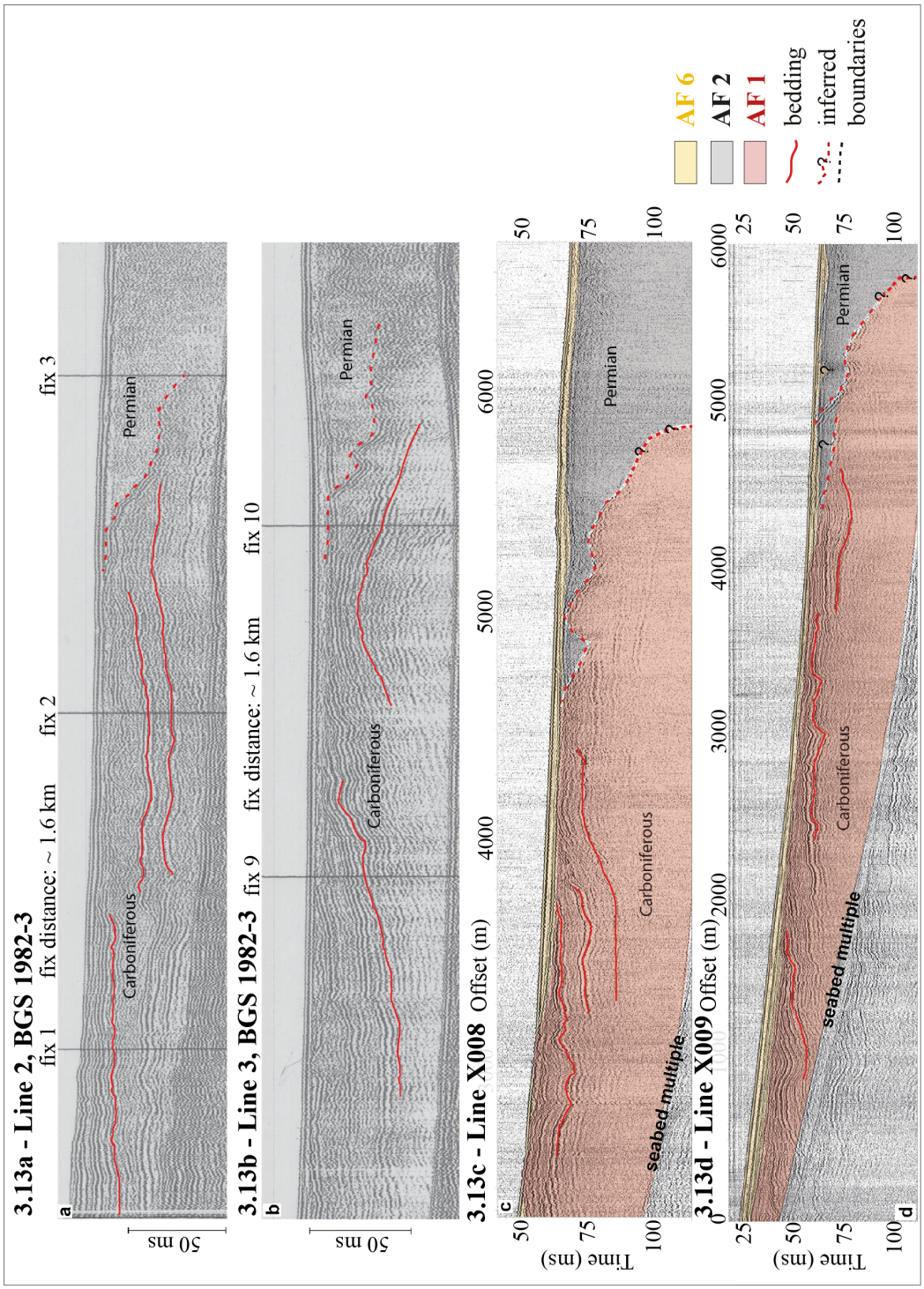

Figure 3.13: BGS 1982-3 survey lines 2 and 3 and Blyth survey lines X008 and X009 and interpreted geological facies.

and evaporites and have been subdivided into five/six clastic-carbonate-anhydrite-salt Zechstein cycles (Z1 - Z6; Taylor, 1990; Tucker, 1991; Cameron *et al.*, 1992; Gatliff *et al.*, 1994). These sediments, and particularly the evaporites, appear to be thicker in the central North Sea, where salt movements occur (Taylor, 1990; Cameron *et al.*, 1992; Gatliff *et al.*, 1994). The Zechstein sediments are in fact known to be characterised by salt diapirism and salt withdrawal, which are believed to have caused deformation of the overlying strata (Taylor, 1990; Cameron *et al.*, 1992; Gatliff *et al.*, 1994; Glennie, 1998). This salt diapirism phenomenon, affecting the Upper Permian sediments, has mainly been reported in the central and northern North Sea and appears to be absent within the study area (Gatliff *et al.*, 1994). From the Blyth survey profiles, we can observe how the Upper Permian strata (AF 2) is characterised by a very irregular upper boundary, that appears wavy (Fig. 3.11), although it is not always possible to follow it throughout the entire survey. Given that this area of the western North Sea is thought not to be affected by halokinesis, we infer that the Zechstein sediments observed here have been influenced and displaced by the presence of faults lower in the sequence, which affected the layers above. In addition, the geometry of the upper boundary of the Permian unit may indicate incision and erosion after deposition. After the last marine incursion during Permian time, much of the British area was low-lying and permitted the accumulation of Triassic sediments. These were deposited in a continental environment and were laid down as fluvial and later aeolian sequences. Fluvial erosion may have resulted in the irregular and incised upper boundary of the Permian sequence (Cameron *et al.*, 1992; Benton *et al.*, 2002).

On top of the Carboniferous and Permian strata, AF 3 - 6 have been mapped along the Blyth profiles. AF 3 is the thickest facies of this upper sequence and the Boomer profiles displayed in Figure 3.8, 3.9 and 3.11 show how the upper boundary of this layer appears flat throughout the entire survey. Although the Blyth profiles appear generally noisy, in some areas it is possible to see that AF 3 is characterised by wavy parallel reflectors (Fig. 3.6). In seismic stratigraphy the presence of parallel reflectors may suggest a uniform rate of sediment deposition and subsidence in an undisturbed environment (Sheriff, 1980; Emery & Myers, 1996). The flat upper boundary of the facies appears to cut out the internal reflectors of AF 3 abruptly, and it is hence thought to be an erosional contact. Because of these particular seismic characteristics, together with the geological information available for the area, we interpret AF 3 as composed of Triassic sediments (Cameron *et al.*, 1992; Gatliff *et al.*, 1994; Glennie, 1998). Triassic sediments have been mapped previously in the Blyth area and are thought to outcrop, below Quaternary facies, in correspondence to the easternmost part of the survey (in violet in Fig. 3.12; Cameron *et al.*, 1992; Gatliff *et al.*, 1994). Typically, the acoustic response of Triassic sediments is characterised by parallel reflectors, which often appear folded and faulted, and the unit is usually found on top of Upper Permian sediments (see also Chapt. 2), and appears to infill the irregular geometry of the Upper Permian formation. Figure 3.14 shows three different segments of Sparker profiles acquired during the BGS 1982-3 survey (the location of these profiles is marked in light blue in Fig. 3.12 with their correspondent figure number). These seismic sections show the different acoustic responses of both Permian and Triassic sediments which were mapped in the area (Fig. 12; BGS DigRock 250k map).

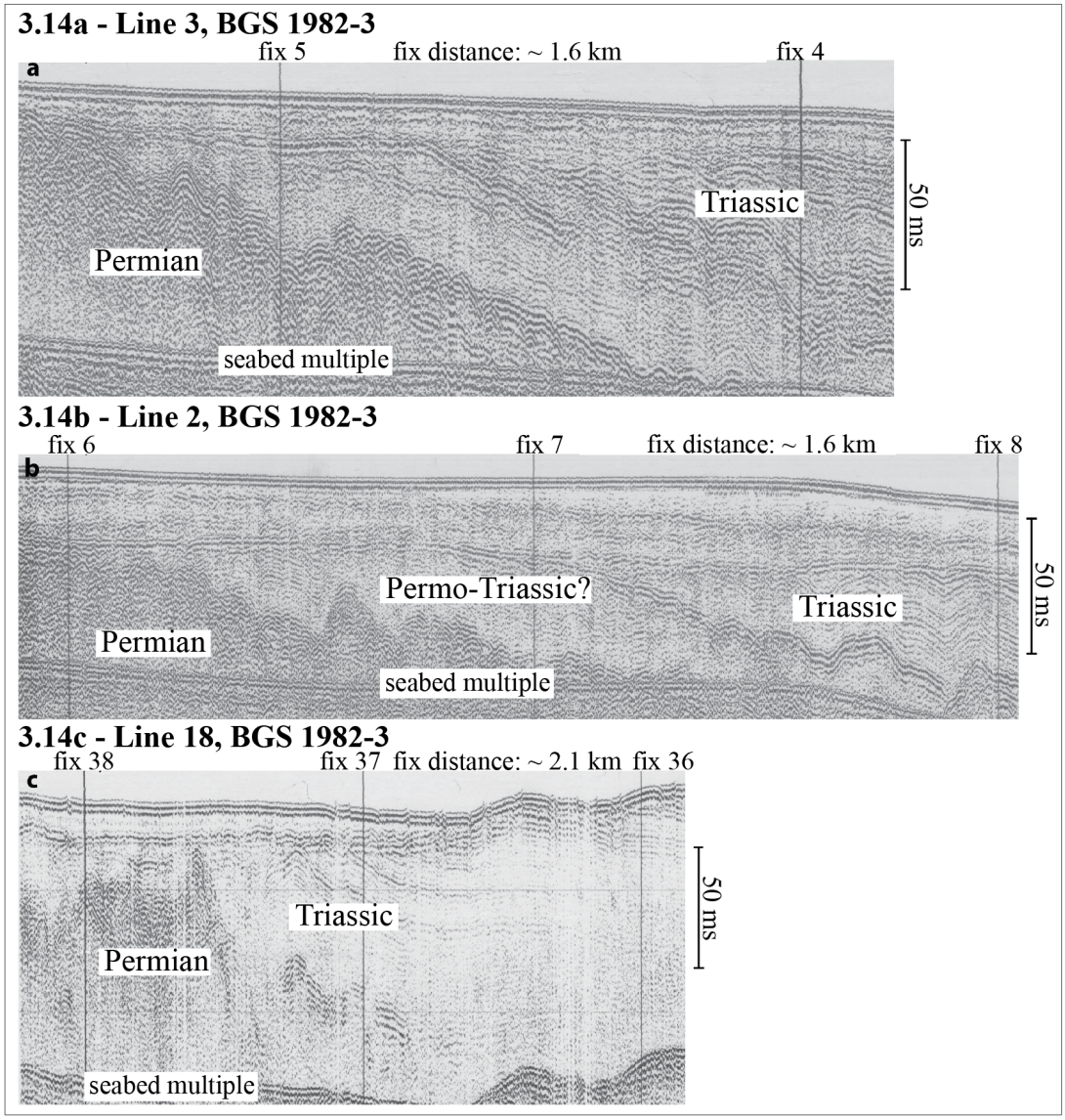

Figure 3.14: BGS 1982-3 Line 3 (3.14a), Line 2 (3.14b) and Line 18 (3.14c) showing the acoustic responses of Permian and Triassic sequences. Interpretations compiled from the BGS Offshore Regional Reports (Cameron *et al.*, 1992; Gatliff *et al.*, 1994). The location of the profiles are indicated in light blue in Fig. 3.12 (3.14a, 3.14b, 3.14c).

The Permian unit is characterised by an irregular and wavy upper boundary and by chaotic reflectors, while the Triassic unit shows wavy parallel reflectors which seem to follow the geometry of the layer underneath. The upper boundary of the Triassic unit appears flat and truncates its reflectors abruptly (e.g. Fig. 3.14b).

In the Blyth survey area, AF 3 is found directly on top of the Upper Permian strata (AF 2; Fig. 3.11). At the bottom boundary, the internal reflectors of AF 3 appear concordant with the underlying geology and the facies seems to infill the basins formed by the Permian formation underneath (Fig. 3.8, 3.9 and 3.11). These characteristics are similar to what can be observed from the BGS 1982-3 profiles shown in Figure 3.14. Line 2 (Fig. 3.14b) of the BGS 1982-3 survey is particularly helpful for comparison because it is located within the Blyth

survey acquisition grid (Fig. 3.12 and 3.15). Part of this profile has been shown in Figure 3.15 together with two cross-profiles of the Blyth survey: N - S orientated Line GEO 061 and W - E orientated Line X009. The flat upper boundary of the Triassic sediments, which truncates the reflectors underneath, has been marked in green on Line 2 (Fig. 3.15a). The upper boundaries of AF 3 along the two Blyth profiles have also been marked in Figure 3.15b and c, and they appear at the same depth below the seabed ($\sim$25 ms) as the Triassic boundary observed in Line 2, which is why it is inferred they are the same feature. Also, the Triassic sediments show a wavy parallel configuration, which correlates to the observation of the internal reflectors of AF 3 (Fig. 3.15b and c). For these reasons, it is inferred that AF 3 is composed of Triassic sediments. As shown above in Figure 3.12, the BGS has previously mapped the presence of Triassic sediments in correspondence to the study area (see also Chapt. 2). Close to the English coasts, these sediments are known to reach up to 500 m in thickness (Gatliff *et al.*, 1994), while they become much thicker towards the central and northern areas of the central North Sea, reaching more than 1500 m in thickness (Gatliff *et al.*, 1994). According to the BGS pre-Quaternary map (Fig. 3.12), the Triassic formation is supposed to be outcropping (below Quaternary sequences) only in the most eastern sector of the Blyth survey (Fig. 3.12). This corresponds to the observed extension of AF 3 in the survey area and thus corroborates the proposed interpretations.

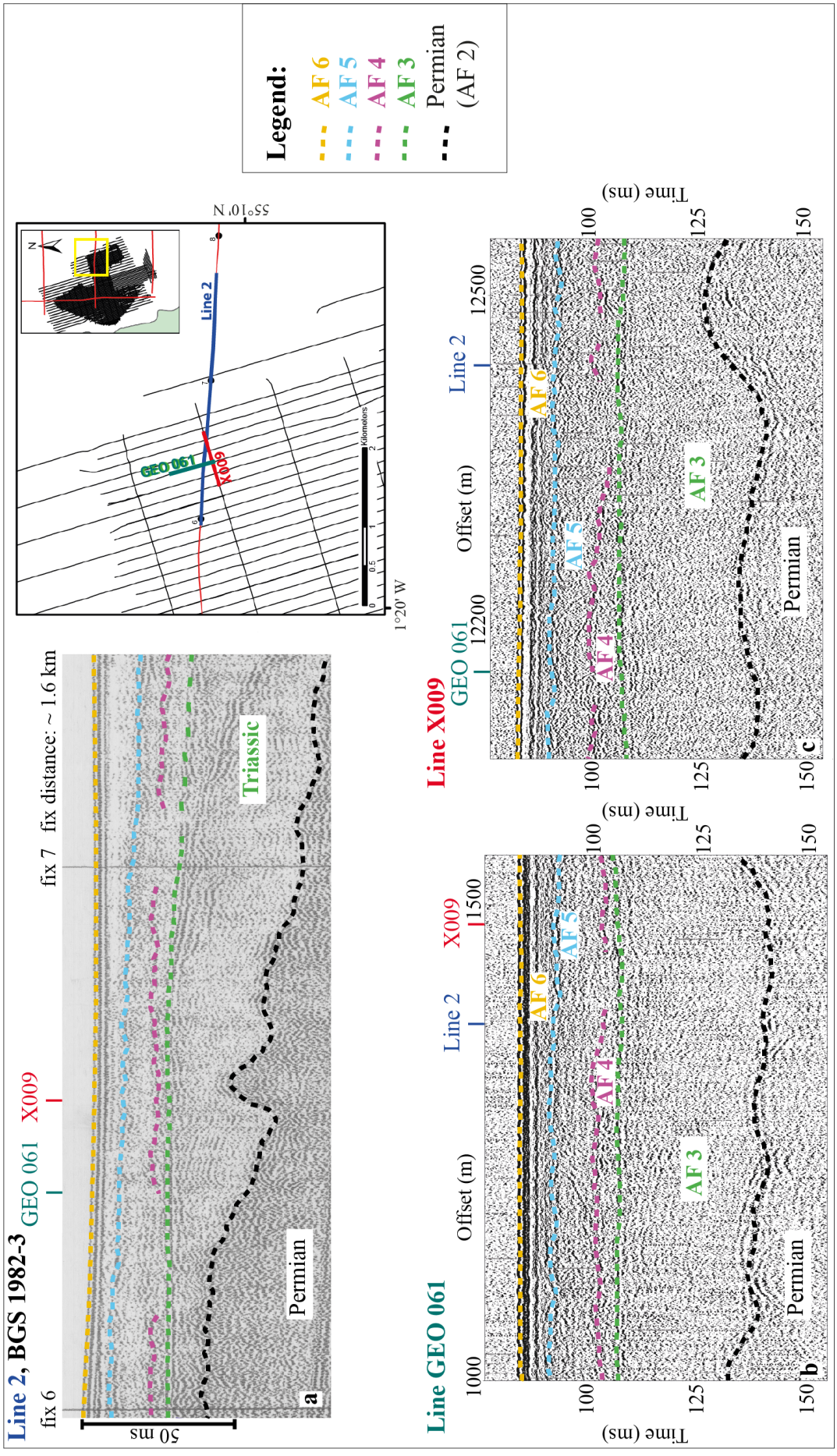

Figure 3.15: a: segment of Line 2 (BGS 1982-3 survey). b, c: cross-profiles of Line GEO 061 and X009 (Blyth survey). Facies upper boundaries are also shown.

3.4.2 Quaternary

As previously discussed in Section 3.1 and Chapter 2, according to the BGS Offshore Regional Reports for the southern and central North Sea, three different formations occur on top of the pre-Quaternary strata in the vicinity of the study area: the Wee Bankie, the St Abbs and the Forth formations (Fig. 3.16, see also Chapt. 2; Gatliff *et al.*, 1994). Figure 3.16 shows how both the St Abbs and the Forth formations are present as lenses in this region of the western North Sea, while the surrounding geology appears to be mainly composed of the Wee Bankie Formation and of pre-Quaternary strata (see also Fig. 2.4, in Chapt. 2). The presence of these three formations has also been observed along Line 2 from the BGS 1982-3 survey displayed in Figure 3.15a, where they lay on top of pre-Quaternary formations. Their upper boundary can be correlated to the upper boundaries of AF 4 - 6 observed along the Blyth profiles (Fig. 3.15b and c), and it could be thus tentatively suggested that AF 4 corresponds to the Wee Bankie Formation, AF 5 to the St. Abbs Formation and AF 6 to the Forth Formation. On seismic profiles, AF 4 and AF 5 generally appear to be very discontinuous and are characterised by a chaotic acoustic response (Fig. 3.6). Such properties could be correlated to the acoustic response given by till sediments, which usually show a chaotic internal geometry or appear transparent, due to the heterogeneous nature of the sediments that characterise them (Cameron *et al.*, 1992; Gatliff *et al.*, 1994; Huuse & Lykke-Anderson, 2000). AF 4 and AF 5 are thus tentatively interpreted to be diamictons, and possibly tills. The BGS described the Wee Bankie Formation in seismic section as a facies characterised by a sheet-like geometry, an uneven thickness and an irregular upper contact, with chaotic internal reflectors (Gatliff *et al.*, 1994; Golledge & Stoker, 2006). The acoustic response of the Wee Bankie Formation therefore appears similar to the response of AF 4 and this could indicate that the two are in fact the same type of facies. From correlation with onshore tills, the Wee Bankie Formation has been inferred to be of Late Devensian age. At times, the facies has also been found directly on top of Triassic sediments (Gatliff *et al.*, 1994). This is consistent with the observations of AF 4.

If AF 4 is the Wee Bankie Formation, it would follow that the overlying AF 5 represents either the St Abbs or the Forth formations, based on the mapped geology of the area (Fig. 3.16; Cameron *et al.*, 1992; Gatliff *et al.*, 1994). The acoustic appearance of the St Abbs Formation has been described as structureless, with only faint and discontinuous subparallel reflectors and the facies has been mapped on top of either the Wee Bankie Formation or of pre-Quaternary strata (Gatliff *et al.*, 1994). The Forth Formation instead has been described as characterised by subparallel or oblique reflectors, with only its more recent member being generally acoustically amorphous (Gatliff *et al.*, 1994). AF 5 does not show subparallel or oblique reflectors, unlike the Forth Formation, and could thus correlate with the structureless appearance of the St Abbs Formation. Nonetheless, the acoustic appearance of AF 5 is very similar to AF 4 (Fig. 3.6), hence the facies was initially interpreted as a second diamicton and possibly a till unit. However, the fact that the BGS and the Blyth surveys were acquired with different equipment needs to be taken into consideration. The Sparker system utilized for the acquisition of the BGS survey, while capable to penetrate deeper below the seabed, is of lower resolution compared to the Boomer system used to acquire the Blyth profiles. Consequently, there is inconsistency between the two surveys, particularly when describing

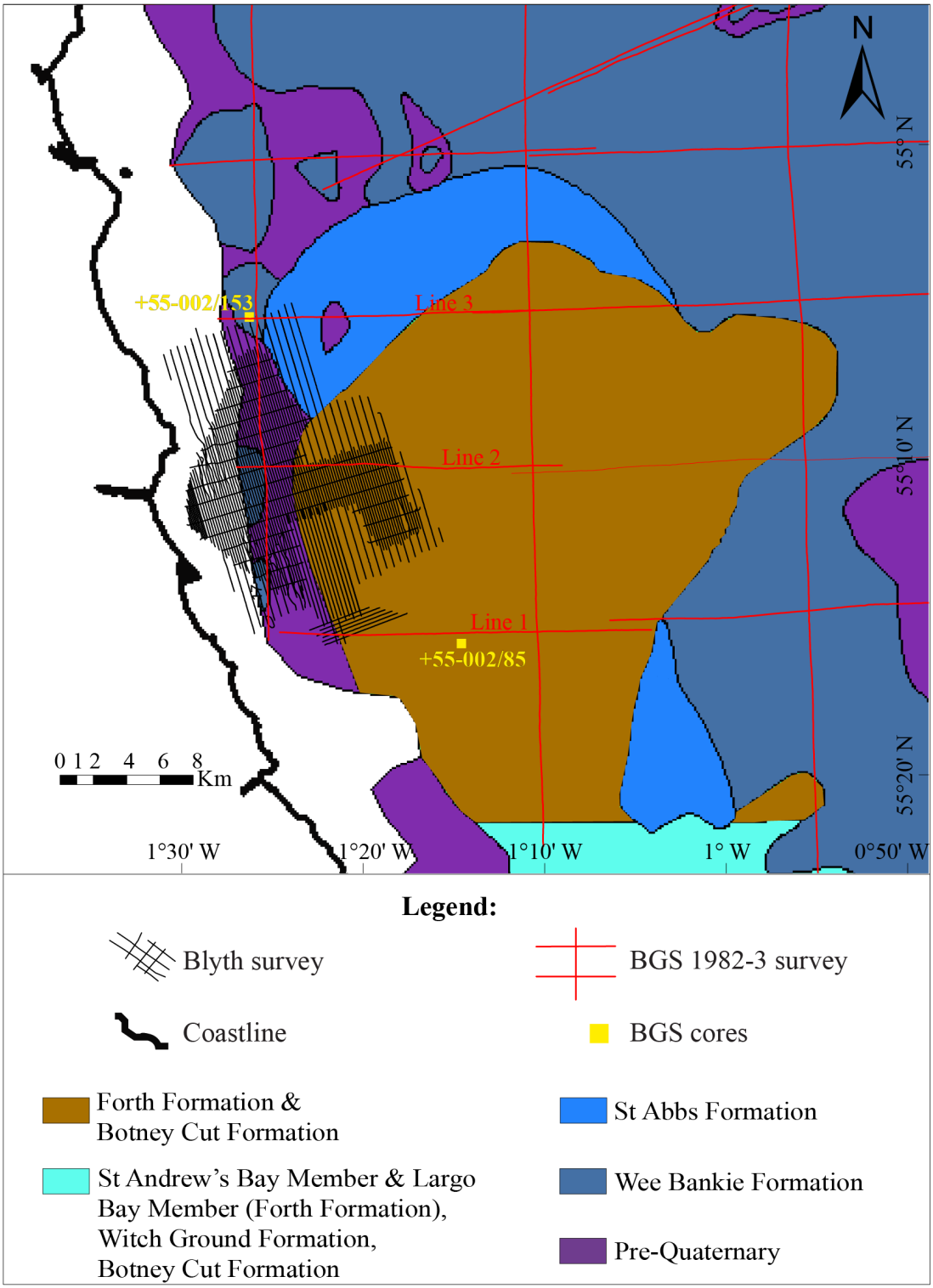

Figure 3.16: Map of the Quaternary sediments in the Blyth survey area, compiled from the British Geological Survey Quaternary Sheets and based on Gatliff *et al.* (1994) and Cameron *et al.* (1992). With the permission of the British Geological Survey.

the internal acoustic responses of the different facies. This appears to be less noticeable only for the responses of high amplitude and strong reflectors, such as the ones of the Carboniferous strata. AF 5 is thus considered to be either a subglacial or a glaciomarine facies, such as the St Abbs Formation.

On top of AF 5, AF 6 has been mapped in the Blyth survey. The BGS mapped the Forth Formation as the uppermost sequence in the area and described it as composed of marine, glaciomarine, fluviomarine and estuarine facies of Late Devensian to Holocene age (Gatliff *et al.*, 1994). As mentioned above, its acoustic appearance has been described as characterised by oblique and subparallel reflectors, although the facies can also be acoustically amorphous (Gatliff *et al.*, 1994). Considering that AF 6b displays chaotic reflectors (Fig. 3.17), and that it is found in correspondence to the area where a lens of Forth Formation (Fig. 3.16) was identified by the BGS, the facies is here correlated to the Forth Formation sequence. In contrast, the acoustic appearance of AF 6a is characterised by parallel reflectors, which would suggest it is composed of Holocene sediments.

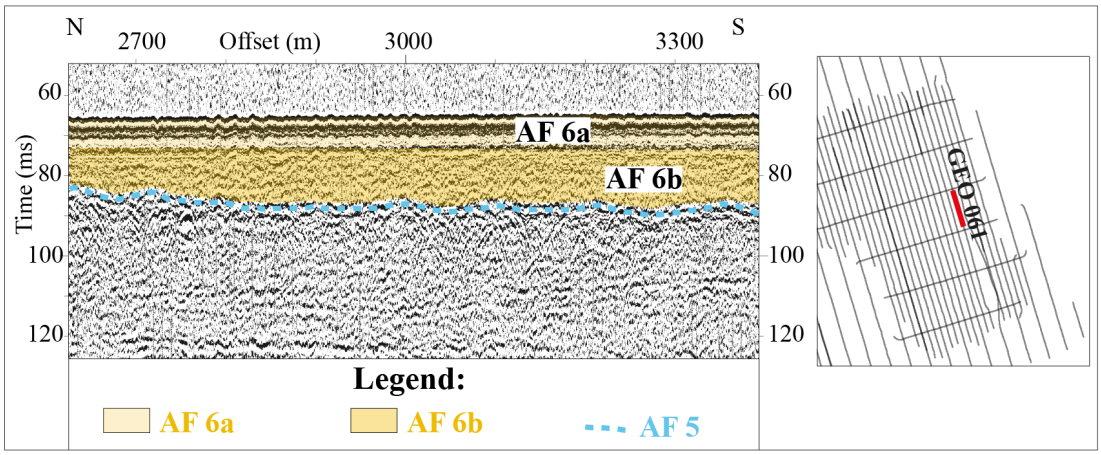

Figure 3.17: Segment of the GEO 061 seismic profile of the Blyth survey (location in the insert map), showing a detail of the acoustic character of AF 6a and AF 6b. The upper boundary of AF 5 is also indicated (dashed light blue line).

The BGS borehole logs and core logs available for the western North Sea were also taken into account during the analyses of the Blyth survey. Two sediment cores were collected relatively close to the Blyth study area, one to the north and the other one to the south-east of the survey (Fig. 3.16), although only a very small amount of sediment was recovered from both cores. The northernmost BGS +55-002/153 sediment core was characterised by only 0.15 m of sediment and was described by the BGS as being composed of dark reddish gray, muddy gravel, with pebbles up to 90 mm in size, on reddish brown till. The second core, BGS +55-002/85, located to the south (Fig. 3.16), was characterised by only 0.25 m of sediments and described as composed of dark brown, clayey sand, on top of sandy mud, on top of stiff brown clay, defined as till. If correlated to the Blyth survey profiles, both cores would only penetrate slightly into the uppermost facies of the sequence, AF 6a. The available documentation for both cores is very limited and not detailed enough to consider the two cores as valid additional evidence. Furthermore, according to the BGS Offshore Regional Reports, sea-bed sediments in the research area are characterised by muddy sand with lenses of gravelly muddy sand and muddy sandy gravel (Gatliff *et al.*, 1994). These sediments, where present, are usually on top of Holocene and Pleistocene deposits or bedrock (Gatliff *et al.*, 1994). These considerations would suggest that the sediments collected from the two BGS cores discussed above could

relate to sea-bed sediments more than to tills. Alternatively, the cores sediments could indicate the presence of diamictons, and possibly till units, close to the seabed. Nevertheless, only the collection of new and deeper sediment samples in the area can clarify these assumptions.

In summary, AF 4 could correlate to the Wee Bankie Formation, AF 5 to the St Abbs Formation or to another diamicton, possibly a till unit, and AF 6b to the Forth Formation, or, as for AF 6a, it could be composed of more recent Holocene and sea-bed sediments. Information collected from onshore studies also needs to be taken into account with respect to these interpretations. The upper LGM till from County Durham, the Horden Till, is thought to be correlative with the Skipsea Member of the Holderness Formation and with the Bolders Bank Formation in the North Sea (see also Chapt. 2; Cameron *et al.*, 1992; Carr *et al.*, 2006; Davies *et al.*, 2009a, 2011, 2012a; Livingstone *et al.*, 2012b). The Bolders Bank Formation is believed to represent the easternmost extension of the NSL and has been described as the south-eastward continuation of the Wee Bankie Formation to the south of 56° N and east of 0° (Gatliff *et al.*, 1994). If AF 4 is in fact the Wee Bankie Formation, it could be inferred to be the correlative of the onshore Horden Till, deposited by the NSL during the Dimlington Stadial (Fig. 3.18; Davies *et al.*, 2012a; Livingstone *et al.*, 2012b). Alternatively, AF 4 could also be the correlative of the Blackhall Till, found onshore along the Durham coast (Fig. 3.18). This unit is also of Late Devensian age, but is thought to have been deposited by ice sourced from north-western England, such as the TGIS (Davies *et al.*, 2009a, 2012b). If AF 5 correlates with the St Abbs Formation (Fig. 3.18), this would imply that it was deposited in glaciomarine conditions after the LGM during regional deglaciation. AF 5, though, displays similar acoustic characteristics to AF 4, and was thus initially interpreted also as a till unit. If AF 4 is considered to be the correlative of the Blackhall Till onshore, i.e. deposited by the TGIS, it could be inferred that AF 5 represents the correlative of the Horden Till, and that it was deposited at a later stage by the NSL. Alternatively, if AF 4 is the Wee Bankie Formation, AF 5 could represent a till unit deposited at a later stage or during an ice re-advance. In an entirely different scenario, AF 4 and AF 5 could be much older than thought and related to earlier Pleistocene glaciations. Evidence of older glaciations has been found on County Durham, where Davies *et al.* (2012b) described the presence of a till unit, the Ash Gill Member of the Warren House Gill Formation, which was interpreted as MIS 8 in age or older (Fig. 3.18; Davies *et al.*, 2012b; Livingstone *et al.*, 2012b). AF 4 could therefore correlate with this older unit and AF 5 with a more recent till, deposited during the Late Devensian, thus replicating offshore the same stratigraphic sequence observed onshore (Fig. 3.18).

However, most of the Quaternary diamictic sediments mapped offshore by the BGS, in correspondence to the Blyth survey area and further to the east, appear to be related to the south-eastern extension of the NSL (e.g. the Wee Bankie and the Bolders Bank formations, see also Chapt. 2; Cameron *et al.*, 1992; Gatliff *et al.*, 1994). In addition, the landforms left by ice on the onshore areas adjacent to the Blyth survey (displayed in Fig. 3.4 and discussed in more detail in Chapt. 2) show how the geomorphological imprint related to the TGIS and thus orientated in a W - E direction is not present close to the coast, and is overprinted by landforms orientated in a N - S direction and related to the action of the NSL. The NSL is indeed known to have been active at a late stage during the Late Devensian, after the TGIS had

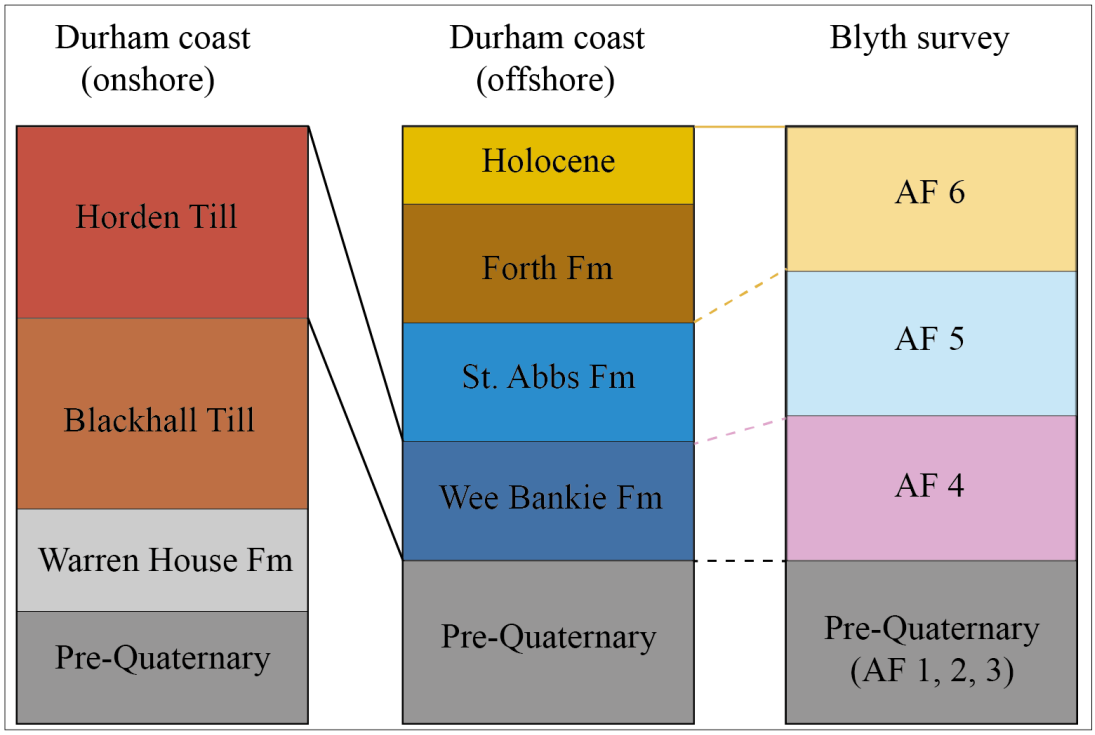

Figure 3.18: Simplified composite stratigraphy of the Durham coast onshore (Davies *et al.*, 2009a, 2012a,b; Livingstone *et al.*, 2012b), offshore (Cameron *et al.*, 1992; Gatliff *et al.*, 1994) and of the Blyth survey area. Dashed lines represent possible correlations of the different facies. In particular, black dash line correlates the Pre-Quaternary strata; pink dash line correlates AF 4 to the Wee Bankie Fm and Horden Till; Yellow dash line correlates the bottom of AF 6 to the bottom of the Forth Fm.

already started to retreat towards the west (see Chapt. 2; Livingstone *et al.*, 2008, 2010, 2012b, 2015). Considering what can be seen onshore, it would be reasonable to assume that the offshore evidence reflect the same scenario. Given the fact that most of the onshore Quaternary diamictic sediments relate to the last glaciation, the late southwards flow of the NSL and the fact that the TGIS imprint onshore is overprinted by the signature of ice coming from the north, it would be reasonable to assume that AF 4 correlates to the Wee Bankie Formation (and onshore Horden Till) and that AF 5 relates to a diamictic deposits (and possibly a till), deposited during a later phase of the NSL. This is based on the internal characteristics of both seismic facies (which are very similar) and on the general geomorphic imprint found onshore. The fact that offshore on the bathymetry data no geomorphological landforms were observed could indicate that any evidence of the passage of the NSL was later covered by the deposition of AF 6, which is here quite thick in comparison to adjacent areas to the east (see also Chapt. 2). Further discussion will follow in chapters 4 and 5.

3.5 Conclusions

This chapter provides an assessment of the bathymetry and seismic stratigraphy that characterise the Blyth survey area. From the analysis of the bathymetry data it was possible

to see how the seabed in this area of the western North Sea is relatively flat, with maximum depths of approximately -60 m. The bedrock strata crop out close to the coast, where the beddings, and at times faults, are visible. Moving away from the coast towards the east, the bedrock is present at a relatively shallow depth below the seabed, which appears flat. No geomorphological landforms were observed on the seafloor, other than a series of regular, rectangular-shaped depressions which are thought to be man-made and possibly related to the collapse of sub-seafloor mine shafts. Six different acoustic facies were recognized and mapped in the region: AF 1 correlates with the Carboniferous (Pennine Coal Measures) sequence; AF 2 correlates with the Upper Permian (Zechstein) sediments; AF 3 is interpreted as composed of Triassic sediments, due to its location and its internal seismic character. These three facies match what was previously mapped and interpreted by the BGS. AF 4 and AF 5 are interpreted as composed of glacigenic diamicts (and possibly tills) due to their seismic characteristics. AF 4 is interpreted to be the correlative of the Wee Bankie Formation (mapped by the BGS in the area) and, as a consequence, of the Horden Till mapped onshore, and is thus thought to have been deposited by the NSL during the Dimlington Stadial. AF 5 shows similar internal characteristics to AF 4 and is thus interpreted as an second till unit deposited after AF 4. Specifically, AF 5 is thought to have been deposited during a re-advance phase of the NSL. This interpretation differs from previous investigations by the BGS, which saw the presence of a glaciomarine facies (the St Abbs Formation) on top of a subglacial one (the Wee Bankie Formation) in the area. The lack of any geomorphological imprint offshore together with the imprint observed from the adjacent onshore area (which shows N - S orientated lineations, related to the NSL, overprinting the W - E orientated lineations, related to the action of the TGIS) suggest the scenario observed offshore is similar to the onshore one, and that the evidence for ice flow left on the seafloor is attributable to the action of the NSL. This is in line with the reconstructions from Livingstone *et al.* (2015), indicating that the TGIS weakened and was already retreating by 18.7 - 17.1 ka BP, while the NSL continued to flow southwards. AF 6, found on top of AF 5, is a thick facies characterised by chaotic to parallel reflectors and has been divided into two different sub-facies. AF 6b at the bottom has been correlated to the Forth Formation while AF 6a at the top is interpreted as composed of Holocene sediments. The deposition of this thick sequence, believed to be of deglacial - marine nature, could also explain the lack of geomorphic evidence from the seafloor, which may have been masked by the deposition of this facies during overall ice retreat. This work thus provides new information on the offshore stratigraphy along the coast of Blyth and adds to what was previously mapped by the BGS, although more data are needed in order to unambiguously identify the seismic facies in the area.

Chapter 4

The geomorphological imprint and sedimentary signature of the North Sea Lobe, and chronology of the last BIIS retreat in the western North Sea

4.1 Introduction

During the Late Quaternary, high elevation areas in the Cheviots, Southern Uplands, Lake District and Pennines formed competing ice-dispersal centres in the central sector of the last BIIS and played an important role in modulating ice flow through the Forth, Tweed, Tyne Gap, Stainmore and North Sea Lobe (NSL) ice streams (Boulton & Hagdorn, 2006; Bradwell *et al.*, 2008b; Hubbard *et al.*, 2009; Davies *et al.*, 2009a, 2012a; Livingstone *et al.*, 2010, 2012b; Yorke *et al.*, 2012). These fast-flowing corridors drained the central and northern sectors of the BIIS and extended offshore into the North Sea (Fig. 4.1), which should thus hold important information on the glacial imprint of the last BIIS. Despite the numerous studies along the east coast of the UK (Evans *et al.*, 2005; Everest *et al.*, 2005; Livingstone *et al.*, 2008, 2010, 2012b, 2015; Davies *et al.*, 2012a; Roberts *et al.*, 2013; Bateman *et al.*, 2015, 2017), which have led to significant improvements in our understanding of the last phases of BIIS recession, substantial gaps still exist in our knowledge of the behaviour of the BIIS in the North Sea. Even though some areas of the basin have been intensively researched with respect to their glacial history (e.g. eastern and northern North Sea and the Norwegian Channel; Sejrup *et al.*, 2000, 2016; Graham *et al.*, 2007; Stewart & Lonergan, 2011; Stewart *et al.*, 2012; Morén *et al.*, 2017), the stratigraphic architecture and the glacial seafloor geomorphology of the western North Sea are still poorly constrained. Recent studies from Dove *et al.* (2017), Cotterill *et al.* (2017) and Roberts *et al.* (In prep.) have provided new information on the offshore glacial history of the southern North Sea and of the Dogger Bank area, yet little is known about the western North Sea and particularly about the area offshore the coasts of north-east England. Despite the datasets collected and published by the British Geological Survey (BGS; Cameron *et al.*, 1992; Gatliff *et al.*, 1994), which reconstruct the stratigraphic and sedimentary architecture of the basin, there is a lack of high resolution data that fully characterises the sedimentary imprint left on the seabed by the passage of the last BIIS, and particularly of the NSL, in the western North Sea. As discussed in the previous chapters, different seismic units of Quaternary age have been mapped in the area by the BGS (Fig. 2.4) and have been divided according to their

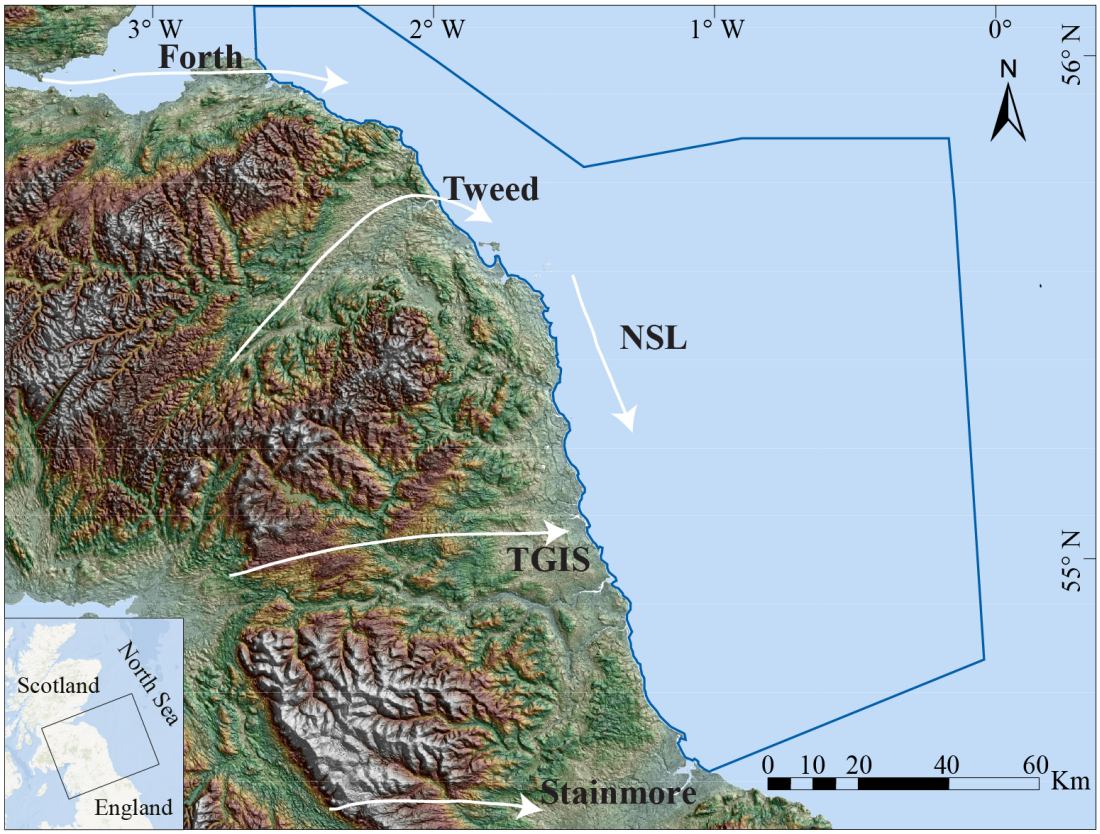

Figure 4.1: NEXTmap image of northern England and southern Scotland (location shown in the insert map) and locations and generalised ice flow directions of the Forth, Tweed, Tyne Gap Ice Stream (TGIS), Stainmore and North Sea Lobe (NSL) ice streams. The location of the Britice-Chrono study area analysed in this chapter is delineated with the blue polygon.

seismic and sedimentary characteristics (Cameron *et al.*, 1992; Gatliff *et al.*, 1994). Outcrops of pre-Quaternary strata are overlain principally by the Wee Bankie Formation/Bolders Bank Formation, which extends from Scotland to Norfolk and south of the Dogger Bank. Despite a confined lens of the Forth Formation, Botney Cut Formation and St Abbs Formation mapped by the BGS closer to the coast off Blyth (as shown and discussed in Chapt. 3), the Wee Bankie Formation appears to be the sole Pleistocene unit characteristic of the western North Sea. The new information presented by Dove *et al.* (2017) for the southern North Sea, and in Chapter 2 in this study, are evidence that this area of the North Sea holds more details than previously thought and that new detailed marine observations are needed to fully characterise the imprint of the last BIIS offshore, and to combine it with the onshore evidence. Furthermore, despite the available chronology from the onshore area, no chronological constraint is yet available for this offshore sector.

As part of the GLANAM project, this research aims to rectify these knowledge gaps by using new geomorphological and sedimentological evidence from the western North Sea. The key aims are:

1. to reconstruct the offshore glacial imprint of the last BIIS, and particularly of the NSL
2. to reconstruct the offshore acoustic architecture of the region, and particularly the glacial

stratigraphy

3. to provide detailed information on the nature of the Quaternary glacial sediments
4. to assess the range of glacial environments associated with the NSL
5. to establish for the first time the pattern and the nature of ice advance and retreat offshore
6. to propose a preliminary chronology for the retreat of the NSL offshore, during the last glacial cycle

This is achieved using a combination of high-resolution multibeam bathymetry datasets, new 2D seismic profiles and five vibro-cores collected off north-east England during the Britice-Chrono JC123 survey in 2015, together with additional datasets gathered from different sources.

4.2 Materials and Methods

The study area of this chapter (the Britice-Chrono survey) is delimited by Dunbar to the north and Hartlepool to the south and is indicated with a blue polygon in Figure 4.1. The datasets analysed here consist of bathymetry, seismic profiles and sediment cores collected during the Britice-Chrono JC123 oceanographic survey on board of the RRS *James Cook*, in July 2015. Additional geophysical datasets, gathered from various sources, were also analysed and interpreted in this chapter, and provide excellent complementary information for the study area.

1. Bathymetry data

A total of ∼340 km of new multibeam bathymetry was acquired during the Britice-Chrono JC123 oceanographic survey in the western North Sea, with the EM710 70-100kHz Multibeam Echosounder (MBES) system, and navigational data were recorded in UTM30N grid coordinates with SIS navigation software. The dataset is composed predominantly of a single acquisition line (black line in Fig. 4.2b and 4.2c) which delineates a triangle in the middle of the study area. Only the northernmost and southernmost tips of the dataset are composed of two parallel acquisition lines. The MBES data resolution varies along the survey line and the instrument sweep at times shows numerous gaps at each side. This was due to changes of weather condition during acquisition. Caris HIPS/SIPS 7.1 software was utilised on board for MBES data processing. The data were later processed using QPS Fledermaus, gridded at 5 m cell size and then exported in ASCII format.

Considering the limited extension of this new MBES dataset (acquired mainly along a single line), supplementary bathymetry for the study area was downloaded from the UK Hydrographic Office (UKHO). The UKHO has been accredited by the Marine Environmental Data and Information Network (MEDIN) as the national Data Archive Centre for bathymetric surveys and provides access to available bathymetric surveys, gathered from various sources, free of charge. The bathymetry obtained from the UKHO and analysed in this chapter (UKHO dataset) contains public sector information licensed under the Open Government Licence v3,

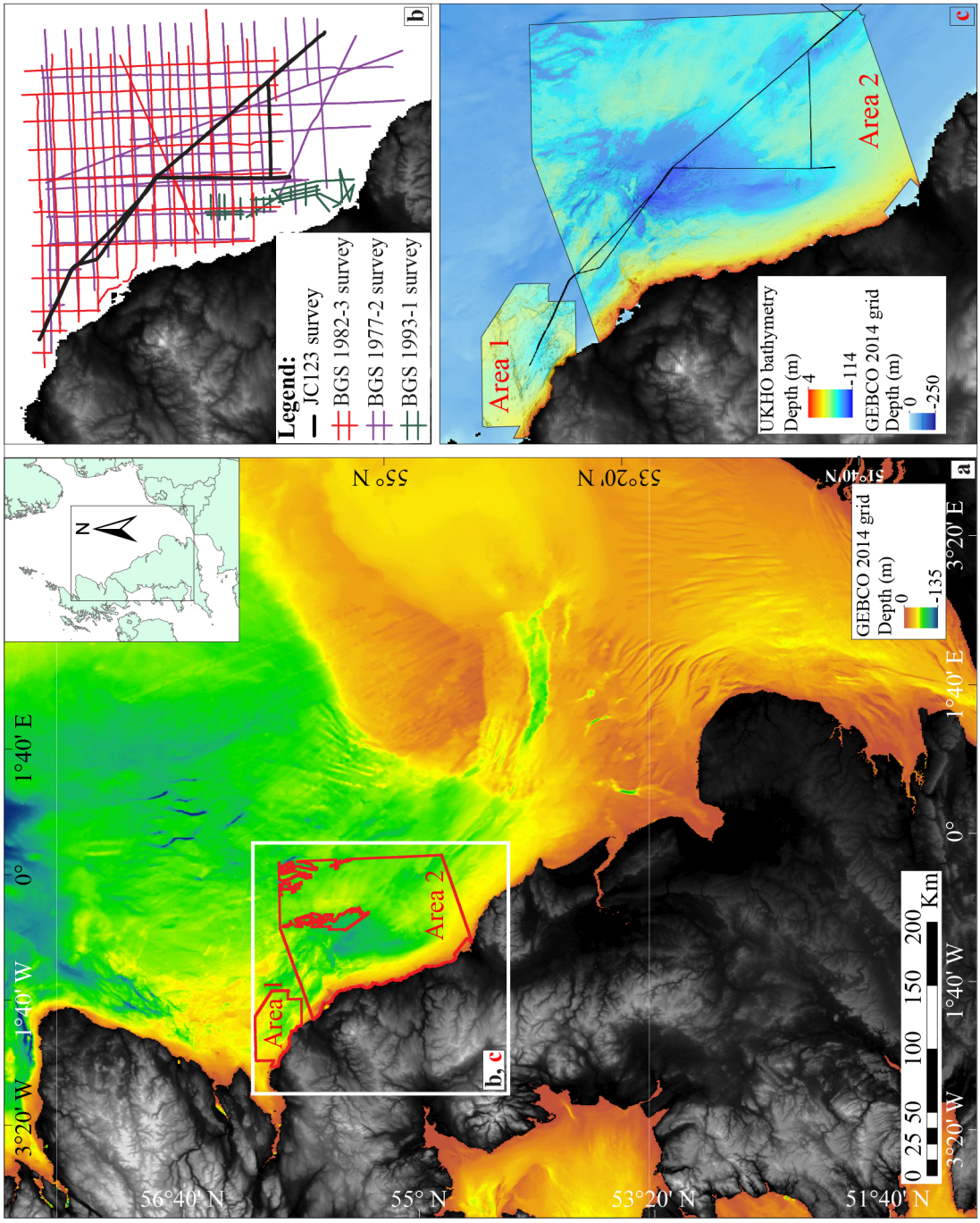

Figure 4.2: a: overview of the North Sea bathymetry (GEBCO, 2014 grid) and location of the Britice-Chrono study area. The white square indicates the location of b and c. b: location of the JC123 survey line (black line) and of the BGS surveys. c: Area 1 and 2 of the UKHO bathymetry dataset (the UKHO bathymetry colour scale used here will be used for all the other images of the chapter).

and is composed of numerous survey lines originally acquired with different methodologies (Singlebeam and Multibeam Echosounder). It covers an area which extends up to ~125 km from the coastline, from North Berwick in the north to Hartlepool in the south, and is divided into two areas, Area 1 and Area 2 (Fig. 4.2c), which are not connected to each other due to missing data points. For the same reason, Area 2 contains some gaps in its central and eastern

sides (Fig. 4.2c). After download from the UKHO website, the two areas were imported in QPS Fledermaus and, depending on the density of the original acquisition grid, were gridded using different cell sizes. A cell size of 50 m was used to grid Area 1 while a cell size of 100 m was used to grid Area 2. This was necessary to achieve full data coverage and means that the two areas have different spatial resolutions: Area 1 has a spatial resolution of 50 m, while Area 2 of 100 m. The grids were mainly analysed using QPS Fledermaus software, which allows for the visualisation of the bathymetry data in 3D and for the creation of 2D cross-profiles. This is extremely helpful in order to better visualise the different landforms found on the seafloor. Considering the study area is characterised by extensive bedrock outcrops (see also Chapt. 2 and 3), it was necessary to analyse the bathymetry data in combination with the available seismic profiles, in order to fully distinguish between bedrock ridges and landforms of glacial origin. For example, if a particular landform was observed on the bathymetry and was thought to be of glacial origin, the seismic profiles (if available at that location) would then be used to visualise the internal structure of such landform and to reach a final interpretation. In addition, if a particular landform was interpreted to be of glacial origin (for example a subglacial lineation), similar landforms found in close proximity to it and with similar geometries and orientations would also be mapped as lineations. The fact that the spatial resolution for the biggest of the two UKHO areas (Area 2) was only of 100 m, meant that smaller landforms may have been lost in the resolution of the grid and were thus not observed and mapped. This could be the case for relatively small drumlins, lineations, ridges, etc. which, if present, were not fully captured in the dataset. Whenever there was uncertainty about specific bedforms, due to the low resolution of the bathymetry data and to the absence of seismic profiles and/or other relevant information, such bedforms were left as undefined and will require further investigations for their characterisation. After the analysis in QPS Fledermaus, the grids were then exported in ASCII format and imported into ArcGIS and Adobe Illustrator for geomorphological mapping and to produce the final images provided in this chapter.

In addition to the UKHO dataset, the Olex database for the North Sea (www.olex.no), which is a collection of Singlebeam data acquired and shared by users, was also taken into account as a guideline for geomorphological mapping, and the GEBCO 2014 grid was downloaded and imported into ArcGIS to provide a regional bathymetric overview of the North Sea and particularly of the areas in close proximity to the Britice-Chrono study area (Fig. 4.2a).

2. Seismic profiles

During the Britice-Chrono survey, a total of ∼340 km of 2D seismic profiles were acquired with the SBP120 Sub-Bottom Profiler, in conjunction with the Multibeam bathymetry data, and along the acquisition line delineated in black in Figure 4.2b and 4.2c. The Sub-Bottom Profiler was able to penetrate up to a maximum depth of 30 millisecond (ms) into the sediment, with approximately 15 - 20 ms average penetration. The 2D seismic profiles were analysed and interpreted with the IHS Kingdom software. The visible horizons were mapped and different seismic facies were identified according to their seismic characteristics and to the geometry of their internal reflectors. Note that all the figures of the seismic profiles shown in this chapter have a depth scale shown in time (ms), instead of meters. An approximate time-depth

conversion is achieved using an average P-wave velocity (speed of sound in the sediments calculated from the the sediment cores) of 1590 m/s, which means that in this chapter 10 ms correspond to ∼8 m.

In addition to the seismic profiles acquired during the Britice-Chrono survey, the BGS 2D paper seismic profiles (location in Fig. 4.2b), acquired during the 1977/2, 1982/3 and 1993/1 surveys, were also analysed, to help characterise the stratigraphic signature of the area. Given that these surveys consist of paper records, it was not possible to import them into IHS Kingdom. The lines, available as .jp2 files, were analysed using CorelDRAW. The BGS geological maps available for the study area also provided valuable background information.

3. Sediment cores

The five vibro-cores JC123-131VC - 135VC (in the text abbreviated to 131, 132, 133, 134 and 135), analysed in this work, were collected during the Britice-Chrono survey using the BGS vibrocore system with a 6-m barrel. The Multibeam swath bathymetric data and Sub Bottom profiles, acquired during the survey, were used to target core localities. The cores are located in the central and southern part of Area 2 of the UKHO dataset (Fig. 4.3; note that core JC128-VC (128) was not analysed in this study together with the other five, but is here shown because it provided an additional radiocarbon date, useful for this work).

Core	Abbreviation	Latitude (N)	Longitude (W)	Length (m)	Water depth (m)
JC123-131VC	131	55° 33.307’	1° 03.774’	2.81	109
JC123-132VC	132	55° 29.469’	0° 55.159’	2.19	108
JC123-133VC	133	54° 56.662’	0° 56.725’	4.46	77
JC123-134VC	134	55° 00.037’	0° 56.921’	4.52	83
JC123-135VC	135	54° 59.961’	0° 13.798’	5.66	90.6

Table 4.1: Vibro-cores information.

The vibro-cores were measured directly on board using the Multi-Sensor Core Logger (MSCL-99) system of the University of Leicester, for Magnetic Susceptibility (MS), Gamma-density, P-wave velocity (V_p) and Electrical resistivity values. MS has been recognized as an effective tool to identify variations in the supply of terrigenous sediments to the oceans (Robinson *et al.*, 1995), although in glaciomarine settings, it can also be used as an indicator of grain size variations in the sediments (Kilfeather *et al.*, 2011; Hogan *et al.*, 2016). The P-wave velocity profiles of each core were also used to calculate core penetration in the seismic section (conversion from milliseconds to meters). The bottom sections of each collected core (and cores 131 and 133 entirely) were also X-rayed using the Geotek X-ray Core Imaging system at the Geotek facilities in Daventry, in order to investigate the possible presence of shells for radiocarbon dating but also to help with the identification of sedimentary structures.

The five vibro-cores were then analysed at Durham University - Geography Department laboratories and sub-sampled for radiocarbon dating and for palaeoenvironmental analyses. 34 x 1 cm slabs of sediment were taken from the cores at chosen intervals and wet sieved using 63

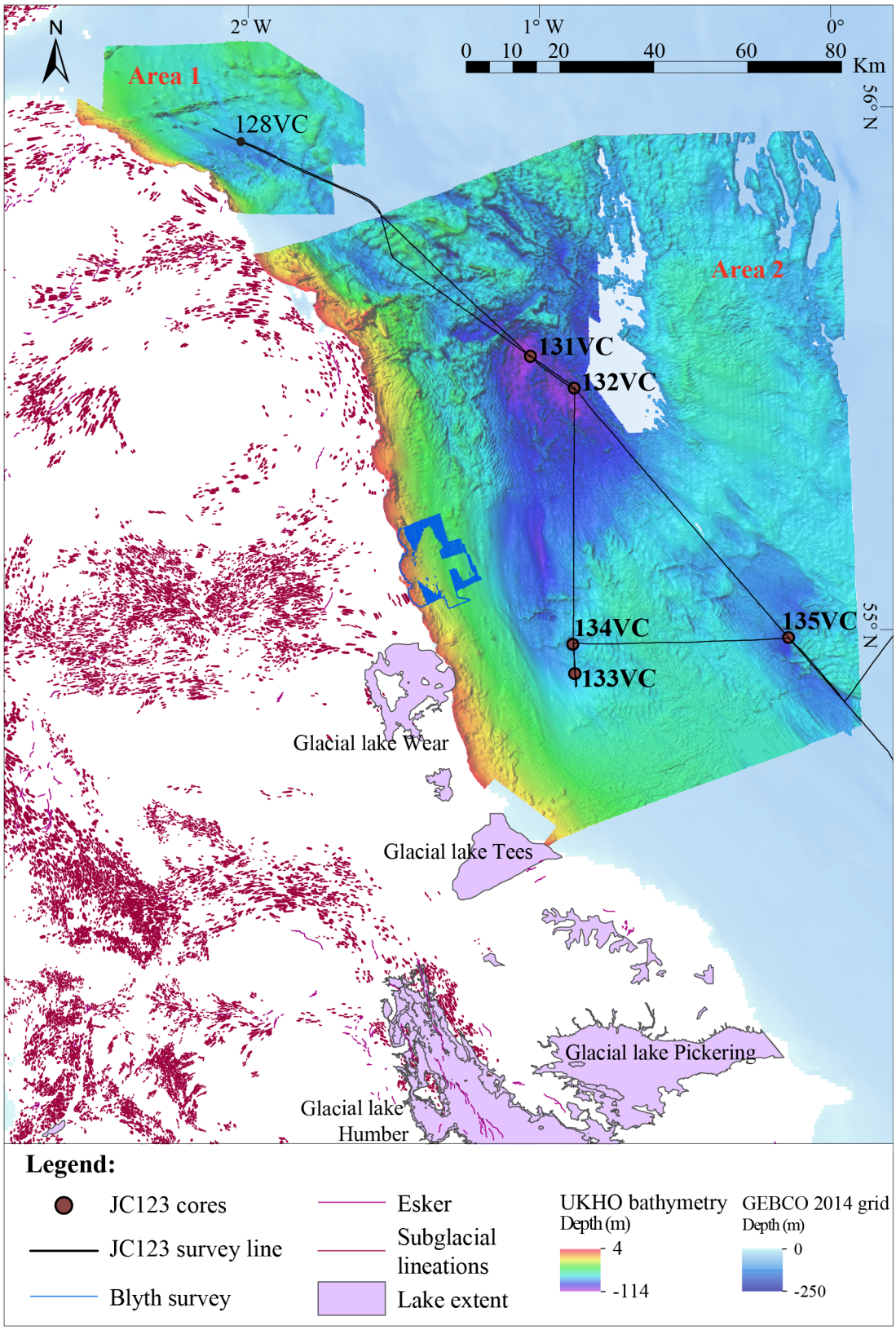

Figure 4.3: Location of the five vibro-cores analysed in this study (131 - 135, in brown) and of core 128 (in black), which provided one radiocarbon date. The Blyth survey and UKHO areas 1 and 2 discussed in Chapters 3 and 4 are also shown. Onshore mapping was downloaded from the BRITICE Glacial Map (Clark *et al.*, 2004a, 2018).

to 500 μm sieves. The 1 cm slabs generally consisted of 3 - 5 millilitres (ml) of sediment, which was measured by water display (each slab of sediment was dropped into a known amount of distilled water and the difference in ml was measured to obtain the total ml of sediment of the sample). The sub-samples locations were chosen particularly in the lower sections of each core, at either lithological changes but also within the same sedimentary facies, to evaluate differences in foraminifera abundance and species diversity. The fraction finer than 63 μm was drained to remove the clay/silt portion while the 63 - 500 μm fraction was retained and dried in the oven at $\sim$60°C. Each sample was then analysed using the Zeiss Stemi SV11 binocular microscope. All five vibro-cores are characterised by a limited number of foraminifera individuals found in each sample. Wherever present, benthic foraminifera were picked primarily for radiocarbon dating but also for palaeoenvironmental analyses. 14 x 1 cm slabs where chosen from cores 132, 134 and 135 for palaeoenvironmental reconstructions. Both benthic and planktonic foraminifera were counted and benthic foraminifera were identified and analysed based on their abundances. Only 1 of the 1 cm slab samples (core 132, 144 cm depth) was sent to NERC laboratories for dating. Core 128 (Fig. 4.3, 55° 58.798', 2° 02.414') was not analysed in detail in this study but is here shown and briefly described, because it provided a second sample for radiocarbon dating (core 128, 280 cm depth). The two samples produced two uncalibrated ages which were then calibrated using a reservoir age (ΔR) of 0, 300 and 700 (Table 4.2). The radiocarbon reservoir ages in the North Atlantic and adjacent shelf seas have varied both in space and time since the LGM, and in glaciated margins the issue is complicated by meltwater entering the marine system that may have been in freshwater reservoirs (e.g. glacier ice) for many thousands of years. As there is still uncertainty as to which reservoir age (ΔR) would be more appropriate for the North Sea basin, in this work the ages calibrated with ΔR = 0 will be used. These are of 16,949 $\pm$ 218 cal. yrs BP for core 128 and of 19,571 $\pm$ 172 cal. yrs. BP for core 132.

Core	**Depth in core (cm)**	**Carbon source**	**CRA (yrs. BP)**	**Cal. age (cal. yrs. BP), ΔR=0**	**Cal. age (cal. yrs. BP), ΔR=300**	**Cal. age (cal. yrs. BP), ΔR=700**
128	280	mixed foraminifera assemblage	14,376$\pm$41	**16,949$\pm$216**	16,488$\pm$218	15,954$\pm$178
132	144	mixed foraminifera assemblage	16,613$\pm$47	**19,571$\pm$172**	19,180$\pm$190	18,766$\pm$118

Table 4.2: Information on the two radiocarbon ages measured from cores 128 and 132. CRA = Conventional Radiocarbon Ages; ΔR = reservoir effect. In this work the dates with ΔR = 0 (in bold) are used.

Studies on benthic foraminifera species for palaeoenvironmental reconstructions usually require a minimum of 200 individuals to obtain a reliable indicator of the species diversity (Thomas *et al.*, 1995; Jennings *et al.*, 2014). In this case, only two out of the 14 x 1 cm samples are characterised by a total number of tests higher than 200, while 9 of them reach less than 100 tests. Considering this is a common characteristic of all cores, all samples are presented in this

chapter, although this will be further considered for the interpretations. Different sedimentary lithofacies and subfacies were identified following the guidelines of Evans & Benn (2004) and then interpreted, based on the combination of all the available datasets and on the different palaeoenvironments.

4.3 Results

4.3.1 Bathymetry data and geomorphology of the seafloor

The North Sea is characterised by relatively shallow waters that do not exceed ∼200 m depth on average, except in the eastern side of the basin, in the Norwegian Channel. Figure 4.2a shows an overview of the seafloor of the UK sector of the North Sea (GEBCO, bathymetric grid 2014). It is noticeable how the entire area is very shallow and waters start to deepen and reach over -130 m only in the most northern part. Nevertheless, the seabed has a very complex geometry and is characterised by the occurrence of numerous landforms. It is known from the BGS pre-Quaternary maps of the North Sea (Cameron *et al.*, 1992; Gatliff *et al.*, 1994), that the western sector is defined by numerous bedrock outcrops, and when not outcropping, the bedrock strata are usually present at a very shallow depth below the seabed. This has had a big influence on the overall topography of the area, and on the glacial imprint that has developed during the Quaternary (Cameron *et al.*, 1992; Gatliff *et al.*, 1994; Sejrup *et al.*, 2000, 2009; Lonergan *et al.*, 2006; Davies *et al.*, 2011; Graham *et al.*, 2011). The two UKHO areas (Fig. 4.2c and 4.4a) analysed in this work, are both characterised by very shallow waters. Area 1, to the north, extends for ∼1220 km^2, from the coast to ∼35 km offshore towards the east, and is characterised by water depths that do not exceed approximately -80 m. Area 2, to the south, extends for ∼13000 km^2, from the coast to ∼220 km offshore. Waters are up to -40 m deep along the coastline and in the south. In the eastern side of the area, water depths are around -70 m on average, while the seafloor deepens into a small basin in the central part of Area 2, and here waters reach the maximum depth of -113 m. (Fig. 4.4a). The two areas are characterised by the presence of numerous landforms which are shown in Figure 4.4b. Four landform categories were identified on the dataset: (1) Ridges, (2) Wedges, (3) Elongate mega-ridges and (4) Channels.

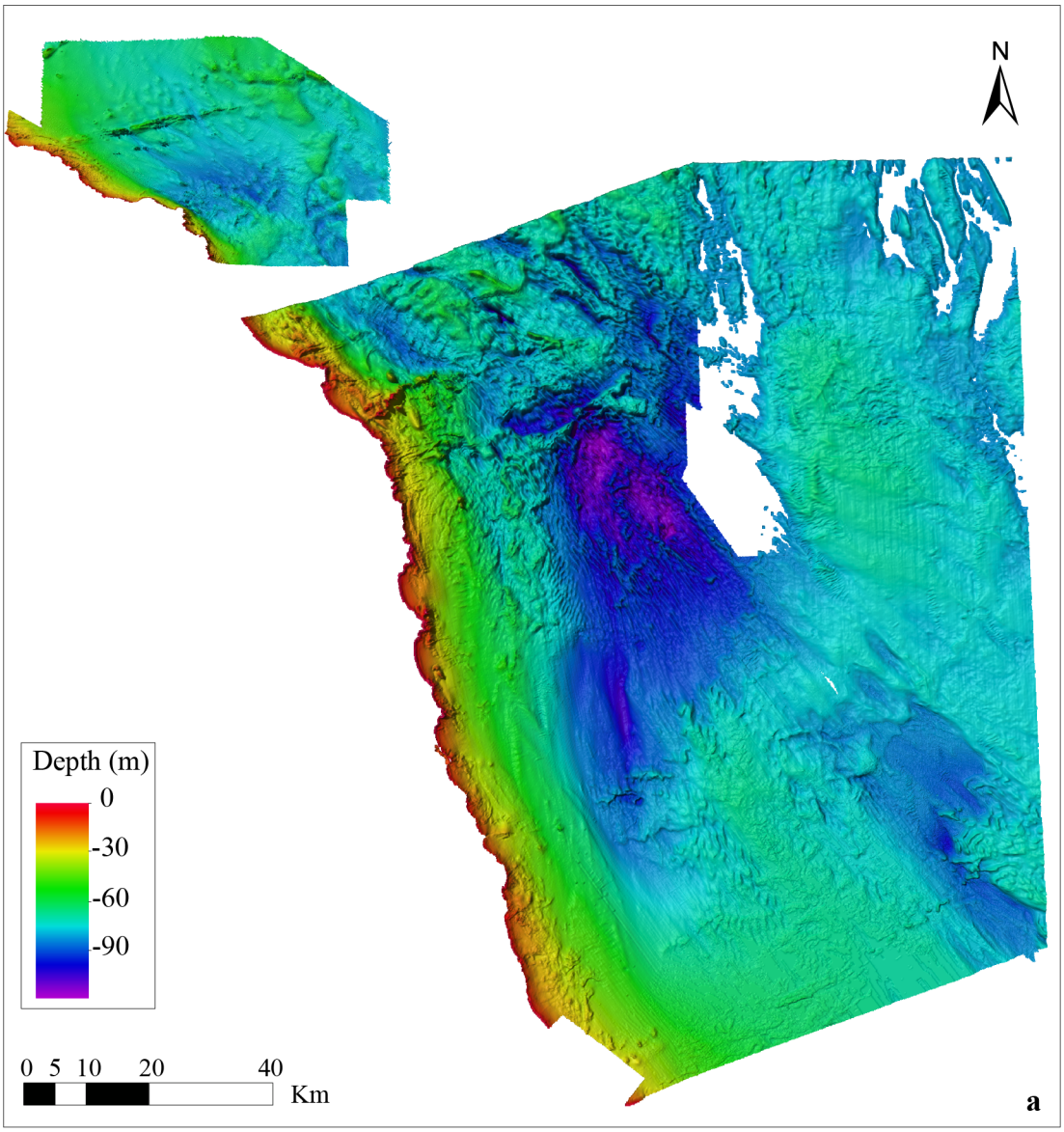

Figure 4.4: a: high resolution bathymetry of the UKHO Area 1 and 2 (shown with 85x vertical exaggeration). Gaps are due to missing data points in the dataset. The location of the two areas is shown in Figure 4.2a and 4.2c.

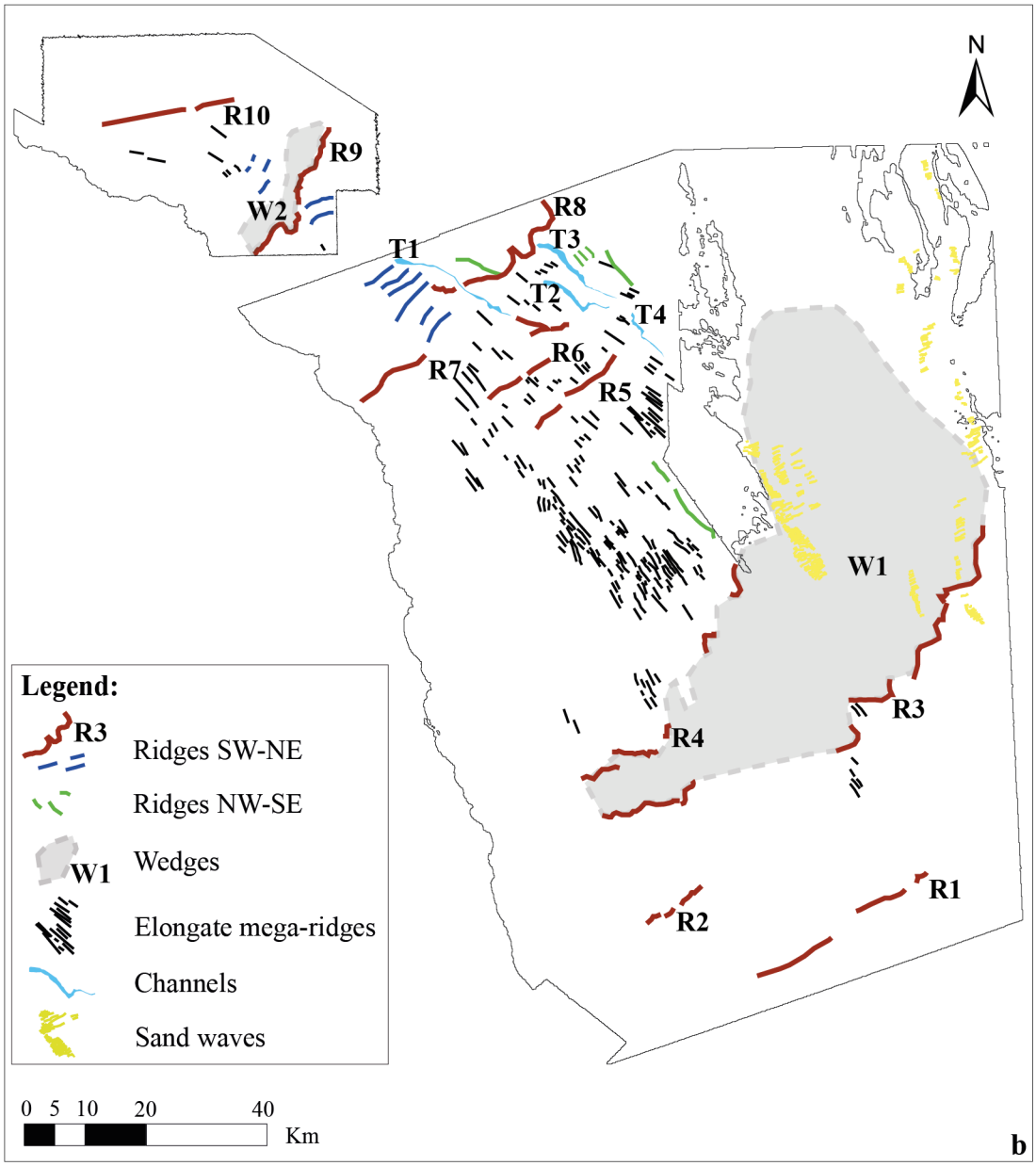

Figure 4.4 (cont.): b: geomorphological map of the UKHO Area 1 and 2.

Ridges

Numerous ridges have been mapped on the UKHO areas and are shown in brown, blue and green in the geomorphological map (Fig. 4.4b). They were divided into three sub-groups, according to their orientations and geometries. The ridges highlighted in brown are numbered from south to north (R1 - R10), and are all orientated in a SW - NE direction (Fig. 4.4b). Some of these ridges are actually composed of different individual and laterally discontinuous smaller ridges, which were grouped together and considered as one ridge feature, due to their similar orientation and the fact that they appear to be part of one big form. This is for example the case for R1, R3 and R4 (Fig. 4.4b). Such a scenario is similar for example to what was mapped in the southern North Sea by Dove *et al.* (2017), where several isolated moraines were considered together as one big feature according to orientation and location (Fig. 2.8), and to the onshore moraine sets mapped in north-east England and shown in Figure 4.3 (Teasdale, 2013; Livingstone *et al.*, 2015), which are made of disconnected smaller ridges. The ridges R1 - R10 occur in both UKHO areas, but do not appear in the very central part of Area 2 (Fig. 4.4b and 4.5). Examples of their cross-profiles are shown in Figure 4.5. R1 and R2 occur in the southernmost part of the study area. These two ridges are both discontinuous and display a relatively straight planform. They occur at approximately -61 m depth and are 1 - 2 m high (Fig. 4.5a). They are both quite narrow, being up to 2 km and 1.2 km wide respectively and, on bathymetric profile, R1 shows steeper slopes. Further north, R3 and R4 are found (Fig. 4.5b). These two ridges have a more curvilinear/lobate planform in comparison to R1 and R2, and they delineate the northern and southern limits of the W1 wedge (Fig. 4.4b). In cross-profiles, R3 displays gentler slopes (Fig. 4.5, R3a and R3b) and both R3 and R4 are up to 5 m in height. R5 - R8 are found in the northernmost part of the UKHO Area 2 (Fig. 4.4b). They are all up to 8 - 10 m high, and R5, R6 and R7 are quite rectilinear in planform, while R8 is more curvilinear (Fig. 4.5c). In cross-profile, R6 and R7 appear multi-crested and R7 in particular has steep and angular slopes and is found in very shallow waters (its crests reach up to approximately -10 m depth). R8 displays a single and rounded crest, and is characterised by gentler slopes, particularly to the north. Finally, R9 and R10 are the two northernmost ridges observed on the dataset and they occur in the UKHO Area 1. R9 is quite curvilinear in shape and delineates the southern limit of the W2 wedge (Fig. 4.4b). In cross-profile, R9 displays gentle slopes while R10 has a more linear planform, displays steep and angular slopes and appears multi-crested (Fig. 4.5d) and is very similar to R7. Both R9 and R10 are up to 10 m high. The ridges highlighted in dark blue in Figure 4.4b are also orientated in a SW - NE direction, but differ from the first sub-group of ridges described above because they are located only in a small sector of the study area, between R7 and R10, and are generally shorter in length. They are mainly characterised by a straight, at times arched, planform and are between $\sim$4 and 8 m high. The close proximity of these ridges to one another and their similar orientation and planform, could resemble the typical characteristics usually observed for retreat moraines (Ottesen & Dowdeswell, 2006; Bradwell & Stoker, 2015a), inferring that these ridges could have been deposited during retreat of the NSL. The internal characteristics of these ridges are explored further in Section 4.4.1. The third sub-group of ridges consists of a few NW - SE orientated landforms marked in green in Figure 4.4b. These ridges are located within Area 2

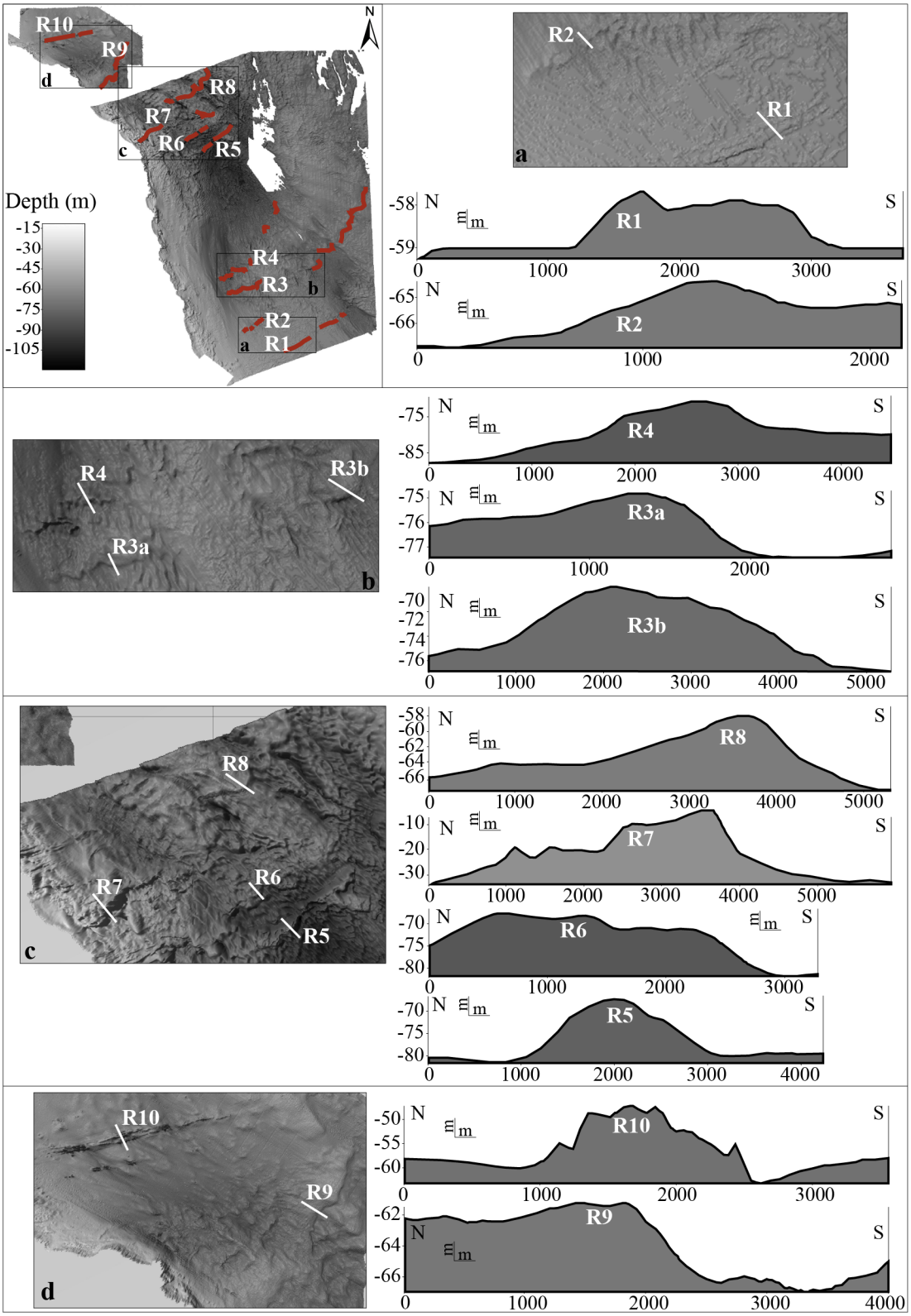

Figure 4.5: N - S cross-profiles of the 10 identified ridges of the first sub-group (R1 - R10). Note that the profiles have been vertically exaggerated.

of the UKHO dataset, and are characterised by a linear planform. They are approximately up to 6 m high and their length can vary. The ridges have been distinguished from the previous two sub-groups mainly because they are orientated almost perpendicularly to the other ridges

(Fig. 4.4b). Considering the presence of bedrock strata in the area, it is essential to analyse the seismic profiles to fully understand the nature of all three sub-groups of ridges (Sect. 4.4.1).

Wedges

Two landforms that display a wedge-like geometry can be seen on the UKHO dataset (W1 and W2, grey polygons, Fig. 4.4b). W1 is the largest of these and is located in the south-eastern part of Area 2. It is approximately 30 km wide, extends for ∼100 km in length from south-west to north-east and is ∼10 - 15 m high. It is also characterised by numerous crests and is at times overlain by sediment waves/dunes, particularly in its central and north-eastern sides (Fig. 4.4b). In cross-profile W1 displays an asymmetric geometry, with steeper slopes on its southern margin and gentler ones towards the north (Fig. 4.6a). It is delimited discontinuously by R3 to the south, and by R4 to the north (Fig. 4.4b and 4.6a).

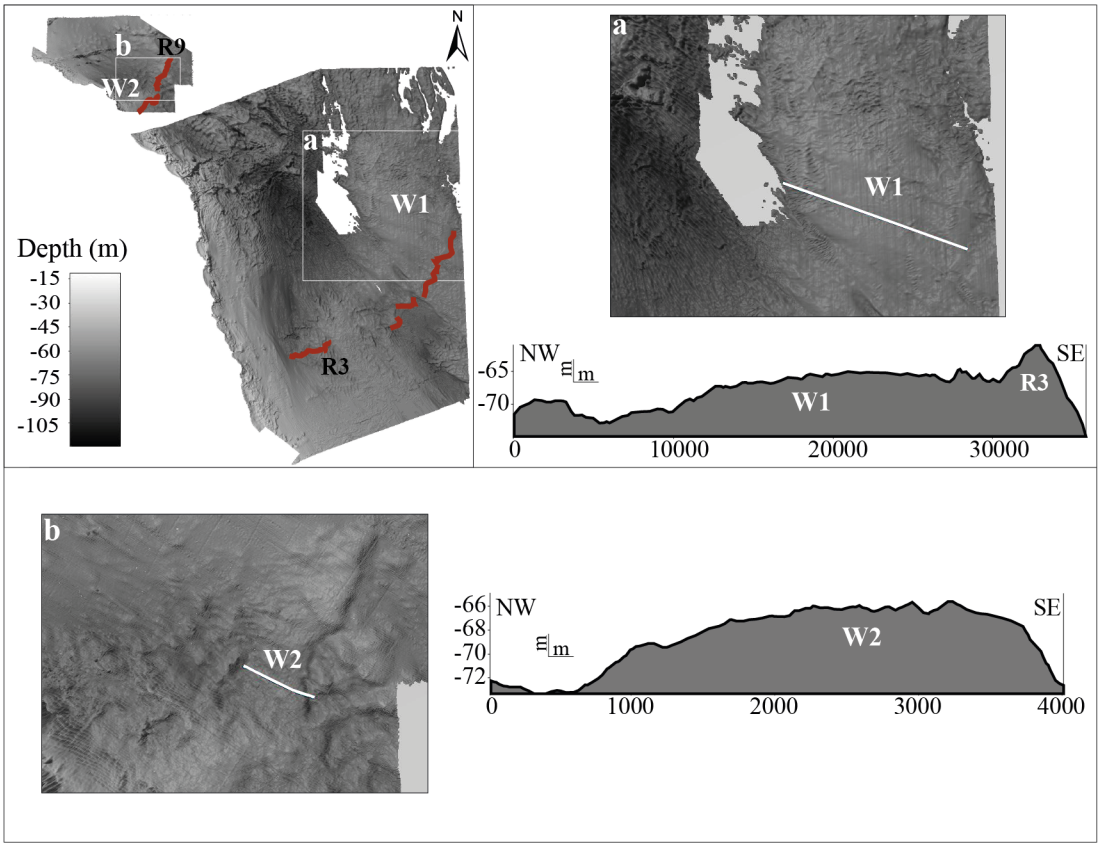

Figure 4.6: Cross-profiles examples of W1 (a) and W2 (b). Note the different horizontal scale used for W1 and W2 (significantly smaller). Also note that the profiles have been vertically exaggerated.

W2 is located in Area 1 and is smaller than W1, being ∼9 - 12 m high, 3 to 5 km wide and approximately 25 km long (Fig. 4.4b). It is characterised by numerous crests and by an asymmetric geometry when observed in cross-profile (Fig. 4.6; also note the smaller horizontal scale used for the cross-profile of W2 in respect to the one used for W1). Similarly to W1, W2 also displays steeper slopes on the southern side and gentler slopes on the northern one (Fig.

4.6b). Its southern limit is delimited by R9.

Elongate mega-ridges

Both Area 1 and 2 are characterised by the presence of elongated and narrow ridges (Fig. 4.4b). These ridges are predominantly present in Area 2 and mainly occur in its northern and central part. This sector is also the deepest of the study area, where water depths reach a maximum of -113 m. None of the elongate ridges were observed close to the coastline. They are characterised by an elongate planform and are generally narrow. Figure 4.7a shows a cross-profile of some of these ridges, which display a narrow geometry, with widths that vary from tens to a few hundred meters, and generally have steep slopes and rounded crests. At times the ridges appear wider on their northern side and more tapered towards their southern tip. In long profile these elongate ridges display gentle slopes and irregular crests (Fig. 4.7b). The length of the ridges spans from a few hundred meters up to ∼6 km and their elongation ratio (maximum length/maximum width) varies between 3:1 to 14:1. At times the ridges are bifurcated (Fig. 4.7b). Their orientation can be used to divide them into two different sets: in Area 1 the bedforms are orientated WNW - ESE to NW - SE and in Area 2 they are mainly orientated NW - SE to NNW - SSE (Fig. 4.4b).

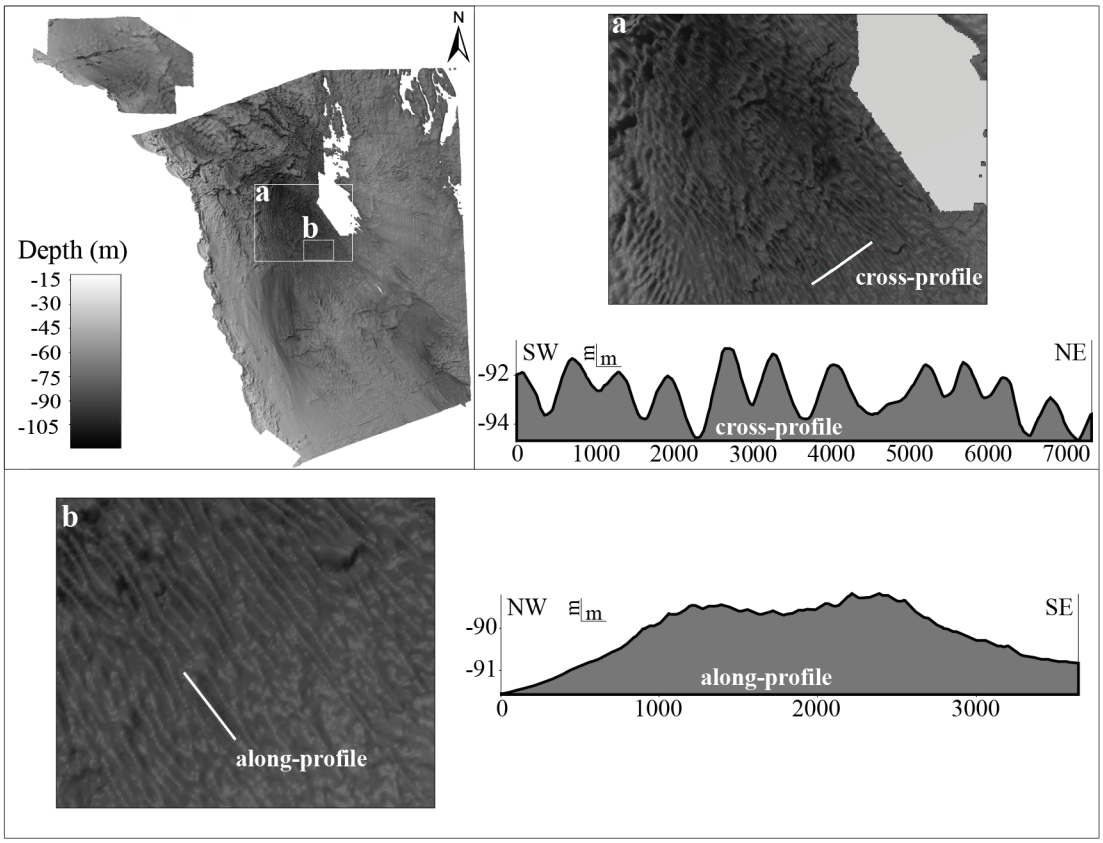

Figure 4.7: Cross- and along-profile examples of the elongate mega-ridges (a and b). Note that the profiles have been vertically exaggerated.

Channels

In the northern part of Area 2, four channels were observed (mapped in light blue in Fig. 4.4b). These depressions are relatively narrow and elongate and are generally orientated NW - SE, with the exception of T4, which is orientated NNW - SSE (Fig. 4.8). T1 is the northernmost of these and cuts through the ridge R8 (as shown in the map in Fig. 4.8), while T2, T3 and T4 are all located south-east of this ridge. The troughs are approximately 10 to 22 km long and generally between ∼400 to ∼2700 m wide. At times, these troughs appear wider towards the northern side and become narrower towards the south (e.g. T2 and T3 in Fig. 4.4b and 4.8). They do not present a linear planform but instead appear sinuous. In cross-profile, they display similar characteristics to one another, being all V-shaped and having generally quite steep flanks (Fig. 4.8). When observed along-profile, the beds of the troughs do not appear flat, but are rather irregular and characterised by an up/down profile (example in Fig. 4.8, profile T2a). Finally, the channels are up to ∼16 m deep.

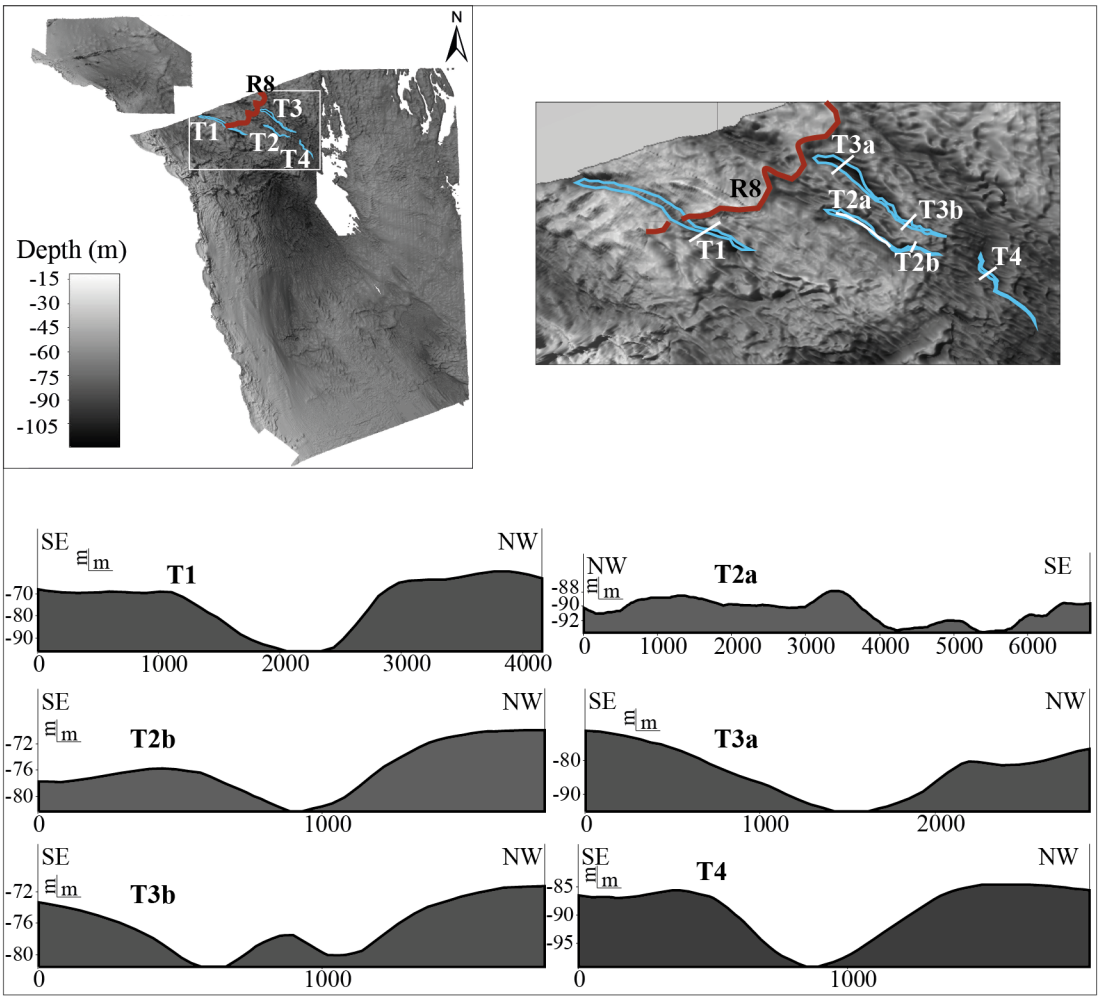

Figure 4.8: Cross-profiles of the T1 - T4 channels and along profile shown for T2 (profile T2a). Note that the profiles have been vertically exaggerated.

4.3.2 Seismic profiles

High resolution Sub-Bottom Profiler (SBP) data were acquired during the Britice-Chrono JC123 oceanographic survey (survey track in black, Fig. 4.2b and 4.2c), and the acoustic signal reached a maximum penetration of ∼35 ms below the seabed. Five different acoustic facies (AF) were recognized along the acquisition line according to their acoustic signature. AF 1 is the lowermost facies of the sequence and consists of pre-Quaternary strata. This assertion is based on the BGS Offshore Regional Reports for the North Sea (Fig. 2.2 and 2.4, in Chapt. 2; Cameron *et al.*, 1992; Gatliff *et al.*, 1994). The bedrock strata (AF 1) are generally present at very shallow depths below the seabed throughout the entire area, though often outcrop at the seafloor, forming some of the irregular topography observed in the bathymetry data (Fig. 4.4a). AF 2 - 5 are present on top of AF 1 and they consist of Quaternary deposits (Cameron *et al.*, 1992; Gatliff *et al.*, 1994). These four facies are not uniformly present in the sequence and appear laterally discontinuous. They are often interrupted by bedrock highs and it is rarely possible to observe the complete sequence AF 1 - 5 at any one location. The seismic appearances of AF 1 - 5 are shown in Figure 4.9 and described below.

AF 1

AF 1 represents the lowermost facies detected by the instrument resolution. This facies generally consists of bedrock strata that, when not outcropping, lie quite close to the seabed. According to the BGS maps, there are five different types of bedrock in the research area. These are: Carboniferous, Permian, Triassic, Jurassic and Cretaceous (Cameron *et al.*, 1992; Gatliff *et al.*, 1994; Glennie, 1998).

AF 1a is generally observed in the western part of the research area and closer to the coast. It shows folded and faulted parallel reflectors that are truncated at their upper boundary (Fig. 4.9). It is present at very shallow depths (up to ∼10 ms, ∼8 m) below the seafloor and, when not outcropping, is overlain by several different acoustic facies. AF 1a has been previously interpreted as Carboniferous strata (Cameron *et al.*, 1992; Gatliff *et al.*, 1994; Glennie, 1998).

AF 1b is characterized by highly deformed, and discontinuous internal reflectors (Fig. 4.9), and is found in correspondence of the Permian strata mapped by the BGS (Cameron *et al.*, 1992; Gatliff *et al.*, 1994; Glennie, 1998). Along the acquisition line, it is difficult to detect the limit between AF 1a (Carboniferous) and AF 1b (Permian), which overlies it, though a clear acoustic change can be seen moving towards the southern and westernmost part of the acquisition line, where AF 1b displays stronger internal reflectors. At the upper boundary of the facies, the reflectors are generally truncated. It is not possible to detect the entire thickness of the facies, but the SBP can generally penetrate into AF 1b for up to ∼30 ms (∼24 m).

AF 1c is characterised by high amplitude and frequency parallel reflectors, which appear folded and faulted (Fig. 4.9). They are also truncated at the top by a relatively flat erosional surface and are observable for up to ∼15 - 20 ms (∼12 - 16 m) in depth before signal loss. AF 1c is generally found in the central part of the acquisition line, in correspondence to the Triassic outcrops previously mapped by the BGS (Cameron *et al.*, 1992; Gatliff *et al.*, 1994), and is thus inferred to be composed of Triassic sediments.

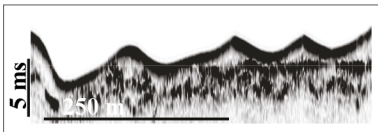	High amplitude seafloor reflector	AF 5
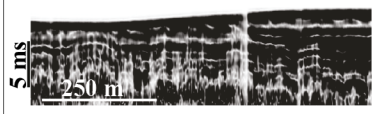	High frequency and amplitude parallel reflectors that appear deformed	AF 4
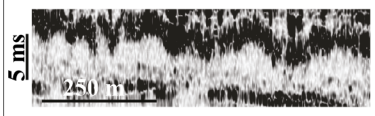	High amplitude and irregular upper boundary. Opaque internal appearance	AF 3
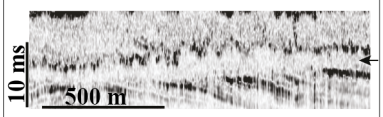	Irregular and discontinuous upper boundary. Transparent internal appearance	AF 2
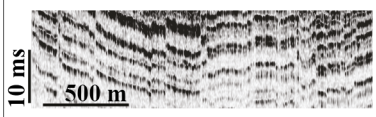	High amplitude parallel reflectors which appear faulted and folded	AF 1e (Cretaceous)
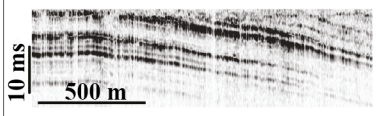	High amplitude parallel reflectors which at times appear folded and faulted	AF 1d (Jurassic)
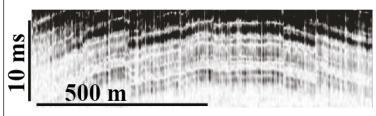	High amplitude and frequency parallel reflectors, which appear folded and faulted	AF 1c (Triassic)
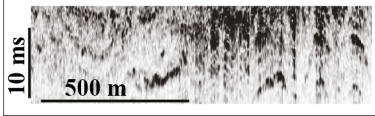	Highly deformed, irregular and discontinuous parallel reflectors	AF 1b (Permian)
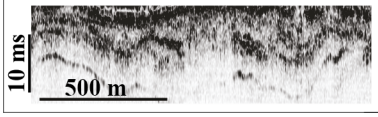	Folded and faulted, low amplitude parallel reflectors	AF 1a (Carboniferous)

Figure 4.9: Acoustic signatures of the different seismic facies observed along the profiles. Interpretation of pre-Quaternary strata based on the BGS literature (Cameron *et al.*, 1992; Gatliff *et al.*, 1994).

AF 1d appears in the southern and south-eastern part of the dataset and is characterised by high amplitude and continuous parallel reflectors that appear folded and at times faulted (Fig. 4.9). It is generally 15 ms (∼12 m) thick, though it is not possible to observe its lower boundary from the profiles. The upper boundary of the facies appears flat and continuous and truncates the reflectors underneath, and is thus considered an erosional boundary. The acoustic response of AF 1d looks very similar to AF 1c (Triassic), but clearly overlies it. The facies is found in correspondence to the outcrops of Jurassic strata, previously interpreted by the BGS (Cameron *et al.*, 1992; Gatliff *et al.*, 1994). When not overlain by different acoustic facies, AF 1d outcrops at the seabed in the most southern part of the survey.

AF 1e is acoustically very similar to AF 1c (Triassic) and AF 1d (Jurassic), being characterised by high amplitude and frequency parallel reflectors, that have been folded and faulted (Fig. 4.9). The reflectors are also truncated at the top by an erosional boundary. When not overlain

by different acoustic facies, AF 1e outcrops at the seabed in the most south-eastern part of the survey. AF 1e is found in correspondence to the occurrence of Cretaceous strata, as previously mapped by the BGS (Cameron *et al.*, 1992; Gatliff *et al.*, 1994), and is thus interpreted to be the same facies. Cretaceous strata have been mapped in the south-eastern tip of the survey line.

AF 2

AF 2 is a thin acoustic facies characterised by a varying thickness, generally between ∼2 - 6 ms (∼1.5 - 4.8 m). Whenever present, the facies lies directly on top of AF 1 (Fig. 4.10). This facies is laterally discontinuous, and has a patchy/lens-like distribution. It is usually found in depressions/small basins between bedrock highs (Fig. 4.10). The facies appears internally transparent on seismic profiles and is characterised at the top by a low amplitude and irregular reflector which marks its upper boundary (Fig. 4.9). It is sometimes difficult to distinguish between AF 2 and the unit above it (AF 3).

AF 3

AF 3 is one of the most common facies along the survey line and is usually found on top of AF 2, or directly on top of bedrock strata. The facies, marked in violet in Figure 4.10, is less discontinuous than AF 2 in the dataset and has a very variable thickness that spans between 4 and 10 ms (∼3 - 8 m). Similarly to AF 2, AF 3 is characterised by a very high amplitude and highly irregular upper reflector (Fig. 4.9), which is usually continuous. Internally, the facies is often acoustically opaque and it is not possible to observe any additional internal structures, with the exception of the rare presence of a few chaotic reflectors. The spatial distribution of AF 3 along the acquisition line varies. It is often found at the very top of the seismic sequence overlain only by AF 5 and by the seabed, but at times, it forms the core of different landforms (e.g. W1 and W2 are mainly composed of AF 3; Fig. 4.10).

AF 4

AF 4 generally overlies AF 3. Occasionally, it is found directly on top of bedrock strata, but is also found as infill in small depressions/basins (Fig. 4.10). Its acoustic appearance is defined by high amplitude and high frequency, at times wavy, parallel reflectors, that appear slightly deformed (Fig. 4.9 and 4.10). The facies has a varying thickness, sometimes of up to ∼10 ms (∼8 m), and is present along much of the seismic line as a series of discontinuous lenses (Fig. 4.10). It is often most ubiquitous in the south-western and south-easternmost parts of the survey line, partially confined between topographic highs (Fig. 4.10). Its upper boundary appears usually flat and the facies is overlain only by AF 5 and the seabed.

AF 5

The uppermost facies of the seismic sequence is represented by AF 5. This facies is generally very thin and is not always observable from the profiles, particularly when bedrock strata outcrop at the seafloor. AF 5 appears acoustically transparent on seismic profile and is bounded at the top by the seabed reflector (Fig. 4.9).

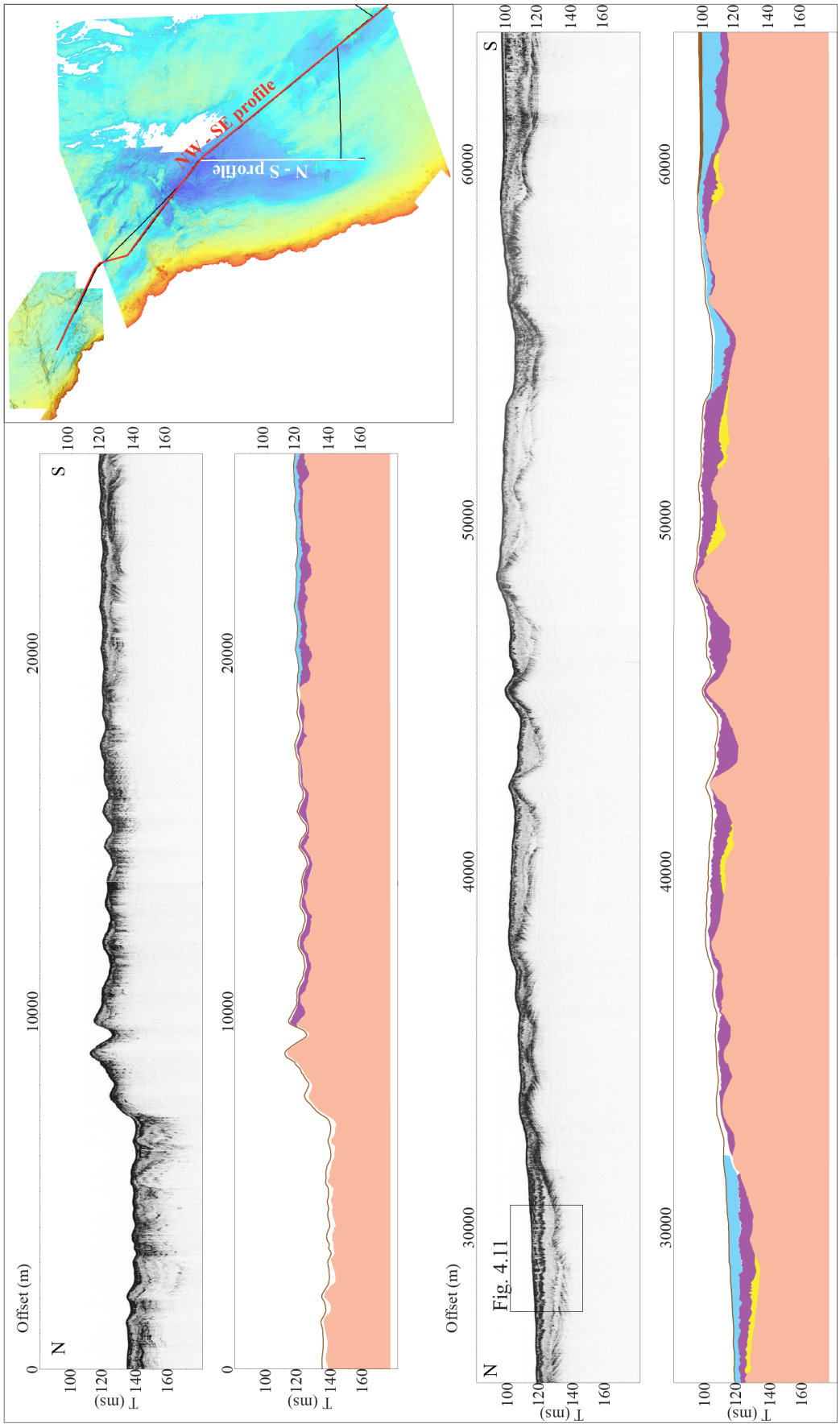

Figure 4.10: N - S seismic profile and facies interpretation. Some of the landforms previously mapped in Figure 4.4b are also indicated. The location of the profile is shown in white in the insert map. The acoustic facies legend is shown below.

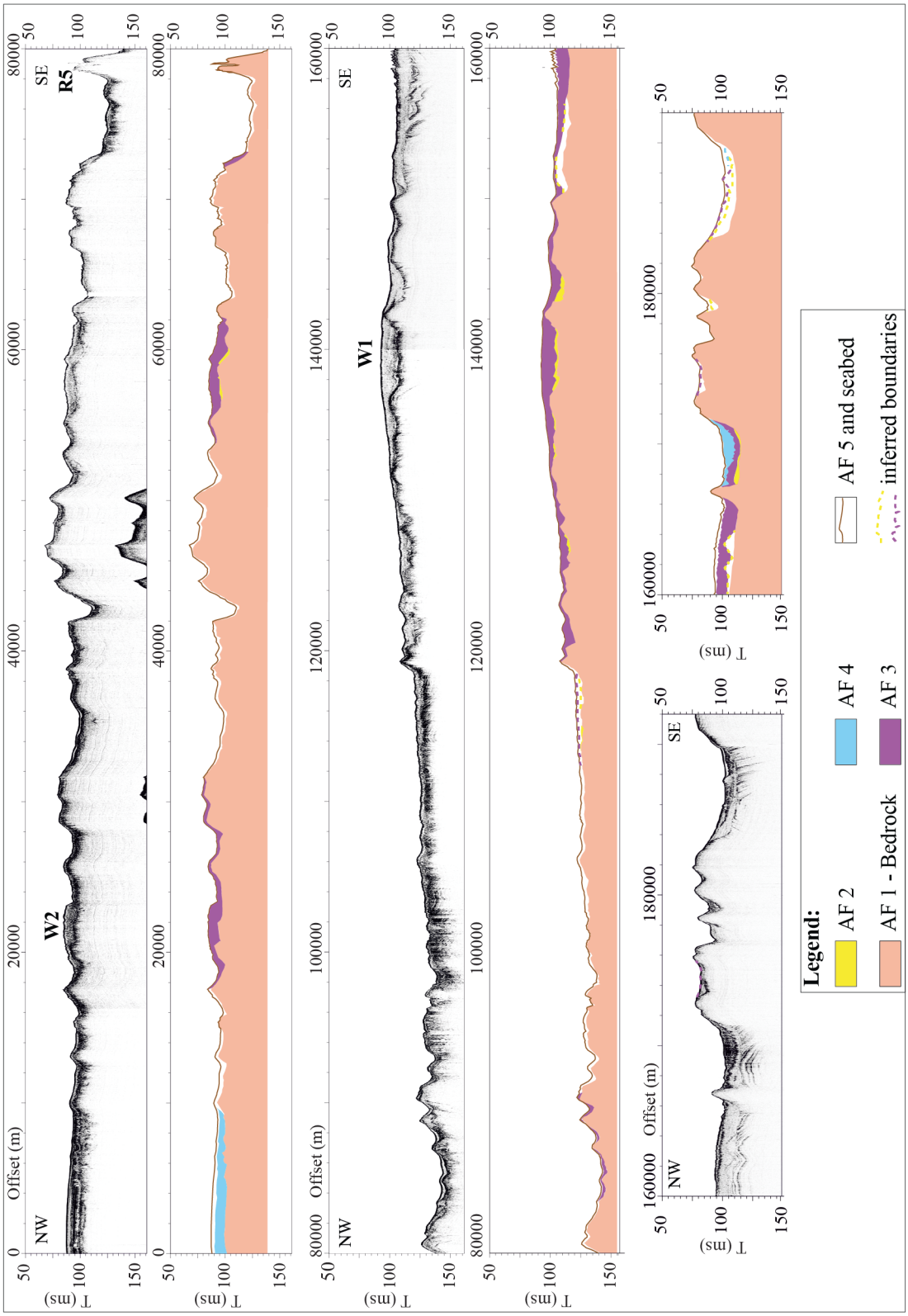

Figure 4.10 (cont.): NW - SE seismic profile and facies interpretation. Some of the landforms previously mapped in Figure 4.4b are also indicated. The location of the profile is shown in red in the insert map above.

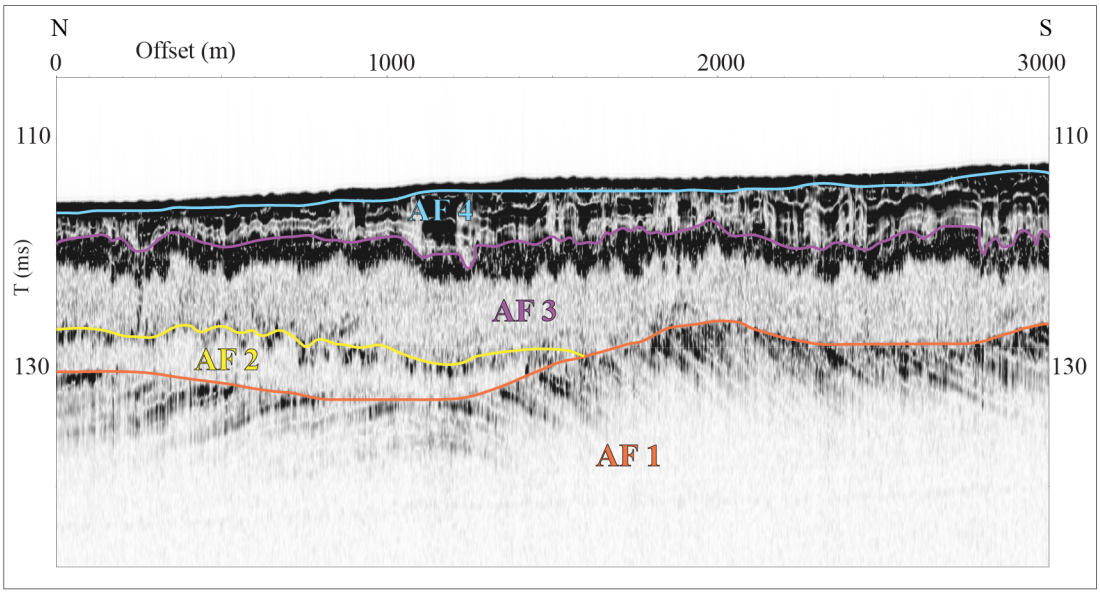

Figure 4.11: Detail view of facies AF 1 - 4. The location of this zoomed in section is shown in Figure 4.10 (black square).

4.3.3 Sediment cores

1. General core location and stratigraphy

The five vibro-cores 131 - 135, analysed in this work, were collected along a transect that stretches NW - SE across the central part of Area 2 of the UKHO dataset (Fig. 4.3). Core 131 was recovered on the flank of one of the elongate mega-ridges mapped on the bathymetry data (Fig. 4.12). The core is 2.70 m long and, when correlated to the seismic profile (Fig. 4.12), it appears to penetrate in the uppermost acoustic facies AF 5 (brown, Fig. 4.12), which has a very high amplitude upper reflector that represents the seafloor, and to reach the very top of AF 3 (violet, Fig. 4.12). Based on the distinct acoustic responses observed on the seismic data and on the BGS Offshore Regional Reports, different bedrock formations (AF 1, see Sect. 4.3.2) are inferred to be present throughout the research area, and Permian sediments are believed to form the substrate underneath AF 3 in correspondence to the location of core 131 (Fig. 4.12; Cameron *et al.*, 1992; Gatliff *et al.*, 1994). Core 132 is located approximately 11.5 km south-west of core 131 (Fig. 4.3). It is 2.17 m long and was also collected from an area characterised by elongate mega-ridges, though it appears to be located in the trough between two of these landforms, where a small lens of AF 4 (light blue, Fig. 4.12) was deposited. Here, AF 4 onlaps AF 3, although core 132 does not penetrate into the latter (Fig. 4.12). Bedrock strata (Triassic) are believed to be present underneath the Quaternary sediments at this location (Cameron *et al.*, 1992; Gatliff *et al.*, 1994). Cores 133 and 134 are located approximately 6 km apart from each other (Fig. 4.3 and 4.12), are 4.24 and 4.50 m long respectively, and are the closest ones to the coast of eastern England. The seafloor geomorphology in this area is characterised by the presence of W1, one of the two wedges recognized on the UKHO dataset (see Fig. 4.4b). The 2D seismic profile in Figure 4.12 shows the presence of bedrock strata (possibly Triassic; Cameron *et al.*, 1992; Gatliff *et al.*, 1994) at a very shallow depth below the seafloor at the

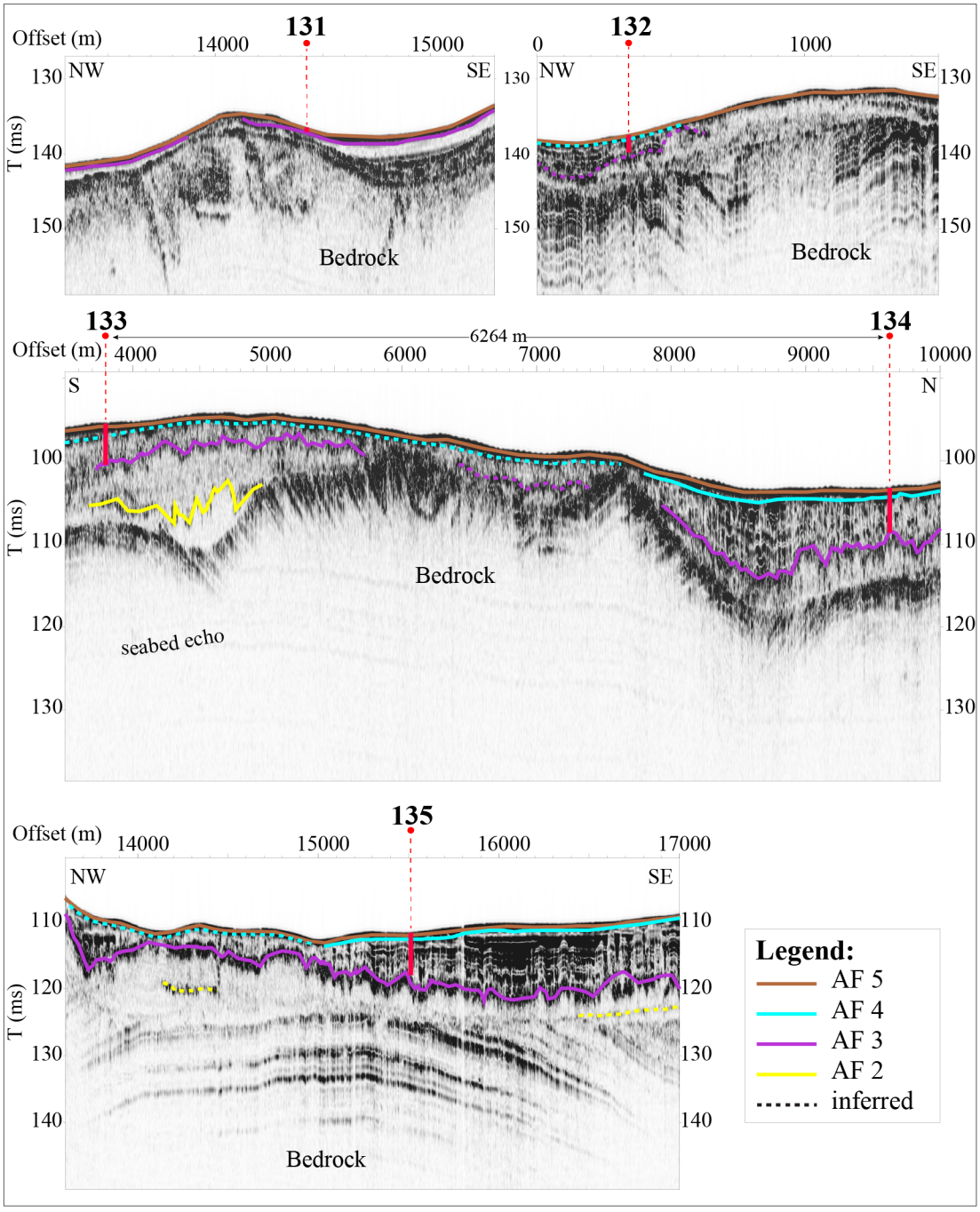

Figure 4.12: Cores 131 - 135 locations in relation to the 2D seismic profiles and the acoustic facies. The cores' penetration into the acoustic sequence was calculated for each core using the average of their P-wave velocities values. Coloured lines represent the upper boundaries of the acoustic facies.

cores' locations, overlain locally by lenses of AF 2 (yellow, Fig. 4.12), and more commonly by AF 3. On top of AF 3, AF 4 is found in this section and both cores 133 and 134 appear to penetrate through it and to just reach the top of AF 3. Finally, core 135 was collected in a small basin located in the south-east sector of the UKHO dataset, between two bedrock highs (Fig. 4.3). The southern limit of W1 is located approximately 16 km north from this core. The core is 5.66 m long and, as shown in Figure 4.12, penetrates AF 4 and just reaches the top of

AF 3. Cretaceous bedrock is believed to form the lowest part of the sequence at this location (Cameron *et al.*, 1992; Gatliff *et al.*, 1994).

2. Sedimentology

Cores 131 - 135 are described below based on visual observations, physical properties measurements and X-rays. A brief description of core 128 is also provided. The cores are described together where appropriate, according to their locations, and outlined in Figure 4.13. The sediments were classified as four different lithofacies and related subfacies that can be summarized as follows: LF 1 - massive (LF 1a) and stratified (LF 1b) diamictons; LF 2 - massive clay (LF 2a) and stratified silt and clay (LF 2b); LF 3 - massive sand (LF 3a) and gravel (LF 3b); LF 4 - massive sand with shells.

Cores 131 and 132

Cores 131 and 132 are the northernmost cores analysed in this research (Fig. 4.3) and also the shortest, being 2.70 and 2.17 m long, respectively. Core 131 consists of four lithofacies. At the bottom, core 131 displays a 5 cm layer of fine, well sorted sand (Fig. 4.13) and a 3 cm thick layer of reddish fine/medium sand (LF 3a). These are overlain by 72 cm of soft, massive, brown/grey (5Y 5/1, 5Y 4/1) silty clay (LF 2a). Above LF 2a, there is another layer (34 cm thick) of dark brown/grey, fine to medium, well sorted sand (LF 3a), overlain by 7 cm of fine gravels (LF 3b). A 75 cm thick layer of diamict (LF 1a) is found on top of the gravel layer and is then overlain by 74 cm of massive sand (LF 4) that constitutes the top of the core (Fig. 4.13). LF 2a is interstratifed with LF 3a found above it, while LF 1a is characterised by firm, massive, brown/reddish (7.5YR 4/2) silty clay with abundant clasts throughout, and contains a lens of medium sand. LF 4 at the top differs from the sands below (LF 3a) due to the presence of numerous shell fragments and clasts of different dimensions. This upper sand is medium/coarse and displays more shell fragments directly on top of the diamict and becomes finer, silty and well sorted at the top of the core (Fig. 4.13). MS measurements down core 131, show higher peaks in values corresponding to the diamictic layer, reaching more than 500 10^{-5} SI (corrected volume specific units) towards its base (Fig. 4.13). This high peak also correlates with peaks in gamma density and electrical resistivity values but also with a drop in V_p (from $\sim$1830 to $\sim$1550 m/s). This is probably related to the presence of the gravel layer, characterised by looser material. All physical properties also show an increase in values corresponding to the medium/coarse sand layer above the diamict and at the bottom of the core, at the boundary between clay and sand. Shear strength measurements collected within the diamictic layer show a gradual increase from 11 kPa at 85 cm depth to 50 kPa at 135 cm depth.

Core 132 consists of three lithofacies and is characterised at the bottom by 79 cm of very soft, thickly horizontally and inclined laminated, slightly silty clay (LF 2b; 7.5YR 4/3, 7.5YR 4/2) that displays colour banding from brown to red to green and occasional clasts (Fig. 4.13 and 4.14). The laminations appear more frequent towards the base of the layer and become more inclined towards the top, although this can be the result of a slight deformation of the sediments during coring. Clayey silt bands $\sim$0.5 - 1 cm thick are also found towards the base. At the top, this unit displays a sharp and highly curved boundary (probably the result of core

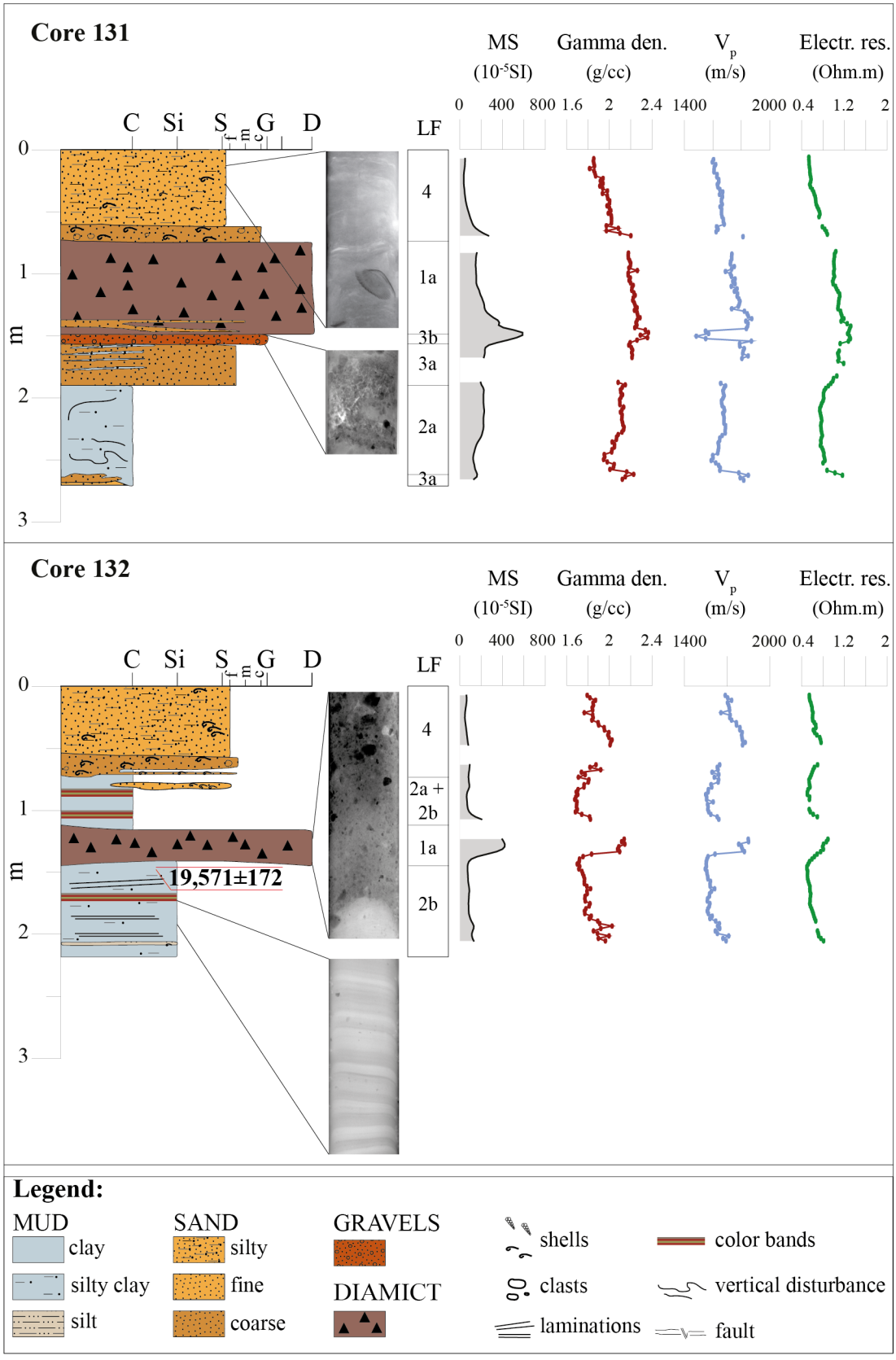

Figure 4.13: Core logs, lithofacies and physical properties measurements of cores 131 and 132. MS: magnetic susceptibility, Vp: P-wave velocity, Electr. resist.: electrical resistivity. Darker colour on the X-rays represents higher density material. The position of the radiocarbon date obtained from core 132 (144 cm depth) is indicated with red lines.

tube disturbance) and is overlain by 26 cm of diamict (LF 1a; 112 - 138 cm depth). This consists of dark-brown/grey (10YR 4/1), soft, silty clay with abundant clasts of various dimensions (Fig. 4.13 and 4.14). On top of the diamict, brown (10YR 4/3), massive, soft clay is present (LF 2a + LF 2b), characterised by colour bands and interdigitated towards the top with a lens of clayey silt/very fine sand, containing shell fragments, and the overlying unit. A 16 cm thick layer of brown, moderately sorted, very fine to fine sand (LF 4) is found on top of the clay and is characterised by abundant shell valves and shell fragments and by numerous clasts. The top of the core consists of 54 cm of dark brown/grey, massive, silty fine sand (LF 4), characterised by the presence of shell fragments and colour banding (Fig. 4.13). A 1 cm sample slab was taken at 144 cm depth from this core (within LF 2b) and sent to NERC laboratories for radiocarbon dating. The sample is located at the very top of the laminated clay layer LF 2b, very close to the lower contact of the diamict (LF 1a; position indicated in red in Fig. 4.13). MS, gamma density, V_p and electrical resistivity all display peaks in concentrations corresponding to the diamictic layer in the central part of the core but are also high within the sand layers at the top of the core and display an increase towards its base (Fig. 4.13). MS values in the diamict reach up to $\sim$420 10^{-5} SI at 129 cm depth.

Cores 133 and 134

Core 133 and 134 were collected closest to the coast, and only a few kilometres from each other (Fig. 4.3). Core 133 is 4.24 m long and consists of three lithofacies. It is characterised at the bottom by a 91 cm thick layer (333 - 424 cm depth) of brown (7.5YR 3/2), soft clay with abundant clasts of different sizes and some colour banding (LF 1b). This diamict differs from the diamictic layers of the other four cores (LF 1a) due to the presence of some small light brown (7.5YR 4/1) lenses of softer clayey silt and silty clay that are also visible from the X-rays (Fig. 4.13). A sharp, slightly inclined boundary separates this unit from the layer above which consists of a 233 cm thick, brown/reddish (7.5YR 4/2, 7.5YR 4/1), soft, massive clayey silt (LF 2b). From the X-rays it is possible to see that this layer displays some horizontal and inclined thin laminations with occasional occurrences of small clasts. It is also characterised by thin lenses of dark brown/grey clayey silt, with abundant visible granules, and by colour bands (Fig. 4.13). The clayey silt is intermixed towards the top with the unit above, which consists of 89 cm of brown/greyish, massive, slightly silty, moderately sorted, fine sand, with very small shell fragments (LF 4). Numerous gastropods are visible in this unit from the X-ray scans, as well as small granules and clasts. At 71 cm depth, the layer displays more abundant shells, shell fragments and clasts. The physical properties of core 133 show higher values of gamma density and electrical resistivity at the top of the core, with higher peaks also in MS corresponding to the interval, in the uppermost layer, characterised by more shells and clasts, which also displays a drop in V_p compared to the values above it (Fig. 4.13). Below this, the MS values are constant throughout the clayey silt layer, though some peaks are visible, which possibly relate to the presence of bands with more granules. Finally, there is a subsequent peak in MS at the interface between clayey silt and diamict, and the other three properties also display an increase in values until the bottom of the core.

Core 134 is 4.50 m long and consists of 3 lithofacies. It is characterised by a diamictic

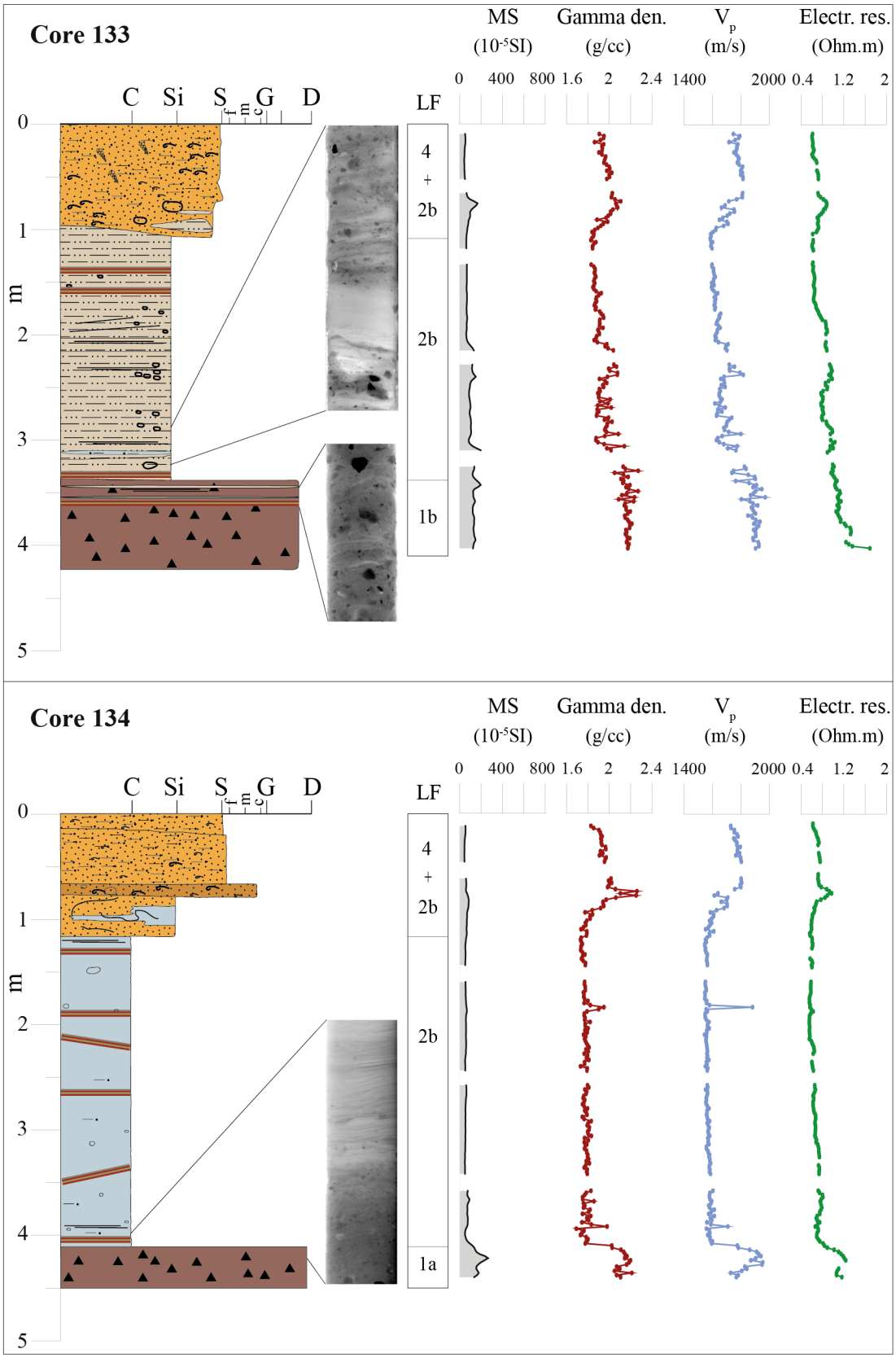

Figure 4.13 (cont.): Core logs, lithofacies and physical properties measurements of cores 133 and 134.

layer (LF 1a) at the base, which consists of a brownish (7.5YR 3/2), soft, silty clay with abundant clasts of various dimensions and lithologies (Fig. 4.13). The diamict does not show evidence of laminations either from visual observation or on X-ray imagery. The upper contact of this layer appears gradational. Above the diamict, a 296 cm thick layer of brown/red (7.5YR 4/2, 7.5YR 4/3), very soft, massive clay is found (LF 2b), which is characterised by numerous horizontal and inclined colour bands and by the presence of occasional granules and clasts. Towards the bottom of the layer, it is possible to see some very small laminae of red silt (Fig. 4.13). There is a change of colour occurring at ∼391 cm depth, where the sediment becomes grey/brown (7.5YR 4/1) and the clay appears more silty and highly laminated. A disturbed layer marks the upper contact of the massive soft clay with the unit above it, which consists of a 7 cm thick silty, coarse, poorly sorted sand (LF 4 + LF 2b), characterised by the presence of abundant clasts, shells and shell fragments. The two layers are interdigitated between 78 and 116 cm depth (Fig. 4.13). At the top, the core is characterised by 57 cm of brown, moderately sorted, massive, silty, very fine to fine sand (LF 4), with visible and usually small shell fragments. This layer is separated by an inclined boundary from the unit above it, which consists of 14 cm of dark grey/green, soft, silty and moderately sorted very fine sand (LF 4) with small shell fragments. MS values are quite constant throughout the entire length of the core, presenting slightly higher values in correspondence to the coarse, poorly sorted sand, which is rich in clasts, and then reaching up to a maximum of ∼267 10^{-5} SI at 419 cm depth, in the diamict. High peaks in gamma density, V_p and electrical resistivity are also present occasionally in the clay, possibly due to the presence of higher density sediments (Fig. 4.13). The diamictic facies displays shear strengths of 20 - 25 kPa throughout.

Core 135

Core 135 is the easternmost core of this research and is 5.66 m long. It consists of 4 lithofacies and is characterised at the bottom by a diamictic layer (Fig. 4.13). This reddish/grey (5YR 3/3, 5YR 4/3), massive, soft silty clay (LF 1a) displays abundant clasts of different dimensions and lithologies that do not appear to show any preferred orientation, based on a crude assessment of the X-ray images. The diamict is 107 cm thick and is interrupted by the presence of a 5 cm thick layer of very bright red (5YR 4/3), soft, clayey silt containing some black pods (LF 2a). The layer above the diamict, separated from it by a sharp and inclined contact, consists of a 417 cm thick, brown (7.5YR 4/1, 7.5YR 4/2), soft, clayey silt (LF 2b) that displays lamination, colour bands and a colour change at 405 cm depth (10YR 4/1). X-rays show the presence of some small clasts within it. The laminations are horizontal to inclined and the core displays micro-faults at ∼410 cm depth (Fig. 4.13 and 4.14). Numerous laminae/strata up to more than 1 cm in thickness, of reddish (7.5YR 5/4, 7.5YR 4/4), very well sorted, very fine sand (LF 3a) are present throughout the entire unit (Fig. 4.14). Above this, there is an 11 cm thick, dark brown/grey moderately sorted, silty fine/medium sand layer (LF 4), full of shell fragments and that displays an uneven lower contact with the layer underneath (Fig. 4.13). Small lenses of this material are also found at the very top of the clayey silt. The top part of the core is characterised by 23 cm of dark grey, moderately sorted, fine/medium sand (LF 4) with visible shell fragments throughout, that overlies a 3 cm thick layer with more abundant shells and shell

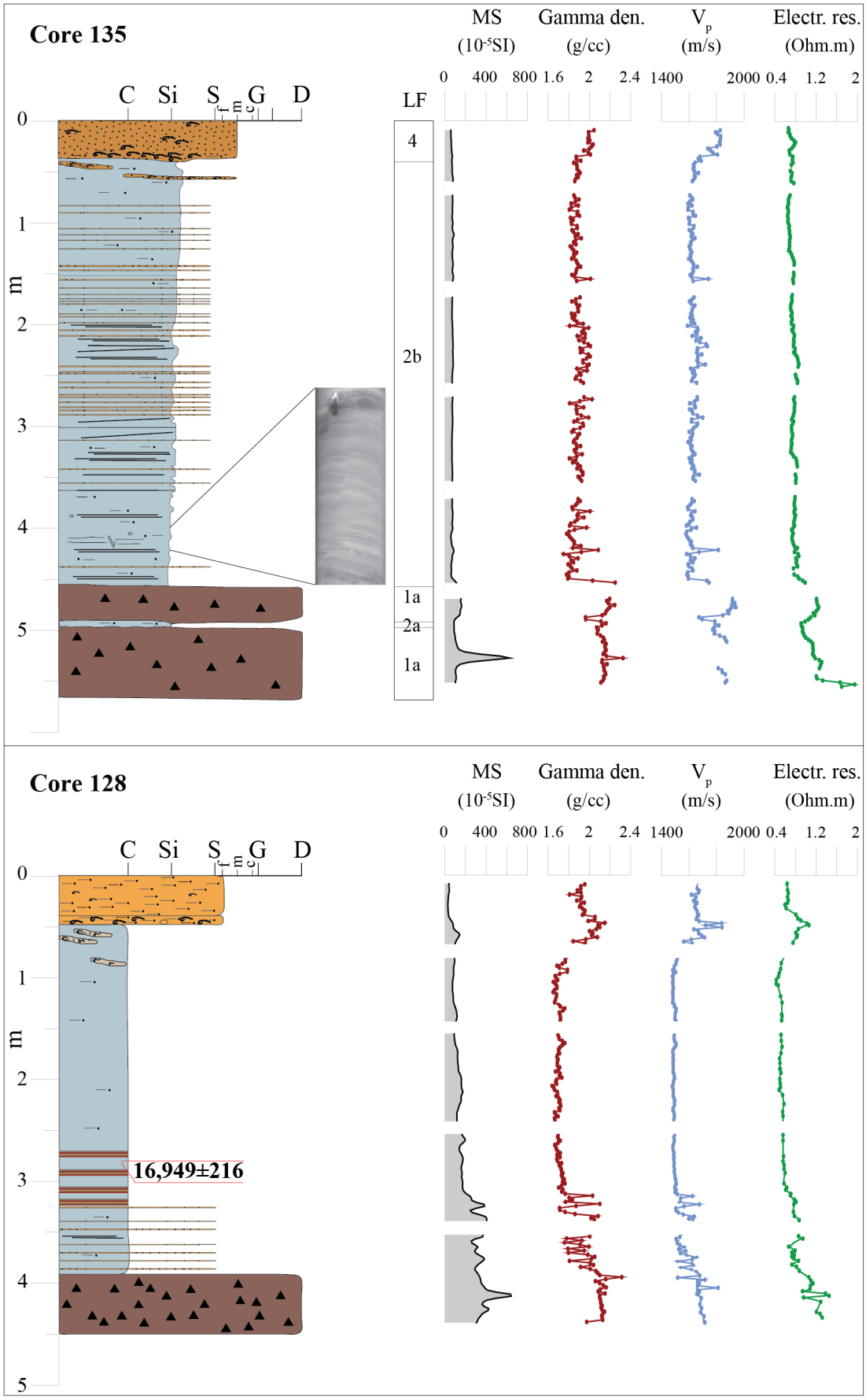

Figure 4.13 (cont.): Core logs, lithofacies and physical properties measurements of cores 135 and 128. The position of the radiocarbon date obtained from core 128 (280 cm depth) is indicated with red lines.

fragments, including one intact valve (∼4.5 cm in diameter). MS data show relatively low and constant values throughout the core until a visible increase above the top of the diamict layer, where values change from ∼65 to ∼150 10^{-5} SI and then reach up to ∼629 10^{-5} SI at 527 cm depth, possibly due to the presence of bigger clasts (Fig. 4.13). The values for gamma density, V_p and electrical resistivity follow the trend of the MS, although more clearly represent the presence of the laminae of very fine sand, showing numerous peaks corresponding to their occurrence. They also display higher values at the top of the core where the sediment is sandy. Shear strengths measurements collected in the diamictic layer show values between ∼40 - 70 kPa.

Core 128

Core 128 was collected within Area 1 of the UKHO dataset (Fig. 4.3), and is briefly described here because it provided an additional radiocarbon age that was used in this study. The core was not analysed together with the other five at the laboratories of Durham University, and this description is thus taken from the core log prepared on-board. The core is 4.50 m long and is characterised at the bottom by 59 cm of massive, brown (7.5YR 3/2) silt with abundant clasts, overlain by a 72 cm thick layer of alternating clayey silt and clay (Fig. 4.13). This unit is then overlain by a 236 cm thick layer of soft, brown (7.5YR 3/2) clay, which displays numerous color bands and is slightly laminated. This layer is interdigitated with small lenses of sandy silt with shell fragments between 48 and 82 cm depth. At the top of the core, a 48 cm thick layer of silty fine sand is found, characterised by occasional shell fragments until 40 cm depth, and highly abundant shell fragments until 48 cm depth. MS measurements display higher values towards the bottom and top of the core, in correspondence with the diamictic and sandy layers. This is also the case for the other three physical properties. Shear strengths measurements within the diamictic layer are between ∼18 - 68 kPa.

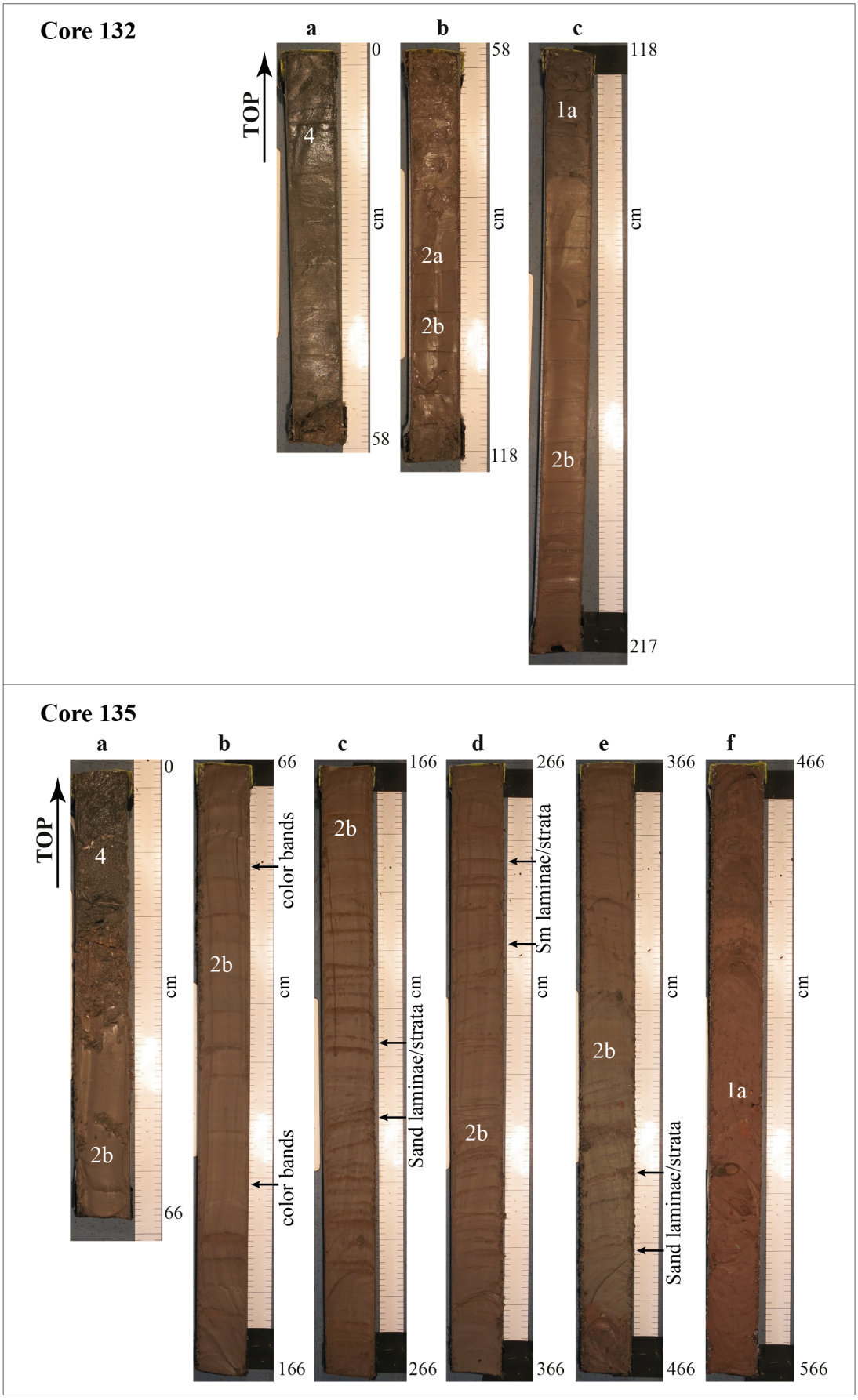

Figure 4.14: Photos of cores 132 (three sections, a - c) and 135 (six sections, a - f). The lithofacies numbers and additional details are indicated.

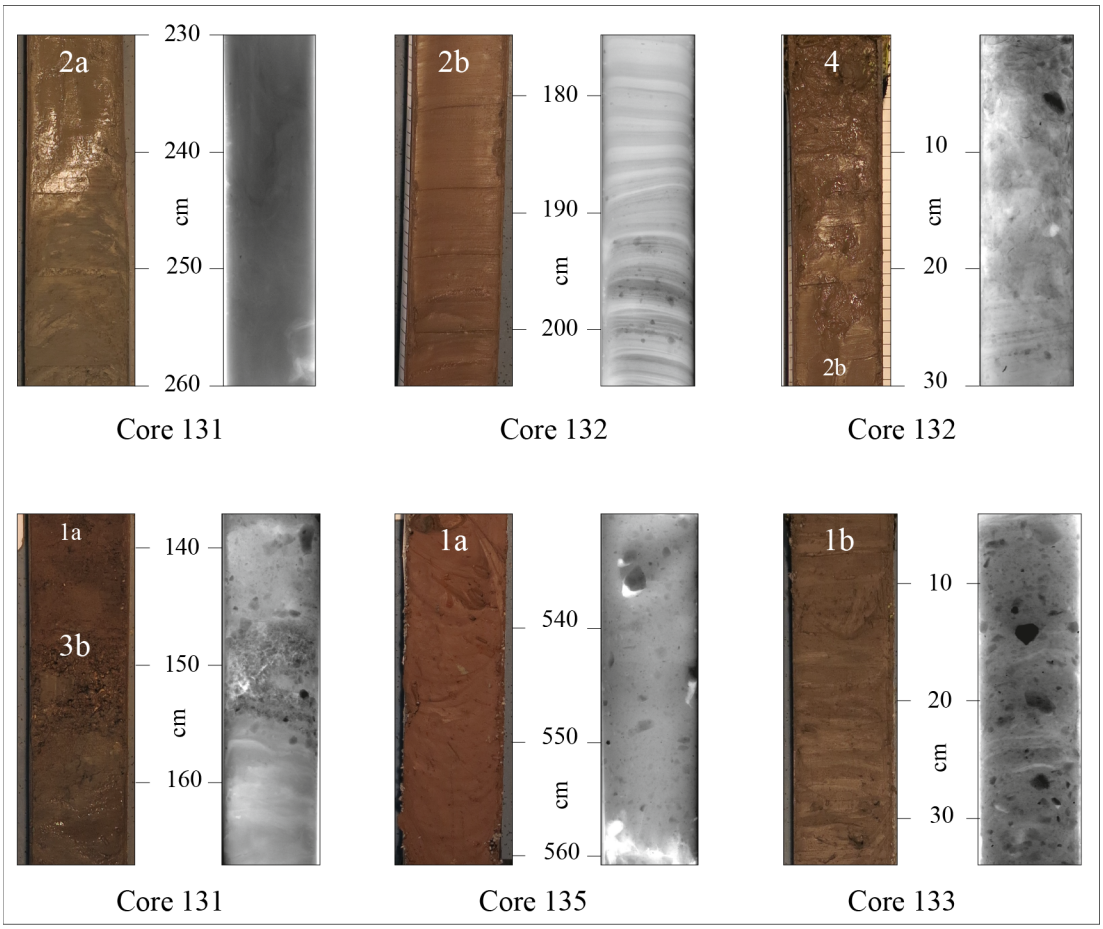

Figure 4.15: Examples of core photos and X-rays of the lithofacies identified in the research area. Note that darker colors on the X-rays represent denser materials.

4.3.4 Micropalaeontology

The five vibro-cores 131 - 135 were analysed for foraminiferal content and for radiocarbon dating, although only one sample contained enough foraminifera tests to be dated (core 132, 144 cm depth). Common to all five cores is the limited number of foraminifera individuals found in each sample. An assessment of the species assemblages was carried out for three cores: 132, 134 and 135. The results are displayed in Figure 4.16 and Table 4.3.

Core 132

Three samples were analysed from core 132. The samples at 84 and 109 cm depth, reveal a total of 9 different foraminifera species (including the unidentified individuals, Fig. 4.16). A 1 cm slab was also taken at 209 cm depth within the lowermost facies of the core (LF 2b), though no foraminifera tests were found. One sample was collected from this core at 144 cm (LF 2b) and sent to NERC laboratories for radiocarbon dating due to the large number of individuals picked. The sample at 109 cm depth was taken from the brown, massive, soft clay facies (LF 2a and 2b, Fig. 4.13) and is characterised mainly by *Elphidium excavatum (clavatum)*, with 80 specimens out of a total of 122, followed in abundance by *Haynesina orbiculare* (17 individuals). *Elphidium albiumbilicatum*, *Elphidium asklundi* and *Elphidium*

excavatum are also present, though in minor percentages (Fig. 4.16). The sample at 84 cm depth was collected from the same layer (LF 2a and 2b) but very close to its upper contact and shows the presence of very similar species to the lower sample, with *Elphidium excavatum (clavatum)* being the most abundant, although the *Cassidulina reniforme* species is also present here, with 29 individuals out of a total of 131.

Core 134

Foraminifera tests are absent from core 134 at 409 cm depth, which is located almost at the lower contact of the silty soft clay layer (LF 2b), close to the upper boundary of the diamict (LF 1a, Fig. 4.13). At 354 cm depth, within the same facies (LF 2b), 67 foraminifera individuals were found, mainly consisting of *Elphidium albiumbilicatum* (62 specimens) and *Haynesina orbiculare* (only 3 specimens; Fig. 4.16). There is a clear change in foraminifera species occurrence between this lower sample and the three collected higher in the core, that are all characterised by the absence of *Elphidium albiumbilicatum* in favour of *Elphidium excavatum (clavatum)*, which is dominant (Fig. 4.16). At 339 cm depth (LF 2b) particularly, this species accounts for 206 individuals out of a total of 308 found, and is followed in number by *Elphidium incertum* which is also absent from the sample at 354 cm. The samples collected at 259 cm and at 169 cm depth were also located within LF 2b (Fig. 4.13) and a total of 53 foraminifera tests were recovered from each. Both samples show a high percentage of *Elphidium excavatum (clavatum)*, while *Haynesina orbiculare*, absent at 339 cm depth, re-appears here with 6 individuals at 259 cm and 2 individuals at 169 cm depth. This uppermost sample is also the only one characterised by the presence of the species *Cassidulina reniforme*, which is here the second most abundant species with 15 specimens out of a total of 53 (Fig. 4.16).

Core 135

Core 135 has the longest record for changes in foraminifera species, with 8 samples collected. No foraminifera were found at 550 cm depth, within the diamict (LF 1a), while only 8 were recovered from 493 cm depth. This sample was collected from the soft clayey silt unit (LF 2a) that interrupts the diamict layer (Fig. 4.13). Interestingly, it is the only sample characterised by the presence of *Cibicides sp.* which is absent from the samples above (Fig. 4.16). A total of 7 samples were collected at different depths within the clayey silt layer (LF 2b). At 371 cm depth, 2 foraminifera tests were found, one of them being planktonic and the other one being *Haynesina orbiculare*. The sample at 334 cm is still very poor in foraminifera individuals, with a total of 8 tests recovered, and is dominated by *Elphidium* genus. This is also the case for the sample at 298 cm depth, though here two tests of planktonic foraminifera are found, out of a total of 22. At 250 cm depth the individuals are 107 in total and they are characterised by 37 *Elphidium excavatum (clavatum)*, 22 *Elphidium incertum* and 20 planktonic. In this sample there is also a high abundance of *Bolivina inflata*, with 12 individuals. At 160 cm depth the foraminifera individuals are much higher in number, with a total of 492 picked, and once again *Elphidium excavatum (clavatum)* and *Elphidium incertum* are the dominant species. The planktonic tests continue to increase in abundance and are here 54 in number. At 80 cm depth

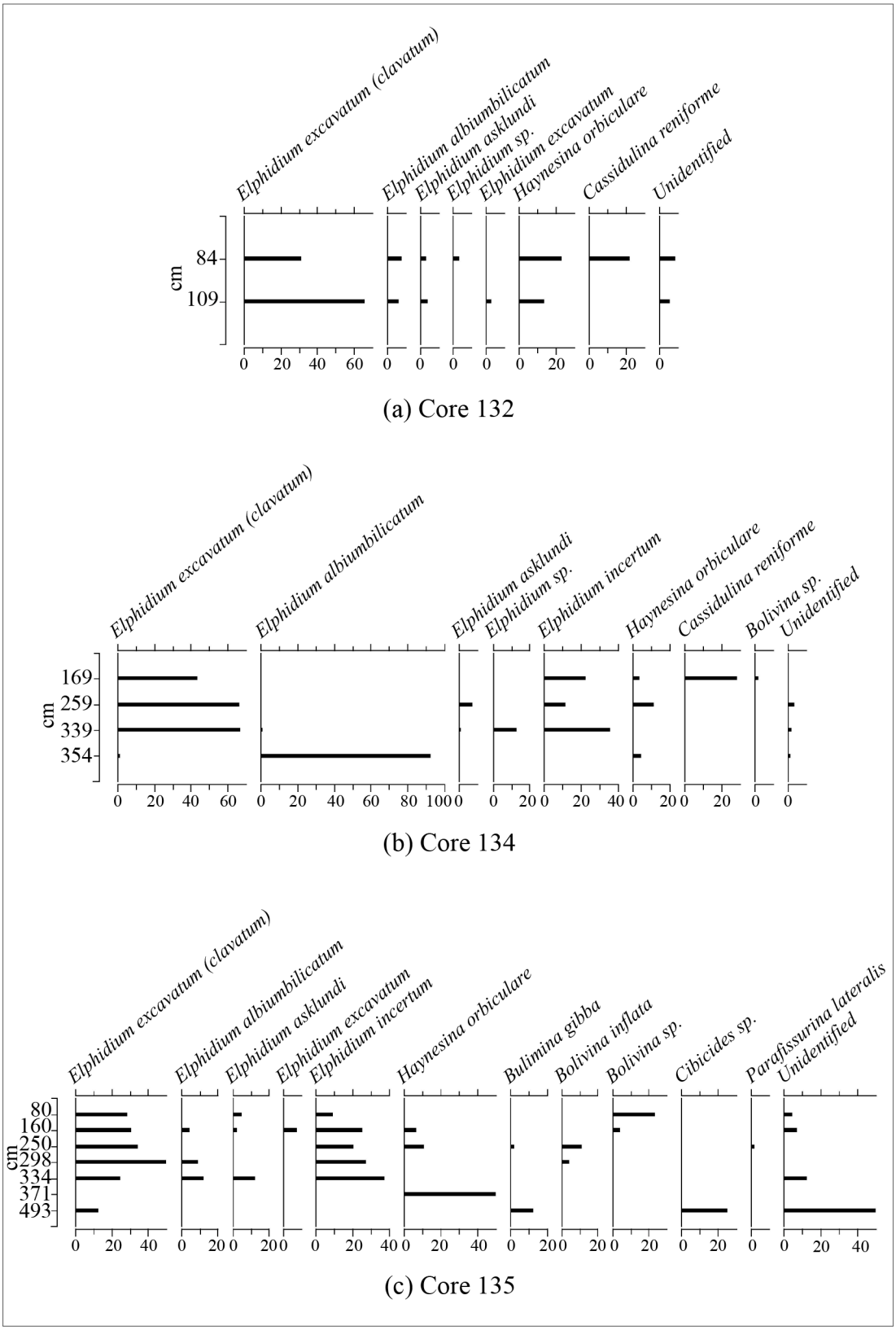

Figure 4.16: Foraminifera relative abundances of cores 132, 134 and 135. Only data values ≥ 1 % are shown.

Core	**132**		**134**				**135**						
Depth (cm)	84	109	169	259	339	354	80	160	250	298	334	371	493
Species	Individuals												
Elphidium excavatum (clavatum)	41	80	23	35	206	1	6	151	37	11	2	0	1
Elphiudium albiumbilicatum	10	8	0	0	3	62	0	22	0	2	1	0	0
Elphidium asklundi	4	5	0	4	3	0	1	11	0	0	1	0	0
Elphidium sp.	5	0	0	0	40	0	0	0	0	0	0	0	0
Elphidium sp. (fragments)	0	0	0	0	21	0	0	0	0	0	0	0	0
Elphidium excavatum	0	4	0	0	0	0	0	37	0	0	0	0	0
Elphidium incertum	0	0	12	6	110	0	2	125	22	6	3	0	0
Haynesina orbiculare	30	17	2	6	1	3	0	33	12	0	0	1	0
Cassidulina reniforme	29	0	15	0	0	0	0	0	0	0	0	0	0
Bulimina gibba	0	0	0	0	0	0	0	0	2	0	0	0	1
Bolivina inflata	0	0	0	0	0	0	0	0	12	1	0	0	0
Bolivina sp.	0	0	1	0	0	0	5	22	0	0	0	0	0
Cibicides sp.	0	0	0	0	0	0	0	0	0	0	0	0	2
Parafissurina lateralis	0	0	0	0	0	0	0	0	2	0	0	0	0
Fissurina sp.	0	0	0	0	0	0	0	1	0	0	0	0	0
Lagena sp.	0	1	0	0	0	0	0	0	0	0	0	0	0
Planktonic	0	0	0	0	0	0	6	54	20	2	0	1	0
Unidentified	12	7	0	2	7	1	1	35	0	0	1	0	4
Total	131	122	53	53	308	67	21	492	107	22	8	2	8

Table 4.3: Absolute abundances of foraminifera species in vibro-cores 132, 134 and 135.

only 21 foraminifera tests were found. 6 *Elphidium excavatum (clavatum)* and 6 planktonic individuals were counted but *Bolivina sp.* and *Elphidium incertum* tests are also present at this depth. The uppermost sample was collected at 20 cm depth from the fine/medium sand lithofacies (LF 4) at the top of the core (Fig. 4.13). This sample was subdivided manually into four parts and one quarter was analysed at the microscope. This was due to the high amount of sediment that remained in the sample after the sieving process (see Sect. 4.2). The sample is characterised by a very high abundance of quartz fragments and other grains of different lithologies and displays a large amount of shell fragments and sea urchin spines. It is barren in foraminifera.

4.4 Interpretations

4.4.1 Correlation of bathymetry and seismic data

Correlation between the bathymetry and the seismic data was necessary to interpret the numerous landforms observed on the seabed. The UKHO bathymetry dataset reveals the area is characterised by a very irregular and rugged seafloor, with numerous topographic highs and lows (as can be seen in Fig. 4.4a), and with extensive bedrock outcrops (as previously discussed in Chapt. 2 and 3). However, there is also a distinctive set of glacial landforms occurring in the study area.

Bedrock and moraine ridges

The SW - NE orientated ridges mapped in Figure 4.4b in brown (R1 - R10), which at times have convex planforms, are quite regularly distributed in the area, from north to south. These ridges could, at first glance, be interpreted as moraine ridges derived from ice flowing along a NW to SE trajectory. Figure 4.17 shows examples of the bathymetric and seismic appearances of R4, R5 and R7 (Fig. 4.17a, 4.17b and 4.17c, respectively). Cross-profiles are shown for R5 and R7, while R4 is shown along-profile. R5 and R7 display similar characteristics to one another. They are defined by steep slopes and have an irregular profile with various crests. R4 is only 5 m high and displays gentler slopes. From the seismic profiles it is possible to see how these three ridges are all characterised internally by bedrock strata, which is present very close or at the seabed (Fig. 4.17b and 4.17c). Ridges R1, R2, R6 and R10 also display similar geometries to R4, R5 and R7 and, when observed on seismic profiles, appear correlated to bedrock highs. It is thus inferred that these ridges are not moraines but bedrock ridges, whose configuration and orientation is principally controlled by bedrock structure. R7, in particular, appears to correspond, at least partly, to the offshore continuation of the Whin Sill complex (Fig. 4.18), an igneous intrusion of Late Carboniferous - Early Permian age, which crops out onshore in northern England, from Holy Island down to Alnwick and Teesdale, and also continues offshore (Gatliff *et al.*, 1994; Stephenson *et al.*, 2003; Liss *et al.*, 2004).

Figure 4.17d and 4.17e show cross-profiles of the second sub-group of ridges (in blue in the insert map, Fig. 4.17). These are also characterised internally by bedrock strata, overlain in places by AF 5. It is thus inferred that these ridges are not moraines but bedrock ridges. This

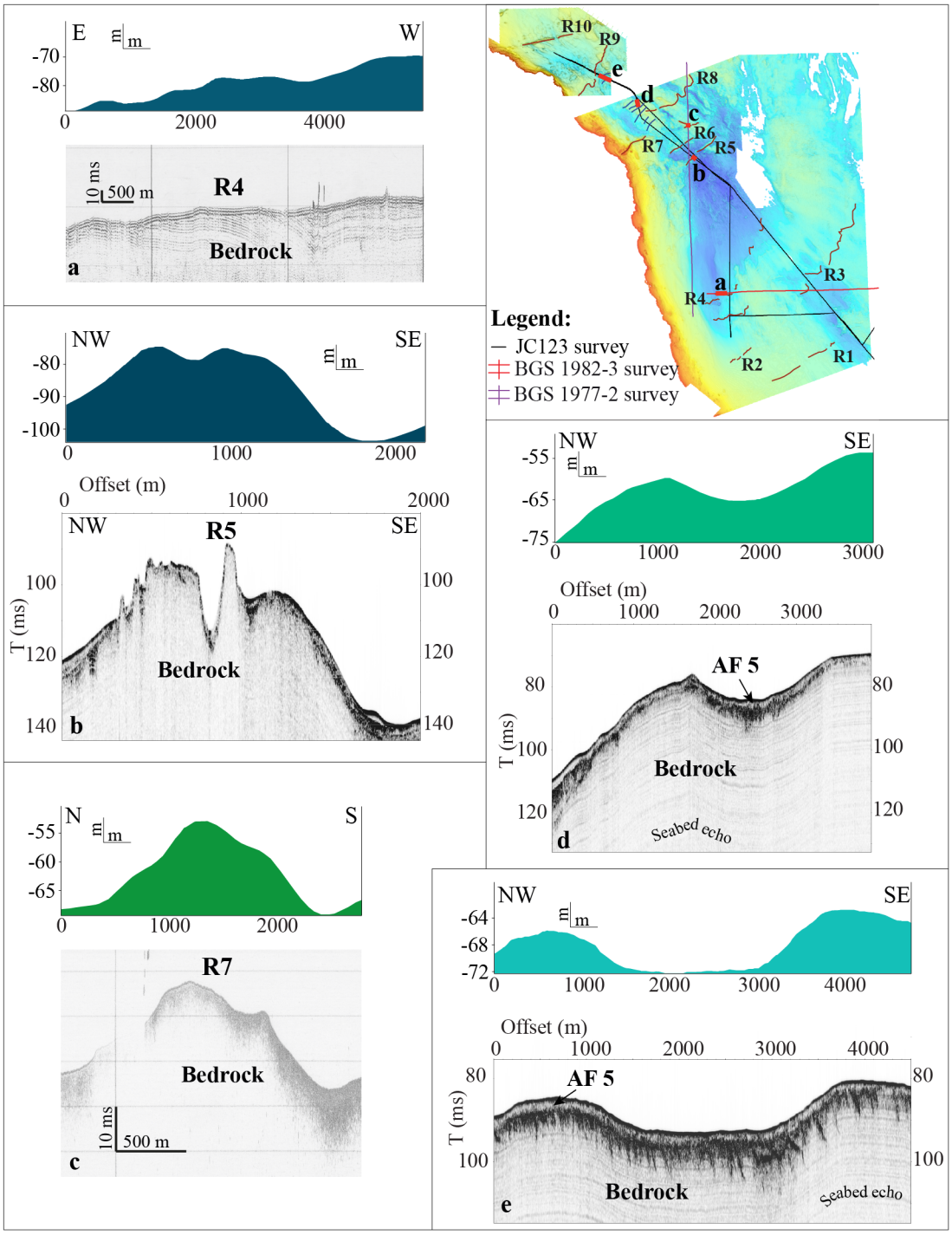

Figure 4.17: Examples of seismic profiles from the JC123 survey and from two BGS lines (red and violet lines) along the ridges R4, R5 and R7 (profiles a, b, c) and along the second sub-group of ridges recognized in Figure 4.4b (mapped in blue; profiles d, e). The locations of the profiles are highlighted in red in the insert map. Note the vertical exaggerations of the bathymetry and seismic profiles. Also note the seabed echo visible in profiles d and e which could be mistaken for internal stratifications.

is also the case for the third sub-group of ridges, orientated in a NW - SE direction (in green in Fig. 4.4b) and previously described in section 4.3.1. On seismic profiles they also appear to be internally characterised by bedrock strata, hence their formation is not considered to be related

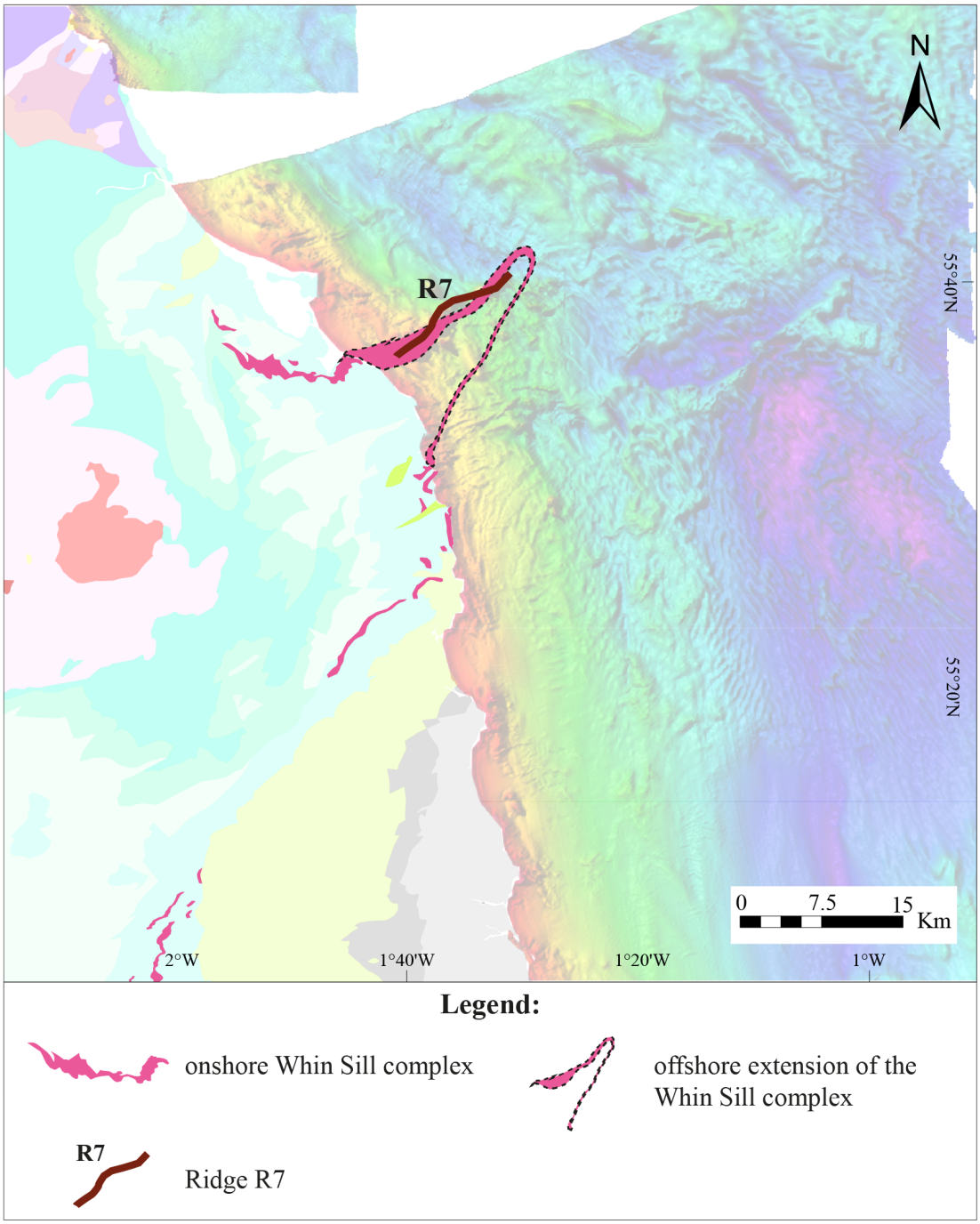

Figure 4.18: Onshore bedrock geology map compiled by the BGS (DiGMapGB-625 Bedrock geology), shown together with the offshore UKHO bathymetry data. The Whin Sill complex is highlighted in pink and its offshore continuation is also shown in pink, delimited by a black dashed line. The position of the ridge R7 is shown in brown. This figure contains British Geological Survey materials.

to the action of ice.

The ridge R8, on the other hand, is different. It is very curvilinear, characterised by a multi-lobe planform and by numerous inflection points (Fig. 4.4b and 4.19). It is concave to the north-west, both its northern and southern slopes are gentle and it does not exceed 10 m in height. Bedrock strata is present close to the seafloor underneath R8, though in

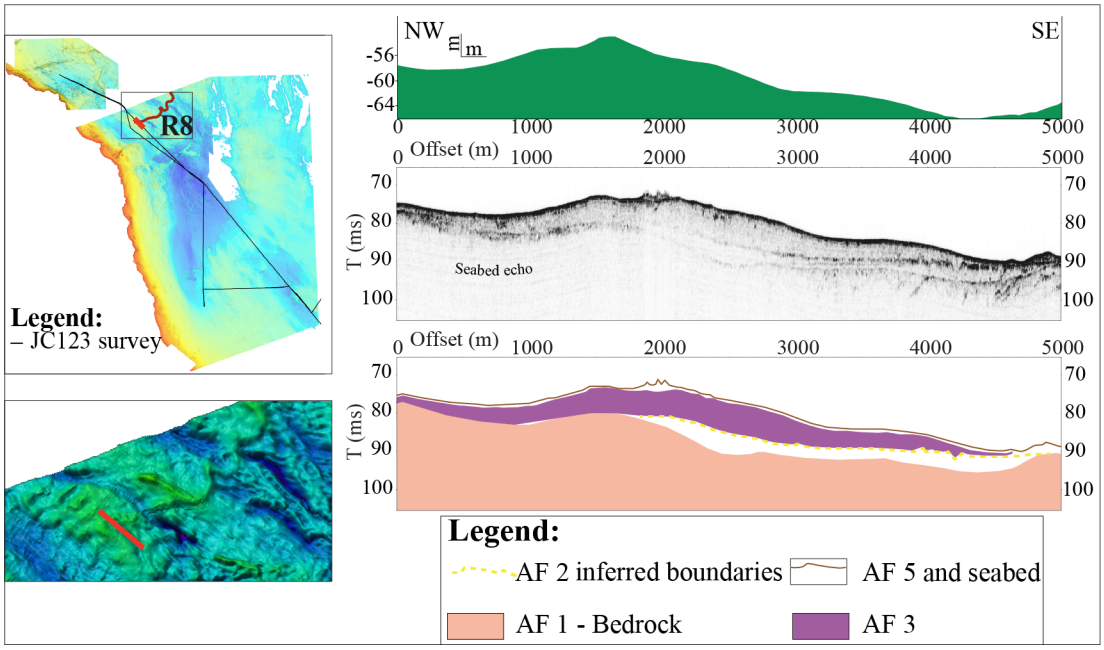

Figure 4.19: Bathymetric and seismic profiles and facies interpretation of R8. Its location and the location of the profile (red line) are shown in the insert map on the left. A detail of the UKHO high resolution bathymetry is also shown (location indicated by the black square in the map). Note the vertical exaggeration of both the bathymetry data and the seismic profile. Also note the seabed echo which could be mistaken for internal stratifications.

this case AF 3 (in violet, Fig. 4.19) is the main facies that forms the core of the actual ridge. The seismic appearance of AF 3 resembles the acoustic response of tills, which is often transparent due to the heterogeneous nature of their sediments (Cameron *et al.*, 1992; Gatliff *et al.*, 1994; Huuse & Lykke-Anderson, 2000). Furthermore, the sediment cores collected in the area during the Britice-Chrono JC123 survey show the presence of diamict (LF 1a and LF 1b) in correspondence to this facies (see Sect. 4.3.3 and Fig. 4.12; this is discussed in more detail in Sect. 4.5). AF 3 is thus interpreted to be a glacigenic diamict (and possibly a till). Combining the morphological and stratigraphic evidence, R8 is interpreted to be a moraine ridge, related to either a stillstand or to an oscillation of an ice-margin. Similar landforms have been observed and mapped offshore of north-west Scotland, where they have been interpreted as ice-marginal and ice-recessional moraines (Bradwell & Stoker, 2015a), and the curvilinear shape of R8 resembles the typical profile of a recessional push moraine (Benn & Evans, 2010; Bradwell & Stoker, 2015a).

Finally, R3 and R9 differ when observed on seismic profiles from the ridges analysed so far. They represent the southernmost limits of W1 and W2 respectively (Fig. 4.4b), and are discussed below.

Grounding zone wedges (GZWs)

The two wedges W1 and W2, are orientated from south-west to north-east. W1 displays a very curvilinear planform and a lobate southern perimeter. It is characterised by a rugged upper surface and is overprinted by sand dunes and sand waves (Fig. 4.4b and 4.20). When observed

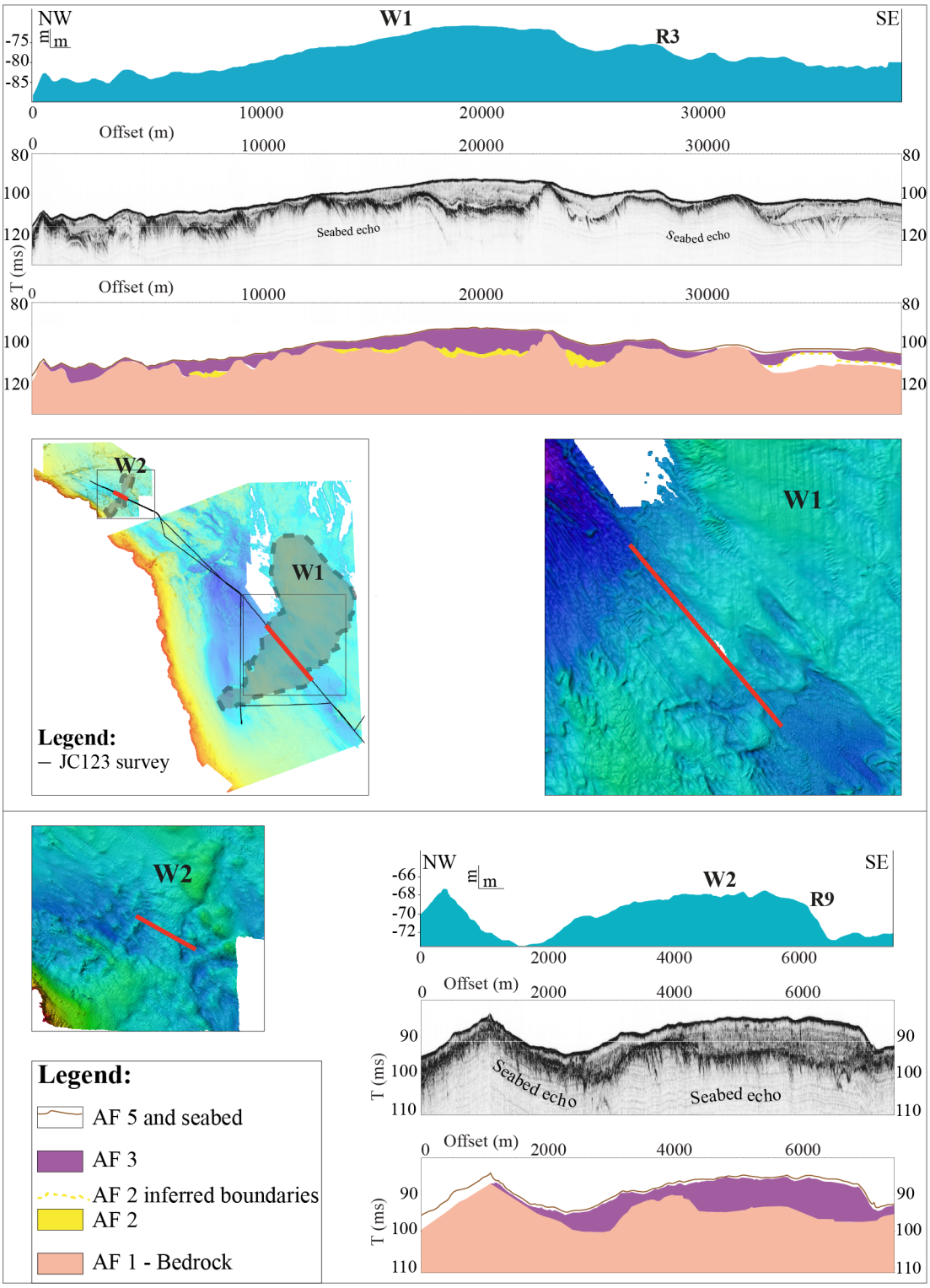

Figure 4.20: Bathymetric and seismic profiles and facies interpretation of W1 and W2. The wedges and the location of the profiles (red lines) are shown in the insert map. UKHO bathymetry close-ups are also shown (locations indicated with black squares in the map). Note that both the bathymetry data and the seismic profiles are vertically exaggerated.

in seismic section, W1 is characterised by the presence of bedrock strata very close to, and at times at, the seafloor, constituting some of the crests of the wedge itself (Fig. 4.20). However, the acoustic facies that mainly constitutes the core of the landform is AF 3 (Fig. 4.20), which

overlies the bedrock strata or is found overlying discontinuous lenses of AF 2 (mapped in yellow, Fig. 4.20). AF 3 is generally acoustically opaque, though at times, chaotic reflectors are also visible. AF 2 on the other hand is very thin and has an irregular upper boundary, while its acoustic appearance is usually transparent. AF 3 was previously interpreted as glacigenic diamicton, due to its acoustic signature and to ground-proofing. Considering that AF 2 is characterised by a lens-like geometry, is acoustically transparent and displays a generally irregular upper boundary, together with the fact that it is found, along the seismic profiles, associated with the presence of AF 3 (Fig. 4.10), this facies is also interpreted as glacigenic diamicton (and possibly a till; Cameron *et al.*, 1992; Gatliff *et al.*, 1994; Huuse & Lykke-Anderson, 2000). Therefore, given its wedge-like geometry and its geological composition, W1 is interpreted to be a grounding zone wedge (GZW). Grounding zone wedges are wedge-shape deposits predominantly composed of glacial diamict or till. They are typically characterised by an asymmetric geometry with steeper ice-distal sides, and are commonly tens of meters high, up to several kilometres wide and tens of kilometres in length (Ottesen *et al.*, 2007; Dowdeswell & Fugelli, 2012; Batchelor & Dowdeswell, 2015). Usually, GZWs appear acoustically semi-transparent to chaotic, reflecting the internal diamictic composition (Batchelor & Dowdeswell, 2015). W1 displays all the above-mentioned characteristics. The bathymetric profiles of Figure 4.21 show how W1 is only a few meters high, but much more extended in width, spanning for $\sim$30 km. The wedge has also an asymmetric profile and displays gentler slopes towards its northern limit and steeper ones facing the south (Fig. 4.20 and 4.21c, 4.21d, 4.21e). This particular geometry indicates that the former ice flow was directed towards the south-east, in accordance with the known glacial history of the area, which suggests that ice flowed south-eastwards from source areas such as the Forth (Fig. 4.1; Everest *et al.*, 2005; Bradwell *et al.*, 2008b; Livingstone *et al.*, 2012b, 2015; Bateman *et al.*, 2015). W2 is the other large wedge-like landform observed on the UKHO bathymetry. The bathymetric profiles shown in Figure 4.20, 4.21a and 4.21b, show how W2 is also characterised by an asymmetric geometry, and displays gentler slopes towards the north-west and steeper ones facing the south-east. When observed on seismic profile, W2 appears to be also composed of acoustic facies AF 3, which lies directly on top of bedrock strata (Fig. 4.20). Considering the similarity to W1, both geometrically and in composition, W2 is interpreted as a second grounding-zone wedge, which further confirms the former ice flow direction, towards the south-east.

Finally, the ridges R3 and R9 appear to be part of W1 and W2 (Fig. 4.20). When observing them on seismic profile, it is possible to see how they are not isolated ridges, but rather part of the two GZWs. This is particularly evident for R3 which is found in association with a bedrock high that comes close to the seabed (Fig. 4.20) and constitutes one of the crests of W1. R3 and R9 are thus considered as part of the GZWs. Therefore, it is inferred that of all the landforms analysed so far, only W1, R8, and W2 are related to the action of ice and represent former ice-margin locations (R3 and R9 being considered as part of the wedges), while the rest of the mapped landforms represent bedrock outcrops in the study area.

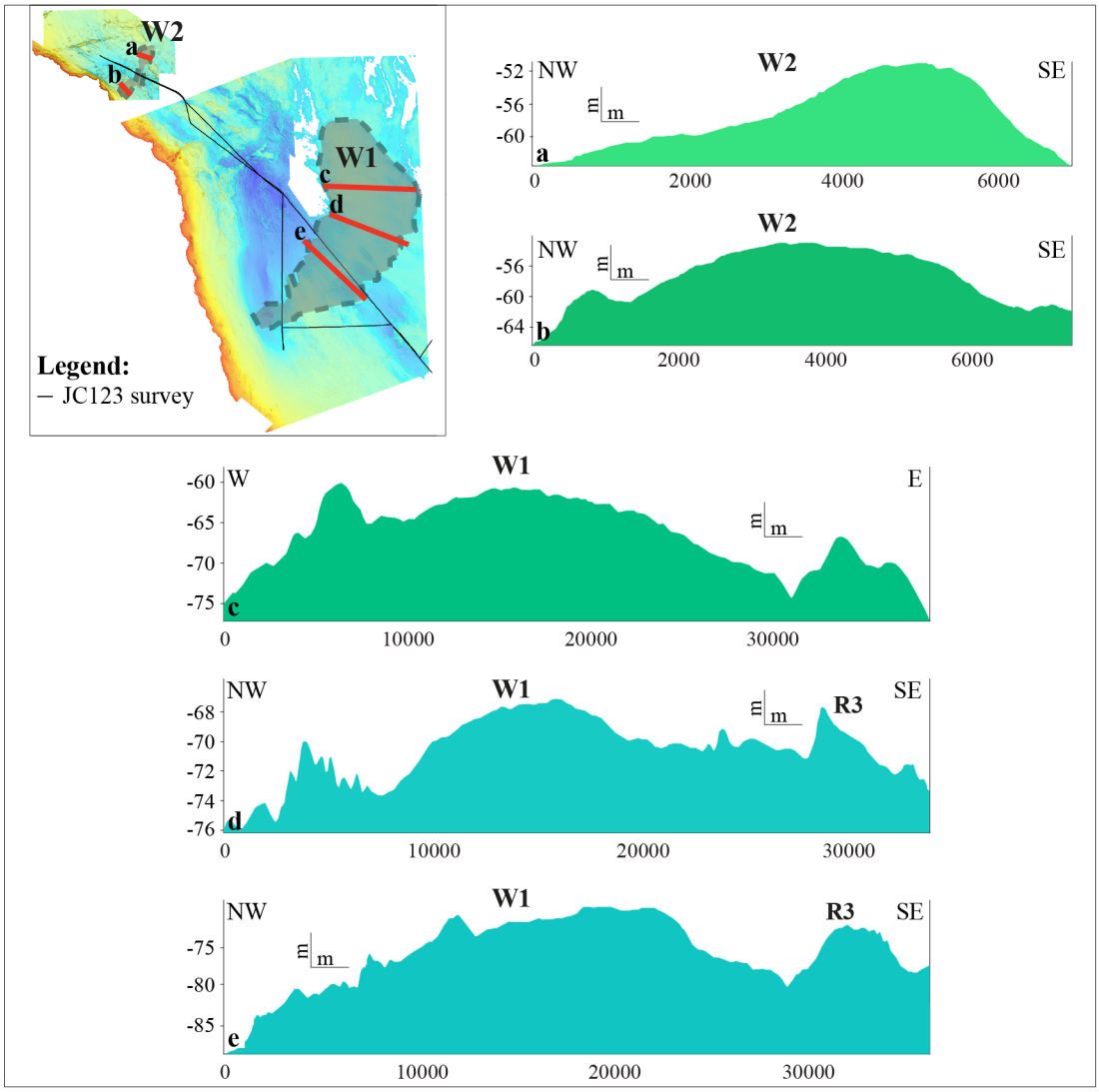

Figure 4.21: NW - SE bathymetric profiles of W1 and W2. The wedges and the location of the profiles (red lines) are shown in the insert map. Note that the profiles are vertically exaggerated. Also note the presence of sand waves on top of W1.

Elongate mega-ridges - Bedrock-cored lineations

Numerous small ridges were observed on the bathymetry data mainly in the central part of the UKHO Area 2 (Fig. 4.4b, black lines). These elongate ridges are orientated mainly NW - SE and only appear to be orientated WNW - ESE within Area 1 (Fig. 4.4b). They are generally between 1 and 4 m in height and their elongation ratio varies between 3:1 and 14:1. When observed on seismic profile, it is possible to see how these bedforms are prevalently composed of bedrock, which comes up at the seabed in correspondence to the crests of the ridges (Fig. 4.22 and 4.23). A localized thin layer of AF 3 is also part of the internal composition of the bedforms, and it generally appears to be thicker in the topographic lows between the ridges (in violet in Fig. 4.22). The bedrock strata, recognized and mapped by the BGS at this location, are of Permian and Triassic age (see also Chapt. 2). As previously described in Section 4.3.2, both Permian and Triassic facies often display deformed internal reflectors that appear folded and faulted and are truncated at the top. These characteristics can also be observed from the

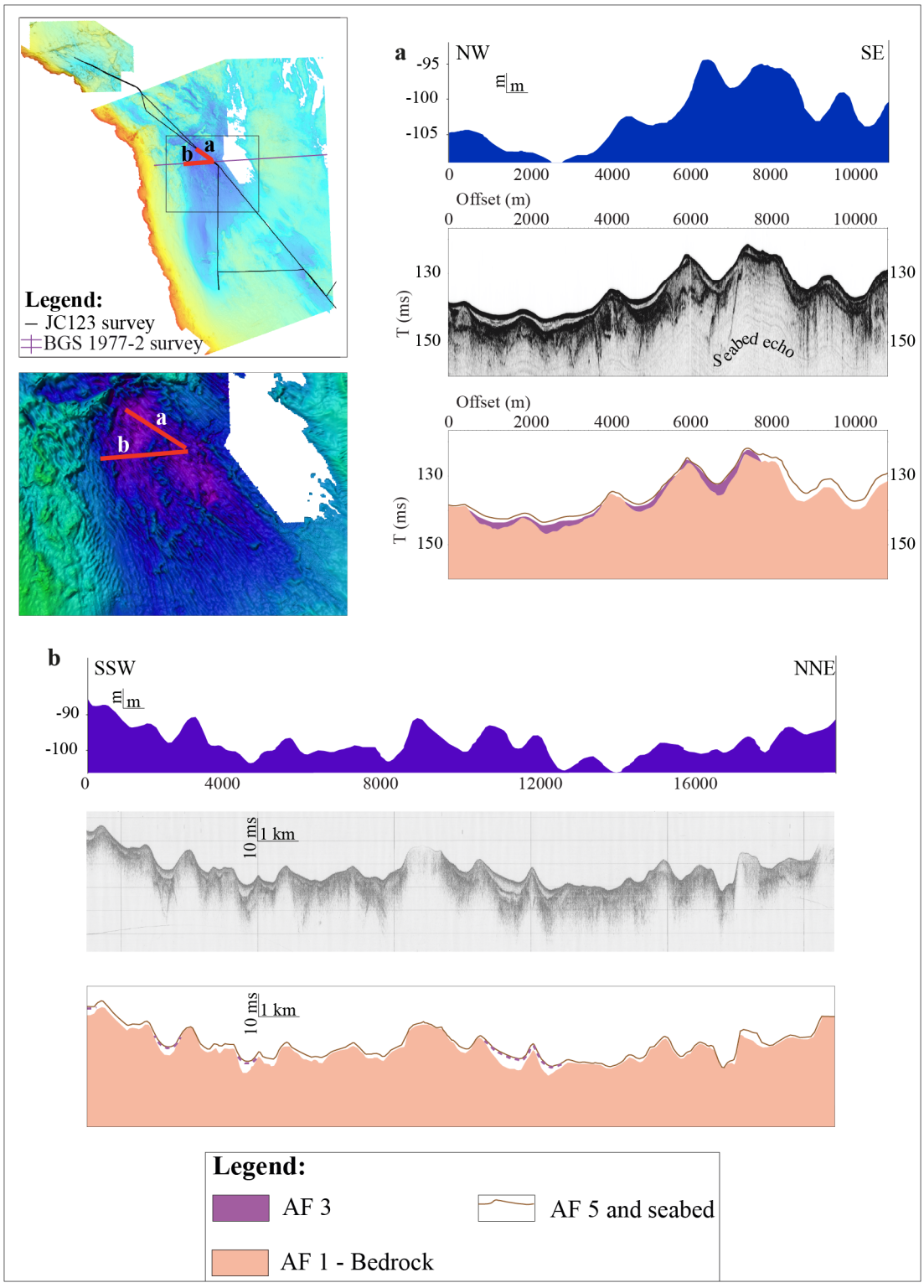

Figure 4.22: Bathymetric and seismic along-profile (a) and cross-profile (b) of the streamlined bedforms. Their locations are shown in the insert map (red lines). A detail of the UKHO high resolution bathymetry is also shown (locations indicated with a black square in the insert map). Note that both the bathymetric and seismic profiles are vertical exaggerated. Also note the seabed echo which could be mistaken for internal stratifications.

seismic along- and cross-profiles shown in Figure 4.23, where it is possible to see the internal bedding planes of the bedrock strata underneath some of the bedforms. This figure shows two segments of seismic profiles, one taken from a BGS line (Fig. 4.23a) and the other from the JC123 acquisition line (Fig. 4.23b) and on both, despite the fact that the BGS line is of lower resolution, it is possible to see the subparallel configuration of the bedrock internal planes (highlighted in the figure with black lines). These bedding planes also appear to be at a relatively high angle in respect to the seabed and often appear folded. Such aspects might infer that the internal structures of the bedrock itself influenced the resultant widths and heights of the bedforms, as discussed by Lane *et al.* (2015).

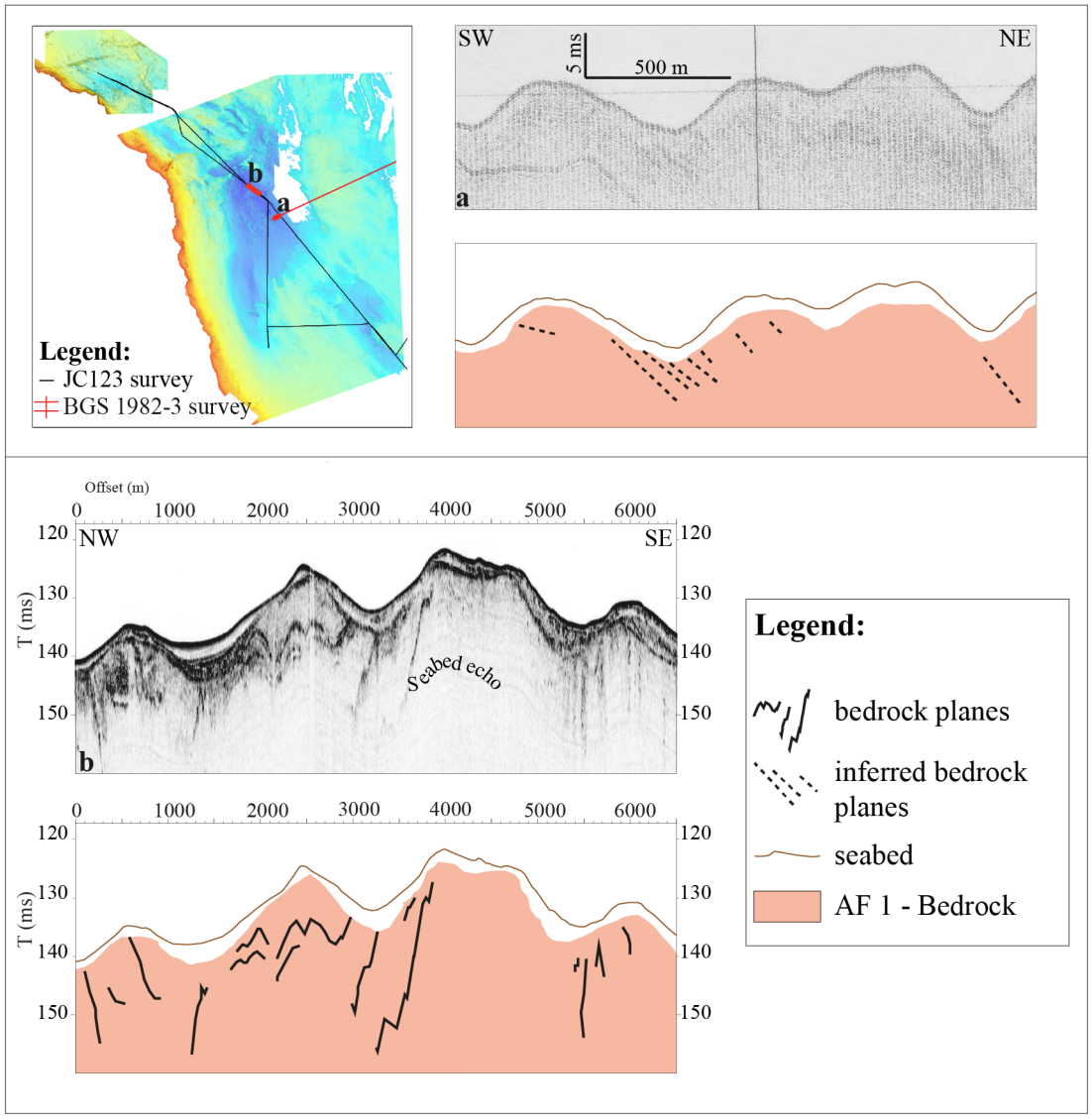

Figure 4.23: Seismic along-profile (a) and cross-profile (b) of the elongate bedforms. Their locations are shown in the insert map (red lines). The internal bedding planes of the bedrock strata are highlighted with black lines. Note that both the seismic and the bathymetry profiles are vertical exaggerated. Also note the seabed echo which could be mistaken for internal stratifications.

Considering their geometries and geological composition, together with their orientation, which is at a right angle in respect to the GZWs (Fig. 4.4b), these bedforms are interpreted to be bedrock-cored lineations, that were created subglacially by ice flowing from north-west. These landforms appear very similar to other bedrock-cored lineations observed onshore eastern England and onshore and offshore north-west Scotland (Bradwell *et al.*, 2008a; Livingstone *et al.*, 2008). In the Tyne Gap area, numerous bedrock moulded lineations were mapped by Livingstone *et al.* (2008). The geometry of subglacial bedforms is believed to be controlled mainly by ice flow direction, although bedrock structure can also play an important role in the resulting morphology of the landforms (Roberts & Long, 2005; Lane *et al.*, 2015). Considering that in the study area, all the mapped ridges show a preferential orientation, from WNW - ESE within UKHO Area 1, to NW - SE within Area 2, and noting that they are arranged perpendicularly to the GZWs, it is inferred that the palaeo-ice flow responsible for the formation of the bedrock-cored lineations was directed mainly NW - SE. The fact that the bedrock-cored lineations are composed mainly of bedrock strata, indicates that these bedforms are erosional, characterised by bedrock that was moulded/plucked by ice flow (Roberts & Long, 2005; Bradwell *et al.*, 2008a; Livingstone *et al.*, 2008; Lane *et al.*, 2015). The formation of these erosive landforms might be ascribed to the action of different glacial cycles, which formed and successively eroded/re-shaped them, instead of a single glacial phase (Roberts & Long, 2005). The layer of AF 3 at times observed on top of the crests of the landforms (as a thin cover) and in the topographic lows between them (thicker layer) represent the final sediment deposited by the ice during the last glacial phase.

Channels - Meltwater channels

Four sinuous, elongated troughs (T1 - T4, Fig. 4.4b and 4.24) were identified on the bathymetric dataset. These negative landforms are all orientated in a NW - SE direction. They have a rather sinuous profile and appear to begin and end abruptly (as previously shown in Fig. 4.8). This is also visible from the UKHO bathymetry inserts in Figure 4.24. T1 appears to continue north outside the bathymetry data (Fig. 4.24), but it was not observed in the UKHO Area 1, so it is believed T1 terminates within the bathymetric data gap between the two areas. The bathymetric and seismic profiles displayed in Figure 4.24, which run diagonally and transversally across T1 and T3, respectively, show how both troughs have steep slopes and appear V-shaped. Additionally, they are sometimes characterised by reversed gradients (e.g. T1, Fig. 4.24, in the UKHO bathymetry insert). On seismic profiles, these depressions appear to cut through bedrock strata, and in the T1 profile an inferred thin layer of AF 3 was also mapped. (Fig. 4.24). These four troughs are interpreted to be meltwater channels and to have formed subglacially (Bradwell *et al.*, 2008b; Smith *et al.*, 2009; Benn & Evans, 2010). This is primarily based on the geometries of these depressions, particularly their abrupt start and end, together with their undulating long profile (up/down profile), their slightly sinuous forms and their incision into bedrock strata (Greenwood *et al.*, 2007; Smith *et al.*, 2009). Similar features have been observed elsewhere in the North Sea, particularly offshore eastern Scotland (Bradwell *et al.*, 2008b), but are also common onshore, in England and Scotland (Clark *et al.*, 2004a, 2018; Evans *et al.*, 2005; Greenwood *et al.*, 2007; Livingstone *et al.*, 2008). A large

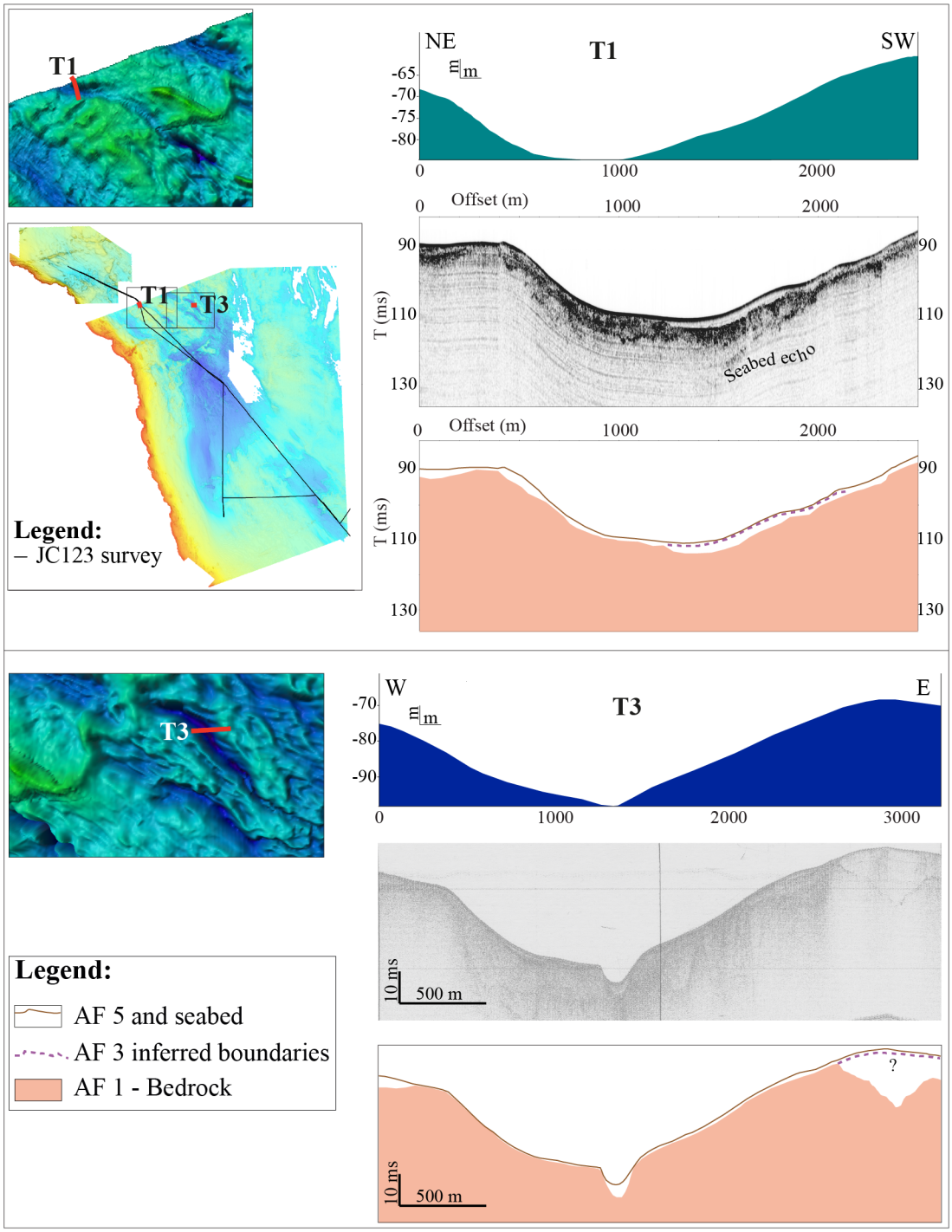

Figure 4.24: Bathymetric and seismic profiles and facies interpretation of the troughs T1 and T3. The location of the profiles (red lines) is shown in the insert map. Details of the UKHO high resolution bathymetry are also shown (locations indicated with black squares in the map). Please note that the discrepancy between the T3 bathymetric and seismic profiles is probably due to the fact that the latter was acquired ∼30 years before the former. Also note the seabed echo which could be mistaken for internal stratifications.

number of meltwater channels were recorded in the BRITICE database for the last BIIS, and they include subglacial meltwater channels, lateral meltwater channels, proglacial channels, and tunnel valleys and the majority of these meltwater channels have been defined as subglacial

(Clark *et al.*, 2004a, 2018; Evans *et al.*, 2005; Greenwood *et al.*, 2007). Comparison of the T1 - T4 meltwater channels identified in this study to the tunnel valleys mapped in the southern North Sea by Dove *et al.* (2017) (see Fig. 2.8), shows how they are smaller, considering the tunnel valleys observed off Holderness are approximately up to 80 m deep, 45 km long and 5 km wide and, more importantly, the tunnel valleys all exhibit a typical U-shape cross-profile (Dove *et al.*, 2017). This is in contrast to the observations of T1 - T4, which display a more sinuous planform and are all characterised by V-shape cross-profiles. For these reasons, T1 - T4 are interpreted as large subglacial meltwater channels. Subglacial meltwater channels are thought to indicate the presence of former ice and the ice flow direction, given that they develop orthogonally to the ice margins (Clark *et al.*, 2004a; Greenwood *et al.*, 2007). Furthermore, they are thought to indicate a warm-based thermal regime, that allows percolation of meltwater to subglacial channels where it can freely erode and circulate (Clark *et al.*, 2004a; Greenwood *et al.*, 2007). T1 - T4 all share the above-mentioned characteristics and are orientated NW - SE, thus indicating that the former ice flow was along the same direction. In addition, they display the same orientation of the bedrock-cored lineations. They are also located in close proximity and perpendicularly to R8 (Fig. 4.4b), and perhaps formed when the ice margin was close to this location. These are all further indicators of a NW - SE former ice flow.

Sediment drapes and the active seafloor

AF 1, AF 2 and AF 3 have been interpreted in the previous sections because they are found in association with some of the landforms identified on the seafloor. To summarize, AF 1 is defined as bedrock strata and AF 2 and AF 3 as composed of glacigenic diamicts (and possibly tills). The acoustic facies AF 4 is generally found within small basins usually constrained by topographic highs. It occurs in small lenses and has a limited and patchy distribution throughout the acquisition line but, wherever present, it is usually found on top of AF 3 (Fig. 4.10). Internally, AF 4 is characterised by high amplitude parallel reflectors, which at times appear deformed, and its lower boundary is generally concordant with the facies underneath (Fig. 4.10 and 4.11). In addition, the sediment cores collected during the JC123 survey show the presence of massive and laminated silts and clays with occasional clasts (LF 2a and LF 2b) in correspondence with AF 4 (Fig. 4.12 and 4.13; this is discussed in detail in Sect. 4.4.2). The geometry of this facies, its occurrence in association with AF 3 (glacigenic diamicts) and with the assemblage of glacial landforms identified above, that comprises grounding-zone wedges, moraines and subglacial bedforms, together with the fact that the facies is composed of stratified and laminated muds, point to a glaciomarine origin (this will be further discussed in Sect. 4.4.2). The seismic appearance of AF 4 further supports this interpretation, being comparable to the acoustic character of glaciomarine sediments identified elsewhere in the North Sea (Cameron *et al.*, 1992; Gatliff *et al.*, 1994, see also Chapt. 2 and 3). Glaciomarine facies were not mapped in this area on the Quaternary map for the North Sea, compiled by the BGS (Fig. 2.4, Chapt. 2). It is inferred that the very high resolution of the seismic profiles analysed in this study permitted its identification.

The uppermost facies of the sequence is AF 5, which is bounded at the top by a high amplitude seafloor reflector and is usually transparent internally (Fig. 4.9). Sediments collected

from this facies during the JC123 survey, are characterised mainly by fine to medium sands with abundant shells and shell fragments (LF 4; Fig. 4.12 and 4.13). According to the BGS Offshore Regional Reports, Holocene sediments are found in the research area overlying Pleistocene or pre-Quaternary strata, as a thin veneer or in the form of mobile landforms (e.g. sand waves; Cameron *et al.*, 1992; Gatliff *et al.*, 1994). Considering the seismic and geological characters of AF 5 and the fact that the facies is found in correspondence to the presence of sand waves along the acquisition line, the facies is interpreted to be of Holocene age. This will be further discussed in Section 4.4.2.

4.4.2 Sedimentary environments

According to the characteristics of the sediments and to the micro-fauna, the lithofacies identified in the cores (Fig. 4.13 and 4.15) are here organized into different depositional environments, which are summarized in Table 4.4 and described below.

LF 1: glaciomarine diamictons - iceberg-rafted

LF 1 consists of the subfacies LF 1a (massive, matrix-supported diamicton) and LF 1b (massive to stratified, matrix-supported diamicton; Fig. 4.15 and Tab. 4.4). These diamicton units occur in all cores, as a thin layer in the middle of cores 131 and 132 (75 and 26 cm thick, respectively) and at the bottom of cores 133, 134 and 135 (Fig. 4.13). They are characterised by abundant clasts dispersed in a soft clay-silt matrix and by MS measurements that usually range between 100 and 629 10^{-5} SI. This variability in MS is probably due to differences in the concentration of magnetic minerals but also to changes in grain sizes (Kilfeather *et al.*, 2011; Hogan *et al.*, 2016). Foraminifera specimens are absent in all diamictic units, while the shear strengths measurements for these facies range between $\sim$11 - 70 kPa. From visual observations and from the analyses of the X-rays images, planar structures are absent within these sediments, as well as any indications for clast alignment (Fig. 4.13 and 4.15). In addition, on seismic profiles, cores 133, 134 and 135 appear to clearly penetrate through the acoustic facies AF 4, characterised by high frequency and amplitude parallel reflectors, and to just reach the very top of AF 3, which is characterised by an opaque internal appearance (Fig. 4.12). AF 3 was interpreted as a glacigenic diamict (and possibly a till), principally due to its acoustic character. The seismic appearance of diamictic sediments and tills is in fact often transparent due to the heterogeneity of their sediments (Cameron *et al.*, 1992; Gatliff *et al.*, 1994; Huuse & Lykke-Anderson, 2000). The fact that this facies is found in association with the bedrock-cored lineations and the GZWs inferred that the sediments that characterise it are subglacial/sub-marginal in origin (Clark, 1993; Stokes & Clark, 2001; Evans & Hiemstra, 2005). Despite the fact that the shear strengths measurements for LF 1 are comparable/exceed the ones observed in "soft" subglacial tills in West Antarctica (Ó Cofaigh *et al.*, 2005), the absence of any visible planar structures or alignment of clast is in contrast with a subglacial origin of these sediments and LF 1 is thus interpreted as ice-proximal, consisting of sediments probably deposited at or in front of the grounding line as undermelt diamicton, or of iceberg-rafted deposits (Gravenor *et al.*, 1984; Ó Cofaigh *et al.*, 2005; Hogan *et al.*, 2016; Evans, In press). This will be discussed

Lithofacies (LF)	Description	Interpretation
1a	Massive, matrix-supported diamicton with abundant clasts. Generally between ∼30 and 100 cm thick (though probably continuing in depth below the bottom of the core), of brown, grey, reddish colour. Clasts of various dimensions and lithologies.	glaciomarine diamicton / iceberg rafting
1b	Massive, matrix-supported diamicton with abundant clasts and very thin beds (∼0.5-2 cm) of softer clayey silt and silty clay. Only present in core 133 where it is 91 cm thick but likely continues in depth below the bottom of the core.	glaciomarine diamicton / iceberg rafting
2a	Massive clay at times exhibiting vertical disturbance and with occasional clasts. Only found in cores 131 and 132.	suspension settling occasionally influenced from meltwater plumes
2b	Silty clay and clayey silt, highly laminated with numerous dropstones of different sizes and often colour banded. Usually found above the diamict layers. Laminae can be ∼0.1 cm thick.	suspension settling from meltwater plumes/ IRD/ turbidity currents
3a	Fine to medium well sorted sand.	iceberg rafting/dumping
3b	Fine gravel layer, 7 cm thick, only found in core 131 at 149 cm depth directly below LF 1a.	iceberg rafting/ dumping
4	Fine to coarse sand, at times silty, with numerous shells of different dimensions and occasional clasts. Coarser sand has higher abundance of both. Mainly found at the top of each core.	post-glacial sedimentation

Table 4.4: Summarized description and interpretation of the different lithofacies identified in cores 131 - 135 (Fig. 4.13) and relation to the depositional environments. These interpretations are based on Thomas & Connell (1985), Dowdeswell *et al.* (1994), Dowdeswell *et al.* (2000), Ó Cofaigh & Dowdeswell (2001), Ó Cofaigh & Evans (2001), Lucchi *et al.* (2013) and Evans (In press).

further in Section 4.5.

LF 2 and LF 3: glaciomarine sediments - interplay of depositional processes

LF 2 consists of the subfacies LF 2a (massive clay) and LF 2b (laminated clay and silt), identified in all the cores, while LF 3 consists of the subfacies LF 3a (massive sand) and LF 3b (massive, clast-supported gravel layer), found only in core 131 below the diamict (LF 1a; Fig. 4.13 and 4.15). The massive and laminated silts and clays (LF 2a and 2b) are found on top of the diamictic units in all but one of the vibro-cores analysed (the only exception occurs in core 131, where the relatively thin diamict layer is overlain by massive sands (LF 3a; Fig. 4.13). LF 2b is usually laminated and often displays colour banding (Fig. 4.13 and 4.14). Numerous clasts are present throughout the lithofacies and appear to become less frequent towards the

top. The lithofacies also displays relatively low MS values in comparison to coarser ones and is characterised by highly variable densities, that are more likely higher in correspondence to clast-rich intervals. Electrical resistivity and V_p measurements are usually low (Fig. 4.13). X-ray images allowed for the observation at high resolution of the different laminations and clasts distribution within LF 2b. These are summarized and genetically interpreted in Figure 4.25. The laminations observed are usually one to a few millimetres thick, although some stratification has also been observed in the facies, where the strata are 1 or 1.5 cm in thickness (Core 132, Fig. 4.13 and 4.15). The laminae are generally planar and parallel and are often disturbed by dropstones or IRD (ice-rafted debris) layers (examples in Fig. 4.25). They are frequent and at times have a rhythmic appearance (Fig. 4.15). Core 133, which was X-rayed in its entire length (Fig. 4.26), displays highly laminated clayey silts disturbed by numerous dropstones and IRD layers, close to the upper boundary of the diamict (Fig. 4.26d and 4.26e), and smaller and fewer clasts upwards through the deposit (Fig. 4.26b and 4.26c).

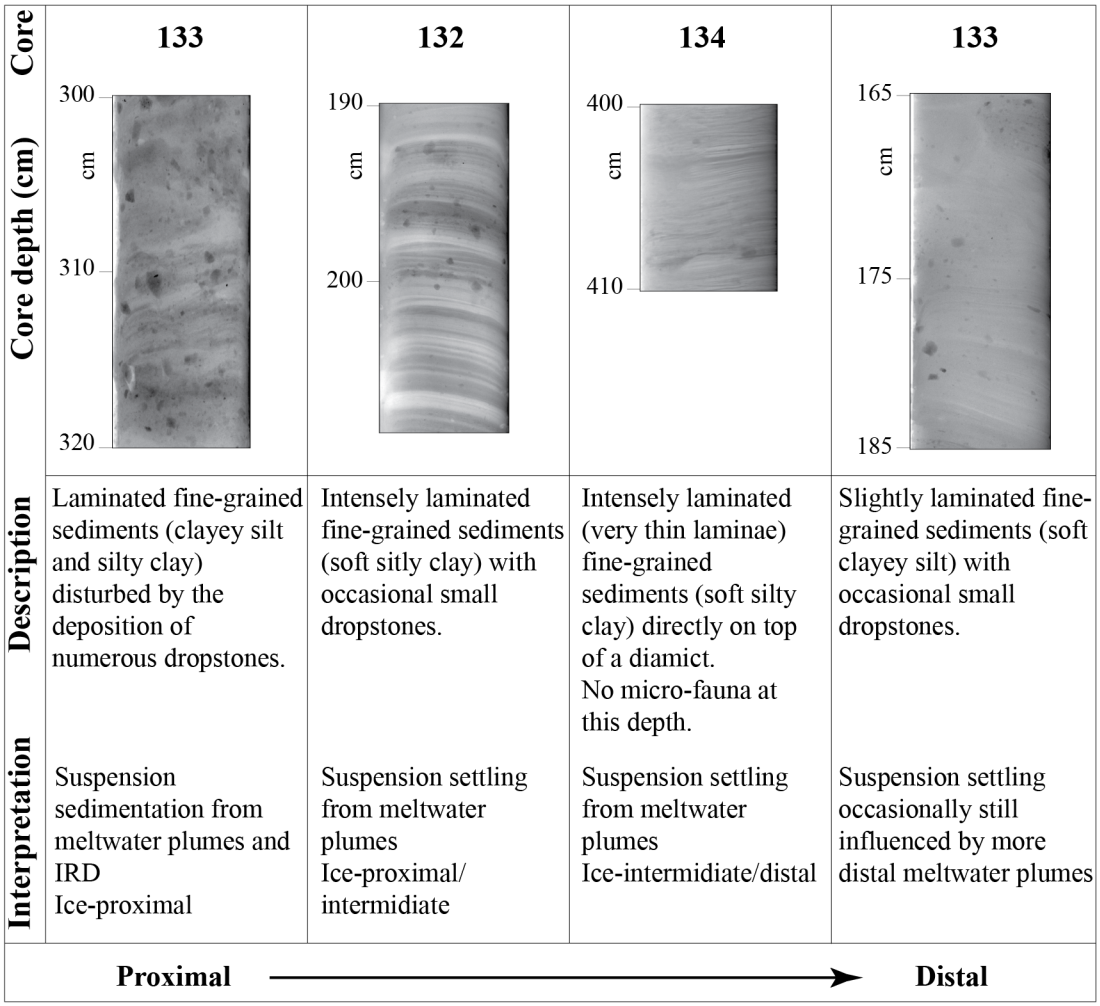

Figure 4.25: Different types of laminations observed in the cores. Interpretations of the laminated sediments are based on Dowdeswell *et al.* (2000) and Ó Cofaigh & Dowdeswell (2001).

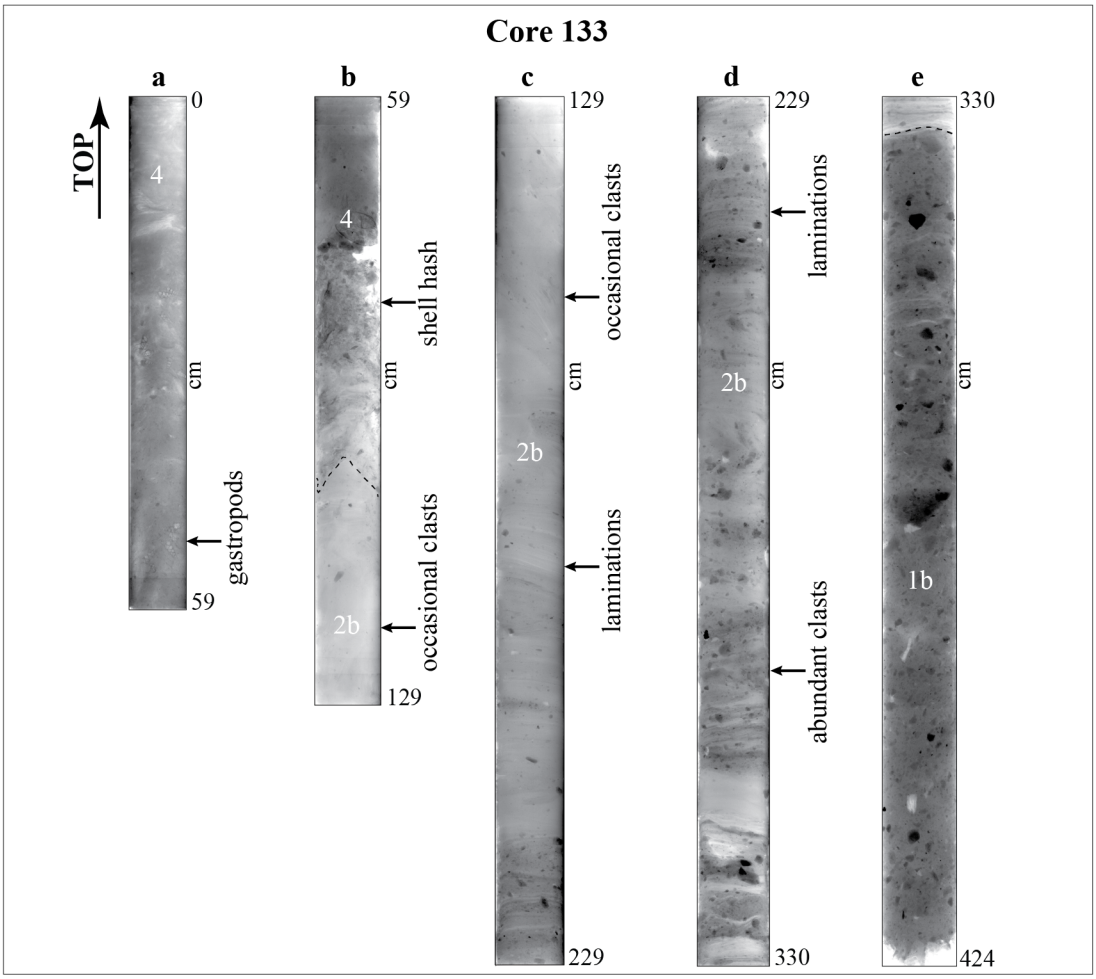

Figure 4.26: X-ray images of core 133. The five sections (a - e) are displayed from top (a, left) to bottom (e, right). The lithofacies numbers and additional details are indicated. Dashed black lines represent lithofacies boundaries.

The foraminifera assemblage identified within LF 2a and 2b is characterised by abundances of *Elphidium excavatum (clavatum)* and by *Cassidulina reniforme*, which are cold temperature species, known to be indicators of extreme glacial marine environments (Fig. 4.16; Feyling-Hanssen, 1972; Hansen & Knudsen, 1995; Peters *et al.*, 2015). In addition, abundances of *Haynesina orbiculare* and of *Elphidium excavatum*, further corroborate the cold marine environment at the time of deposition (McCabe *et al.*, 1986; Knudsen & Sejrup, 1993).

Considering the characteristics of this lithofacies, the presence of laminations and dropstones, together with evidence from the micro-fauna, LF 2a and 2b are interpreted to represent glaciomarine sediments deposited by a combination of different processes, such as suspension settling from proximal to distal meltwater plumes, gravitational processes such as turbidity currents, and ice rafting. The laminated sediments characterised by high abundances of clasts and IRD layers, found generally at the top of the diamictic units (Fig. 4.25 and 4.26), are believed to record ice-proximal to intermediate environments (Fig. 4.25), and to have been deposited mainly from suspension settling of turbid meltwater plumes emanating from the ice margin (Dowdeswell *et al.*, 2000; Ó Cofaigh & Dowdeswell, 2001; Lucchi *et al.*, 2013). The clayey silt and silty clay sediments observed at the top of the diamictic layers usually

display more pronounced laminations and stratifications, and are characterised by abundant clasts, considered to be evidence of more glacial proximal settings (Cowan & Powell, 1990; Ó Cofaigh & Dowdeswell, 2001). The presence of more irregular laminations characterised by the occurrence of sandy beds found intercalated to soft clay silts, could indicate that sediment deposition was also influenced by episodic bottom processes, such as turbidity currents, which are also significant in locations proximal to the ice-margin (Mackiewicz *et al.*, 1984; Cowan *et al.*, 1999; Ó Cofaigh & Dowdeswell, 2001). Towards the top of the core, these sediments are characterized by sparser clasts and the laminations become very thin, to absent (example in Fig. 4.26). These characteristics are probably related to the development of more distal conditions and to a reduction in IRD flux, associated to a recessional ice margin (Dowdeswell *et al.*, 2000; Ó Cofaigh & Dowdeswell, 2001; Ó Cofaigh & Evans, 2001). LF 3a and 3b, observed below the diamict in core 131 (Fig. 4.13), are thought to be evidence for deposition by iceberg rafting/dumping (Thomas & Connell, 1985; Dowdeswell *et al.*, 1994). These sediments are immediately above the massive clay (LF 2a) and underneath the diamict layer (LF 1a; Fig. 4.13) and could indicate a greater influence on sedimentation by icebergs at that time.

LF 4: post-glacial sediments

LF 4 consists of the massive, at times silty, sands that are found at the top of all vibro-cores (Fig. 4.13 and 4.15). These sediments are often characterised by abundant shells and shell fragments (gastropods clearly visible in Fig. 4.26a), as well as clasts. The lithofacies correlates to the uppermost acoustic facies identified on the seismic profiles (AF 5, Fig. 4.12; Sect. 4.4.1). This acoustic facies is characterised by a very high amplitude and continuous reflector (which represents the seabed) and a transparent acoustic appearance internally. A foraminifera sample was taken at 20 cm depth in core 135 within LF 4 (Fig. 4.13), which shows great abundance of quartz clasts, as well as shell fragments and sea urchin spines, but rare foraminifera. Only one foraminifera individual was recognized to belong to the Bulimina genus, although it was not possible to identify the species. Considering the higher density of the sediments of LF 4 in comparison to LF 2a and 2b, and the general absence of finer-grained sediments, together with the high abundance of macro-fauna, not found in any of the other samples analysed, LF 4 is interpreted to consist of post-glacial and Holocene sediments. These sediments are believed to have deposited in open/modern marine conditions, from fluvial transport and coastal erosion and to be reworked by present bottom/tidal currents (Cameron *et al.*, 1992; Gatliff *et al.*, 1994; De Haas *et al.*, 1997).

4.5 Discussion

4.5.1 The offshore imprint of the NSL

The identification of specific glacial landform assemblages offshore provides new information on the dynamic behaviour and retreat dynamics of the BIIS. Here, both the advance phase subglacial signal of the NSL and the nature of the dynamic retreat of the ice across the region are considered.

Subglacial imprint

Evidence for subglacial processes can be firstly ascribed to the presence of elongate bedforms, in the central part of both the UKHO areas 1 and 2 (Fig. 4.4b and 4.22). These bedforms, previously interpreted as bedrock-cored lineations, differ from the surrounding topography as they are elongate and appear slightly tapered, at times being wider to the north and narrower to the south, and they also appear to have seed points, suggesting that bedrock bumps are close to the surface and possibly trigger bedform initiation. Glacial lineations form subglacially, parallel to ice flow, and can be indicators of either prolonged or fast former ice flow (Clark, 1993; Stokes & Clark, 2001, 2002; Bradwell *et al.*, 2007; Golledge *et al.*, 2008; Livingstone *et al.*, 2008). Streamlined bedforms can form by erosion (bedrock moulded or till eroded) or by deposition (till deposition; Clark, 1997; Livingstone *et al.*, 2008; Eyles, 2012; Eyles *et al.*, 2016; Eyles & Doughty, 2016). The fact that the lineations identified in the study area are predominantly bedrock-cored, indicates that they were probably formed initially as erosional features, with pre-existing bedrock being eroded by the action of ice. They are are believed to have formed in response to basal abrasion and plucking, probably during different ice flow phases and not just during the last one (Roberts & Long, 2005; Livingstone *et al.*, 2008; Bradwell & Stoker, 2015a; Krabbendam *et al.*, 2016). This is further discussed in Chapter 5. It is also possible that the bedrock structure influenced the final widths and heights of the bedforms (Roberts & Long, 2005; Lane *et al.*, 2015), as discussed previously in Section 4.4.1 and shown in Figure 4.23. The bedrock strata in the region appear to be often characterised by subparallel internal bedding planes that are faulted and folded and sometimes dip at a rather high angle in relation to the seabed and to the inferred former ice flow (Fig. 4.23). Such a configuration was also previously observed and discussed in Chapter 3 for the Blyth survey area, which is characterised by outcrops of bedrock strata close to the coast (see Fig. 3.3b, in Chapt. 3). The Carboniferous bedding planes in particular, clearly visible in Figure 3.13, appear folded and faulted and display low to relatively high dip angles. The presence of different bedrock facies within the study area, that either crop out or are generally buried at a very shallow depth below the seabed, together with the fact that they all display bedding planes that often dip at a relatively high angle, could have played an important role in the final geometries of the bedrock-cored lineations observed on the seafloor.

The orientation of these bedrock-cored lineations gives an indication on the ice flow direction responsible for their formation. In Section 4.4.1 it was inferred that the ice was directed WNW - ESE within the UKHO Area 1, and NW - SE within Area 2. In Figure 4.27, the subglacial bedforms mapped in the research area (black lines) are shown together with the onshore subglacial lineations recorded in the BRITICE database for the last BIIS (red lines; Clark *et al.*, 2004a, 2018; Evans *et al.*, 2005). Despite the fact that only few lineations were observed on the bathymetry dataset of the UKHO Area 1, the ice flow direction was here inferred to be orientated WNW - ESE to NW - SE in correspondence of the subglacial lineations of Area 2. This interpretation seems to relate well with the onshore evidence. From Figure 4.27 it is possible to see how the lineations mapped onshore in close proximity to the UKHO Area 1 (in the North Berwick/Dunbar area) show a SW - NE to WSW - ENE orientation, thus further indicating that the ice flow coming from this area (white arrow in Fig. 4.27) turned from an

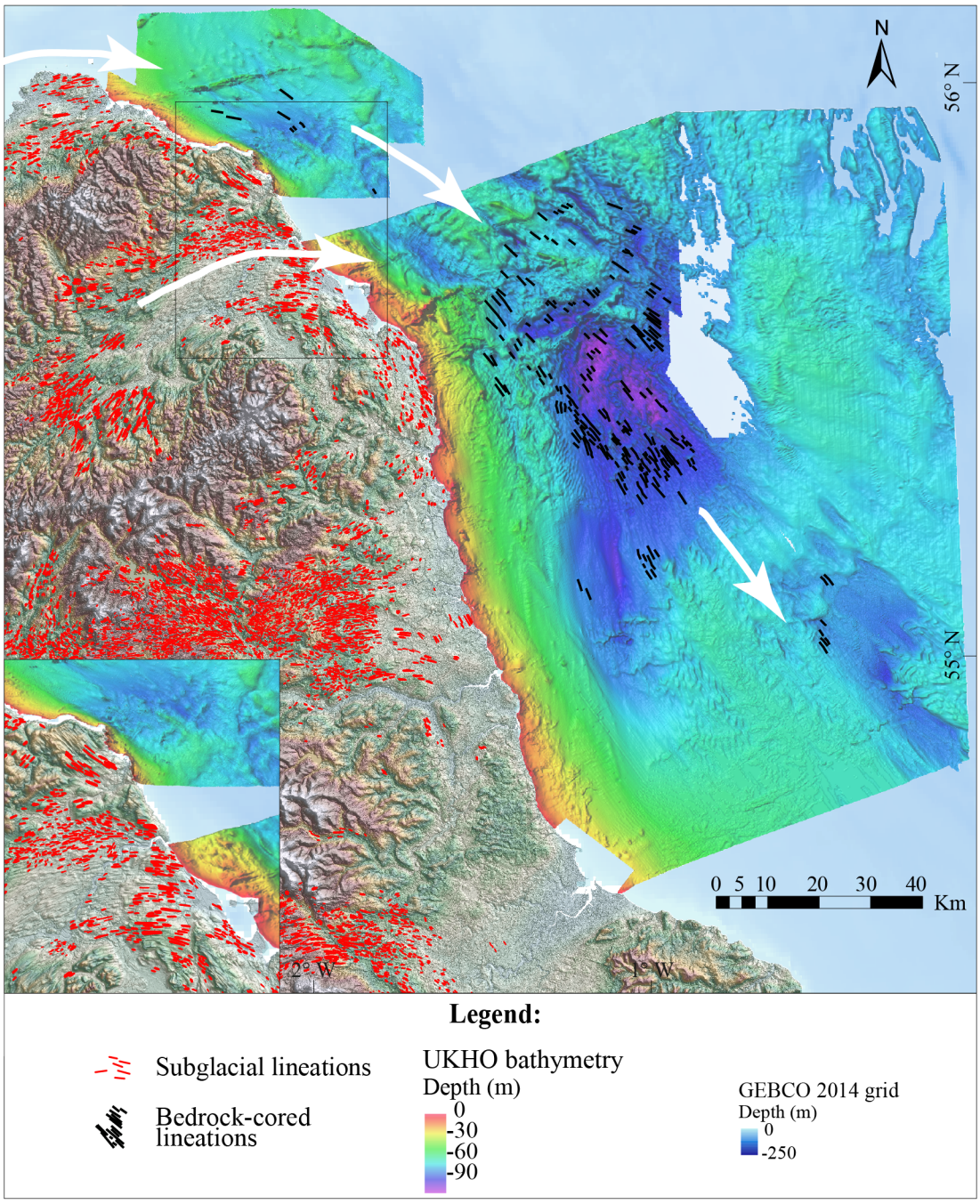

Figure 4.27: The bedrock-cored lineations (black lines) mapped in this study are shown together with the onshore subglacial lineations (red lines) recorded in the BRITICE database (Clark *et al.*, 2004a, 2018; Evans *et al.*, 2005). The white arrows represent the inferred former ice flow direction. The insert map shows a zoomed in view of the Tweed area.

original SW - NE/WSW - ENE direction to WNW - ESE/NW - SE in the offshore sector. This is confirmed by the arrangement of the subglacial lineations mapped in the Tweed valley (see detail view in Fig. 4.27), which show an actual turn in their orientation, from SW - NE inland to NW - SE close to the coast, suggesting they were probably deflected by ice coming from the north. Finally, no evidence was found in the study area for ice flow directed towards the east and it is thus believed that the ice responsible for the formation of the bedrock-cored lineations was mainly directed towards the south-east in this sector of the North Sea (Fig. 4.27).

An additional indicator of subglacial imprint and of the former ice flow direction, is represented by the presence of the four channels T1 - T4, mapped in the northern part of the UKHO Area 2 and interpreted as subglacial meltwater channels (Fig. 4.8 and 4.24). These troughs are all orientated NW - SE and have comparable widths to the tunnel valleys mapped in the southern, central and northern North Sea, of up to 5 km, but are generally smaller in length and less deep, given these tunnel valleys are generally up to 50 to more than 100 km long and can be more than 100 m deep (Lonergan *et al.*, 2006; Bradwell *et al.*, 2008b; Graham *et al.*, 2011; Stewart & Lonergan, 2011; Dove *et al.*, 2017). More importantly, T1 - T4 display a rather sinuous planform (Fig. 4.8). Tunnel valleys generally display straight planforms, are usually characterised by steep flanks, relatively flat bottoms and display U-shape cross-sections (Ó Cofaigh, 1996; Benn & Evans, 2010). T1 - T4 were identified as meltwater channels considering their V-shaped cross-sections, their up/down long profiles and their high sinuosity (Greenwood *et al.*, 2007). They are also believed to have formed subglacially, at the ice bed and their orientation is thus indicative of the ice flow direction, considering subglacial meltwater channels form along the ice flow (Greenwood *et al.*, 2007; Benn & Evans, 2010). The fact that these channels are found orientated perpendicularly to R8, further confirms a NW - SE ice flow direction.

The deposition of the two acoustic facies AF 2 and AF 3, interpreted as glacigenic diamicts (possibly tills), represents additional evidence for subglacial processes. It was not possible to sample AF 2 during the JC123 survey, but sediments correlating to the very top of AF 3, the facies above it, are characterised by glacigenic diamicts (LF 1a and 1b). Seismically, AF 2 and AF 3 are quite similar, and it was concluded that AF 2 could represent a subglacial till. Its seismic appearance indeed resembles a typical seismic character generally described for till deposits (Cameron *et al.*, 1992; Gatliff *et al.*, 1994; Huuse & Lykke-Anderson, 2000; Ó Cofaigh *et al.*, 2005). AF 3 displays a similar seismic character and is found in association with the bedrock-cored lineations, thus suggesting a subglacial origin. The fact that the facies is also found at the core of the two GZWs recognized in the area (W1 and W2), suggests glacial sub-marginal thickening (Boulton, 1996a,b; Evans & Hiemstra, 2005). AF 3 is thus believed to have a subglacial to sub-marginal origin (further discussion in Chapt. 5).

These two facies offshore could tentatively be correlated to the findings from Chapter 3 (Blyth survey) but also to the onshore stratigraphy of eastern England. Firstly, within the Blyth survey area, two acoustic facies were also identified on top of bedrock strata, that share some of the acoustic characters of AF 2 and AF 3, and that were interpreted as possible glacial tills. Given that there is a lack of geological evidence and age constraints for the Blyth facies in question AF 4 and AF 5 (from now on referred to as BL-AF 4 and BL-AF 5), the proposed interpretations were based on the seismic characters of both and on what was previously mapped by the BGS in the area. It was previously discussed in Chapter 3 that BL-AF 4 could be correlated to the Wee Bankie Formation, a Late Devensian unit found usually on top of bedrock strata and known to be characterised by an uneven thickness, a sheet-like geometry, and an irregular upper boundary (see Fig. 2.4 in Chapt. 2; Gatliff *et al.*, 1994; Golledge & Stoker, 2006). The facies AF 3, identified in this chapter, could be also tentatively correlated to the Wee Bankie Formation. This is due to the similar acoustic appearance, the extensive presence

of AF 3 throughout the study area, and also to the fact that the Wee Bankie Formation has also been described as a possible subglacial till (Gatliff *et al.*, 1994). Furthermore, a correlation of AF 2 and AF 3 to the onshore sediments of eastern England could be proposed. As previously discussed in Chapter 2 and 3, different till facies are found along the eastern coast of England and their deposition has been related to the last glacial phase. The Blackhall Till is found on the Durham coast and is thought to have been deposited by ice sourced in north-western England, such as the TGIS (Davies *et al.*, 2009a, 2012b). The Horden Till of County Durham, correlative of the Skipsea Till of Yorkshire and of the offshore Wee Bankie Formation and Bolders Bank Formation (see also Chapt. 2), and the Withernsea Till of Holderness are both interpreted as subglacial to sub-marginal sediments and believed to relate to the action of the NSL (Carr *et al.*, 2006; Davies *et al.*, 2009a, 2011, 2012a,b; Evans & Thomson, 2010; Bateman *et al.*, 2015). If AF 3 is in fact the Wee Bankie Formation, it would infer that the facies also correlates to the onshore Horden Till and that it was deposited by the NSL. AF 2, which has a general patchy appearance, is mainly preserved as a thin lens usually between topographic highs, and lies directly on top of pre-Quaternary strata (Fig. 4.10), could be interpreted as either an early deposit laid by an initial advance phase of the NSL and successively eroded and overprinted by AF 3, or could be considered the offshore correlative of the Blackhall Till. This would infer that its deposition was related to an advance of the TGIS and that successively the facies was eroded during the late NSL re-advance phase (see also Chapt. 2). Although, given its patchy appearance, the deposition of AF 2 could also have taken place during an earlier glaciation and the facies could also be correlated to the onshore Ash Gill Member of the Warren House Gill Formation found on County Durham and dated to be of MIS 8 age or older (Davies *et al.*, 2012b; Livingstone *et al.*, 2012b). Nonetheless, the identification of AF 2 and AF 3 on top of bedrock strata, indicates that the previous Quaternary maps available for the western North Sea were lacking this level of detail (Fig. 2.4, Chapt. 2) and infers that the Wee Bankie Formation is not the sole subglacial Quaternary unit present in the area.

Deglacial imprint

The presence of two grounding-zone wedges (W1 and W2) in the study area provides information on the dynamics of ice retreat in this region. GZWs are defined as ”asymmetric sedimentary depo-centres which form through the rapid accumulation of glacigenic debris along a line-source at the grounding zone of marine-terminating ice sheets during stillstands in ice-sheet retreat” (Batchelor & Dowdeswell, 2015). They are often found as part of landform assemblages specific to ice stream flow, generally in association with Mega-Scale Glacial Lineations (MSGLs), lateral moraines and till sheets (Ottesen & Dowdeswell, 2009; Batchelor & Dowdeswell, 2015). In numerous high-latitude continental shelves, GZWs have been observed in association with, and overriding MSGLs, which can be also found in turn superimposed on their surfaces (Dowdeswell *et al.*, 2008; Dowdeswell & Fugelli, 2012; Batchelor & Dowdeswell, 2015). The occurrence of GZWs suggests that ice retreat was not rapid and that was interrupted by temporary stillstands in grounding-line position during deglaciation (Dowdeswell *et al.*, 2008; Dowdeswell & Fugelli, 2012). Their presence indicates the locations of significant phases of temporary stability (at least tens to hundreds of years)

and the location at which they form is often controlled by the geometry of the continental shelf (Dowdeswell *et al.*, 2008; Batchelor & Dowdeswell, 2015). The fact that the western North Sea is today characterised by very shallow waters and by various bedrock outcrops that constitute topographic highs, probably helped to provide pinning points during the overall retreat, allowing temporary stability. As previously shown in Figure 4.10 and 4.20, both W1 and W2 are located within areas characterised by bedrock highs and were laid down between bedrock ridges that often come up to the surface. These characteristics are thought to have favoured grounding-zone stabilisation through increasing basal and lateral drag (Batchelor & Dowdeswell, 2015). Whenever GZWs display streamlined lobes along their down-ice margins, and are overprinted by MSGLs, they record that the ice was still actively streaming during retreat (Dowdeswell *et al.*, 2008). Despite the fact that W1 and W2 do not appear to be overprinted by MSGLs, it is possible to see from the bathymetry data how the upper surface of W1 appears slightly streamlined, and how its southern margin is rather lobate (Fig. 4.4a). It is believed that W1 and W2 thus formed during ice retreat across the study area, by the subglacial deposition and build-up of sediments delivered at the grounding line, and that their presence in the glacial assemblage observed on the seafloor, indicates that the NSL retreat was characterised by at least two phases of stillstands (Dowdeswell *et al.*, 2008; Dowdeswell & Fugelli, 2012; Batchelor & Dowdeswell, 2015). GZWs are also indicators of the former ice flow direction, being found at a right angle to glacial lineations and thus being orientated transverse to the direction of ice flow. This is also the case for W1 and W2, which are found transverse in respect to the bedrock-cored lineations in the study area. In addition, the steeper slopes of GZWs are known to be located on their ice-distal sides (Batchelor & Dowdeswell, 2015). Both W1 and W2 display steeper slopes towards the south (Fig. 4.20), thus confirming that the ice was flowing from NW to SE. The fact that W2 is much smaller than W1 could indicate a shorter phase of grounding line stability and perhaps a reduced sediment flux to the grounding zone (Dowdeswell & Fugelli, 2012; Batchelor & Dowdeswell, 2015).

The ridge R8, interpreted to be a moraine ridge related to either a stillstand or to an oscillation of an ice-margin, based on its geological and geomorphological characteristics (Sect. 4.4.1), is found between the locations of W1 and W2 (Fig. 4.4b) and has a multi-lobate planform which resembles a terminal/push-moraine (Benn & Evans, 2010; Bradwell & Stoker, 2015a). It could thus be evidence for an ice re-advance during overall retreat. The NW - SE seismic profile shown in Figure 4.10, shows the presence of a big wedge-like feature, also characterised at the core by AF 3, in close proximity to R8, in the northern part of the UKHO Area 1. Considering that numerous bedrock ridges were observed in this area (second sub-group of ridges, in blue in Fig. 4.4b), it could be tentatively suggested that this wedge-like feature is actually a third grounding-zone wedge, and that it represents an additional location at which the ice stopped during overall retreat, possibly facilitated by the presence of bedrock highs that acted as pinning points. However, it is important to note that this wedge-like feature is not clearly apparent from the bathymetry data, contrary to what was observed from W1 and W2. R8 could then represent a stillstand/re-advance event that occurred while the ice margin was still close to this location.

In summary, it is believed that ice retreat had started by the time W1 was deposited,

and continued after a period of stillstand at this location. Between W1 and W2, thus before retreating to the location of W2, a second stillstand phase might have occurred, and an ice re-advance resulted in the deposition of R8. Alternatively, after the deposition of W1, the ice could have retreated all the way back to the location of W2 and have been stable here long enough to deposit the wedge, and could have then successively re-advanced, allowing for the formation of R8, before the deglacial phase continued towards the north-west.

The different landforms identified in this research indicate that the former ice flow was directed towards the south-east. Both bedrock-cored lineation and GZW orientations reflect an ice flow mainly directed WNW - ESE in the most north-eastern part of the study area (UKHO Area 1), that turned slightly and was directed NW - SE in the most central and southern part (UKHO Area 2). The bedrock-cored lineations within the UKHO Area 1 indicate that the ice flow was coming from south-east Scotland (Fig. 4.4b) and that the deposition of the landforms observed on the seafloor is ascribable to the action of the NSL, sourced mainly from the Firth of Forth. This fast-flowing ice lobe was still active at a very late stage during the last glaciation, constraining dates from the Yorkshire coast suggesting the NSL operated between 21.7 - 15.5 ka BP (Bateman *et al.*, 2011, 2015, 2017; Livingstone *et al.*, 2012b, 2015; Roberts *et al.*, 2013). Although all the glacial landforms observed on the dataset appear to point to the action of ice coming from the north-west, it is known that this particular area was also affected by the flow of the TGIS, which drained the last BIIS flowing from west to east (Fig. 4.1; Livingstone *et al.*, 2008, 2012b, 2015). The lack of any geomorphological evidence attributable to an eastward orientated ice flow, appears to further confirm the model compiled by Livingstone *et al.* (2015), which shows how the TGIS had retreated from the eastern coasts of England, allowing for the formation of Glacial Lake Wear, sometimes before ∼18.7 to 17.1 ka, and how the central sector of the last BIIS underwent extensive collapse while the NSL continued to stream southwards during this time (see also Fig. 2.6 in Chapt. 2). The only evidence that could be related to the action of the TGIS offshore, is the presence of the patchy AF 2, mapped directly on top of bedrock strata and overlain by AF 3. As previously discussed in this section, AF 2 could correlate to the onshore Blackhall Till, deposited by the TGIS. Overall, the bedrock-cored lineations point to a former ice flow mainly sourced from south-eastern Scotland, although the orientation of the mapped lineations onland in the Tweed valley (Fig. 4.27) indicate that the Tweed ice stream might also have fed into the NSL, turning its course towards the south in the offshore area.

Additionally, the geomorphology observed on the seafloor indicates that the NSL did not undergo a catastrophic retreat event, but rather retreated sequentially, and the presence of the two (or three) GZWs and a moraine indicates at least two periods of ice stillstand. This oscillatory behaviour of the NSL has also been recorded onshore, where evidence from the Yorkshire coast has shown how the NSL was characterised by different advance and retreat phases, and was thus highly dynamic (Evans & Thomson, 2010; Bateman *et al.*, 2015; Evans *et al.*, 2017). Furthermore, new evidence from the southern North Sea also suggests that the southern margin of the NSL was an oscillating ice margin, which occupied different stillstand positions before its final retreat (Dove *et al.*, 2017).

The NSL is thus thought to have flowed southwards and re-advanced due to internal reorganization (Bateman *et al.*, 2015), though little is known on the timings of its retreat and disintegration. From the analysed bathymetry and seismic dataset, it is inferred that deglaciation was not rapid, but rather characterised by different phases of stillstand and ice re-advance. New evidence on the timing for the NSL final retreat is discussed in Section 4.5.2. The evidence provided in this section suggests that the western North Sea is characterised by a mixed bed assemblage which include five components: bedrock ridges, bedrock-cored lineations, meltwater channels, moraine and grounding-zone wedges. The set of landforms recognized on the seafloor suggests both hard- and soft-bedded imprint. This is further discussed in Chapter 5.

4.5.2 Sedimentary signature and palaeoenvironments - LGM and early deglaciation

The four LFs and subfacies identified in this research record changes in the depositional processes that were dominant in the western North Sea during the last glaciation and after the onset of deglaciation (Ó Cofaigh *et al.*, 2005). LF 1a and 1b, which are characterised by massive, matrix-supported and occasional stratified diamictons (Table 4.4), constitute the base of cores 133, 134 and 135, but also occur in the central sections of cores 131 and 132 (Fig. 4.13). On visual observation, these diamictons generally appear as massive silts and clays with clasts, the abundance of which becomes evident on X-rays images, and the sediments resemble the appearance of subglacial tills (Fig. 4.26; Dowdeswell *et al.*, 2000; Evans *et al.*, 2005; Lucchi *et al.*, 2013; Peters *et al.*, 2016). In addition, LF 1a and 1b are relatively soft and not overconsolidated. Despite the fact that subglacial tills are usually characterised by high shear strengths, softer subglacial tills have also been recorded from western Antarctica (Dowdeswell *et al.*, 2004; Evans *et al.*, 2005; Kilfeather *et al.*, 2011), hence indicating that this characteristic on its own cannot be used as the primary evidence to discriminate this type of sediments. Nevertheless, subglacial tills often display shear structures, which are evidence for deposition underneath grounded ice (Ó Cofaigh & Dowdeswell, 2001; Ó Cofaigh *et al.*, 2005; Evans *et al.*, 2005; Carr *et al.*, 2006). However, LF 1a and 1b have a massive appearance and lack any indications of clast alignments, and/or no deformation or planar structures are evident.

As previously mentioned in Section 4.3.3, vibro cores 133, 134 and 135 appear to reach the very upper boundary of acoustic facies AF 3, although they do not seem to penetrate into it (Fig. 4.12). AF 3 has been previously interpreted as composed of glacigenic diamicts of subglacial/sub-marginal origin. The heterogeneous nature of diamictic sediments, characterised by a mixture of grain sizes, result in an acoustically homogeneous character when observed on seismic profile (Hogan *et al.*, 2016). This is consistent with the observations of AF 3. In addition to this, AF 3 displayed a varying thickness, a very strong and irregular upper boundary, and was found as the core of subglacial and sub-marginal landforms such as bedrock-cored lineations and GZWs (Sect. 4.4.1). For these reasons, AF 3 is believed to record subglacial to sub-marginal deposition. The Quaternary map compiled by the BGS for the western North Sea shows the presence of a patchy Wee Bankie Formation off the east

coasts of Scotland and northern England, interrupted by bedrock outcrops (see Fig. 2.4, in Chapt. 2). This formation was previously described as a stiff diamicton that displays interbeds of sand, pebbly sand and silty clay and is assumed to be of Late Devensian age (Gatliff *et al.*, 1994; Carr *et al.*, 2006). It also displays sub-angular and sub-rounded clasts that are thought to indicate a Scottish provenance, and numerous small-scale deformation features, that led to the interpretation of the formation as a subglacial till unit (Carr *et al.*, 2006; Davies *et al.*, 2011). According to their widespread extensions, acoustic characters, and irregular upper boundaries, a correlation between AF 3 and the Wee Bankie Formation was suggested (Sect. 4.4).

The fact that cores 133, 134 and 135 reach only the very top of AF 3 and do not penetrate into the acoustic facies, could imply that LF 1 (which is found at the bottom of all three cores) does not represent the direct correlative of AF 3. In addition, LF 1 is overlain by LF 2 in the cores, that has been correlated to AF 4 (Fig. 4.12), interpreted to be a deglacial acoustic facies, composed of glaciomarine sediments. Considering the internal characteristics of LF 1, and the fact that this facies is found at the boundary between AF 3 (subglacial to sub-marginal) and AF 4 (glaciomarine), the sediments of LF 1 are inferred to be transitional diamictons, and to represent the transition from subglacial to glaciomarine sedimentation. It is believed that this "transitional facies" was not deposited subglacially but possibly still close to the ice margin, as a glaciomarine diamicton at or in front of the grounding line or as ice-rafted deposits (Hogan *et al.*, 2016). The fact that this soft diamicton appears stratified in close proximity to its upper boundary and to the contact with the overlying glaciomarine sediments (Fig. 4.26e), also implies that at the time of its deposition, the ice margin was probably still very close but was starting to retreat, and icebergs were becoming more dominant in releasing material to the seafloor (Gravenor *et al.*, 1984; Ó Cofaigh & Dowdeswell, 2001; Ó Cofaigh & Evans, 2001; Evans, In press). This would further corroborate an increasing distance of the ice margin going upwards in the sequence.

On top of LF 1, LF 2 has been identified in the cores, and interpreted as a glaciomarine unit. As previously observed from the core logs (Fig. 4.13) and from the X-rays (Fig. 4.15, 4.25 and 4.26), LF 2 is characterised by fine-grained sediments that are strongly laminated. These laminations are disturbed by dropstones and, at times, IRD layers and are believed to document a change in the type of depositional environment, and the onset of deglaciation (Ó Cofaigh *et al.*, 2005). Meltwater plumes from an ice margin have been known to be responsible for the deposition of sediments similar to LF 2 (Ó Cofaigh & Dowdeswell, 2001) and it is thus suggested that LF 2 was deposited mainly by suspension settling from turbid meltwater plumes in proximal to more distal conditions (Ó Cofaigh & Dowdeswell, 2001). The sediments within this lithofacies association also display abundances of cold temperature foraminifera species, that are known to be indicators of extreme glacial marine environments and are also found in modern glaciomarine settings (Sect. 4.3.4 and Fig. 4.16; Feyling-Hanssen, 1972; Hansen & Knudsen, 1995; Peters *et al.*, 2015). This thus supports the interpretations. In addition, LF 2 is found in association to the acoustic facies AF 4 (Fig. 4.12), internally characterised by strong parallel reflectors, which resemble the seismic appearance of glaciomarine sediments observed in other regions of the North Sea (Cameron *et al.*, 1992; Gatliff *et al.*, 1994). Core 133 displays the best example of LF 2 (Fig. 4.26). As clearly visible from the X-rays, at

the top of the slightly laminated diamicton found at the base of the core (LF 1b, Fig. 4.26e), LF 2 displays highly laminated sediments, strongly disturbed by the presence of abundant clasts. This type of sediments has been interpreted in previous studies to be evidence for a proximal ice-margin, responsible for discharging meltwater plumes and depositing a large amount of material close to the grounding line (Ó Cofaigh & Dowdeswell, 2001). In core 133, this proximal condition can be observed in section d (Fig. 4.26d), while sections c and b (Fig. 4.26c and 4.26b) indicate more distal conditions. With increasing distance from the ice margin and decrease in sedimentation rates, glaciomarine sediments usually display thinner laminae and are characterised by smaller grain-sizes (Ó Cofaigh & Dowdeswell, 2001). This can be observed in sections c and b of core 133 (Fig. 4.26c and b). In addition, the amount of dropstones and presence of IRD layers is also reduced as more distal conditions developed (Ó Cofaigh & Dowdeswell, 2001). This reduction in the abundance of laminations and dropstones is clearly recorded in core 133. Furthermore, more distal conditions lead to the deposition of massive muds that do not display laminations and are often bioturbated (Ó Cofaigh & Dowdeswell, 2001). This facies is also found in the analysed cores (LF 2a, Fig. 4.13). LF 2 found offshore clearly indicates that the NSL retreated in a glaciomarine environment in the western North Sea. This facies differs from what can be observed onshore north-east England, in the Tyne Gap and river Tyne Valley, where different sands and gravels facies have been identified (at times on top of diamictic facies) and interpreted to record deposition in a glacifluvial to glaciolacustrine proximal-distal environment (Yorke *et al.*, 2012; Davies *et al.*, 2013; Livingstone *et al.*, 2015). The presence of LF 2 also differs from what was observed in the southern North Sea off Holderness by Dove *et al.* (2017), where the presence of subglacial and glaciofluvial sediments associated with the NSL points to a terrestrial environment. This is further discussed in Chapter 5.

4.5.3 First chronology for ice retreat in the western North Sea

Two radiocarbon dates were obtained from foraminifera tests found within the glaciomarine lithofacies (LF 2b) of cores 132 and 128 (Fig. 4.3). The oldest date comes from core 132, where an age of 19,571±172 cal. yrs. BP was obtained. Further north, a second radiocarbon age of 16,949±218 cal. yrs. BP was obtained from core 128 (Fig. 4.28). These two ages represent two minimum ages for ice retreat, given that they were not recovered right at the contact between diamicton and glaciomarine sediments (location in the cores highlighted in Fig. 4.13). The fact that the oldest date is found towards the south while the youngest of the two comes from the northwesternmost core, suggests that the ice was retreating in a north-west direction, towards southern Scotland. This is in line with the proposed interpretations which, based on the geophysical data collected from the area, indicated a north-west direction for ice retreat (Sect. 4.5.1).

Considering the locations of these two dates, particularly in relation to the location of the GZWs identified on the seafloor (Fig. 4.28, it could be inferred that the ice margin was located north of core 132 by 19,571±172 cal. yrs. BP, and retreated to a location north of core 128 by 16,949±218 cal. yrs (as schematized in Fig. 4.28). However, it must be noted that these two dates are at odds with deglacial dates collected onshore from the Holderness region, where

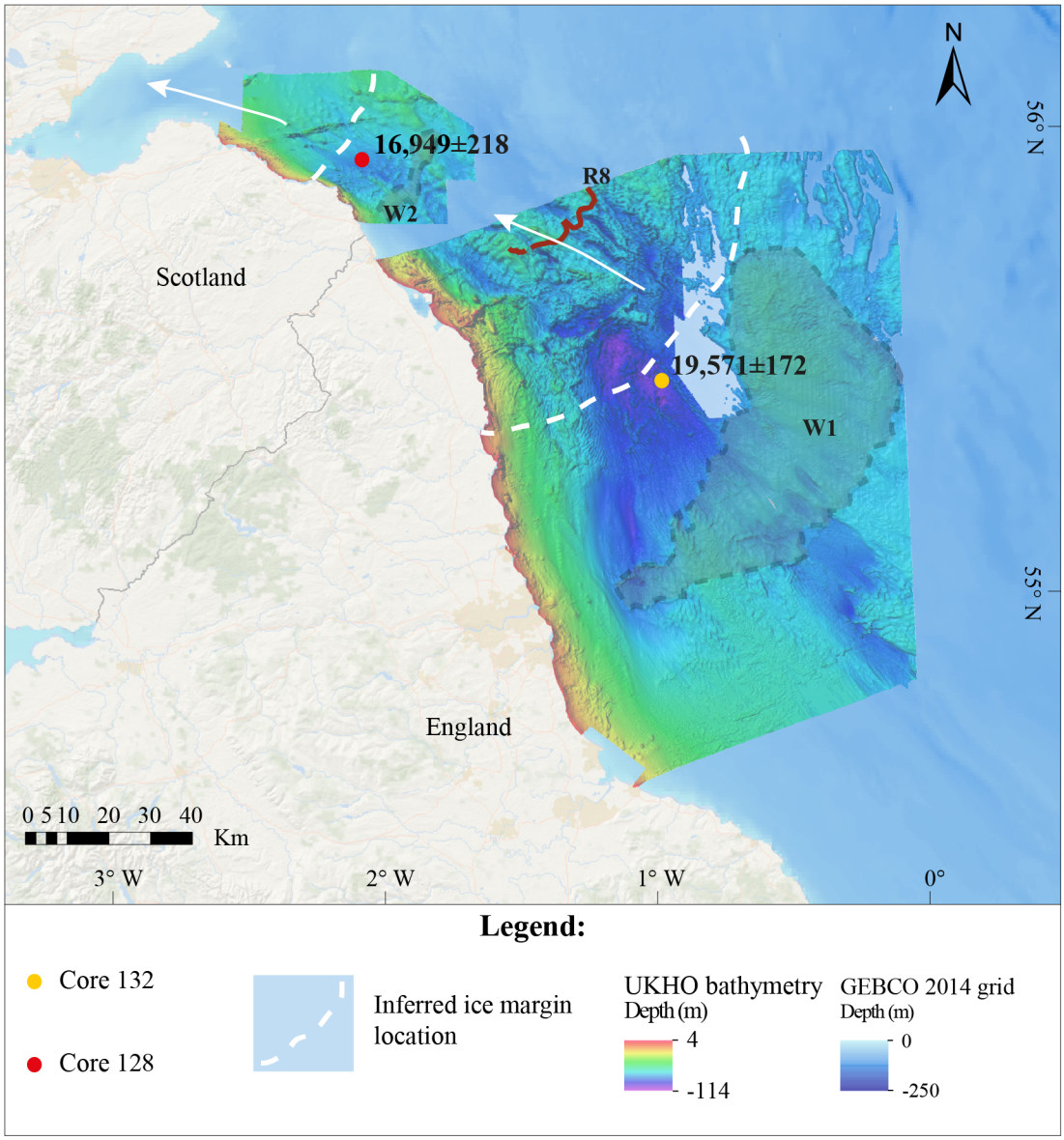

Figure 4.28: Location of the two radiocarbon ages obtained from cores 128 and 132 and inferred ice margin positions (white dashed lines). The positions of W1, W2 and R8 are also shown. The ages are shown in cal. yrs BP.

a series of near-synchronous ice advances, including the Withernsea Till advance, occurred as late as ~16.8 ka BP (Livingstone *et al.*, 2012b, 2015; Roberts *et al.*, 2013; Bateman *et al.*, 2015, 2017). A successive ice re-advance could have taken place after the deposition of the dated glaciomarine sediments, which would also be coherent with the onshore chronology. However, no sedimentary evidence for a possible ice re-advance appears from the cores. In core 132, the dated glaciomarine sediments are overlain by a 26 cm of diamict (LF 1; Fig. 4.13), although this thin layer might rather be the result of iceberg dumping/overturning, more than evidence for an advancement of the ice margin. Furthermore, this diamictic layer is then overlain by laminated to massive muds, which suggest increasing distance from the ice front. From the data analysed in this work, considering the distance between the two dated cores (~88.96 km), and the obtained radiocarbon dates, a retreat rate of ~33.92 m/yr can be tentatively suggested,

although additional radiocarbon dates are necessary to fully constrain the timings of ice retreat from the western North Sea.

4.6 Conclusions

High resolution bathymetry, seismic and core data reveal new information on the seafloor geomorphology, seismic stratigraphy and sedimentary imprint that characterise the western North Sea. This new evidence builds on the current knowledge of the glacial history of the area and suggests a new reconstruction for the evolution of the NSL in the western North Sea. A variety of landforms are recognized on the seafloor and include (1) bedrock-ridges, (2) bedrock-cored lineations orientated WNW - ESE to NW - SE, that are believed to have formed subglacially during ice advance by ice flowing from north-west. (3) Two (possibly three) grounding-zone wedges, orientated perpendicularly to the lineations, which are believed to be evidence of an episodic ice retreat, punctuated by different periods of stillstand. (4) A moraine, related to either a stillstand or to an oscillation of an ice-margin and (5) different subglacial meltwater channels which are also indicative of the former ice flow direction. Five different acoustic facies are also recognized from the datasets and record the presence of bedrock strata at or close to the seafloor (AF 1), together with subglacial/sub-marginal tills (AF 2 and AF 3), glaciomarine sediments (AF 4) and post-glacial to Holocene sediments (AF 5). Sediments recovered from five vibro-cores in the area record the last glacial-deglacial phase of the NSL during the Late Devensian. The presence of relatively soft, massive, matrix-supported diamictons (LF 1), also characterised by the apparent absence of planar structures, are believed to record the transition from subglacial to glaciomarine depositions, as they are also correlated to the boundary between acoustic facies AF 3 and AF 4. These sediments are overlain by fine, soft and laminated glaciomarine silts and clays (LF 2), which display strong laminations and abundance of clasts at the bottom (LF 2b), and thinner laminae and fewer clasts towards the top (LF 2a), and by massive sand (LF 3a) and gravel (LF 3b) lithofacies. They are believed to record deposition by suspension settling from meltwater plumes, iceberg rafting, and possibly turbidity currents, and to be evidence of a retreating ice margin, from a relatively proximal location in the lower sections of the cores, to a more distal position going upwards in the sedimentary sequence. LF 2a and LF 2b have been correlated to AF 4, which is characterised by high amplitude parallel reflectors that further corroborate the glaciomarine origin, and are also characterised by cold temperature foraminifera species, known to be indicators of extreme glacial marine environments. LF 4 found at the top of the sequence is composed by massive sands with abundant shells and is inferred to represent Holocene sediments. Additionally, two new radiocarbon dates collected within the glaciomarine lithofacies (LF 2) provide new information for ice retreat in the western North Sea. These ages record that the NSL was retreating from the central part of the study area around 19,571$\pm$172 cal. yrs. BP, and that by 16,949$\pm$218 cal. yrs. BP the ice had retreated north-west of core 128, located in the northern part of the study area and closer to southern-Scotland. The two dates provide a tentatively suggested slow retreat rate of $\sim$33.92 m/yr. The evidence provided in this chapter demonstrates that the NSL was responsible for the formation of the subglacial landforms

orientated from WNW - ESE and NW - SE and that it was fed by Scottish ice. This is further confirmed by the orientations of the GZWs which indicate that ice retreated towards southern Scotland. In addition, the imprint on the seafloor reveals that ice retreat in the western North Sea was characterised by different phases of stillstand, which resulted in the formation of the two GZWs observed, and which were possibly facilitated by the presence of pinning points. The characteristics observed from the sediment cores suggest that the NSL retreated in a glaciomarine environment in this part of the North Sea. Further discussion will follow in Chapter 5.

Chapter 5

Discussion

The North Sea Lobe (NSL) is known to have flowed in the North Sea and to have deposited sediments along the eastern coast of England, and many studies have analysed the glacigenic sequences exposed at Holderness (east Yorkshire) as well as at County Durham (NE England), relating to the advance and retreat of the NSL (Carr *et al.*, 2006; Davies *et al.*, 2009a, 2011, 2012a; Evans & Thomson, 2010; Bateman *et al.*, 2011, 2015, 2017; Livingstone *et al.*, 2012b, 2015; Evans *et al.*, 2017). Using onshore sedimentological and geomorphological evidence of NSL activity, Livingstone *et al.* (2008, 2012b) proposed a multi-stage model for ice flow phases for the central sector of the last British and Irish Ice Sheet (BIIS; see also Chapt. 2). Despite the aforementioned onshore signal, offshore reconstructions of ice sheet activity in the western North Sea are still tentative in nature, especially in relation to the final phases of the last BIIS before deglaciation. Furthermore, there is a lack of ice retreat chronology for this particular area. The new high resolution geophysical datasets collected in this sector of the North Sea basin from the Blyth and Britice-Chrono study areas, permitted to better define the glacial history of the region. The compilation of a new geomorphological map that highlighted the presence of numerous landforms, allowed to characterise for the first time the imprint of the NSL and the patterns of retreat offshore (Chapt. 4). In addition, the new set of sediment cores collected from the area allowed the characterisation of subglacial, ice-marginal and glaciomarine conditions during NSL retreat. By combining the new data with the pre-existing knowledge of NSL activity, this chapter aims to propose a new model for the dynamic history of the NSL offshore from County Durham and Northumberland, during the Last Glacial Maximum (LGM).

5.1 NSL: New offshore evidence and implications for BIIS dynamics

The new datasets analysed in this study provide evidence for the imprint of an ice lobe on the seafloor of the western North Sea. The analysis of the UKHO high resolution multibeam bathymetry (Chapt. 4) identified numerous sets of landforms, that are indicators of the NSL flow pathway and advance, but also essential indicators of the dynamics of its retreat during deglaciation. The glacial landforms recognized and mapped in Chapter 4 are shown together with the adjacent onshore topography in Figure 5.1. Here, the onshore subglacial lineations

and ice-dammed lake extents, downloaded from the BRITICE Glacial Map (a map and GIS database of glacial landforms and features related to the last British Ice Sheet; Clark *et al.*, 2004a, 2018), are also shown, so to permit a correlation between the onshore and offshore geomorphology. The orientations and directions of the Forth, Tweed, Tyne Gap Ice Stream (TGIS), Stainmore and NSL ice streams are also indicated (white arrows).

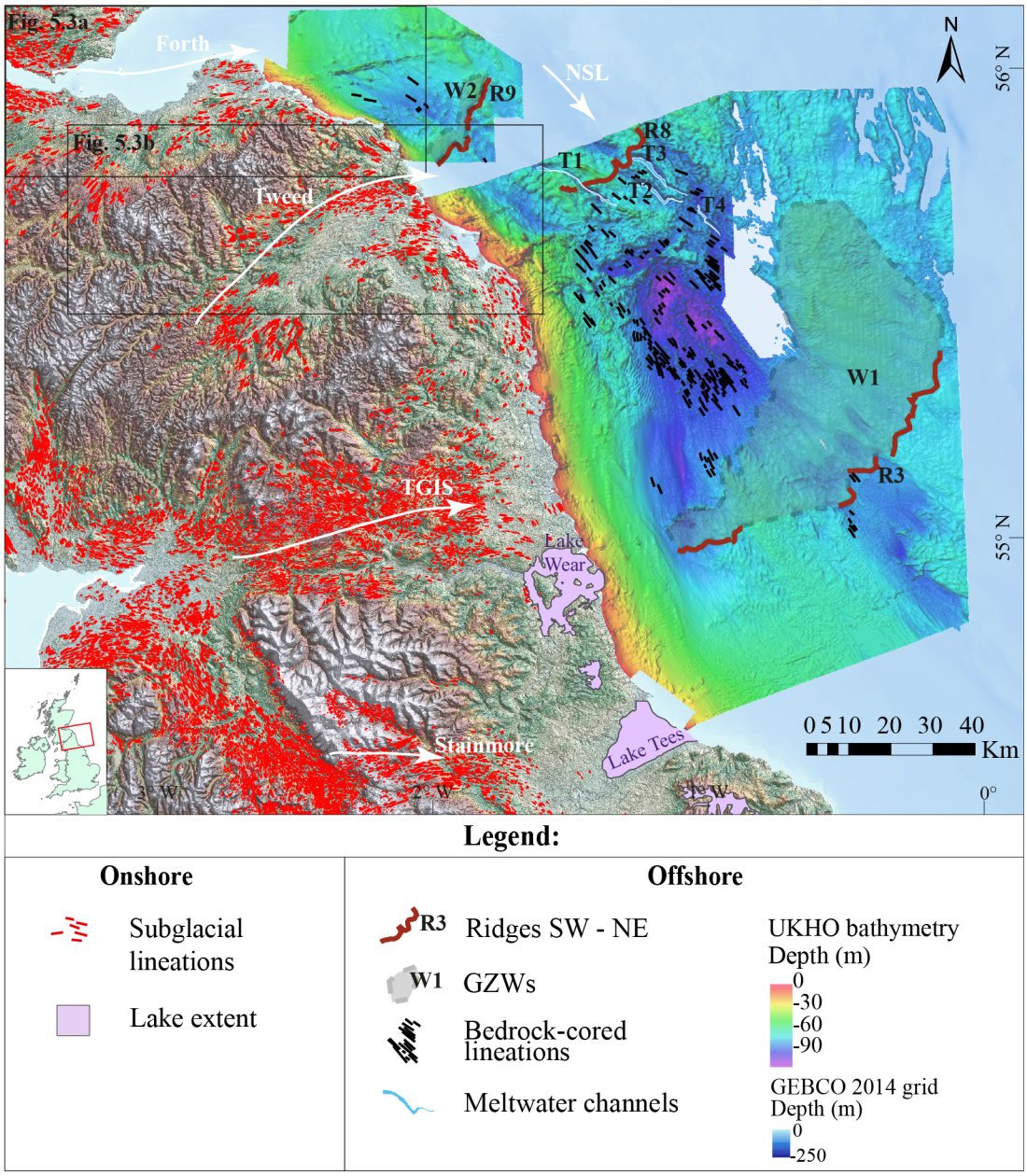

Figure 5.1: UKHO bathymetry dataset and interpreted glacial landforms (Chapt. 4), shown together with the onshore glacial signal. Onshore mapping of subglacial lineations and ice-dammed lake extents were downloaded from the BRITICE Glacial Map (Clark *et al.*, 2004a, 2018). The ice flow directions of the Forth, Tweed, Tyne Gap Ice Stream (TGIS), Stainmore and NSL ice streams are indicated with white arrows. The location of the shown area is indicated in the insert map with a red square. The locations of Figure 5.3a and 5.3b are indicated with black squares. NEXTMap onshore topography.

5.1.1 The advance phase signal: sedimentary and geomorphological evidence for NSL flow

One of the most important characteristics discovered on the seabed in the study area, is represented by the presence of the parallel/subparallel, elongated bedforms, interpreted in Chapter 4 as subglacial bedrock-cored lineations (in black in Fig. 5.1; see also Fig. 4.22 and 4.23, in Chapt. 4). These bedforms are discontinuous and relatively short (in comparison to Mega-Scale Glacial Lineations (MSGLs); Clark, 1993), and their lengths vary from a few hundred meters up to 6 kilometres. Similar types of bedrock-moulded landforms have been observed onshore eastern England, for example in the Tyne Gap region (Livingstone *et al.*, 2008, 2010), onshore and offshore north-west Scotland (Bradwell *et al.*, 2008b; Krabbendam & Glasser, 2011; Bradwell & Stoker, 2015a; Dove *et al.*, 2015), as well as in West Greenland (Lane *et al.*, 2015). They are well-known indicators of palaeo-ice flow direction and are thought to form due to the action of either fast or prolonged ice flow (Clark, 1993; Stokes & Clark, 2001; Roberts & Long, 2005; Bradwell *et al.*, 2008b; Livingstone *et al.*, 2008; Roberts *et al.*, 2010). The bedforms observed in the western North Sea suggest the ice flow was orientated mainly NW - SE (Chapt. 4). They are believed to be mainly erosional, due to the fact that they are generally characterised by bedrock cores, and to have formed in response to basal abrasion and plucking, probably during different phases of ice flow (Roberts & Long, 2005; Livingstone *et al.*, 2008; Bradwell & Stoker, 2015a; Krabbendam *et al.*, 2016). This is because hard-bed streamlining is believed to form over a longer time frame, when compared to the streamlining characterised internally by soft sediments, and requires more energy to be eroded. Their formation can thus be the result of numerous glacial phases (Roberts & Long, 2005; Krabbendam *et al.*, 2016).

In addition, it is believed that the bedrock strata present in the area might have had an influence on the resulting morphology of the lineations observed, which are elongated and narrow and display rounded crests (see Chapt. 4). As previously discussed in Chapter 4, the bedrock strata found in correspondence to these lineations are of Carboniferous, Permian and Triassic age (Cameron *et al.*, 1992; Gatliff *et al.*, 1994), and display parallel internal bedding planes that are folded and dip at different angles in respect to the inferred palaeo-ice flow direction (see also Chapt. 4). These bedding planes display evidence of erosion, as they appear truncated at their upper boundary. From the available seismic lines in the study area, it was observed that the bedrock strike appears generally parallel to the ice flow (although it should not be assumed that this is the case for the entire area), and it was inferred that this may have facilitated the development of such elongated bedforms. Lane *et al.* (2015) suggested that the presence of stratified bedrock characterised by gently dipping to folded strata, with strike parallel to ice flow, constitutes one of the cases where highly elongate rock bedforms can occur. Krabbendam *et al.* (2016) have described the phenomena for the Tyne Gap region, where rock megagrooves and megaridges appear to be well developed in areas where the ice flow was parallel to the bedrock strike, rather than transverse to it, and thus appear to be strike-controlled (Livingstone *et al.*, 2008; Krabbendam *et al.*, 2016). The bedrock strata that characterise this area are mainly of Carboniferous age, and it is thus believed that the offshore bedforms are comparable to the ones observed onshore, and that the characteristics of the bedrock strata

might have played a role in the resulting morphology of the lineations.

Despite the fact that these bedforms are mainly bedrock-cored, a patchy distribution of acoustic facies AF 3, interpreted as composed of glacigenic diamicts (Chapt. 4), is also present in the area, and often thickens in the depressions between the bedforms and is generally thinner or is absent on top of the crests (Fig. 5.2). Hence, due to the presence of both hard and soft materials in the area, the landform assemblage observed on the UKHO bathymetry is defined as a mixed-bed assemblage (Eyles *et al.*, 2016). It is believed the bedforms observed offshore were formed through streamlining beneath grounded ice and that the seafloor shows evidence for abrasion/erosion as well as sediment deposition, although additional data are needed to fully discriminate the internal nature of these landforms and better characterise the distribution of soft sediments. The Tyne Gap region onshore eastern England provides a clear analogue for this type of landsystem, with both hard-bed lineations and numerous till-cored drumlins that are found together as part of the footprint of the TGIS (Fig. 5.1; Livingstone *et al.*, 2008; Krabbendam *et al.*, 2016). Figure 5.2 shows a simplified reconstruction of the central part of the UKHO Area 1, where these lineations are observed.

The landforms observed in the study area also provide information on the orientation of the former ice flow. As previously discussed (see also Chapt. 4), the lineations mapped on the seabed show a preferred orientation that is directed WNW - ESE in the northern part of the bathymetry data (UKHO Area 1) and NW - SE in the central part of the survey, where the majority of the bedforms were observed (Fig. 5.1; UKHO Area 2). This orientation suggests a former ice flow mainly directed NW - SE. This is further supported by the disposition of the other glacial landforms observed on the seabed. The two GZWs (W1 and W2) are both orientated transverse to the lineations (Fig. 5.1), thus indicating that the ice flow was coming mainly from north-west, as GZWs are known to develop perpendicular to the direction of ice flow (Batchelor & Dowdeswell, 2015). In addition, the arcuate ridge R8 together with the subglacial meltwater channels also document former ice flow direction towards the south-east. It is thus inferred that the landforms observed in the western North Sea are evidence for the action of the NSL, which was fed by the Forth ice stream and was flowing out of south-east Scotland, extending offshore, turning southwards and impinging the eastern coast of England (Fig. 5.1, see also Chapt. 4). This is further corroborated by the orientation of the bedrock-cored lineations in the northern part of the UKHO dataset, where they appear to be directed towards southern Scotland, and to be well correlated to the subglacial lineations mapped immediately onshore (Fig. 5.1 and 5.3).

Analyses on till provenance in Yorkshire and County Durham also indicated that the NSL was responsible for the deposition of these sedimentary packages, which are characterised by lithologies originated in southern Scotland, the Cheviots and the east coast of England (Catt, 2007; Davies *et al.*, 2009a, 2011; Evans & Thomson, 2010; Boston *et al.*, 2010; Busfield *et al.*, 2015). This southern extension of the NSL is also fully corroborated by the striking streamlined appearance of the Tweed valley onshore (Fig. 5.1 and 5.3). Here, the streamlined landforms bend around the Cheviots and display a clear switch in orientation from SW - NE, in the main corridor, to NW - SE in close proximity to the coast (Fig. 5.3). The Tweed ice stream is in fact thought to have joined (or more likely was deflected by) the NSL flow coming from northern

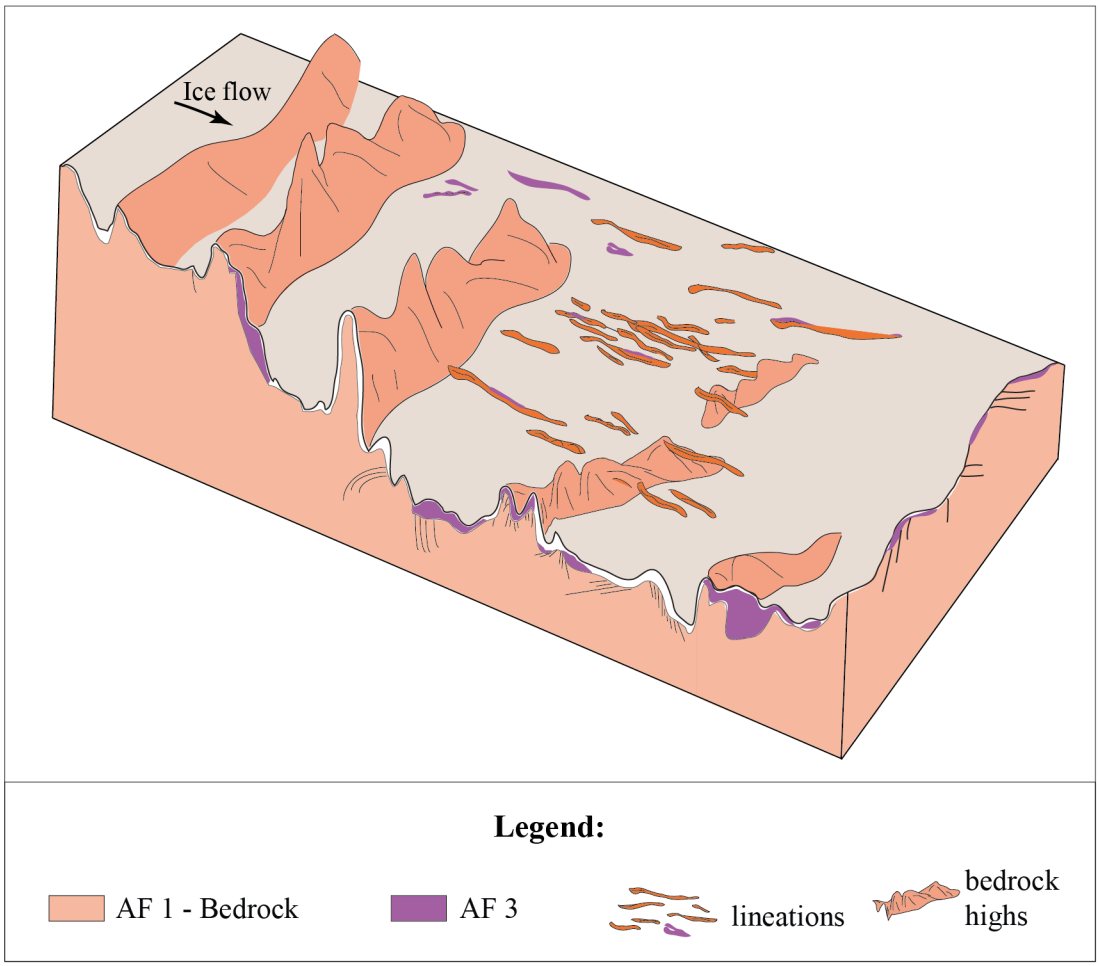

Figure 5.2: Highly simplified 3D representation of the mixed-bed assemblage observed in the study area, showing the presence of different bedrock ridges/outcrops, together with numerous bedrock-cored lineations, which are at times overlain by lenses of AF 3. The light brown colour represents the seabed. Note that the facies on top of AF 3 were not included in this diagram and are left blank.

areas and continued its course towards the south (Livingstone *et al.*, 2012b). The fact that the NSL deflected towards the south and flowed parallel to the eastern coast of England, has been a matter of interest in numerous studies. This is because, considering the very flat and shallow nature of the western North Sea (with maximum depths in the study area of approximately -113 m, and average depths of approximately -70 m; Chapt. 4), it would be logical to assume that the ice stream flowed eastward towards the central North Sea after flowing out of the Firth of Forth. Instead, no evidence for this eastward flow in the research area is found, and only a strong signal for ice flow directed towards the south/south-east is recognized. Furthermore, along the offshore corridor of the study area, no evidence was found on the bathymetry dataset for ice flow directed from west to east, and thus related to the action of ice coming from the Tyne Gap (Fig. 5.1, see also Chapt. 2 and 3). The only evidence that could possibly be related to the action of the TGIS is represented by the acoustic facies AF 2 observed in the Britice-Chrono survey (Chapt. 4), which has a general patchy appearance and was interpreted as a glacigenic diamicton (and possibly a till), and the acoustic facies BL-AF 4 observed in

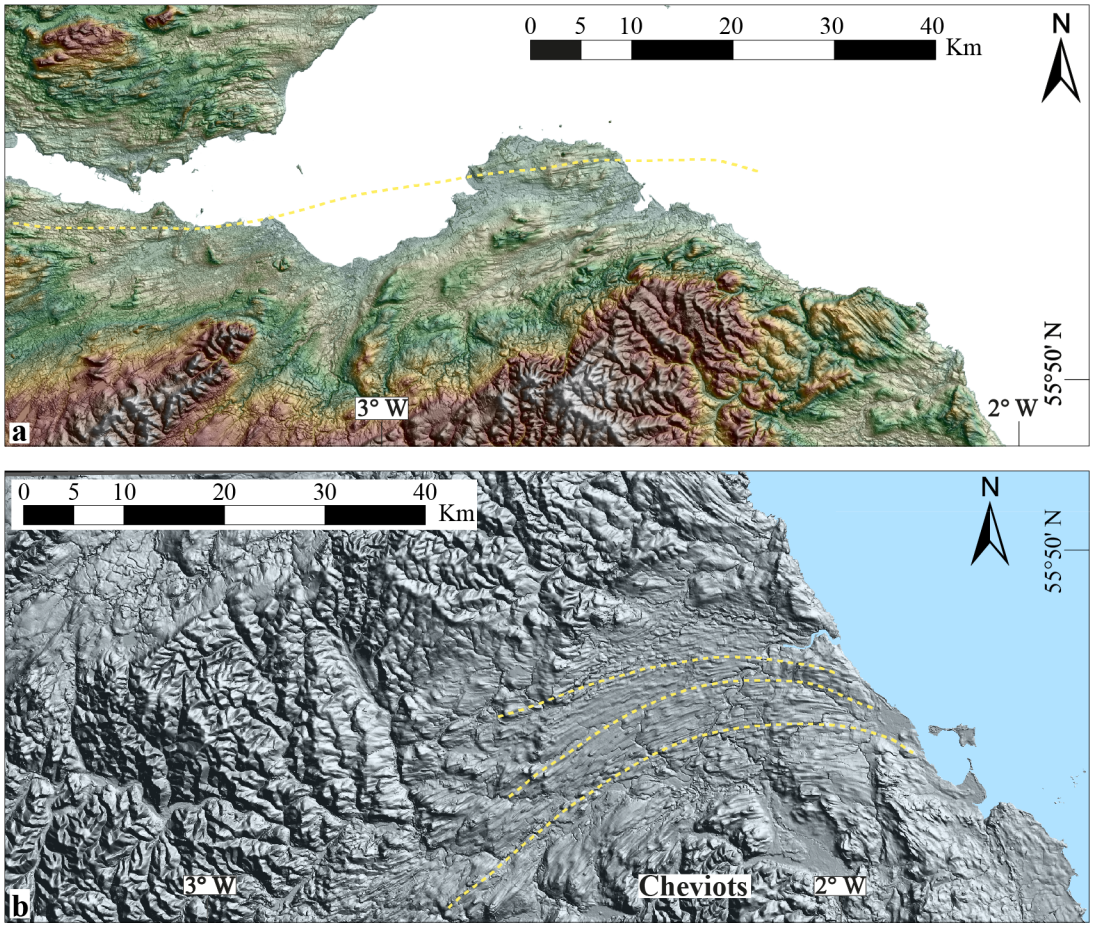

Figure 5.3: NEXTMap images of the Forth (a) and Tweed (b) basins showing the preferred orientations of the subglacial landforms and the inferred ice flow direction (yellow lines). Figure 2b shows the clear switch in orientations of these landforms which here bend around the Cheviots and turn towards the south-east. Modified from Hughes *et al.* (2010). The location of the images is shown in Figure 5.1.

the Blyth survey (Chapt. 3), which has a chaotic internal geometry and was interpreted as a glacigenic diamicton (and possibly a till). Ice is known to have come out of the Tyne Gap, towards the east, at some point, as reconstructed by Livingstone *et al.* (2012b) and AF 2 could thus be the offshore correlative of the Blackhall Till. However, any geomorphological evidence for this ice flow was probably later overprinted by ice coming from the north. Some evidence for this overprint can be found onshore in the Tyne Gap region as recognized by Livingstone *et al.* (2015), and previously shown in Chapter 2 and 3. In addition, BL-AF 4 was correlated to the Wee Bankie Formation rather than to a facies deposited by the TGIS due to its internal characteristics, the fact that it was also observed on top of pre-Quaternary strata and was found in an area where the presence of this formation was mapped by the BGS (see Chapt. 2 and 3).

Following the reconstructions of Livingstone *et al.* (2015) and Bateman *et al.* (2015), this study also suggests that the NSL was still active and flowing southwards at a later stage after the LGM and was, by that point, the sole contributor to the glacial imprint that characterises the present-day seafloor, while both the TGIS (sometimes before ~18.7 to 17.1 ka, Livingstone *et al.*, 2015), and the Stainmore ice streams had retreated inland. The reasons to explain this

sudden turn of the NSL have been discussed in many studies and are diverse. Clark *et al.* (2012) proposed the possible presence of a persistent ice dome in the central/southern North Sea as a plausible scenario to explain the presence of ice along the eastern coasts of England at a late stage during the last glacial period. However, this reconstruction is now being revised by the Britice-Chrono project with the collection of new geophysical and sedimentary evidence from the North Sea basin. The presence of Scandinavian ice to the east, which would have constrained the NSL flow and deflected it towards the south, was also considered as one of the possible causes for this sharp turn by Davies *et al.* (2011), however, the latest reconstruction of the extent of the SIS and BIIS in the North Sea from Sejrup *et al.* (2016), suggests that the final unzipping of the two ice sheets was close to 18.5 ka (see Fig. 2.5 in Chapt. 2). At this time, the NSL is known to have re-advanced towards Holderness (Clark *et al.*, 2012; Evans & Thomson, 2010; Boston *et al.*, 2010; Livingstone *et al.*, 2012b, 2015; Bateman *et al.*, 2015; Dove *et al.*, 2017), regardless of the absence of lateral constraint from the east. This is in line with the reconstructed models of the last BIIS (Lee *et al.*, 2002; Boulton & Hagdorn, 2006; Patton *et al.*, 2016; Hughes *et al.*, 2016), which support a southwards BIIS spread in the North Sea basin without the presence of Scandinavian ice to the east.

The NSL could have turned southwards due to favourable bed conditions, possibly caused by the presence of soft and deformable substrate in the western North Sea and on eastern England (Lee *et al.*, 2002; Catt, 2007; Boston *et al.*, 2010; Busfield *et al.*, 2015). In fact, the presence of deformable Jurassic and pre-existing Quaternary sediments (see also Chapt. 2) are believed to be a possible trigger for fast ice flow in this region (Catt, 2007; Bateman *et al.*, 2015). Furthermore, the proposed flow pathway of the NSL (Chapt. 4) is situated between two areas of higher ground, the Dogger Bank on the eastern side (an extensive SW - NE orientated bathymetric high situated in the central North Sea, see Sect. 5.2 and Chapt. 2), interpreted as a large thrust moraine complex (Roberts *et al.*, In prep.; Cotterill *et al.*, 2017), and the North York Moors and the Yorkshire Wolds on the western side (Bateman *et al.*, 2015; Busfield *et al.*, 2015), both of which could have further contributed to the southern expansion of the NSL by constraining it on both margins. The data analysed in this study thus confirm the proposed former pathway of the NSL (Evans & Thomson, 2010; Davies *et al.*, 2011; Clark *et al.*, 2012; Livingstone *et al.*, 2012b, 2015; Roberts *et al.*, 2013; Bateman *et al.*, 2015), and provide new evidence for ice stream flow direction towards the south-east in the western North Sea, which left numerous landforms indicative of its passage, both onshore (Hughes *et al.*, 2010; Livingstone *et al.*, 2012b, 2015) and offshore (Fig. 5.1, see also Chapt. 4). It is also believed that the NSL was active at a late phase during the last glacial period while other sectors of the BIIS had started their retreat towards land, as previously thought (Evans & Thomson, 2010; Livingstone *et al.*, 2015; Bateman *et al.*, 2015). This is confirmed by the new chronology proposed in this study (Chapt. 4), which is discussed in further detail in section 5.2.

5.1.2 The retreat phase signal: evidence for periods of ice stillstand

The subglacial landforms that were created during phases of ice advance in the study area, have been subsequently overprinted by the deposition of landforms during active retreat. As previously discussed in Chapter 4, two GZWs were recognized in the area (Fig. 5.1),

and provide important information on the type of ice retreat that characterised this sector of the North Sea. GZWs are known to be diamictic wedges that form at the grounding zone by the constant and rapid accumulation of glacigenic debris from active ice, as this continues to deliver sediments to its margin (Powell & Alley, 1997; Dowdeswell *et al.*, 2008; Ottesen & Dowdeswell, 2009; Batchelor & Dowdeswell, 2015). GZWs thus form beneath actively fast-flowing ice and their presence in the geomorphic record represents evidence of phases of grounding zone stability during ice retreat (Powell & Alley, 1997; Dowdeswell & Fugelli, 2012; Batchelor & Dowdeswell, 2015). The schematic model published by Ottesen & Dowdeswell (2009) and modified by Batchelor & Dowdeswell (2015), shown in Figure 5.4, is a reconstruction of the different landform assemblages that can be found at the beds of fast flowing ice streams (Fig. 5.4a) or slow flowing ice (Fig. 5.4b) on a continental margin.

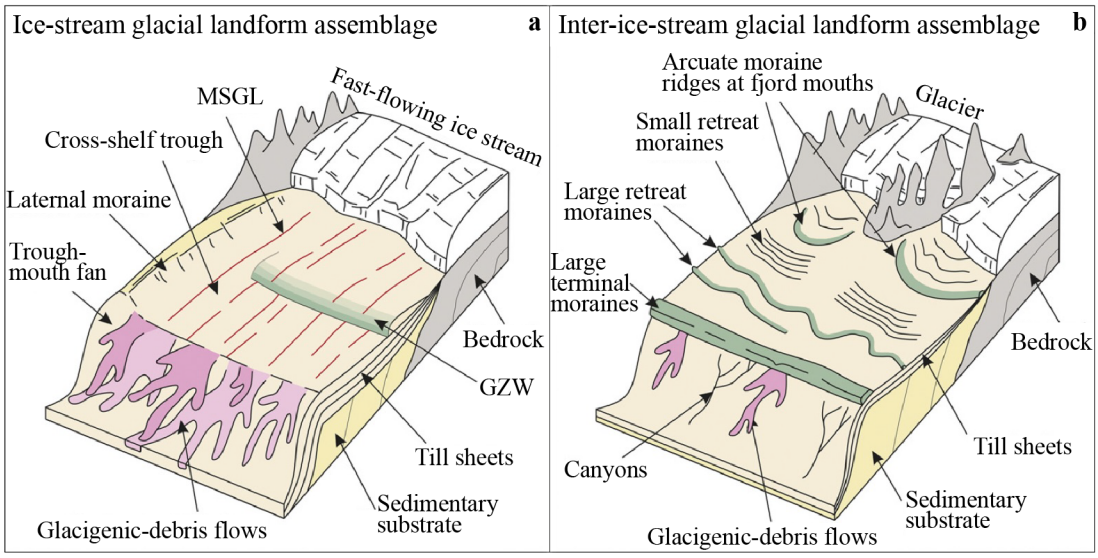

Figure 5.4: a: Typical ice stream landform assemblage produced by fast, ice stream flow on a continental margin. b: Typical inter-ice stream landform assemblage produced by slow-flowing ice on a continental margin. GZW: Grounding-Zone Wedge. MSGL: Mega-Scale Glacial Lineations. From Ottesen & Dowdeswell (2009) and Batchelor & Dowdeswell (2015).

Generally, the presence of GZWs, orientated transversally to MSGLs, represents evidence of fast ice and indicates that the ice retreat was episodic, characterised by temporary stillstands (Ó Cofaigh *et al.*, 2008; Dowdeswell *et al.*, 2008; Dowdeswell & Fugelli, 2012; Batchelor & Dowdeswell, 2015). On the other hand, the presence of sets of large and small transverse moraine ridges record slower-flowing ice, that was characterised by a relatively slow retreat (Ó Cofaigh *et al.*, 2008; Dowdeswell *et al.*, 2008; Ottesen & Dowdeswell, 2009).

Different factors can control the formation of GZWs, although the location of any stillstand during ice retreat is strongly influenced by the topography of the seafloor. Many high latitude GZWs have been observed at locations characterised by the presence of topographic/sedimentary highs in the underlying bathymetry (Ottesen *et al.*, 2007; Dowdeswell & Fugelli, 2012; Batchelor & Dowdeswell, 2015). Lateral and vertical pinning points increase lateral and basal drag, thus promoting grounding zone stability. Therefore, the presence of vertical pinning points, such as bedrock highs for example, can favour the formation of GZWs

by reducing the water depth of the seafloor (Ottesen *et al.*, 2007; Dowdeswell & Fugelli, 2012; Batchelor & Dowdeswell, 2015). Furthermore, as mentioned previously, the orientation of GZWs also gives indication on the former ice flow direction, as the wedges are built transversally to the ice margin (Fig. 5.4a; Ottesen *et al.*, 2007; Dowdeswell *et al.*, 2008; Ottesen & Dowdeswell, 2009; Batchelor & Dowdeswell, 2015).

The two GZWs observed in the study area display the above-mentioned characteristics. They are found in association with glacial lineations, as outlined in Figure 5.4a, and appear to have formed in relatively more shallow areas, characterised by the presence of bedrock highs (Chapt. 4), which possibly provided pinning points in relatively shallow water. It is thus inferred that the NSL underwent phases of stillstand/re-advance during overall retreat, back-stepping and stopping at the locations of W1 at first and then of W2 for enough time to build up both landforms. In addition, the fact that W1 and W2 are orientated SW - NE, are perpendicular to the lineations (Fig. 5.1) and display steeper slopes towards the south-east and gentler ones towards the north-west, is a further confirmation that the former ice flow was directed NW - SE (see also Chapt. 4). Despite this preferred orientation, it is believed that the ice flow might have been unconstrained, especially during the final retreat phase. This is particularly suggested by the lobate planform of W1 (Fig. 5.1), which infers the NSL was not channelised, but was rather flowing into an unrestricted lobate front, and by the glacial imprint that can be observed on this area of the western North Sea, which does not support the presence of lateral shear margins. It is thus inferred that the NSL was behaving as a piedmont lobe during overall northwards retreat.

5.2 New chronology: onshore/offshore correlation

One of the most important and still debated questions regarding the last BIIS relates to the timing of its final retreat. Understanding the dynamics and rates of retreat of past ice sheets is in fact crucial to improve the compilation of more accurate glaciological, isostatic and palaeoclimatic models, that can guide our understanding of current and future ice sheet changes (Hughes *et al.*, 2016; Clark *et al.*, 2012). Different studies have generated a retreat chronology from scattered onshore locations of the last BIIS, by collecting numerous retreat dates using various methodologies (radiocarbon, cosmogenic, thermal luminescence (TL), optically stimulated luminescence (OSL), etc.; Bateman *et al.*, 2008, 2011, 2017; Ballantyne, 2010; Hughes *et al.*, 2011; Clark *et al.*, 2012; Livingstone *et al.*, 2015; Evans *et al.*, 2017). But despite this, the offshore sector still remains the least explored, and there is yet a lack of data points indicating ice retreat in the offshore regions of the last BIIS, particularly in the western North Sea (Hughes *et al.*, 2011; Bateman *et al.*, 2015). The Britice-Chrono project is in the process of developing a new and more accurate reconstruction of the timings of retreat of this ice sheet. As part of the project, this study takes into consideration the two new radiocarbon dates collected in study area and discussed in Chapter 4, and includes additional chronology information gathered from the North Sea region during the JC123 oceanographic survey.

5.2.1 Former eastern margin of the last BIIS: new and published chronology

In this section, the main chronology for ice advance and retreat recorded on the former eastern margin of the last BIIS from Hughes *et al.* (2011) and other successive studies (Bateman *et al.*, 2011, 2015, 2017; Yorke *et al.*, 2012; Livingstone *et al.*, 2015; Fairburn & Bateman, 2016; Evans *et al.*, 2017) are summarized and shown together with the new information gathered from the cores in the western North Sea (Fig. 5.5).

On at least two occasions the NSL is believed to have oscillated along the eastern coast of England during the last glacial phase. These oscillations have been correlated to the deposition of the Skipsea Till and of the Withernsea Till (Bateman *et al.*, 2011, 2015, 2017). Penny *et al.* (1969) obtained radiocarbon ages measured on moss samples from the Dimlington silts, which underlie both the Skipsea and the Withernsea tills in Holderness, east Yorkshire. These dates indicate that the NSL reached its maximum extent after 23.0 - 20.8 cal. ka BP (18.25 $\pm$ 0.25 ka BP) and 22.3 - 20.9 cal. ka BP (18.5 $\pm$ 0.4 ka BP; Penny *et al.*, 1969). The two dates marked in red in Figure 5.5 at Holderness, represent the mean values of the dates listed above and indicate that there was an ice advance after 21.8 $\pm$ 0.3 and 22.0 $\pm$ 0.5 cal. ka BP. Similarly, Bateman *et al.* (2008) recorded an ice advance after 23.3 $\pm$ 1.5 ka from a sample underlying a glacial diamict at Ferrybridge, Yorkshire (in red, Fig. 5.5). In addition, new OSL ages from ongoing work further south, at Garett Hill on the Norfolk coast, suggest that BIIS ice arrived in the region immediately after 23.4 - 20.2 ka (Roberts *et al.*, In prep.). Evidence for ice retreat also comes from Dimlington and Ferrybridge (dates in green, Fig. 5.5). Bateman *et al.* (2011) published new OSL dates from the Dimlington typesite, measured from four samples collected from silts and sands located between the Skipsea Till and the Withernsea Till. The measured ages bracket the period between 16.9 $\pm$ 0.9 and 14.4 $\pm$ 0.8 ka and indicate that the NSL was still active at a late stage during the last glacial period (Bateman *et al.*, 2011; Yorke *et al.*, 2012). These ages were revised from Bateman *et al.* (2017), and dated sediments directly overlying the Skipsea Till at Dimlington and Skipsea indicate that the NSL retreated offshore before 17.0 $\pm$ 0.9 ka before re-advancing. Further inland, at Ferrybridge, Yorkshire, Bateman *et al.* (2008) obtained an OSL date of 16.6 $\pm$ 1.2 ka from the Lake Humber region (Fig. 5.5). This date is thought to indicate the age of the 33 m lake level and to represent a late stage during which the NSL impounded Lake Humber (Bateman *et al.*, 2008; Fairburn & Bateman, 2016), and after which the final retreat of the NSL took place. Bateman *et al.* (2017), provide new evidence from the Humber Gap region, and suggest that the deposition of the Skipsea Till occurred around 21.6 ka $\pm$ 1.3 ka, which was followed by a series of ice re-advances, including the one responsible for the deposition of the Withernsea Till, around 16.8 $\pm$ 0.8 ka. Ice is thought to have fully withdrawn from the region by $\sim$15 ka (Bateman *et al.*, 2017). In addition, new OSL chronology from the former Lake Pickering in the Yorkshire region, appears to indicate that the NSL was located east of the Flamborough Moraine by 17.3 ka (Fig. 1 and 8 in Evans *et al.*, 2017). Furthermore, there are two dates, of ages 15.7 $\pm$ 0.4 cal. ka BP and 12.6 $\pm$ 0.8 cal. ka BP, indicating final ice retreat from the region of glacial Lake Tees (in green, Fig. 5.5; Hughes *et al.*, 2011). Moving towards the north, analyses on the former eastern margin of the TGIS from Livingstone *et al.* (2015), constrain the timing of retreat of the TGIS and its uncoupling from the NSL. These dates (Fig. 5.5) record the westwards retreat of the TGIS

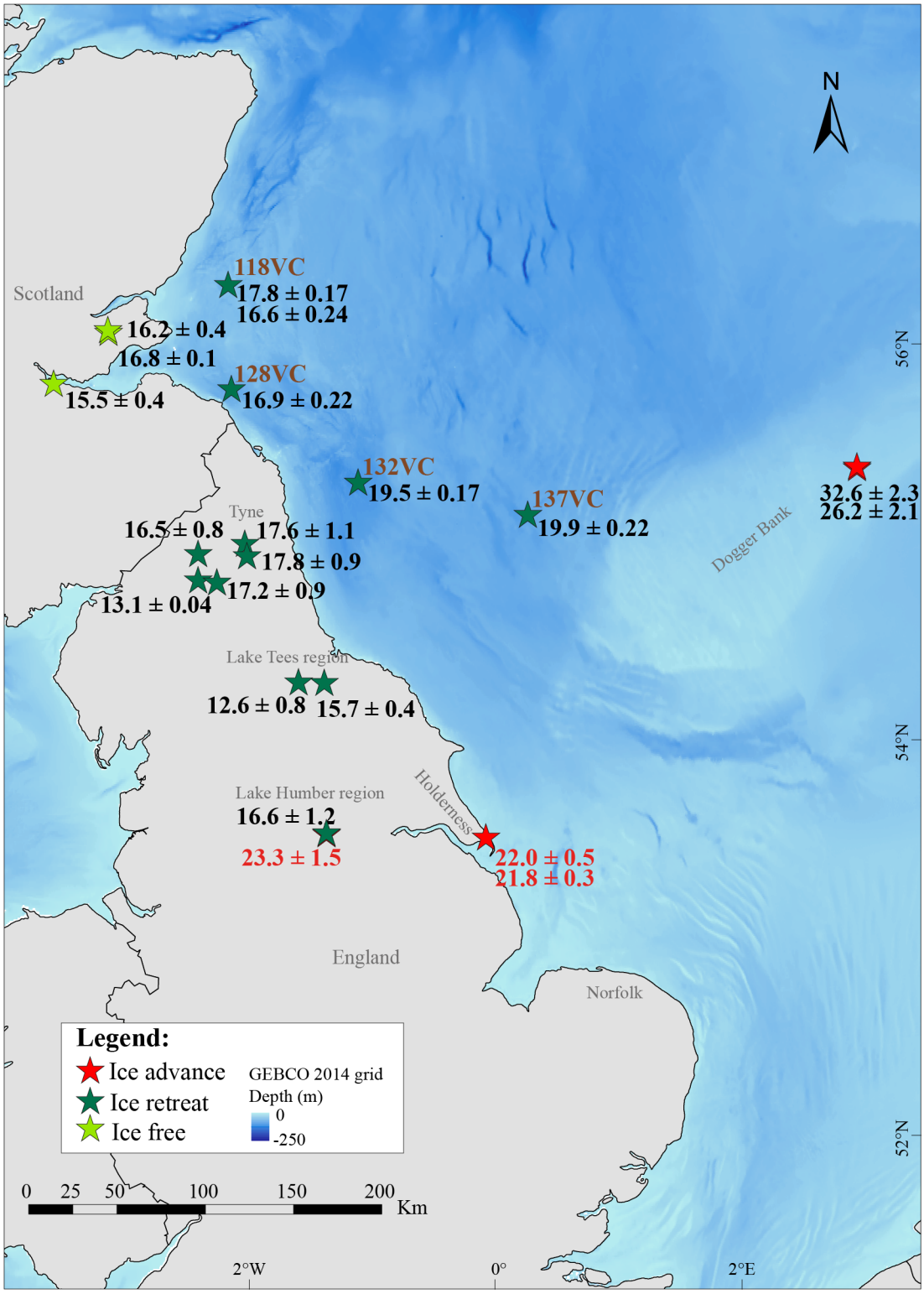

Figure 5.5: Compilation of published and new dates constraining the final phases of the NSL ice stream. Modified from Hughes *et al.* (2011). The ages are expressed in ka BP.

from the coast, from 18.7 - 17.1 ka BP eastward to the Solway Lowlands by 16.4 - 15.7 ka BP (Fig. 10 in Livingstone *et al.*, 2015). The uncoupling of the TGIS from the NSL is recorded by the presence of a moraine located 10 - 15 km inland of the present-day coast (Crowden Hill Moraine, Fig. 4 in Livingstone *et al.*, 2015, see also Chapt. 2). Finally, ice-free conditions are

recorded at 15.5 ± 0.4, 16.8 ± 0.1 and 16.2 ± 0.4 cal. ka BP (in light green in Fig. 5.5) in south-eastern Scotland (Holloway *et al.*, 2002; Hughes *et al.*, 2011), and numerous dates from central and southern Scotland suggest that Scottish ice had retreated substantially by 16 - 14 ka BP and was in the vicinity of the Loch Lomond Stadial configuration by 14 ka BP (Everest & Kubik, 2006; Clark *et al.*, 2012; Hughes *et al.*, 2011).

A set of new dates from the Britice-Chrono project provides new evidence for ice retreat from the offshore sector affected by the NSL. New OSL dates from the Dogger Bank region (Fig. 5.5), record the deposition of glaciolacustrine sediments between 32.6 and 24.1 ka BP (Roberts *et al.*, In prep.). Ice is thought to have overridden the Dogger Bank and to have then retreated back northwards by 27.5 - 23.5 ka BP (Roberts *et al.*, In prep.). After this time, it is believed that the ice was mainly located to the west of the Dogger Bank and extended southwards towards Norfolk (Roberts *et al.*, In prep.). Amongst the sediment cores analysed and discussed in Chapter 4, cores 128VC (128) and 132VC (132) provided two new radiocarbon ages from the study area. These two cores are located within the UKHO Area 2 and 1 respectively (Fig. 5.5), and their sediments were correlated to the seafloor geomorphology and the seismic stratigraphy of the area (Fig. 5.1; see also Chapt. 4). In addition to these two cores, cores 118VC (118) and 137VC (137) are here included. They were collected during the JC123 oceanographic survey outside the study area, but provide two additional radiocarbon dates that can help to better contextualize the ice retreat chronology of the region.

As previously analysed in Chapter 4, the sedimentary imprint of the western North Sea comprises different lithofacies that were correlated to the acoustic facies identified in the area (Chapt. 4). Generally, it was observed that the regional stratigraphy of this sector of the North Sea is characterised by the presence of outcrops/subcrops of pre-Quaternary strata (AF 1), and by a patchy distribution of glacigenic diamictic facies (AF 2 and AF 3), overlain in places by a glaciomarine facies (AF 4), and by Holocene sediments (AF 5). The diamictic and glaciomarine sedimentary packages are laterally discontinuous, and are found repeatedly in the seismic sequence (see Chapt. 4). They are believed to be evidence for subglacial/sub-marginal to glaciomarine sediment deposition during the last glacial phase. The type of acoustic and sedimentary imprint observed in the study area can be correlated to the typical landform/sediment assemblage observed at the front of tidewater margins. This is defined by different subaquatic zones (ice contact, marginal, proximal and distal; Powell, 1984; Hart & Roberts, 1994) where the accumulation of distinct types of sediments takes place, depending on the relative proximity of the ice margin, and on the influence from meltwater plumes, icebergs, etc. (Fig. 5.6). In essence, the datasets suggest that during phases of ice advance, subglacial to sub-marginal sediments were deposited (AF 2 and AF 3), and are found at the base of the glaciomarine sequences (AF 4). As the ice retreated in the region, it stopped at the location of W1 and deposited the GZW, while proximal to more distal glaciomarine sediments were also deposited at the front of its margin (Fig. 5.6). Successively, the ice continued its retreat towards southern Scotland and the process was repeated with the deposition of glaciomarine sediments and the build up of the second GZW (W2; Fig. 5.1).

The two radiocarbon ages obtained from samples of mixed foraminifera assemblages collected within the glaciomarine muds from cores 132 and 128 (Fig. 5.7) are believed to

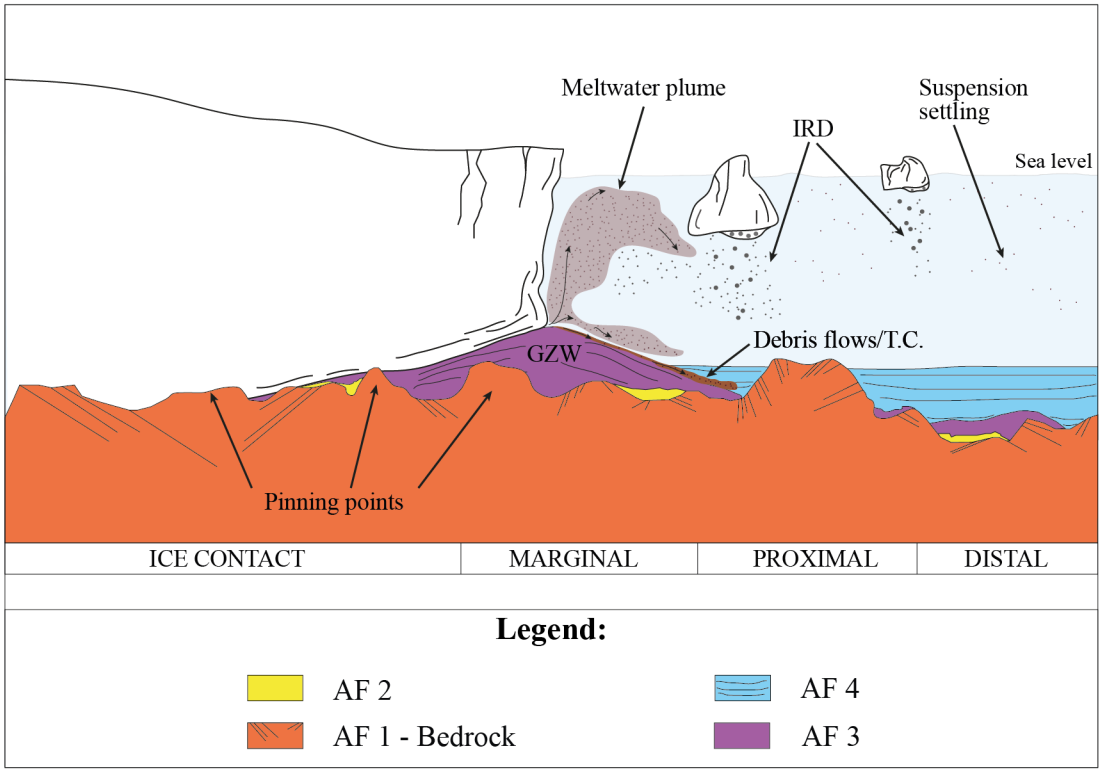

Figure 5.6: Schematic model of the NSL margin, which shows sub-marginal thickening and the formation of a grounding-zone wedge (GZW), and glaciomarine sedimentation at the margin front. These sediments are deposited through a combination of different processes. IRD: Ice Rafted Debris. T.C.: Turbidity currents. Adapted from Hart & Roberts (1994).

be minimum ages for ice retreat (see also Chapt. 4). The measured ages of 19.5 $\pm$ 0.17 cal. ka BP and 16.9 $\pm$ 0.22 cal. ka BP infer that, at that time, the ice margin was located to the north/north-west of the cores' location, given the established direction of the NSL overall retreat towards southern Scotland (Chapt. 4). Two additional dates were obtained from cores 137 and 118. Core 137 was collected at 80 m depth at a location $\sim$34 km east of the UKHO Area 1 and $\sim$95 km south-east of core 132 (Fig. 5.7). It is characterised by a thick layer of silt and silty/very fine sand that are interlaminated, and are overlain by a massive silty sand with abundant shells. One radiocarbon date was obtained from a mixed foraminifera assemblage sample taken at 552 - 555 cm depth in the core, with a resulted measured age of 19.9 $\pm$ 0.22 cal. ka BP (Fig. 5.7). Core 118 was collected further north, at 69 m depth, and is located $\sim$ 57 km north of core 128 and $\sim$39 km east of south-east Scotland (Fig. 5.7). The core is characterised at the bottom by a layer of medium sand with small pebbles and a gravelly layer, overlain by a thick layer of soft massive silty clay with occasional clasts, and by a massive sand with shell fragments at the top. Two radiocarbon ages were obtained from a sample at 240 - 242 cm depth in the core, within the silty clay facies, one from a shell of *Nuculana pernula*, and the other from a mixed foraminifera assemblage sample taken at the same depth interval. From the bivalve sample an age of 17.8 $\pm$ 0.17 cal. ka BP was measured, while an age of 16.6 $\pm$ 0.24 cal. ka BP was obtained from the foraminifera tests (Fig. 5.7). The samples taken for radiocarbon dating from both cores 118 and 137, were collected from the silty clay and

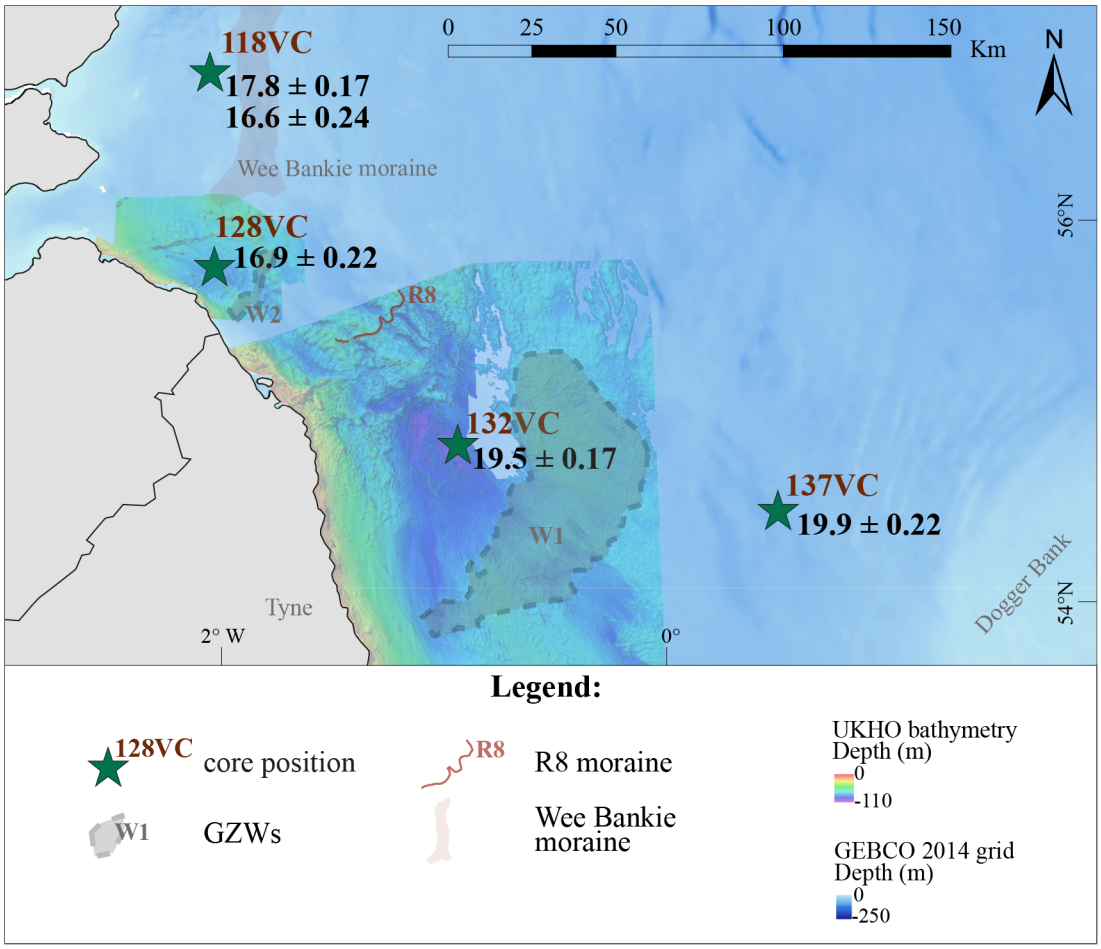

Figure 5.7: Location of cores 118, 128, 132 and 137. The measured radiocarbon ages (cal. ka BP) are shown in the map. Note the position of the cores in respect to the two GZWs and the moraine R8 (Chapt. 4). The location of the Wee Bankie moraine (Clark *et al.*, 2004a) is also indicated.

silt sediments, interpreted as glaciomarine, which are thought to have deposited in ice distal conditions. All the ages presented here are thus considered minimum ages for ice retreat at the cores location, and the start of the deglaciation phase could have been even earlier. It also to be noted, that the ages were all calibrated using a ΔR of 0, as previously discussed in Chapter 4, therefore they could be slightly different if a ΔR of 300 or 700 is applied (see Table 4.2, in Chapt. 4).

Considering all the ages obtained from the North Sea, the timing of ice retreat from the basin can be tentatively better constrained and can be correlated with the onshore chronology (Fig. 5.5). The dates measured from the northernmost offshore cores (118 and 128) of 17.8 ± 0.17 cal. ka BP and 16.6 ± 0.24 cal. ka BP, and 16.9 ± 0.22 cal. ka BP, appear to correlate well with each other and, most importantly, they also seem in accordance with the onshore retreat ages of south-east Scotland, indicated in Figure 5.5. They are thus in agreement with previous reconstructions of ice retreat and suggest that the ice margin was located relatively close to the Scottish coast by ∼17.1 cal. ka BP. Core 118 is also located immediately to the west of the Wee Bankie Moraine (Fig. 5.7), which is a morainal system interpreted to be evidence of an ice re-advance, and to have been deposited approximately between 18 - 24 ka BP (Bradwell

et al., 2008b). The ages recorded from core 118 are thus also in accordance with the proposed age of the Wee Bankie moraine, as they are younger and they are found further along the ice retreat direction.

The other two cores (132 and 137) located further south contain very similar radiocarbon ages, of 19.5 $\pm$ 0.17 cal. ka BP and 19.9 $\pm$ 0.22 cal. ka BP (Fig. 5.7), respectively. The fact that the oldest age was recorded in the southernmost core is in line with the previous interpretations, suggesting that ice retreated towards the north-west. However, these two ages are much older than the surrounding onshore chronology (Fig. 5.5). It is known that the NSL was characterised by an oscillatory behaviour and underwent different advance phases that resulted in the deposition of the Skipsea and later the Withernsea Tills, approximately around 16.8 ka (Bateman *et al.*, 2017). Despite this, the offshore dates are minimum ages for ice retreat and thus suggest that the ice was already retreating by that early time. An ice re-advance that overrode the two core locations and the dated glaciomarine sediments could be a possible scenario to explain this age discrepancy between offshore and onshore sectors, although no evidence for an ice re-advance from the sediments of cores 132 and 137 was observed. The glaciomarine facies are generally overlain by massive sands characterised by the presence of numerous shells and shell fragments. Only in core 132, a thin layer (26 cm) of diamictic sediments was observed (LF 1a, Chapt. 4) lying on top of the glaciomarine sediments from which the radiocarbon age was measured. Nevertheless, due to its small thickness and to the fact that the layer is then overlain by massive muds interpreted to be glaciomarine sediments deposited in more distal conditions, it was suggested that this diamictic facies was possibly an iceberg dump deposit. It is thus not considered to be evidence of an ice re-advance in the area (Chapt. 4). Consequently, the 19.5 cal. ka BP age is thought to represent a minimum age for final ice retreat in this sector of the western North Sea (Chapt. 4). Despite the fact that recent modelling reconstructions from Patton *et al.* (2016, 2017) do not envisage an ice re-advance in the western North Sea at a late stage, the reconstructions based on empirical observations proposed by Hughes *et al.* (2016), depict that the NSL re-advanced down the English coastline around 17 ka. In addition, there are numerous onshore evidence for such a late re-advance along the eastern coast of England (Evans & Thomson, 2010; Davies *et al.*, 2011; Bateman *et al.*, 2011, 2015, 2017; Roberts *et al.*, 2013; Livingstone *et al.*, 2015; Evans *et al.*, 2017), and the new offshore dates are also out of phase with the dates obtained from the Tyne Gap region (Livingstone *et al.*, 2015, Fig. 5.5, see also Chapt. 2). Nevertheless, the ages presented in this study from the western North Sea region all point to an earlier retreat of the NSL towards south-eastern Scotland than previously thought and they are in conflict with reconstructions from coastal regions of eastern England, as previously discussed. The NSL could have differentially retreated in order to explain these age discrepancies, but considering the geomorphological imprint left on the seafloor and the presence and morphology of both W1 and W2, that would seem unlikely. Therefore, this study highlights the need to secure more dates particularly from the offshore region to better constrain the NSL retreat. Despite these considerations, by compiling all the dates shown in Figure 5.5, it can be inferred that the NSL was active in a time window constrained between $\sim$22 and $\sim$16 ka BP.

5.3 Drivers for deglaciation

Different factors are thought to have forced the onset of deglaciation of the last BIIS. Changes in the Earth's orbital parameters and increasing levels of solar insolation in the northern hemisphere are thought to be the primary drivers for the deglaciation period, although other factors, such as sea-level rise, changes in the atmospheric CO_2 concentrations, and internal changes in ice sheet mass balance and configuration are believed to play a big role as amplifying processes (Alley *et al.*, 2005; Clark *et al.*, 2012). The last BIIS was a partially marine terminating ice sheet, known to have extended in the North Sea and up to the shelf break in the north, where it met the North Atlantic and deposited numerous trough mouth fans (Graham *et al.*, 2007, 2011; Bradwell *et al.*, 2008b; Clark *et al.*, 2012; Finlayson *et al.*, 2014; Bradwell & Stoker, 2015a; Sejrup *et al.*, 2016; Patton *et al.*, 2017). The southern North Sea, in contrast, is thought to have been dry land at the time (Peltier *et al.*, 2002; Ward *et al.*, 2006; Sejrup *et al.*, 2016; Roberts *et al.*, In prep.), and characterised by a vast ice-damned lake in the Dogger Bank region, which developed south of the ice margin in response to the coalescence of the BIIS and SIS ice sheets (Fig. 2.5; Sejrup *et al.*, 2016; Roberts *et al.*, In prep.; Patton *et al.*, 2017). This convergence is thought to have favoured the formation of such a large lake in the southern North Sea region, as the two ice sheets would have acted as a barrier to meltwater and to the river discharges of the Thames and the rivers originated from mainland Europe, and prevented their escape towards the north (Toucanne *et al.*, 2010; Clark *et al.*, 2012).

Marine-terminating ice sectors are known to be sensitive to sea-level changes. An increase in sea-level can lead to calving events and consequent ice loss, as can be observed today in marine-terminating sectors of contemporary ice sheets (Bradwell *et al.*, 2008b; Clark *et al.*, 2012). Considering that the northern margins of both BIIS and SIS in the North Sea were marine and influenced by the Atlantic waters, and that calving events are known to be the main cause of mass loss in contemporary ice sheets, it can be assumed that both palaeo-ice sheets were affected by the same processes (Bradwell *et al.*, 2008b; Clark *et al.*, 2012). The presence of Mega-Scale Glacial Lineations (MSGLs) in the Witch Ground Basin area (northern North Sea) and of numerous subglacial landforms observed offshore north-west and northern Scotland, as well as in the eastern North Sea, infers that ice was grounded in this region (Ottesen *et al.*, 2005; Graham *et al.*, 2007; Bradwell & Stoker, 2015a,b; Sejrup *et al.*, 2015, 2016). Both the BIIS and SIS are believed to have been grounded at some point in the North Sea and to have caused depression of the crust due to their glacio-isostatic load (Peltier *et al.*, 2002; Ward *et al.*, 2006; Bradwell *et al.*, 2008b). This lowering in the northern North Sea areas might have induced an increase in relative sea-level, possibly leading to calving events (Clark *et al.*, 2004c; Bradwell *et al.*, 2008b; Clark *et al.*, 2012). A similar situation has been proposed for the Irish Sea, where a sea-level rise, induced in response to isostatic loading, is believed to have caused initial deglaciation (Clark *et al.*, 2004c; Bradwell *et al.*, 2008b). Deglaciation of the North Sea may have thus started in the northern part of the basin, with calving events that led to ice instability. Sejrup *et al.* (2016) suggest that the Norwegian Channel Ice Stream (NCIS; see Fig. 2.5 in Chapt. 2), increased its velocity between 20 and 19 ka, with flow acceleration and calving triggering rapid retreat and ice loss (Bradwell *et al.*, 2008b; Sejrup *et al.*, 2016). The NCIS

is thought to have successively back-stepped towards southern Norway, as recorded by the presence of grounding zone wedges and moraines on the seafloor in the eastern North Sea, thus allowing the marine inundation of the newly ice-free area (see Fig. 2.5 in Chapt. 2; Bradwell *et al.*, 2008b; Sejrup *et al.*, 2016; Morén *et al.*, 2017). New evidence from Morén *et al.* (2017) suggests that the grounding line of the NCIS started to retreat from the continental shelf edge at ∼19 ka and that the Norwegian channel was fully deglaciated by ∼17.5 ka. The uncoupling of the BIIS and SIS, with the debuttressing and recession of the NCIS and inundation of the northern North Sea, are believed to have triggered marginal instability of both ice sheets and ice flow reorganization. This affected the former eastern margin of the BIIS, which had become unconstrained and experienced re-advances (Fig. 2.5; Sejrup *et al.*, 2016). The lack of lateral constraint to the east is believed to have caused reorganization of the Forth, Tweed, TGIS and Stainmore ice streams flow, which eventually resulted in the final imposition and advance of the NSL towards the south. The NSL is known to have re-advanced, reaching the south-eastern coasts of England, while possibly thinning and accelerating (Hubbard *et al.*, 2009; Bateman *et al.*, 2015). This could have been further intensified due to enhanced basal sliding over deformable pre-existing sediments at its base, which lowered the ice marginal profile (Busfield *et al.*, 2015; Bateman *et al.*, 2015).

Sea-level reconstructions for the North Sea basin also suggest that marine waters inundated the northern part of the North Sea first, and only reached the southern North Sea at the beginning of the Holocene (Peltier *et al.*, 2002; Shennan *et al.*, 2006; Bradley *et al.*, 2011; Sturt *et al.*, 2013; Roberts *et al.*, In prep.; Ward *et al.*, 2016; Patton *et al.*, 2017). Recent reconstructions from Bradley *et al.* (2011) indicate that at ∼9 ka, sea-level offshore north-east England was approximately -16 meters lower than the present-day coastline (Fig. 5.8). Consequently, despite the fact that marine transgression in the Dogger Bank area and in the southern North Sea happened at a later stage, it is known that it happened earlier in the study area and that the NSL retreated in a marine environment. This is further confirmed by the glaciomarine sediments and marine microfauna found in all vibro-cores analysed in this study (see Chapt. 4). The foraminifera assemblages observed in the cores, with abundances of *Elphidium excavatum (clavatum)* and *Cassidulina reniforme*, are known indicators of extreme glacial marine environments (Feyling-Hanssen, 1972; Hansen & Knudsen, 1995; Peters *et al.*, 2015). In addition, abundances of other Elphidium species, and of *Elphidium excavatum* and *Haynesina orbiculare* (see Chapt. 2), together with the presence of IRD layers and dropstones in the cores, further indicate deposition in a cold marine environment (McCabe *et al.*, 1986; Knudsen & Sejrup, 1993). It is believed that the opening of a marine embayment in the northern areas of the North Sea, eventually expanded to reach the NSL margin and prompted successive instability and calving, leading to further retreat of the ice lobe. The new radiocarbon ages presented in this study record glaciomarine deposition already by ∼19.9 cal. ka BP to the north of the Dogger Bank region and by ∼19.5 cal. ka BP to the north of the GZW W1 (see Fig. 5.7), thus suggesting that marine inundation reached this region earlier than previously thought.

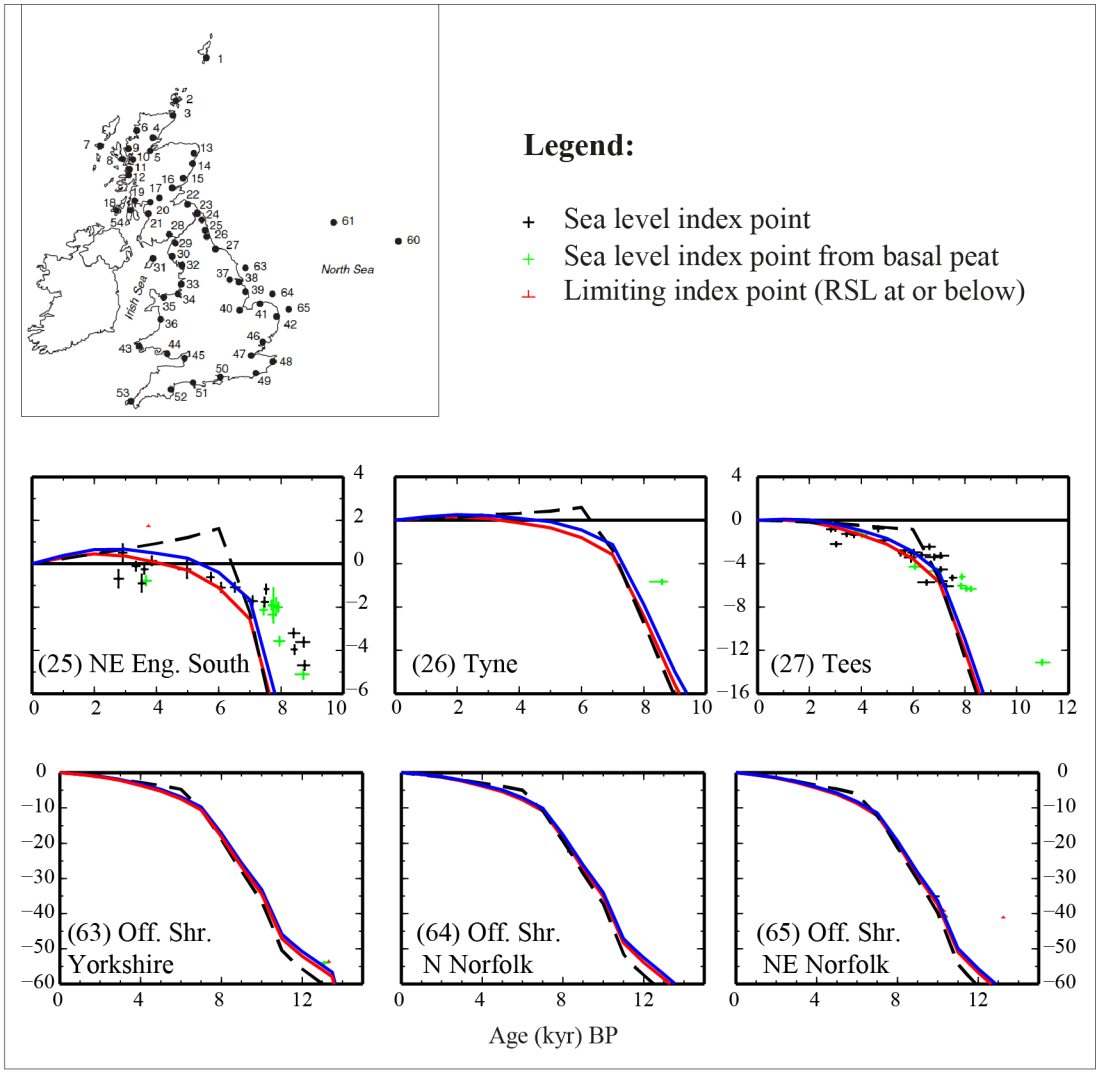

Figure 5.8: Comparison of predicted and observed sea-level at different locations across the study region. From Bradley *et al.* (2011). Predictions based on the optimum earth model inferred in Bradley et al. (2009) - lithosphere thickness 71 km, upper mantle viscosity 0.5×10^{21} Pa s, lower mantle viscosity 3×10^{22} Pa s - are shown for the Brooks et al./Bassett et al. ice model (dashed black line) and the new ice model presented in this analysis (black line). The solid grey line is for the new ice model and an earth model that is identified from χ^2 results. This earth model is identical to the one inferred in Bradley et al. (2009), except that the viscosity in the lower mantle is higher, at 6×10^{22} Pa s.

5.4 Reconstruction of the final phases of the NSL

The evidence and information provided so far in this research permit us to constrain and reconstruct the NSL advance and retreat behaviour in more detail than ever before. After the collapse and retreat of the NCIS, the NSL re-advanced towards south-east England (Fig. 2.5; Sejrup *et al.*, 2016). Given the timings of the NCIS retreat, it is believed that such a re-advance took place without the presence of an ice mass acting as a barrier on the eastern side of the NSL (see also Fig. 2.5 in Chapt. 2). Recent reconstructions from the southern North Sea region, off the coasts of Holderness and Norfolk, provide evidence for an oscillating

ice margin, characterized by different advance and retreat phases, before final retreat towards the north (Dove *et al.*, 2017; Roberts *et al.*, In prep.). Dove *et al.* (2017) recognized distinct, arcuate till wedges and associated moraines on the seafloor in the southern North Sea (see Fig. 2.8, in Chapt. 2), which were interpreted as sub-marginal till wedges formed through complex accretionary processes during at least four major stillstand phases of the NSL, before the ice stream retreated towards Scotland. This evidence from the southern North Sea region for an episodic style of retreat of the NSL is in line with the reconstructions of the NSL retreat from the study area further north. In addition, despite the fact that marine inundation is thought to have reached the southern North Sea at a later stage, and that the NSL imprint recognised by Dove *et al.* (2017) offshore Holderness suggests a terrestrial piedmont lobe, the data presented in this study suggest that in the western North Sea, ice retreated in a marine environment and that the NSL retreat phase was characterised by two or more phases of stillstand in the region.

Figure 5.9 shows a 3D schematic model which reconstructs the last phases of activity of the NSL in the western North Sea. In Figure 5.9a the ice margin is located at the position of the southernmost grounding-zone wedge of the study area, W1 (see also Fig. 5.1). This phase reconstructs a first episode of stillstand during ice retreat, possibly triggered by the presence of pinning points (bedrock subcrops), that allowed the ice to experience temporary stability. This resulted in the build up of W1, through subglacial sediment delivery and sub-marginal till thickening at the ice margin (Boulton, 1996a,b; Evans & Hiemstra, 2005). While the ice stream was stable at this location, subglacial to sub-marginal sediments (AF 3, in violet in Fig. 5.9) were deposited at the grounding zone, while glaciomarine sediments were deposited at the front of the ice margin (AF 4, in blue in Fig. 5.9), through different sedimentary processes (see Fig. 5.6), and are found draping conformably AF 3 along the seismic profiles. As previously discussed in Chapter 4, the fact that AF 2 is often found as a patchy deposit underneath AF 3 (Fig. 5.9a) could indicate that this subglacial facies was deposited (1) during an earlier glaciation, (2) by the action of the TGIS ice stream that extended offshore or (3) during an initial advance phase of the NSL, which was successively eroded and overprinted by AF 3. After this first phase of stillstand, the ice retreated further back towards the north-west uncovering W1 at the seafloor (Fig. 5.9b), while glaciomarine sedimentation (proximal to distal) continued in front of its margin.

In Figure 5.9c the ice margin is located further back, closer to southern Scotland and is experiencing another phase of stability during overall retreat, possibly triggered once again by the presence of numerous bedrock highs in the area, and which resulted in the build up of the second grounding-zone wedge, W2. To the south of the ice margin, additional landforms such as the bedrock-cored lineations and the moraine R8 are exposed on the seabed. The deposition of R8, which is found between W1 and W2 (see also Fig. 5.1), is believed to represent an ice re-advance or an additional phase of stillstand during overall retreat. This is also suggested due to the presence along the seismic lines of a wedge-like feature, characterised internally by AF 3, found in the vicinity of R8 (Chapt. 4). It is worth mentioning though that this feature was not observed on the bathymetry datasets. The last model shown in Figure 5.9d shows W2 exposed at the seabed and the imprint left in the western North Sea by the passage of the NSL and after its final retreat towards south-east Scotland, which was then followed by the

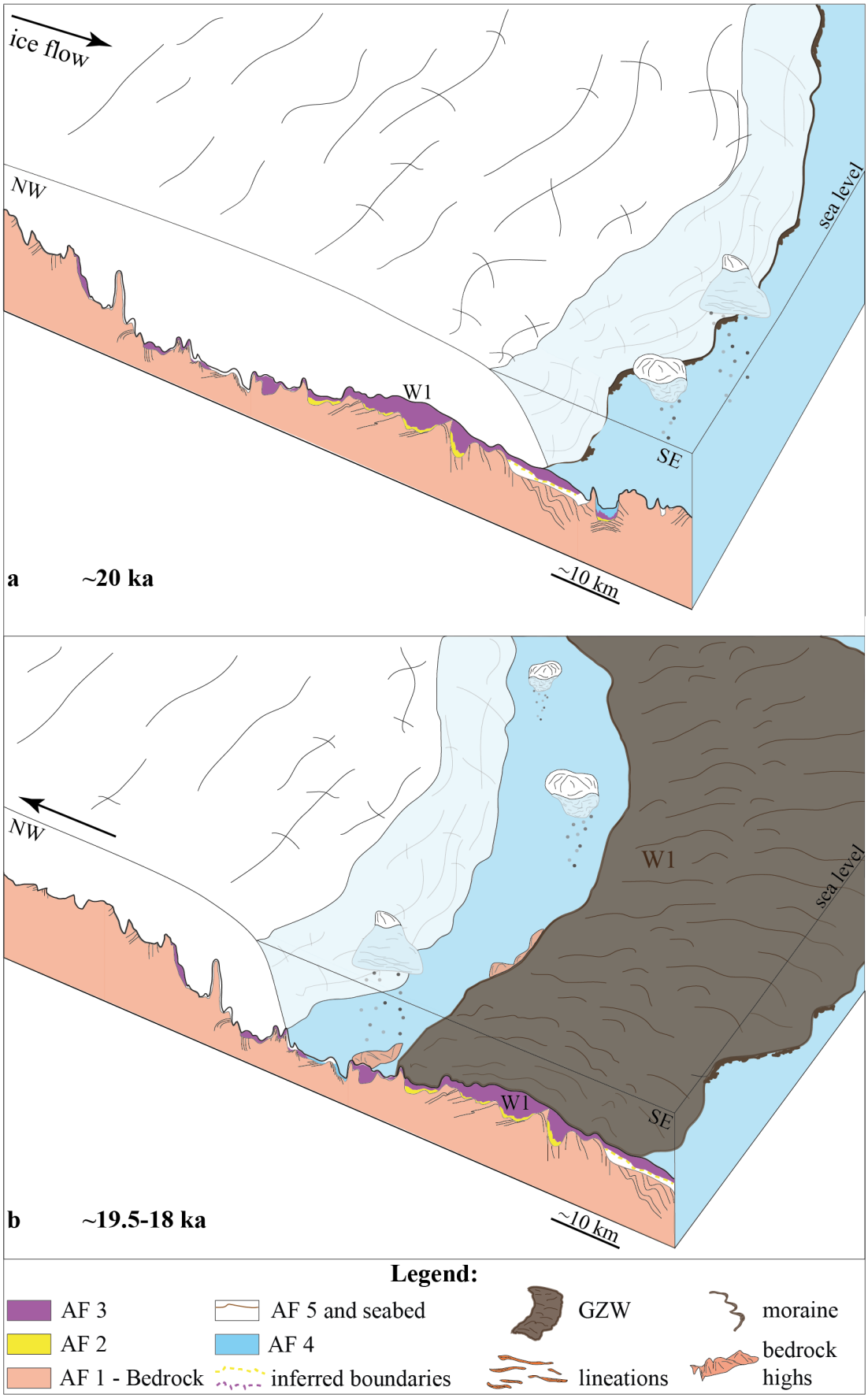

Figure 5.9: 3D schematic models reconstructing the last phases of the NSL ice stream. a: first stillstand during NSL retreat, with the build up of W1. b: ice retreats towards the north-west and glaciomarine sediments are deposited on top of AF 3.

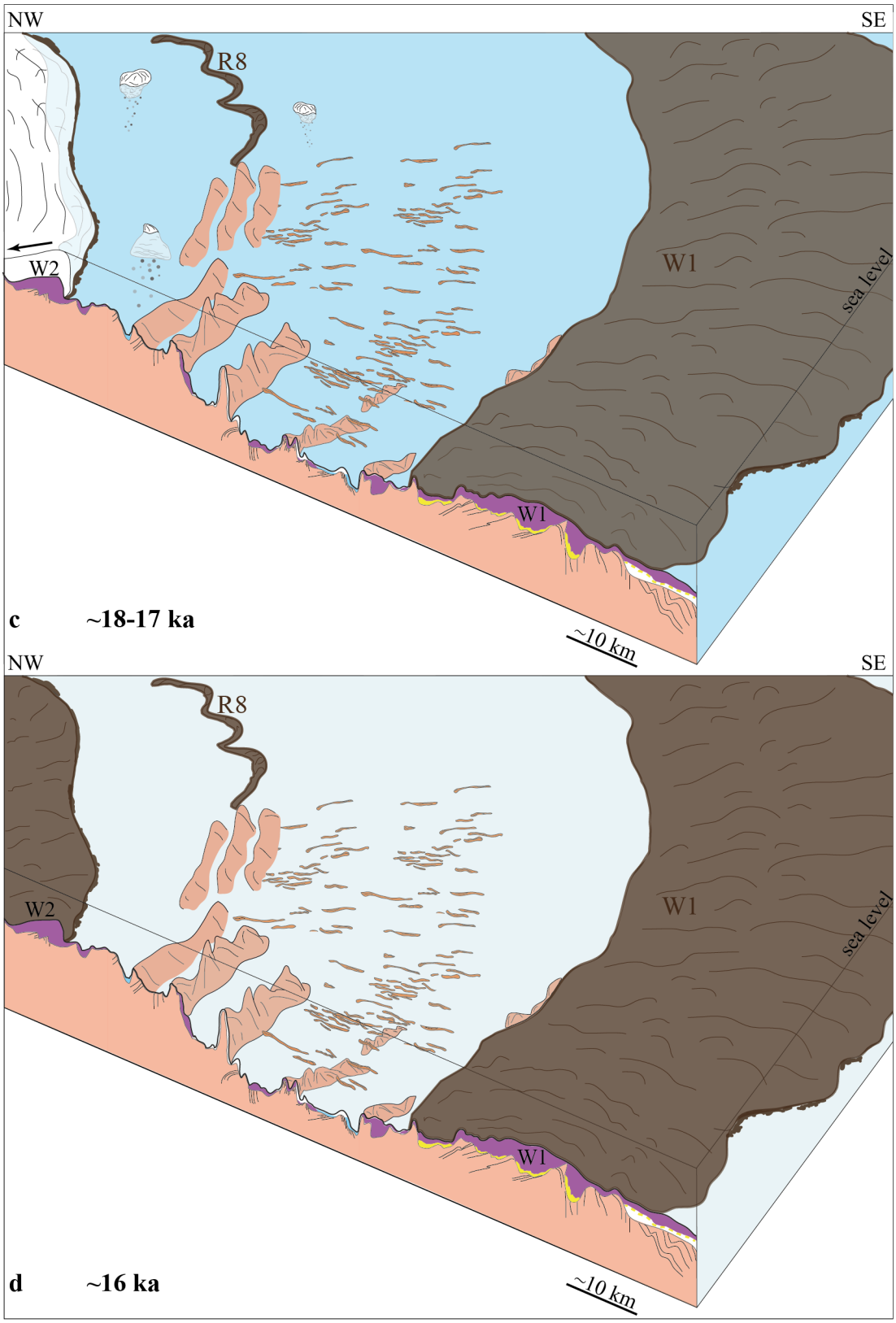

Figure 5.9 (cont.): c: numerous subglacial landforms are uncovered after the ice retreats further and stops for a second time to deposit W2. Glaciomarine sediments are deposited on top of AF 3. d: ice retreats towards southern Scotland and its imprint is uncovered on the seafloor.

deposition of post-glacial to Holocene sediments (AF 5, see Chapt. 4).

Overall, the landforms found today on the seafloor of the western North Sea represent a mixed-bed landsystem and are evidence of the passage of a grounded ice lobe whose retreat phase was characterised by an oscillatory behaviour and by episodes of ice stability in a glaciomarine environment.

Chapter 6

Conclusions

This study investigated the landforms, acoustic facies and lithofacies in two different areas of the western North Sea (the Blyth survey and the Britice-Chrono survey) in order to reconstruct the glacial imprint left by the BIIS, and particularly by the NSL, in the region and to assess the dynamics and the timings of ice retreat. The analyses of different bathymetric, seismic and sedimentary datasets provided an assessment of the Quaternary acoustic and sedimentary imprint characterising the study area, and added information to previous mapping from the BGS and other research. The new key findings and main conclusions of this work are as follows:

- Analyses of both the Blyth and Britice-Chrono surveys highlighted the importance of bedrock strata on the North Sea floor. From both study areas it was observed how bedrock strata generally outcrop close to the coast and are otherwise present at a relatively shallow depth below the seabed moving towards the east. The presence of bedrock at or so close to the seafloor is thought to have favoured the formations of the two GZWs observed on the bathymetry data. Bedrock strata are indeed thought to have provided pinning points, permitting periods of ice stillstands during overall retreat. Both W1 and W2 are located in areas characterised by bedrock highs and were laid down between bedrock ridges that often come up to the surface. The presence of these wedges on the seafloor indicates that retreat was not rapid and was interrupted by periods of temporary stability.
- Bedrock strata are also thought to have influenced the formation of the bedrock-cored lineations observed on the seafloor in the central part of the research area. These lineations are discontinuous and have lengths that vary from a few hundred meters up to a few kilometres. They are thought be mainly erosional, due to the fact that they are generally characterised by bedrock cores, and to have formed in response to basal abrasion and plucking, together with subglacial sediment deposition. Considering that hard-bed streamlining is believed to form over a longer time frame, when compared to the streamlining characterised internally by soft sediments, and requires more energy to be eroded, these bedforms suggest that their formation probably happened during different glacial phases (and thus not just during the most recent one). In addition, the fact that the bedrock strata are characterised by bedding planes that are faulted and folded and often dip at a relatively high angle, could have played an important role in the final

geometries of the lineations.

- Different acoustic facies were recognised from the analyses of the seismic datasets from both the Blyth and the Britice-Chrono surveys. Six acoustic facies were recognised in the Blyth survey (BL-AF 1 - 6): BL-AF 1, BL-AF 2 and BL-AF 3 are believed to be composed of bedrock strata of Carboniferous, Permian and Triassic age, respectively. This corresponds to what was previously mapped in the area by the BGS. BL-AF 4 and BL-AF 5 display very similar internal characteristics to one another and have been interpreted to be composed of glacigenic diamicts (and possibly tills). In particular, BL-AF 4 is thought to be the correlative of the Wee Bankie Formation, a Late Devensian diamictic facies mapped extensively in the area and interpreted to have been deposited by the NSL. This would imply that BL-AF 4 is also the correlative of the Horden Till, found onshore on the eastern coasts of County Durham. BL-AF 5 was initially thought to be the correlative of the St. Abbs Formation, a glaciomarine facies which was previously mapped in the area by the BGS. Although, considering the facies acoustic character, this interpretation was discarded, and BL-AF 5 is also inferred to have deposited by the action of the NSL, during a later phase. BL-AF 6 (divided into 6a and 6b) is believed to correlate to the Forth Formation (6b) previously mapped by the BGS in the area, and to be composed of Holocene sediments at the top (6a). Despite the fact that sedimentary information is not yet available for this area and is needed to better define the facies observed, the analysis of these new seismic profiles provides additional detail in the stratigraphic architecture of the region and adds to what was previously mapped by the BGS.

  Five acoustic facies were recognised in the Britice-Chrono survey (AF 1 - 5): AF 1 is interpreted to be composed of pre-Quaternary deposits, and specifically of bedrock strata of Carboniferous, Permian, Triassic, Jurassic and Cretaceous age. AF 2 and AF 3 are characterised by internal transparency and are interpreted to be composed of subglacial to sub-marginal till sediments. These two facies are believed to (1) either have been both deposited by the NSL during an initial advance phase (AF 2), which was successively eroded and overprinted by a re-advance phase (AF 3). Or (2), AF 2 could have been deposited by the TGIS (and be the offshore correlative of the Blackhall Till onshore), and could have been later overprinted by the final advance of the NSL (AF 3). AF 4 is interpreted to be composed of glaciomarine sediments and AF 5 of post-glacial to Holocene sediments. The recognition of these acoustic facies in the Britice-Chrono survey also adds detail to previous mapping by the BGS in the area.

- Different landforms were observed on the seafloor in the research area, which together constitute a distinct geomorphological imprint. In addition to the bedrock ridges, the GZWs and the bedrock-cored lineations already mentioned, different meltwater channels and a moraine ridge were found on the bathymetry data analysed from the Britice-Chrono survey. The GZWs and the moraine ridge (R8) are all orientated perpendicularly to the bedrock-cored lineations, thus indicating that the ice flow was coming mainly from north-west, as GZWs are known to develop perpendicular to the direction of ice flow. The meltwater channels are instead orientated transverse to R8. Overall, the glacial imprint

found on the seafloor infers that the former ice flow was directed NW - SE and is evidence for the action of the NSL, which was fed by the Forth ice stream and was flowing out of south-east Scotland, extending offshore, turning southwards and impinging the eastern coast of England. This is also in accordance with what can be seen onshore in eastern England (orientation of subglacial lineations in the Tweed valley and along the coastline). Ice retreat was directed towards south-east Scotland, as clearly marked by the positions of W1 and W2. It is important to note that despite the numerous amount of landforms observed on the Britice-Chrono bathymetry data, no glacial landforms were observed on the Blyth survey area, where the seabed appears very flat and is only characterised by the presence of numerous bedrock outcrops close to the coast. It is believed that any evidence for ice flow in the area could have been later overprinted during the deglacial phase and the Holocene.

- No evidence was found on the bathymetry datasets for ice flow directed W - E and thus related to the action of the TGIS. As can be seen from the onshore areas in the Tyne Gap region, evidence for ice flow directed towards the east seems to cease before reaching the coast and is thought to be overprinted by ice coming from the north. It is believed that a similar scenario can be seen offshore, where all recognised landforms point to an ice flow directed NW - SE. The only possible evidence for TGIS activity is represented by the acoustic facies BL-AF 4 from the Blyth survey area (although the interpretation of this facies as deposited by the action of the NSL is favoured) and by AF 2 from the Britice-Chrono survey as previously mentioned.

- The sediments recovered in the Britice-Chrono area provide new information on the sedimentary imprint left on the seabed and on the paleoenvironments that characterised the retreat of the NSL. Different lithofacies (LF) were recognised: LF 1 is composed of relatively soft, massive, matrix-supported diamictons, characterised by the apparent absence of planar structures, and is believed to record the transition from subglacial to glaciomarine depositions. This is also because the facies correlates to the boundary between acoustic facies AF 3 and AF 4. LF 2 is composed of fine, soft and laminated silts and clays, that display strong laminations and abundance of clasts at the bottom (LF 2b), and thinner laminae and fewer clasts towards the top (LF 2a). The facies correlates to AF 4 and has been interpreted to be composed of proximal to distal glaciomarine sediments. This is confirmed by the presence of abundances of cold temperature foraminifera species, that are known to be indicators of extreme glacial marine environments and are also found in modern glaciomarine settings. LF 3 is composed by massive sand (LF 3a) and gravel (LF 3b). Both LF 2 and LF 3 are believed to record deposition by suspension settling from meltwater plumes, iceberg rafting, and possibly turbidity currents, and to be evidence of a retreating ice margin. LF 4 found at the top of the cores is characterised by massive sands with abundant shells and has been interpreted to be composed of Holocene sediments. Overall, the evidence provided in this research indicates that the ice retreated from the region in a glaciomarine environment.

- New ages measured from the glaciomarine facies in the study area provide new

information for ice retreat in the western North Sea. These ages record that the NSL was retreating from the central part of the study area around 19.5 $\pm$ 0.17 cal. ka BP, and that by 16.9 $\pm$ 0.22 cal. ka BP the ice had retreated north-west of core 128, located in the northern part of the study area and closer to southern-Scotland. These new ages record that the deglaciation of the NSL started much earlier than previously thought and are not in accordance to the ages recorded from previous studies onshore eastern England. In addition, it is believed that marine waters inundated the North Sea basin after the unzipping of the BIIS and SIS ice sheets in the northern area of the basin and reached the research area earlier than the southern North Sea. The NSL is thus thought to have been a marine-terminating ice lobe during retreat in the study region.

This research thus presents new information on the last phases of activity of the NSL and contributes to advances in the knowledge of the glacial geology and geomorphology of the western North Sea. Despite this, it is believed that additional information on the timings of the deglacial phase is needed and can be an asset to better constrain the last phases of the NSL. The collection of supplementary radiocarbon dates from the western North Sea can help to better constrain the chronology of ice retreat and can result in a greater picture of the last phase of activity of this ice lobe. Furthermore, this study demonstrates how improved and high resolution marine datasets can provide an added level of detail and are an asset to better recognise and interpret past ice sheets dynamic and behaviour.

Bibliography

Alley, R. B., Clark, P. U., Huybrechts, P., & Joughin, I. 2005. Ice-Sheet and Sea-Level Changes. *Science*, **310**(5747), 456–460.

Alley, R. B., Andrews, J. T., Brigham-Grette, J., Clarke, G. K. C., Cuffey, K. M., Fitzpatrick, J. J., Funder, S., Marshall, S. J., Miller, G. H., Mitrovica, J. X., *et al.* 2010. History of the Greenland Ice Sheet: paleoclimatic insights. *Quaternary Science Reviews*, **29**(15), 1728–1756.

Artemieva, I. M., & Thybo, H. 2013. EUNAseis: A seismic model for the Moho and crustal structure in Europe, Greenland, ande the North Atlantic region. *Tectonophysics*, **609**, 97–153.

Ballantyne, C. K. 2010. Extent and deglacial chronology of the last British–Irish Ice Sheet: implications of exposure dating using cosmogenic isotopes. *Journal of Quaternary Science*, **25**(4), 515–534.

Batchelor, C. L, & Dowdeswell, J. A. 2015. Ice-sheet grounding-zone wedges (GZWs) on high-latitude continental margins. *Marine Geology*, **363**, 65–92.

Bateman, M. D., & Catt, J. A. 1996. An absolute chronology for the raised beach and associated deposits at Sewerby, East Yorkshire, England. *Journal of Quaternary Science*, **11**(5), 389–395.

Bateman, M. D., Buckland, P. C., Chase, B., Frederick, C. D., & Gaunt, G. D. 2008. The Late-Devensian proglacial Lake Humber: new evidence from littoral deposits at Ferrybridge, Yorkshire, England. *Boreas*, **37**(2), 195–210.

Bateman, M. D., Buckland, P. C., Whyte, M. A., Ashurst, R. A., Boulter, C., & Panagiotakopulu, E. 2011. Re-evaluation of the Last Glacial Maximum typesite at Dimlington, UK. *Boreas*, **40**(4), 573–584.

Bateman, M. D., Evans, D. J. A., Buckland, P. C., Connell, E. R., Friend, R. J., Hartmann, D., Moxon, H., Fairburn, W. A., Panagiotakopulu, E., & Ashurst, R. A. 2015. Last glacial dynamics of the Vale of York and North Sea lobes of the British and Irish Ice Sheet. *Proceedings of the Geologists' Association*, **126**(6), 712–730.

Bateman, M. D., Evans, D. J. A., Roberts, D. H., Medialdea, A., Ely, J., & Clark, C. D. 2017. The timing and consequences of the blockage of the Humber Gap by the last British- Irish Ice Sheet. *Boreas*.

Beets, D.J., Meijer, T., Beets, C.J., Cleveringa, P., Laban, C., & Van der Spek, A.J.F. 2005. Evidence for a Middle Pleistocene glaciation of MIS 8 age in the southern North Sea. *Quaternary International*, **133**, 7–19.

Benn, D. I., & Evans, D. J. A. 2010. Glaciers and Glaciation. *Hodder Education, London*.

Benton, M. J., Cook, E., & Turner, P. 2002. *Permian and Triassic red beds and the Penarth Group of Great Britain*. Vol. 24. Joint Nature Conservation Committee.

Boston, C. M., Evans, D. J. A., & Ó Cofaigh, C. 2010. Styles of till deposition at the margin of the Last Glacial Maximum North Sea lobe of the BritisheIrish Ice Sheet: an assessment based on geochemical properties of glacigenic deposits in eastern England. *Quaternary Science Reviews*, **29**, 3184–3211.

Boulton, G., & Hagdorn, M. 2006. Glaciology of the British Isles Ice Sheet during the last glacial cycle: form, flow, streams and lobes. *Quaternary Science Reviews*, **25**, 3359–3390.

Boulton, G. S. 1990. Sedimentary and sea level changes during glacial cycles and their control on glacimarine facies architecture. *Geological Society, London, Special Publications*, **53**(1), 15–52.

Boulton, G. S. 1996a. The origin of till sequences by subglacial sediment deformation beneath mid-latitude ice sheets. *Annals of Glaciology*, **22**(1), 75–84.

Boulton, G. S. 1996b. Theory of glacial erosion, transport and deposition as a consequence of subglacial sediment deformation. *Journal of Glaciology*, **42**(140), 43–62.

Bradley, S. L., Milne, G. A., Shennan, I., & Edwards, R. 2011. An improved glacial isostatic adjustment model for the British Isles. *Journal of Quaternary Science*, **26**(5), 541–552.

Bradwell, T., & Stoker, M. S. 2015a. Asymmetric ice-sheet retreat pattern around northern Scotland revealed by marine geophysical surveys. *Earth and Environmental Science Transactions of the Royal Society of Edinburgh*, **105**(04), 297–322.

Bradwell, T., & Stoker, M. S. 2015b. Submarine sediment and landform record of a palaeo-ice stream within the British- Irish Ice Sheet. *Boreas*, **44**(2), 255–276.

Bradwell, T., Stoker, M., & Larter, R. 2007. Geomorphological signature and flow dynamics of The Minch palaeo-ice stream, northwest Scotland. *Journal of Quaternary Science*, **22**(6), 609–617.

Bradwell, T., Stoker, M., & Krabbendam, M. 2008a. Megagrooves and streamlined bedrock in NW Scotland: the role of ice streams in landscape evolution. *Geomorphology*, **97**(1), 135–156.

Bradwell, T., Stoker, M. S., Golledge, N. R., Wilson, C. K., Merritt, J. W., Long, D., Everest, J. D., Hestvik, O. B., Stevenson, A. G., Hubbard, A. L., Finlayson, A. G., & Mathers, H. E. 2008b. The northern sector of the last British Ice Sheet: Maximum extent and demise. *Earth-Science Reviews*, **88**, 207–226.

Bridgland, D. R., Howard, A. J., White, M. J., White, T. S., & Westaway, R. 2015. New insight into the Quaternary evolution of the River Trent, UK. *Proceedings of the Geologists Association.*, **126**(4-5), 466–479.

Busfield, M. E., Lee, J. R., Riding, J. B., Zalasiewicz, J., & Lee, S. V. 2015. Pleistocene till provenance in east Yorkshire: reconstructing ice flow of the British North Sea Lobe. *Proceedings of the Geologists' Association*, **126**(1), 86–99.

Cameron, T. D. J., Crosby, A., Balson, P. S., Jeffrey, D. H., Lott, G. K., Bulat, J., & Harrison, D. J. 1992. *United Kingdom offshore regional report: the geology of the southern North Sea*. London: HMSO for the British Geological Survey.

Carr, S. J., Holmes, R., Van Der Meer, J. J. M., & Rose, J. 2006. The Last Glacial Maximum in the North Sea Basin: micromorphological evidence of extensive glaciation. *Journal of Quaternary Science*, **21(2)**, 131–153.

Catt, J. A. 2007. The Pleistocene glaciations of eastern Yorkshire: a review. *Proceedings of the Yorkshire Geological Society*, **56**, 177–207.

Clark, C. 1993. Mega-scale glacial lineations and cross-cutting ice-flow landforms. *Earth surface processes and landforms*, **18**(1), 1–29.

Clark, C. D. 1997. Reconstructing the evolutionary dynamics of former ice sheets using multi-temporal evidence, remote sensing and GIS. *Quaternary Science Reviews*, **16**(9), 1067–1092.

Clark, C. D., Evans, D. J. A., Khatwa, A., Bradwell, T., Jordan, C. J., Marsh, S. H., Mitchell, W. A., & Bateman, M. D. 2004a. Map and GIS database of glacial landforms and features related to the last British Ice Sheet. *Boreas*, **33**(4), 359–375.

Clark, C. D., Gibbard, P. L., & Rose, J. 2004b. Pleistocene glacial limits in England, Scotland and Wales. *Quaternary GlaciationsExtent and Chronology*, **1**.

Clark, C. D., Hughes, A. L. C., Greenwood, S. L., Jordan, C., & Sejrup, H. P. 2012. Pattern and timing of retreat of the last British-Irish Ice Sheet. *Quaternary Science Reviews*, **44**, 112–146.

Clark, C. D., Ely, J. C., Greenwood, S. L., Hughes, A. L. C., Meehan, R., Barr, I. D., Bateman, M. D., Bradwell, T., Doole, J., Evans, D. J. A., Jordan, C. J., Monteys, X., Pellicer, X. M., & Sheehy. 2018. BRITICE Glacial Map, version 2: a map and GIS database of glacial landforms of the last British-Irish Ice Sheet. *Boreas*, **47**, 11–e8.

Clark, P. U., McCabe, A. M., Mix, A. C., & Weaver, A. J. 2004c. Rapid rise of sea level 19,000 years ago and its global implications. *Science*, **304**(5674), 1141–1144.

Cotterill, C. J., Phillips, E., James, L., Forsberg, C. F., Tjelta, T. I., Carter, G., & Dove, D. 2017. The evolution of the Dogger Bank, North Sea: A complex history of terrestrial, glacial and marine environmental change. *Quaternary Science Reviews*, **171**, 136–153.

Cowan, E. A., & Powell, R. D. 1990. Suspended sediment transport and deposition of cyclically interlaminated sediment in a temperate glacial fjord, Alaska, USA. *Geological Society, London, Special Publications*, **53**(1), 75–89.

Cowan, E. A., Seramur, K. C., Cai, J., & Powell, R. D. 1999. Cyclic sedimentation produced by fluctuations in meltwater discharge, tides and marine productivity in an Alaskan fjord. *Sedimentology*, **46**(6), 1109–1126.

Davies, B. J., Roberts, D. H., Ó Cofaigh, C., Bridgland, D. R., Riding, J. B., Philipps, E. R., & Teasdale, D. A. 2009a. Interlobate ice-sheet dynamics during the Last Glacial Maximum at Whitburn Bay, County Durham, England. *Boreas*, **38**, 555–578.

Davies, B. J., Bridgland, D. R., Roberts, D. H., Ó Cofaigh, C., Pawley, S. M., Candy, I., Demarchi, B., Penkman, K. E. H., & Austin, W. E. N. 2009b. The age and stratigraphic context of the Easington Raised Beach, County Durham, UK. *Proceedings of the Geologists Association*, **120**, 183–198.

Davies, B. J., Roberts, D. H., Bridgland, D. R., Ó Cofaigh, C., & Riding, J. B. 2011. Provenance and depositional environments of Quaternary sediments from the western North Sea Basin. *Journal of Quaternary Science*, **26(1)**, 59–75.

Davies, B. J., Roberts, D. H., Bridgland, D. R., & Ó Cofaigh, C. 2012a. Dynamic Devensian ice flow in NE England: a sedimentological reconstruction. *Boreas*, **41**(3), 337–336.

Davies, B. J., Roberts, D. H., Bridgland, D. R., Ó Cofaigh, C., Riding, J. B., Demarchi, B., Penkman, K. E. H., & Pawley, S. M. 2012b. Timing and depositional environments of a Middle Pleistocene glaciation of northeast England: New evidence from Warren House Gill, County Durham. *Quaternary Science Reviews*, **44**, 180–212.

Davies, B. J., Yorke, L., Bridgland, D. R., & Roberts, D. H. 2013. *The Quaternary of Northumberland, Durham and North Yorkshire: Field Guide*. Quaternary Research Association: London.

De Haas, H., Boer, W., & Van Weering, T. C. E. 1997. Recent sedimentation and organic carbon burial in a shelf sea: the North Sea. *Marine Geology*, **144**(1), 131–146.

Dove, D., Arosio, R., Finlayson, A., Bradwell, T., & Howe, J. A. 2015. Submarine glacial landforms record Late Pleistocene ice-sheet dynamics, Inner Hebrides, Scotland. *Quaternary Science Reviews*, **123**, 76–90.

Dove, D., Evans, D. J. A., Lee, J. R., Roberts, D. H., Tappin, D. R., Mellett, C. L., Long, D., & Callard, S. L. 2017. Phased occupation and retreat of the last British–Irish Ice Sheet in the southern North Sea; geomorphic and seismostratigraphic evidence of a dynamic ice lobe. *Quaternary Science Reviews*, **163**, 114–134.

Dowdeswell, J. A. 2006. The Greenland ice sheet and global sea-level rise. *Science*, **311**(5763), 963–964.

Dowdeswell, J. A., & Fugelli, E. M. G. 2012. The seismic architecture and geometry of grounding-zone wedges formed at the marine margins of past ice sheets. *Geological Society of America Bulletin*, **124**(11-12), 1750–1761.

Dowdeswell, J. A., Whittington, R. J., & Marienfeld, P. 1994. The origin of massive diamicton facies by iceberg rafting and scouring, Scoresby Sund, East Greenland. *Sedimentology*, **41**(1), 21–35.

Dowdeswell, J. A., Whittington, R. J., Jennings, A. E., Andrews, J. T., Mackensen, A., & Marienfeld, P. 2000. An origin for laminated glacimarine sediments through sea-ice build-up and suppressed iceberg rafting. *Sedimentology*, **47**, 557–576.

Dowdeswell, J. A., Ó Cofaigh, C., & Pudsey, C. J. 2004. Thickness and extent of the subglacial till layer beneath an Antarctic paleo–ice stream. *Geology*, **32**(1), 13–16.

Dowdeswell, J. A., Ottesen, D., Evans, J., Ó Cofaigh, C., & Anderson, J. B. 2008. Submarine glacial landforms and rates of ice-stream collapse. *Geology*, **36**(10), 819–822.

EGS. 2012. *NAREC Geophysical Survey: Technical Report. Revision 3 - Final*. Tech. rept.

Ehlers, J. 1990. Reconstructing the dynamics of the north-west European Pleistocene ice sheets. *Quaternary Science Reviews*, **9**(1), 71–83.

Ehlers, J., & Gibbard, P. 2007. The extent and chronology of Cenozoic global glaciation. *Quaternary International*, **164**, 6–20.

Ehlers, J., & Gibbard, P. 2008. Extent and chronology of Quaternary glaciation. *Episodes*, **31**(2), 211–218.

Emery, D., & Myers, K. J. 1996. *Sequence Stratigraphy*. BP Exploration, Stocklety Park, Uxbridge, London.

Evans, D. J. A. In press. *Till - A Glacial Process Sedimentology*.

Evans, D. J. A., & Benn, D. (eds). 2004. *A practical guide to the study of glacial sediments*. Routledge.

Evans, D. J. A., & Hiemstra, J. F. 2005. Till deposition by glacier submarginal, incremental thickening. *Earth Surface Processes and Landforms*, **30**(13), 1633–1662.

Evans, D. J. A., & Thomson, S. A. 2010. Glacial sediments and landforms of Holderness, eastern England: a glacial depositional model for the North Sea Lobe of the British–Irish Ice Sheet. *Earth Science Reviews*, **101**(3), 147–189.

Evans, D. J. A., Clark, C., & Mitchell, W. A. 2005. The last British Ice Sheet: A review of the evidence utilised in the compilation of the Glacial Map of Britain. *Earth-Science Reviews*, **70 (3-4)**, 253–312.

Evans, D. J. A., Bateman, M. D., Roberts, D. H., Medialdea, A., Hayes, L., Duller, G. A. T., Fabel, D., & Clark, C. 2017. Glacial Lake Pickering: stratigraphy and chronology of a proglacial lake dammed by the North Sea Lobe of the British–Irish Ice Sheet. *Journal of Quaternary Science*, **32**(2), 295–310.

Everest, J., Bradwell, T., & Golledge, N. 2005. Subglacial landforms of the Tweed Palaeo-Ice stream. *The Scottish Geographical Magazine*, **121**(2), 163–173.

Everest, J. D., & Kubik, P. 2006. The deglaciation of eastern Scotland: cosmogenic 10Be evidence for a Lateglacial stillstand. *Journal of Quaternary Science*, **21**(1), 95–104.

Eyles, N. 2012. Rock drumlins and megaflutes of the Niagara Escarpment, Ontario, Canada: a hard bed landform assemblage cut by the Saginaw–Huron Ice Stream. *Quaternary Science Reviews*, **55**, 34–49.

Eyles, N., & Doughty, M. 2016. Glacially-streamlined hard and soft beds of the paleo-Ontario ice stream in Southern Ontario and New York state. *Sedimentary Geology*, **338**, 51–71.

Eyles, N., McCabe, A. M., & Bowen, D. Q. 1994. The stratigraphic and sedimentological significance of Late Devensian ice sheet surging in Holderness, Yorkshire, UK. *Quaternary Science Reviews*, **13**(8), 727–759.

Eyles, N., Putkinen, N., Sookhan, S., & Arbelaez-Moreno, L. 2016. Erosional origin of drumlins and megaridges. *Sedimentary Geology*, **338**, 2–23.

Fairburn, W. A., & Bateman, M. D. 2016. A new multi-stage recession model for Proglacial Lake Humber during the retreat of the last British–Irish Ice Sheet. *Boreas*, **45**(1), 133–151.

Feyling-Hanssen, R. W. 1972. The foraminifer Elphidium excavatum (Terquem) and its variant forms. *Micropaleontology*, 337–354.

Finlayson, A., Fabel, D., Bradwell, T., & Sugden, D. 2014. Growth and decay of a marine terminating sector of the last British–Irish Ice Sheet: a geomorphological reconstruction. *Quaternary Science Reviews*, **83**, 28–45.

Fish, P. R., & Whiteman, C. A. 2001. Chalk micropalaeontology and the provenancing of Middle Pleistocene Lowestoft Formation till in eastern England. *Earth Surface Processes and Landforms*, **26**(9), 953–970.

Gatliff, R. W., Richards, P. C., Smith, K., Graham, C. C., McCormac, M., Smith, N. J. P., Long, D., Cameron, T. D. J., Evans, D., Stevenson, A. G., Bulat, J., & Ritchie, J. D. 1994. *United Kingdom offshore regional report: the geology of the central North Sea*. London: HMSO for the British Geological Survey.

Gibbard, P., & Cohen, K. M. 2008. Global chronostratigraphical correlation table for the last 2.7 million years. *Episodes*, **31**(2), 243–247.

Glennie, K. W. (Ed). 1998. *Petroleum Geology of the North Sea: basic concepts and recent advances. fourth ed.* Blackwell Science Ltd.

Golledge, N. R., & Stoker, M. S. 2006. A palaeo-ice stream of the British Ice Sheet in eastern Scotland. *Boreas*, **35**(2), 231–243.

Golledge, N. R., Finlayson, A. G., Bradwell, T., & Everest, J. D. 2008. The last glaciation of Shetland, north Atlantic. *Geografiska Annaler: Series A, Physical Geography*, **90**(1), 37–53.

Graham, A. G. C., Lonergan, L., & Stoker, M. S. 2007. Evidence for Late Pleistocene ice stream activity in the Witch Ground Basin, central North Sea, from 3D seismic reflection data. *Quaternary Science Reviews*, **26**, 627–643.

Graham, A. G. C., Stoker, M. S., Lonergan, L., Bradwell, T., & Stewart, M. A. 2011. *Quaternary Glaciations: Extent and Chronology: a Closer Look. Developments in Quaternary Science*. Elsevier. Chap. The Pleistocene Glaciations of the North Sea Basin, pages 261–268.

Gravenor, C. P., Von Brunn, V., & Dreimanis, A. 1984. Nature and classification of waterlain glaciogenic sediments, exemplified by Pleistocene, Late Paleozoic and Late Precambrian deposits. *Earth-Science Reviews*, **20**(2), 105–166.

Greenwood, S. L., Clark, C. D., & Hughes, A. L. C. 2007. Formalising an inversion methodology for reconstructing ice-sheet retreat patterns from meltwater channels: application to the British Ice Sheet. *Journal of Quaternary Science*, **22**(6), 637–645.

Hamblin, R. J. O., Moorlock, B. S. P., Rose, J., Lee, J. R., Riding, J. B., Booth, S. J., & Pawley, S. M. 2005. Revised Pre-Devensian glacial stratigraphy in Norfolk, England, based on mapping and till provenance. *Netherlands Journal of Geosciences*, **84**(2), 77–85.

Hansen, A., & Knudsen, K. L. 1995. Recent foraminiferal distribution in Freemansundet and Early Holocene stratigraphy on Edgeøya, Svalbard. *Polar Research*, **14**(2), 215–238.

Hart, J. K., & Roberts, D. H. 1994. Criteria to distinguish between subglacial glaciotectonic and glaciomarine sedimentation, I. Deformation styles and sedimentology. *Sedimentary Geology*, **91**(1-4), 191–213.

Hogan, K. A., Ó Cofaigh, C., Jennings, A. E., Dowdeswell, J. A., & Hiemstra, J. F. 2016. Deglaciation of a major palaeo-ice stream in Disko Trough, West Greenland. *Quaternary Science Reviews*.

Holloway, L. K., Peacock, J. D., Smith, D. E., & Wood, A. M. 2002. A Windermere Interstadial marine sequence: environmental and relative sea level interpretations for the western Forth valley, Scotland. *Scottish Journal of Geology*, **38**(1), 41–54.

Hubbard, A. L., Bradwell, T., Golledge, N., Hall, A., Patton, H., Sugden, D., Cooper, R., & Stoker, M. S. 2009. Dynamic cycles, ice streams and their impact on the extent, chronology and deglaciation of the British–Irish ice sheet. *Quaternary Science Reviews*, **28**(7), 758–776.

Hughes, A. L. C., Clark, C., & Jordan, C. 2010. Subglacial bedforms of the last British Ice Sheet. *Journal of Maps*, **6**(1), 543–563.

Hughes, A. L. C., Greenwood, S. L., & Clark, C. 2011. Dating constraints on the last British-Irish Ice Sheet: a map and database. *Journal of Maps*, **7**(1), 156–184.

Hughes, A. L. C., Clark, C. D., & Jordan, C. J. 2014. Flow-pattern evolution of the last British Ice Sheet. *Quaternary Science Reviews*, **89**, 148–168.

Hughes, A. L. C., Gyllencreutz, R., Lohne, Øystein S., Mangerud, J., & Svendsen, J. I. 2016. The last Eurasian ice sheets–a chronological database and time-slice reconstruction, DATED-1. *Boreas*, **45**(1), 1–45.

Huuse, M., & Lykke-Anderson, H. 2000. Overdeepened Quaternary valleys in the eastern Danish North Sea: morphology and origin. *Quaternary Science Reviews*, **19**, 1233 – 1253.

Jennings, A. E., Walton, M. E., Ó Cofaigh, C., Kilfeather, A., Andrews, J. T., Ortiz, J. D., De Vernal, A., & Dowdeswell, J. A. 2014. Paleoenvironments during Younger Dryas-Early Holocene retreat of the Greenland Ice Sheet from outer Disko Trough, central west Greenland. *Journal of Quaternary Science*, **29**(1), 27–40.

Kilfeather, A. A., Ó Cofaigh, C., Lloyd, J. M., Dowdeswell, J. A., Xu, S., & Moreton, S. G. 2011. Ice-stream retreat and ice-shelf history in Marguerite Trough, Antarctic Peninsula: Sedimentological and foraminiferal signatures. *Geological Society of America Bulletin*, **123**(5-6), 997–1015.

Knudsen, K. L., & Sejrup, H. P. 1993. Pleistocene stratigraphy in the Devils Hole Area, Central North Sea: Foraminiferal and amino-acid evidence. *Journal of Quaternary Science*, **8**(1), 1–14.

Krabbendam, M., & Glasser, N. F. 2011. Glacial erosion and bedrock properties in NW Scotland: abrasion and plucking, hardness and joint spacing. *Geomorphology*, **130**(3), 374–383.

Krabbendam, M., Eyles, N., Putkinen, N., Bradwell, T., & Arbelaez-Moreno, L. 2016. Streamlined hard beds formed by palaeo-ice streams: A review. *Sedimentary Geology*, **338**, 24–50.

Lane, T. P., Roberts, D. H., Rea, B. R., Ó Cofaigh, C., & Vieli, A. 2015. Controls on bedrock bedform development beneath the Uummannaq Ice Stream onset zone, West Greenland. *Geomorphology*, **231**, 301–313.

Lee, J. R., Rose, J., Riding, J. B., Moorlock, B. S. P., & Hamblin, R. J. O. 2002. Testing the case for a Middle Pleistocene Scandinavian glaciation in Eastern England: evidence for a Scottish ice source for tills within the Corton Formation of East Anglia, UK. *Boreas*, **31**(4), 345–355.

Lee, J. R., Busschers, F. S., & Sejrup, H. P. 2012. Pre-Weichselian Quaternary glaciations of the British Isles, The Netherlands, Norway and adjacent marine areas south of 68 N: implications for long-term ice sheet development in northern Europe. *Quaternary Science Reviews*, **44**, 213–228.

Liss, D., Owens, W. H., & Hutton, D. H. W. 2004. New palaeomagnetic results from the Whin Sill complex: evidence for a multiple intrusion event and revised virtual geomagnetic poles for the late Carboniferous for the British Isles. *Journal of the Geological Society*, **161**(6), 927–938.

Livingstone, S. J., Ó Cofaigh, C., & Evans, D. J. A. 2008. Glacial geomorphology of the central sector of the last British-Irish Ice Sheet. *Journal of Maps*, **4:1**, 358–377.

Livingstone, S. J., Ó Cofaigh, C., & Evans, D. J. A. 2010. A major ice drainage pathway of the last BritishIrish Ice Sheet: the Tyne Gap, northern England. *Journal of Quaternary Science*, **25**, 354–370.

Livingstone, S. J., Ó Cofaigh, C., Stokes, C. R., Hillenbrand, C., Vieli, A., & Jamieson, S. S. 2012a. Antarctic palaeo-ice streams. *Earth-Science Reviews*, **111**(1), 90–128.

Livingstone, S. J., Evans, D. J. A., Ó Cofaigh, C., Davies, B. J., Merritt, J. W., Huddart, D., Mitchell, W. A., Roberts, D. H., & Yorke, L. 2012b. Glaciodynamics of the central sector of the last British–Irish Ice Sheet in Northern England. *Earth-Science Reviews*, **111**, 25–55.

Livingstone, S. J., Roberts, D. H., Davies, B. J., Evans, D. J. A., Ó Cofaigh, C., & Gheorghiu, D. M. 2015. Late Devensian deglaciation of the Tyne Gap Palaeo-Ice Stream, northern England. *Journal of Quaternary Science*, **30(8)**, 790–804.

Lonergan, L., Maidment, S. C. R., & Collier, J. S. 2006. Pleistocene subglacial tunnel valleys in the central North Sea basin: 3-D morphology and evolution. *Journal of Quaternary Science*, **21(8)**, 891–903.

Lucchi, R. G., Camerlenghi, A., Rebesco, M., Colmenero-Hidalgo, E., Sierro, F. J., Sagnotti, L., Urgeles, R., Melis, R., Morigi, C., Bárcena, M.-A., *et al.* 2013. Postglacial sedimentary processes on the Storfjorden and Kveithola trough mouth fans: Significance of extreme glacimarine sedimentation. *Global and planetary change*, **111**, 309–326.

Mackiewicz, N. E., Powell, R. D., Carlson, P. R., & Molnia, B. F. 1984. Interlaminated ice-proximal glacimarine sediments in Muir Inlet, Alaska. *Marine Geology*, **57**(1-4), 113–147.

McCabe, A. M., Haynes, J. R., & Macmillan, N. F. 1986. Late-Pleistocene tidewater glaciers and glaciomarine sequences from north County Mayo, Republic of Ireland. *Journal of Quaternary Science*, **1**(1), 73–84.

Mona Lisa Working Group. 1997. MONA LISA - Deep seismic investigations of the lithosphere in the southeastern North Sea. *Tectonophysics*, 1–19.

Morén, B. M., Sejrup, H. P., Hjelstuen, B. O., Borge, M. V., & Schäuble, C. 2017. The last deglaciation of the Norwegian Channel–geomorphology, stratigraphy and radiocarbon dating. *Boreas*.

Ó Cofaigh, C. 1996. Tunnel valley genesis. *Progress in Physical Geography*, **20**(1), 1–19.

Ó Cofaigh, C., & Dowdeswell, J. A. 2001. Laminated sediments in glacimarine environments: diagnostic criteria for their interpretation. *Quaternary Science Reviews*, **20**(13), 1411–1436.

Ó Cofaigh, C., & Evans, D. J. A. 2001. Sedimentary evidence for deforming bed conditions associated with a grounded Irish Sea glacier, southern Ireland. *Journal of Quaternary Science*, **16**(5), 435–454.

Ó Cofaigh, C., Dowdeswell, J. A., Allen, C. S., Hiemstra, J. F., Pudsey, C. J., Evans, J., & Evans, D. J. A. 2005. Flow dynamics and till genesis associated with a marine-based Antarctic palaeo-ice stream. *Quaternary Science Reviews*, **24**(5), 709–740.

Ó Cofaigh, C., Dowdeswell, J. A., Evans, J., & Larter, R. D. 2008. Geological constraints on Antarctic palaeo-ice-stream retreat. *Earth Surface Processes and Landforms*, **33**(4), 513–525.

Ó Cofaigh, C., Dowdeswell, J. A., Jennings, A. E., Hogan, K. A., Kilfeather, A., Hiemstra, J. F., Noormets, R., Evans, J., McCarthy, D. J., Andrews, J. T., *et al.* 2013. An extensive and dynamic ice sheet on the West Greenland shelf during the last glacial cycle. *Geology*, **41**(2), 219–222.

Ottesen, D., & Dowdeswell, J. A. 2006. Assemblages of submarine landforms produced by tidewater glaciers in Svalbard. *Journal of Geophysical Research: Earth Surface*, **111**(F1).

Ottesen, D., & Dowdeswell, J. A. 2009. An inter–ice-stream glaciated margin: Submarine landforms and a geomorphic model based on marine-geophysical data from Svalbard. *Geological Society of America Bulletin*, **121**(11-12), 1647–1665.

Ottesen, D., Dowdeswell, J. A., & Rise, L. 2005. Submarine landforms and the reconstruction of fast-flowing ice streams within a large Quaternary ice sheet: The 2500-km-long Norwegian-Svalbard margin (57–80 N). *Geological Society of America Bulletin*, **117**(7-8), 1033–1050.

Ottesen, D., Dowdeswell, J. A., Landvik, J. Y., & Mienert, J. 2007. Dynamics of the Late Weichselian ice sheet on Svalbard inferred from high-resolution sea-floor morphology. *Boreas*, **36**(3), 286–306.

Ottesen, D., Stokes, C. R., Bøe, R., Rise, L., Longva, O., Thorsnes, T., Olesen, O., Bugge, T., Lepland, A., & Hestvik, O. B. 2016. Landform assemblages and sedimentary processes along the Norwegian Channel Ice Stream. *Sedimentary Geology*, **338**, 115–137.

Patton, H., Hubbard, A., Andreassen, K., Winsborrow, M., & Stroeven, A. P. 2016. The build-up, configuration, and dynamical sensitivity of the Eurasian ice-sheet complex to Late Weichselian climatic and oceanic forcing. *Quaternary Science Reviews*, **153**, 97–121.

Patton, H., Hubbard, A. L., Andreassen, K., Auriac, A., Whitehouse, P. L., Stroeven, A. P., Shackleton, C., Winsborrow, M. C. M., Heyman, J., & Hall, A. M. 2017. Deglaciation of the Eurasian ice sheet complex. *Quaternary Science Reviews*, **169**, 148–172.

Pawley, S. M., Rose, J., Lee, J. R., Moorlock, B. S. P., & Hamblin, R. J. O. 2004. Middle Pleistocene sedimentology and lithostratigraphy of Weybourne northeast Norfolk, England. *Proceedings of the Geologists' Association*, **115**(1), 25–42.

Pawley, S. M., Bailey, R. M., Rose, J., Moorlock, B. S. P., Hamblin, R. J. O., Booth, S. J., & Lee, J. R. 2008. Age limits on Middle Pleistocene glacial sediments from OSL dating, north Norfolk, UK. *Quaternary Science Reviews*, **27**(13), 1363–1377.

Peltier, W. R.and Shennan, I., Drummond, R., & Horton, B. 2002. On the postglacial isostatic adjustment of the British Isles and the shallow viscoelastic structure of the Earth. *Geophysical Journal International*, **148**(3), 443–475.

Penny, L. F., Coope, G. R., & Catt, J. A. 1969. Age and insect fauna of the Dimlington Silts, East Yorkshire. *Nature*, **224**, 65–67.

Peters, J. L., Benetti, S., Dunlop, P., & Ó Cofaigh, C. 2015. Maximum extent and dynamic behaviour of the last British–Irish Ice Sheet west of Ireland. *Quaternary Science Reviews*, **128**, 48–68.

Peters, J. L., Benetti, S., Dunlop, P., Ó Cofaigh, C., Moreton, S. G., Wheeler, A. J., & Clark, C. D. 2016. Sedimentology and chronology of the advance and retreat of the last British-Irish Ice Sheet on the continental shelf west of Ireland. *Quaternary Science Reviews*, **140**, 101–124.

Powell, R. D. 1984. Glacimarine processes and inductive lithofacies modelling of ice shelf and tidewater glacier sediments based on Quaternary examples. *Marine Geology*, **57**(1-4), 1–52.

Powell, R. D., & Alley, R. B. 1997. Grounding-Line Systems: Processes, Glaciological Inferences and the Stratigraphic Record. *Geology and seismic stratigraphy of the Antarctic Margin, 2*, 169–187.

Preece, R. C., Parfitt, S. A., Coope, G. R., Penkman, K. E. H., Ponel, P., & Whittaker, J. E. 2009. Biostratigraphic and aminostratigraphic constraints on the age of the Middle Pleistocene glacial succession in north Norfolk, UK. *Journal of Quaternary Science*, **24**(6), 557–580.

Roberts, D. H., & Long, A. J. 2005. Streamlined bedrock terrain and fast ice flow, Jakobshavns Isbrae, West Greenland: implications for ice stream and ice sheet dynamics. *Boreas*, **34**(1), 25–42.

Roberts, D. H., Dackombe, R. V., & Thomas, G. S. P. 2007. Palaeo-ice streaming in the central sector of the BritishIrish Ice Sheet during the Last Glacial Maximum: evidence from the northern Irish Sea Basin. *Boreas*, **36**(2), 115–129.

Roberts, D. H., Long, A. J., Davies, B. J., Simpson, M. J. R., & Schnabel, C. 2010. Ice stream influence on west Greenland Ice Sheet dynamics during the Last Glacial Maximum. *Journal of Quaternary Science*, **25**(6), 850–864.

Roberts, D. H., Evans, D. J. A., Lodwick, J., & Cox, N. J. 2013. The subglacial and ice-marginal signature of the North Sea Lobe of the BritishIrish Ice Sheet during the Last Glacial Maximum at Upgang, North Yorkshire, UK. *Proceedings of the Geologists' Association*, **124**, 503–519.

Roberts, D. H., Evans, D. J. A., Callard, S. L., Dove, D., Bateman, M. D., Medialdea, A., Saher, M., Ó Cofaigh, C., Chiverrell, R. C., Moreton, S. G., Cotterill, C. J., & Clark, C. D. In prep.. The MIS II Limit of the British-irish Ice Sheet in the Southern North Sea.

Robinson, S. G., Maslin, M. A., & McCave, I. N. 1995. Magnetic susceptibility variations in Upper Pleistocene deep-sea sediments of the NE Atlantic: Implications for ice rafting and paleocirculation at the last glacial maximum. *Paleoceanography*, **10**(2), 221–250.

Sejrup, H. P., Haflidason, H., Aarseth, I., King, E., Forsberg, C. F., Long, D., & Rokoengen, K. 1994. Late Weichselian glaciation history of the northern North Sea. *Boreas*, **23**, 1–13.

Sejrup, H. P., Larsen, E., Landvik, J., King, E. L., Haflidason, H., & Nesje, A. 2000. Quaternary glaciations in southern Fennoscandia: evidence from southwestern Norway and the northern North Sea region. *Quaternary Science Reviews*, **19**, 667–685.

Sejrup, H. P., Larsen, E., Haflidason, H., Berstad, I. M., Hjelstuen, B. O., Jonsdottir, H. E., King, E. L., Landvik, J., Longva, O., Nygård, A., *et al.* 2003. Configuration, history and impact of the Norwegian Channel Ice Stream. *Boreas*, **32**(1), 18–36.

Sejrup, H. P., Hjelstuen, B. O., Nygård, A.e, Haflidason, H., & Mardal, Ivar. 2015. Late Devensian ice-marginal features in the central North Sea–processes and chronology. *Boreas*, **44**(1), 1–13.

Sejrup, H. P., Clark, C. D., & Hjelstuen, B. O. 2016. Rapid ice sheet retreat triggered by ice stream debuttressing: Evidence from the North Sea. *Geology*, **44**(5), 355–358.

Sejrup, H.P., Nygrda, A., Hall, A.M., & Haflidason, H. 2009. Middle and Late Weichselian (Devensian) glaciation history of south-western Norway, North Sea and eastern UK. *Quaternary Science Reviews*, **28**, 370–380.

Shennan, I., Bradley, S., Milne, G., Brooks, A., Bassett, S., & Hamilton, S. 2006. Relative sea-level changes, glacial isostatic modelling and ice-sheet reconstructions from the British Isles since the Last Glacial Maximum. *Journal of Quaternary Science*, **21**(6), 585–599.

Shepherd, A., Ivins, E. R., Geruo, A., Barletta, V. R., Bentley, M. J., Bettadpur, S., Briggs, K. H., Bromwich, D. H., Forsberg, R., Galin, N., *et al.* 2012. A reconciled estimate of ice-sheet mass balance. *Science*, **338**(6111), 1183–1189.

Sheriff, R. E. 1980. *Seismic Stratigraphy*. IHRDC, Publishers, Boston, MA 02116.

Smith, J. A., Hillenbrand, C., Larter, R. D., Graham, A. G. C., & Kuhn, G. 2009. The sediment infill of subglacial meltwater channels on the West Antarctic continental shelf. *Quaternary Research*, **71**(2), 190–200.

Stephenson, D., Loughlin, S. C., Millward, D., Waters, C. N., & Williamson, I. T. 2003. *Carboniferous and Permian Igneous Rocks of Great Britain North of the Variscan Front*. Vol. 27. Joint Nature Conservation Committee.

Stewart, M., Lonergan, L., & Hampson, G. 2012. 3D seismic analysis of buried tunnel valleys in the Central North Sea: tunnel valley fill sedimentary architecture. *Geological Society, London, Special Publications*, **368**(1), 173–184.

Stewart, M. A., & Lonergan, L. 2011. Direct evidence for seven glacial cycles in the Middle-Late Pleistocene of NW Europe. *Geology*, **39**, 283–286.

Stewart, M. A., Lonergan, L., & Hampson, G. 2013. 3D seismic analysis of buried tunnel valleys in the central North Sea: morphology, cross-cutting generations and glacial history. *Quaternary Science Reviews*, **72**, 1–17.

Stoker, M. S., & Bent, A. 1985. Middle Pleistocene glacial and glaciomarine sedimentation in the west central North Sea. *Boreas*, **14**, 325 – 332.

Stoker, M. S., Skinner, A. C., Fyfe, J. A., & Long, D. 1983. Paleomagnetic evidence for early Pleistocene in the central and northern North Sea. *Nature*, **304**, 332–334.

Stoker, M. S., Balson, P. S., Long, D., & Tappin, D.R. 2011. An overview of the lithostratigraphical framework for the Quaternary deposits on the United Kingdom continental shelf. *British Geological Survey Research Report, RR/11/03. 48pp.*

Stokes, C. R., & Clark, C. D. 2001. Palaeo-ice streams. *Quaternary Science Reviews*, **20**(13), 1437–1457.

Stokes, C. R., & Clark, C. D. 2002. Are long subglacial bedforms indicative of fast ice flow? *Boreas*, **31**(3), 239–249.

Stokes, C. R., Tarasov, L., Blomdin, R., Cronin, T. M., Fisher, T. G., Gyllencreutz, R., Hättestrand, C., Heyman, J., Hindmarsh, R. C. A., Hughes, A. L. C., *et al.* 2015. On the reconstruction of palaeo-ice sheets: Recent advances and future challenges. *Quaternary Science Reviews*, **125**, 15–49.

Stroeven, A. P., Hättestrand, C., Kleman, J., Heyman, J., Fabel, D., Fredin, O., Goodfellow, B. W., Harbor, J. M., Jansen, J. D., Olsen, L., *et al.* 2016. Deglaciation of fennoscandia. *Quaternary Science Reviews*, **147**, 91–121.

Sturt, F., Garrow, D., & Bradley, S. 2013. New models of North West European Holocene palaeogeography and inundation. *Journal of Archaeological Science*, **40**(11), 3963–3976.

Taylor, B. J., Burgess, I. C., Land, D. H., Mills, D. A. C., Smith, D. B., & Warren, P. T. 1971. *Northern England (British Regional Geology)*. London: HMSO.

Taylor, J. C. M. 1990. Upper PermianZechstein. *Petroleum Geology of the North Sea: Basic Concepts and Recent Advances, Fourth Edition*, 174–211.

Teasdale, D. 2013. *QRA Field Guide: The Quaternary of Northumberland, Durham and Yorkshire*. Quaternary Research Association: Cambridge. Chap. Evidence for the western limits of the North Sea Lobe of the BIIS in North East England., pages 106–121.

Thomas, E., Booth, L., Maslin, M., & Shackleton, N. J. 1995. Northeastern Atlantic benthic foraminifera during the last 45,000 years: changes in productivity seen from the bottom up. *Paleoceanography*, **10**(3), 545–562.

Thomas, G. S. P., & Connell, R. J. 1985. Iceberg drop, dump, and grounding structures from Pleistocene glacio-lacustrine sediments, Scotland. *Journal of Sedimentary Research*, **55**(2).

Toucanne, S., Zaragosi, S., Bourillet, J., Gibbard, P., Gibbard, ., Giraudeau, J., Turon, J. L., Cremer, M., Cortijo, E., Martinez, P., *et al.* 2009. A 1.2 Ma record of glaciation and fluvial discharge from the West European Atlantic margin. *Quaternary Science Reviews*, **28**(25), 2974–2981.

Toucanne, S., Zaragosi, S., Bourillet, J., Marieu, V., Cremer, M., Kageyama, M., Van Vliet-Lanoë, B., Eynaud, F., Turon, J., & Gibbard, P. L. 2010. The first estimation of Fleuve Manche palaeoriver discharge during the last deglaciation: evidence for Fennoscandian ice sheet meltwater flow in the English Channel ca 20–18ka ago. *Earth and Planetary Science Letters*, **290**(3), 459–473.

Tucker, M. E. 1991. Sequence stratigraphy of carbonate-evaporite basins: models and application to the Upper Permian (Zechstein) of northeast England and adjoining North Sea. *Journal of the Geological Society*, **148**(6), 1019–1036.

Ward, I., Larcombe, P., & Lillie, M. 2006. The dating of Doggerland – post-glacial geochronology of the southern North Sea. *Environmental Archaeology*, **11**(2), 207–218.

Ward, S. L., Neill, S. P., Scourse, J. D., Bradley, S. L., & Uehara, K. 2016. Sensitivity of palaeotidal models of the northwest European shelf seas to glacial isostatic adjustment since the Last Glacial Maximum. *Quaternary Science Reviews*, **151**, 198–211.

Westaway, R., Bridgland, D. R., White, T. S., Howard, A. J., & White, M. 2015. The use of uplift modelling in the reconstruction of drainage development and landscape evolution in the repeatedly glaciated Trent catchment, English Midlands, UK. *Proceedings of the Geologists' Association*, **126**(4-5), 480–521.

White, T. S., Bridgland, D. R., Westaway, R., Howard, A. J., & White, M. J. 2010. Evidence from the Trent terrace archive, Lincolnshire, UK, for lowland glaciation of Britain during the Middle and Late Pleistocene. *Proceedings of the Geologists' Association*, **121**(2), 141–153.

Yorke, L., Rumsby, B. T., & Chiverrell, R. C. 2012. Depositional history of the Tyne valley associated with retreat and stagnation of Late Devensian Ice Streams. *Proceedings of the Geologists' Association*, **123**, 608–625.